SAFETY ANALYSIS REPORT
FOR
JRC-80Y-20T

2022

JAPAN ATOMIC ENERGY AGENCY

CONTENTS

Chapter III : Maintenance conditions of transport packaging and handling method of package ························ **(III)-A-1**

LIST OF FIGURES

LIST OF TABLES

Chapter Ⅰ : Package description

A. Introduction

This packaging is dry type, and is named JRC-80Y-20T. The transportation appearance is shown in (Ⅰ)-Fig.A.1.

The JRC-80Y-20T packaging is used to transport spent fuels from reactors for research (JRR-3) of Japan Atomic Energy Agency (former Japan Atomic Energy Research Institute) to reprocessing plants in foreign countries.

A.1. Name of the packaging

JRC-80Y-20T

A.2. Type

Type B(U) package for fissile material

A.3. Allowable number of packages and allowable arrangement of packages

Allowable number of packages : Unlimited

Allowable arrangement of packages : No restriction

A.4. Transport index and criticality safety index

Transport index : Less than 5.8

Criticality safety index : 0

A.5. Maximum weight of the package

23.2×10^3 kg (at loading the basket for box type fuel)

A.6. Size of the packaging (at body lifting lug)

Diameter approx. 1.9m

Height approx. 2.1m

A.7. Maximum weight of the packaging

22.8×10^3 kg (at loading the basket for box type fuel)

A.8. Materials

1) Main parts : Stainless steel (SA-182 [redacted])

2) Basket : Stainless steel (SA-182 [redacted], SA-240 [redacted]), [redacted]

3) Fin (for heat dissipation and shock absorbing) :Stainless steel (SA-240 [redacted]

A.9. Component of the packaging

1) Body

2) The basket (The following baskets are used for the fuel types below.)

- The basket for box type fuel
- The basket for MNU type fuel

A.10. Fuel elements contained in the packaging.

Type, number of assemblies, and number of rods to be loaded in the transport container are shown below sorted by fuel basket:

- The basket for box type fuel 40 pieces (maximum)

1) JRR-3 standard silicide type fuel

2) JRR-3 follower silicide type fuel

3) Fuels combined the above fuels 1) through 2)

(Herein, the fuel element 1) is called the standard type fuel element, and the fuel element 2) is called the follower type fuel element)

- The basket for MNU type fuel 160 pieces

1) JRR-3 MNU* type fuel

A.11. Planned years of use

1) Planned years of use: 70 years

2) Number of times used for transport per year: once or less

3) Number of days required per transport: 365 days or less

B. Type of package

B.1. Type

---

* MNU means Metallic Natural Uranium.

B(U) package for fissile material

This package corresponds to the requirement for Type B(U) package because the radioactivity exceeds the A2 value as shown in (I)-Table D.2. Additionally, it corresponds to requirements for packages containing fissile material because it is loaded with spent fuels where the enrichment is 20wt% or less, and which contains more than 15g of uranium-235, as shown in table (I)-Table D.1.

B.2. Allowable number of packages

No restriction

[redacted]

(I)-Fig.A.1　Package transport condition

C. Package description - packaging

C.1. Summary of design

(I)-Fig.C.1 shows the external appearance of this package. (I)-Fig.C.2 shows the general view of this package.

The packaging is cylindrical, which consists of the body (shell and body bottom plate) and lid. The packaging contains a basket. The basket is taken in and out of the top of the body, and the lid is fastening to the body by [redacted].

Also, the lid is provided with the vent valve for air-drain, and the bottom portion of the body is provided with the drain valve for water-drain, and the portions of the lid and the body connection are sealed with [redacted] O-ring [redacted]

. During the transport, the packaging is held on the skid in the vertical position (See (I)-Fig.C.3), and is fixed by the tie down device.

The packaging is held in the vertical position when it is handled in JRR-3 Reactor, JRR-4 Reactor or the house of reprocessing plant.

The fuels are put in the basket lodgments of the basket contained in the packaging. The fuel elements are taken in and out of the top of the packaging in the vertical position.

Handling of the packaging is carried out by using the lifting lug attached to the packaging. In order to absorb the drop impact and dissipate the decay heat, the top and bottom portions of the packaging are provided with the fins fixed by welding.

The shell of the packaging has the intensity to bear the penetration due to drop. The fins to facilitate dissipation of decay heat generated from the contained fuel elements are installed on the outer surface of the packaging.

The containment boundary of the packaging, as shown in (I)-Fig.C.4, consists of the body, the lid, O-ring [redacted], the vent valve, and the drain valve.

The main shielding material of the packaging is stainless steel, which consists of the body, the lid, and the basket, and is used for gamma ray and neutron shield.

For the purpose of subcritical control of the package, [redacted] are installed to the basket for box type fuel (except the basket for MNU type fuel) as neutron poison.

[redacted].

[redacted]

(I)-Fig.C.1 The external appearance of the package

[redacted]

(Ⅰ)-Fig.C.2　The general view of the packaging

[redacted]

(Ⅰ)-Fig.C.3　Tie down device

[redacted]

(Ⅰ)-Fig.C.4　The containment boundary of the packaging

C.2. Structure

The packaging, as shown in (I)-Fig.C.1 and (I)-Fig.C.2, consists of the body, the lid, and the basket, which is provided with the skid and tie down device as the attachments.

The materials, dimensions and weights of these are shown in (I)-Fig.C.3～(I)-Fig.C.5.

C.2.1 Body

(I)-Fig.C.5 shows the section view of the body of the packaging without the basket. The main structures of the body are the shell, the body bottom plate, heat dissipating and shock absorbing fins, the base plate, drain valve, and body lifting lugs. The shell is cylindrical, [redacted]mm in inner diameter, [redacted]mm in thickness, and [redacted]mm in inside height, and is made of a solid forging with the bottom plate ([redacted]mm in thickness). The shell and the body bottom plate serve as shielding.

The heat dissipating and shock absorbing fins are divided mainly into two kinds of lateral fins and bottom fins. The lateral fins are installed to the side of the shell and the bottom fins are installed to the bottom corner. These are installed by welding. The configuration of each fins is shown in (I)-Fig.C.6 and (I)-Fig.C.8.

As shown in (I)-Fig.C.6, the lateral fins are 5mm in thickness and 200mm in height, and are installed to all around the shell at the pitch of 10°. The lower extremities of the lateral fins are connected with the bottom fins.

The fins adjacent to the body lifting lug are cut at the upper extremities in order to prevent when it is lifted.

As shown in (I)-Fig.C.7 and (I)-Fig.C.8, the bottom fins are 30 mm in thickness and 189mm in height, and are installed to around the corner of the body bottom plate at the pitch of 5°. The length of fins has three kinds, that enlarge the shock absorbing effect and are structured to be able to absorb the shock step by step. Also, the longest fins (4 pieces) are welded to the base plate in order to supports the packaging body.

The structure of drain valve, which is used on loading or unloading of fuel elements in the packaging, is shown in (I)-Fig.C.9 and (I)-Fig.C.10. The valve body is so arranged as to assemble parts into a complete unit that is fixed to the valve housing by [redacted] and is maintained its containment [redacted] with [redacted] O-rings.

Furthermore, the leak test hole to verify the containment is [redacted], and the valve is a structure capable of applying test pressure after removing the plug. The valve is [redacted]. [redacted] can be opened by opening the valve after [redacted].

The containment of the valve is confirmed by applying the test pressure with removal of the outlet plug. Also, it is structured that [redacted] to prevent from [redacted].

This protection cover ((Ⅰ)-Fig.C.11) has the heat dissipating and shock absorbing fins which are the same structure as the fins of body.

(Ⅰ)-Fig.C.12 shows the body lifting lug. A pair of lugs is installed on the outer surface of the shell by welding, which is used for handling the package and the packaging.

[redacted]

A

(Ⅰ)-Fig.C.5　The sectional view of the packaging

[redacted]

(I)-Fig.C.6　The sectional view of lateral fin

[redacted]

(Ⅰ)-Fig.C.7 Bottom fin and base plate

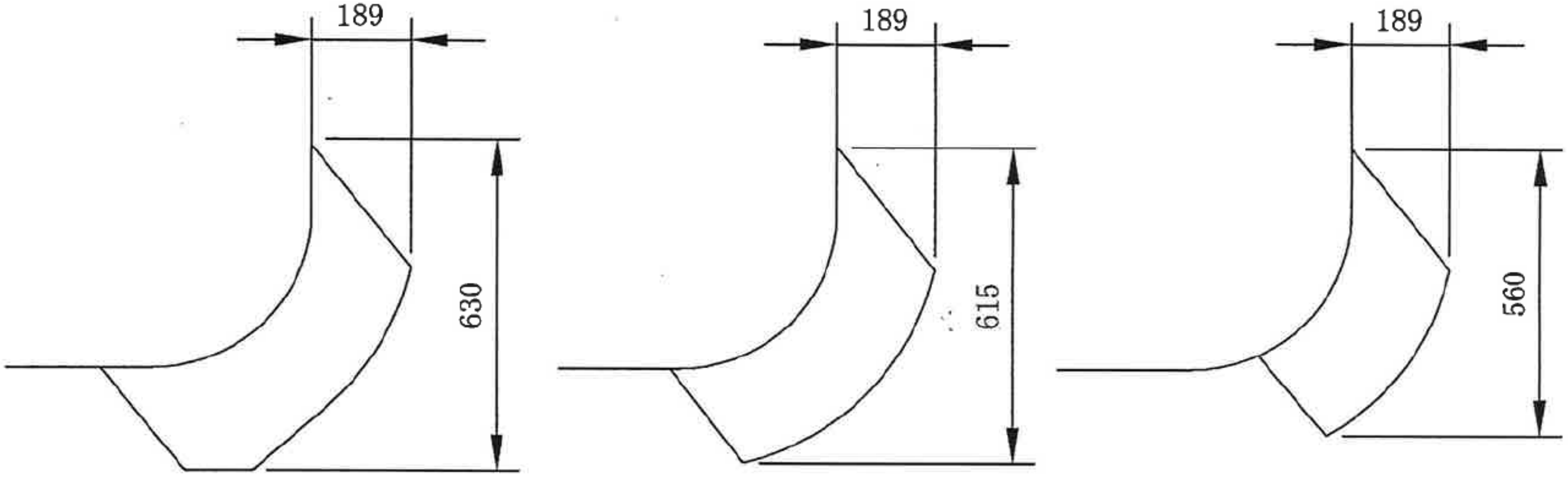

Fin a (Thickness : 30)

Fin b (Thickness : 30)

Fin c (Thickness : 30)

(Unit : mm)

(I)-Fig.C.8 Configuration of bottom fin

[redacted]

(Ⅰ)-Fig.C.9　The sectional view of vent and drain valves

[redacted]

(Ⅰ)-Fig.C.10 The plan of vent and drain valves (without protection cover)

[redacted]

(Ⅰ)-Fig.C.11　Drain valve protection cover

[redacted]

(I)-Fig.C.12　Body lifting lug

C.2.2 Lid

(I)-Fig.C.13 and (I)-Fig.C.14 show the structural view of the lid. The configuration of the top fins is shown in (I)-Fig.C.15.

The lid ([redacted]mm in thickness) is fixed to the shell flange by [redacted]. [redacted].

The flange faces of the contact portion of the lid and the shell are flat, and the containment of the contact portion is kept by [redacted] O-ring among those O-rings in [redacted] of grooves prepared in the lid. In order to verify the containment, the leak test hole is in [redacted] O-rings, as shown in (I)-Fig.C.16, where the test pressure can be applied after removal of the plug. Also, the shell flange is provided with the centering pins (2 pieces) to facilitate the centering and installation of the lid. On the outer surface of the lid, the heat dissipating and shock absorbing fins, which are called top fins, are installed by welding as shown in (I)-Fig.C.14 and (I)-Fig.C.15.

These fins are 30mm or 33mm in thickness and 190mm in height, and are installed all around the circumference of the top corner. The length of the fins is divided into 7 kinds. There are fins that are chamfered off among these fins, and the structure is made to enlarge the shock absorbing effect by fins and to enable to absorb the shock step by step.

The [redacted] is in the middle of the lid, and the vent valve is installed on the outer surface of the lid to be used when loading or unloading of the fuel elements is carried out. Except the protective cover, the structure of the vent valve is exactly the same as that of the drain valve, which is shown in (I)-Fig.C.9 and (I)-Fig.C.10, and is so arranged to assemble parts into a complete unit that the vent valve is fixed to the valve housing by [redacted] and its containment is kept by the [redacted] O-rings.

The fins, which are attached to the protection cover for the drain valve (See (I)-Fig.C.17), are not attached to the protection cover for the vent valve.

A pair of the lid lifting lugs is installed to the lid by welding, and has enough strength to be undestroyed, if the package is lifted up by mistake by any chance.

The protection cover is set up so as not to lift up the package mistakenly by the lug in transport. To enlarge the shock absorbing effect, the lid lifting lugs also have chamfers as well as the top fin. (Ⅰ)-Fig. C.18 shows the lid lifting lugs.

[redacted]

(I)-Fig.C.13 The sectional view of the lid

[redacted]

(Ⅰ)-Fig.C.14 The plan of the lid

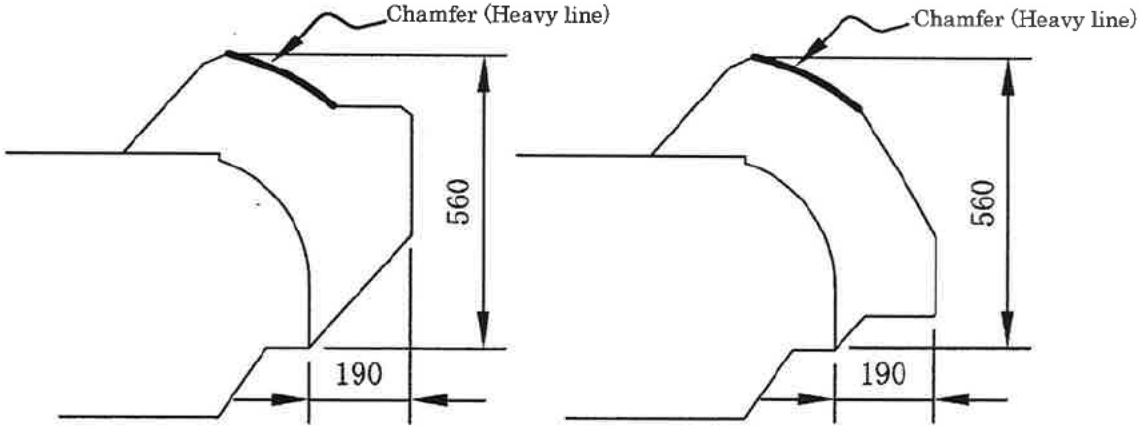

Fin A (Thickness : 30)

Fin B (Thickness : 30)

(Unit : mm)

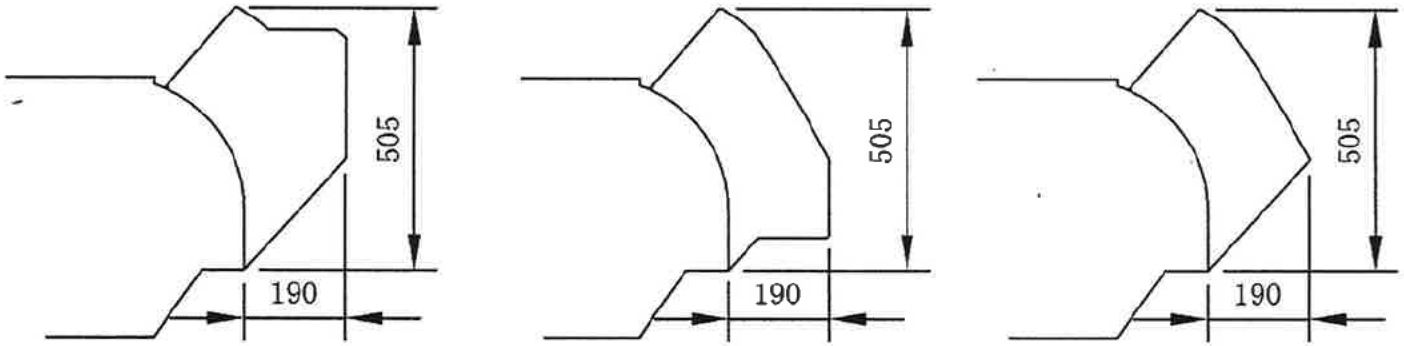

Fin C (Thickness : 30) or
Fin F (Thickness : 33)

Fin D (Thickness : 30) or
Fin E (Thickness : 33)

Fin G (Thickness : 33)

(Ⅰ)-Fig.C.15 Configuration of top fin

[redacted]

(Ⅰ)-Fig.C.16　Leak test hole and plug

[redacted]

(I)-Fig.C.17 Vent valve protection cover

[redacted]

(Ⅰ)-Fig.C.18　Lid lifting lug

C.2.3 Basket

The basket is for use of containing individual fuel elements in the packaging. It is given consideration not to break up or gather the fuel elements during transport and to hold them in subcritical condition.

There are 2 kinds of the basket as follows ;

- Basket for box type fuel as shown in (I)-Fig.C.19, 20.
- Basket for MNU type fuel as shown in (I)-Fig.C.21, 22.

For the basket for box type fuel, the [redacted] are assembled in the baskets as neutron poison.

The basket for box type fuel is structured that it consists of the compartment plates made of stainless steel which surrounds the boral plates and the partition plates made of only stainless steel.

40 basket lodgements (the side of square : [redacted]mm for the basket for box type fuel) are made of the above compartment plates and partition plates, and the above whole basket lodgements are supported by a frame of the forged stainless steel to bear the strength. This frame made of forged stainless steel serves also as shield. They are all of welded structure.

As shown in (I)-Fig.D.1 to (I)-Fig.D.2, the size in the section of the follower fuel elements which are loaded with the basket for box type fuel is smaller than that of the standard type fuel elements. A large space ([redacted]mm when the fuel element is put aside in the lodgement.) arises between the inside of the basket lodgment and the fuel elements. Therefore, when follower type fuel elements are loaded in a basket for box type fuel, an aluminum alloy spacer shown in (I)-Fig. C.23 shall be placed between a fuel element and a fuel element insertion hole for the purpose of using it as a heat transfer component and reducing fuel shaking during transportation.

The basket for MNU type fuel consists mainly of 160 channels made of stainless steel, and is all of welded structure.

[redacted]

(Ⅰ)-Fig.C.19 Basket for box type fuel

[redacted]

(Ⅰ)-Fig.C.20 The general view of the basket for box type fuel

[redacted]

(Ⅰ)-Fig.C.21　Basket for MNU type fuel

[redacted]

(Ⅰ)-Fig.C.22　The general view of the basket for MNU type fuel

[redacted]

(Ⅰ)-Fig.C.23　Configuration of the adapter

C.3. Material

C.3.1 Body

(1) Shell	Stainless steel
(2) Body bottom plate	Stainless steel
(3) Heat dissipation and shock absorbing fin	Stainless steel
(4) Body lifting lug	Stainless steel

C.3.2 Lid

(1) Lid plate	Stainless steel
(2) Lid bolt	Stainless steel
(3) O-ring	[redacted]
(4) Lid lifting lug	Stainless steel

C.3.3 Vent and drain valves

(1) Body	Stainless steel
(2) Valve seat	Stainless steel, [redacted]
(3) Bellows	Stainless steel
(4) O-ring	[redacted]
(5) Gasket	[redacted]
(6) Plug	Stainless steel
(7) Bolt	Stainless steel
(8) Protection cover	Stainless steel

C.3.4 Basket (for box type fuel)

(1) Neutron poison	[redacted]
(2) Frame	Stainless steel
(3) Bottom plate	Stainless steel
(4) Compartment plate	Stainless steel, [redacted]
(5) Partition plate	Stainless steel
(6) Adapter	Aluminum alloy

C.3.5 Basket (for MNU type fuel)	
(1) Square shape pipe	Stainless steel
(2) Bottom plate	Stainless steel
(3) Support bar	Stainless steel
(4) Gusset	Stainless steel
(5) Support plate	Stainless steel
(6) Guide plate	Stainless steel
C.3.6 Lifting lug	Stainless steel, Mild steel
C.3.7 Tie down device	High-tensile steel, Stainless steel

C.4. Dimensions

	Dimension	Reference figure
C.4.1 The whole packaging		(I)-Fig.C.2
Outer diameter	1,840mm (Maximum width：1,860mm)	
Height	2,100mm	
C.4.2 Body		
(1) Shell		
Outer diameter	[redacted]	(I)-Fig.C.5
Plate thickness	[redacted]	
Inside	[redacted]	
(2) Bottom plate thickness		
(Outer circumference)	[redacted]	(I)-Fig.C.5
Plate thickness (Center part)	[redacted]	
(3) Lateral fin		(I)-Fig.C.6
Height	200mm	
Thickness	5mm	
Length	980mm	
Number of fins	36 sheets	
(4) Bottom fin		(I)-Fig.C.7, C.8

	Height	Thickness	Length	Number of fins
a.	189mm	30mm	630mm	4 sheets
b.	189mm	30mm	615mm	32 sheets
c.	189mm	30mm	560mm	36 sheets

		Dimension	Reference figure
C.4.3 Lid			(I)-Fig.C.13, C.14

(1) Lid

Outer diameter [redacted]

Thickness [redacted]

(2) Top fin

	height	thickness	length	number of fins
A.	190mm	30mm	560mm	16 sheets
B.	190mm	30mm	560mm	16 sheets
C.	190mm	30mm	505mm	16 sheets
D.	190mm	30mm	505mm	12 sheets
E.	190mm	33mm	505mm	4 sheets
F.	190mm	33mm	505mm	4 sheets
G.	190mm	33mm	505mm	4 sheets

C.4.4 Basket (I)-Fig.C.19～(I)-Fig.C.23

(1) Basket for box type fuel

Height [redacted]

Outer diameter [redacted]

Inside of basket lodgement sectional area [redacted]

(2) Basket for MNU type fuel

Height [redacted]

Outer diameter [redacted]

Inside of basket lodgement sectional area [redacted]

(3) Adapter

Height [redacted]mm

Outside [redacted]mm × [redacted]mm

Inside [redacted]mm × [redacted]mm

		Dimension	Reference figure
C.4.5 Tie down device			(I)-Fig.C.3
		<u>Skid and tie down device</u>	
	Length	[redacted]	
	Width	[redacted]	
	Height	[redacted]	
C.4.6 Lifting device			
	Length	about 4,200mm	

C.5. Weight

(a) Body (with fins)	a : [redacted]kg
(b) Lid, lid bolt	
(1) Lid (with fins)	b_1 : [redacted]kg
(2) Lid bolt	b_2 : [redacted]kg
(c) Basket	
(1) Basket for box type fuel	c_1 : [redacted]kg
(2) Basket for MNU type fuel	c_2 : [redacted]kg
(3) Spacer (40 pieces)	c_3 : [redacted]kg
(d) Tie down device	d : 1.9×10^3 kg
(e) Lifting device	e : 0.2×10^3 kg

(f) Fuel element

(1) Standard type fuel element	40 pieces	f_1 :	[redacted] kg
(2) Follower type fuel element (with the adapters)	40 pieces	f_2 :	[redacted] kg
(3) JRR-3 MNU type fuel element	160 pieces	f_3 :	[redacted] kg

(g) Water (the weight of water when the inner cavity is filled with water)

(1) Standard type, or follower type fuel element	g_1 :	[redacted] kg
(2) JRR-3 MNU type fuel element	g_2 :	[redacted] kg

(h) Total weight of the package (The maximum weight is used at containing standard type fuel)

(1) At containing standard type, or follower type fuel elements

(a)+(b)+(c_1)+(f_1), or (f_2)	23.2×10^3 kg

(2) At containing JRR-3 MNU type fuel elements

(a)+(b)+(c_2)+(f_3)	23.0×10^3 kg

(i) Total weight when lifted up

(1) At containing standard type, or follower type fuel elements

(a)+(b)+(c_1)+(d)+(e)+(f_1), or (f_2)	25.3×10^3 kg

(2) At containing JRR-3 MNU type fuel elements

(a)+(b)+(c_2)+(d)+(e)+(f_3)	25.1×10^3 kg

D. Contents of package

Contents of the package are spent fuel elements of JRR-3.

The fuel plates of standard type and follower type fuel elements are the fuel meats of uranium silicone aluminum dispersion type alloy covered with aluminum alloy.

The metallic natural uranium of JRR-3 MNU type fuel element is covered with aluminum alloy. The fuel elements are shown in (I)-Fig.D.1 through (I) -Fig.D.4. The standard type fuel element are shown in (I)-Fig.D.1, the follower type fuel element are shown in (I)-Fig.D.2 and JRR-3 MNU type fuel element are shown in (I)-Fig.D.3 through (I) -Fig.D.4, respectively.

The standard type fuel elements are cut off its top and bottom portions which do not contain uranium, so as to be a prescribed length, before being loaded in the container, and then inserted into the fuel basket.

The follower type fuel elements are not cut off, and are loaded in the basket. JRR-3 MNU type fuels elements are cut into 3 pieces from the connection, and are loaded in the basket.

The specification of the fuel elements used for the safety evaluation of the package is shown in (I)-Table D.1. The quantities of main radionuclides contained in each fuel element are shown in (I)-Table D.2.

The integrity of these fuels are confirmed at the inspection before shipment.

On the other hand, the packaging containing the fuel elements is treated to close the vent valve and the drain valve before shipment till the thermal equilibrium is obtained, and to open them once again to release the internal pressure to the air.

After that, each valve is closed again. Therefore, the pressure rise in the packaging will not occur by the decay heat of fuel elements during transport.

[redacted]

(I)-Fig.D.1　JRR-3 Standard Silicide Type Fuel

[redacted]

(Ⅰ)-Fig.D.2　JRR-3 Follower Silicide Type Fuel

[redacted]

(Ⅰ)-Fig.D.3　JRR-3 MNU Type Fuel (Top, Middle Fuel)

[redacted]

(Ⅰ)-Fig.D.4　JRR-3 MNU Type Fuel (Bottom Fuel)

(I)-Table D.1 Specification of contents

Classifi-cation / Item				
	Basket	Box type	Box type(with Adapters)	MNU type
	Reactor	JRR-3	JRR-3	JRR-3
	Fuel element	Standard silicide type	Follower silicide type	MNU type
Fuel type		Plate fuel	Plate fuel	Rod fuel
Number of fuel elements (piece)		40 or less	40 or less	160 or less
Initial enrichment (%) 1)		[redacted]	[redacted]	[redacted]
Total mass of ^{235}U (g/piece) 1)		[redacted]	[redacted]	[redacted]
Total mass of U (g/piece) 1)		[redacted]	[redacted]	[redacted]
Burnup (%) 2)		[redacted]	[redacted]	[redacted]
Cooling time (day)		[redacted]	[redacted]	[redacted]
Total activity (Bq/package)		[redacted]	[redacted]	[redacted]
Decay heat (W/package)		2.24×10^3 or less	1.43×10^3 or less	7.24×10^1 or less
Fuel material	Fuel meat	Uranium silicon aluminum dispersion type alloy	Uranium silicon aluminum dispersion type alloy	Metallic natural uranium
	Clad	Aluminum alloy	Aluminum alloy	Aluminum alloy
	Side plate, etc.	Aluminum alloy	Aluminum alloy	――
Dimension at contained 3) width×height×length (mm)		[redacted]	[redacted]	[redacted]
Weight at contained (kg/piece)		[redacted]	[redacted]	[redacted]

spent standard silicide type fuel elements and spent follower silicide type fuel elements can be loaded together in one transport container.

1) The value in the nuclear specification shows an upper value which contains fabrication tolerance.
2) Burn up (%) = ((All depletion weight of ^{235}U) ÷ (Initial weight of ^{235}U))×100
3) The dimension of the contained fuels is within the dimension specified in (I)-Fig. D.1 through (I)-Fig. D.4.

(I)-Table D.2 Quantities of major radionuclides (per package)

<table>
<tr><td rowspan="2">Classifi-cation</td><td>Basket</td><td>Box type</td><td>Box type (with Adapters)</td><td>MNU type</td></tr>
<tr><td>Reactor</td><td>JRR-3</td><td>JRR-3</td><td>JRR-3</td></tr>
<tr><td>Item</td><td>Fuel element</td><td>Standard silicide type</td><td>Follower silicide type</td><td>MNU type</td></tr>
<tr><td colspan="2">Noble gas, etc.
H −3
Kr−85
I −129
I −131
Xe−131m

Heavy element
Pu−238
Pu−239
Pu−240
Pu−241
Am−241
Cm−242
Cm−244

F.P.
Sr−89
Sr−90
Y −90
Y −91

Zr−95
Nb−95
Ru−103
Ru−106
Te−129m
Cs−134
Cs−137
Ba−140
Ce−141
Pr−143
Ce−144
Pm−147

Others</td><td>(Bq)
[redacted]</td><td>(Bq)
[redacted]</td><td>(Bq)
[redacted]</td></tr>
<tr><td colspan="2">Total</td><td>[redacted]</td><td>[redacted]</td><td>[redacted]</td></tr>
</table>

Chapter Ⅱ : Safety analyses

This package is designed to comply with the IAEA Regulations for the Safe Transport of Radioactive Material 2012 Edition concerning Type B(U) package containing fissile material. This chapter shows the summary of each analysis for the package.

(1) Structural analysis

In the structural analysis of the package, the evaluation of the thermal stress and internal pressure under normal and accident conditions of transport is performed by means of finite element method code ABAQUS etc. Also, the evaluation for drop tests is performed by numerical analysis using finite element method code LS-DYNA.

As the results, it is confirmed that the package sufficiently satisfies all the requirements specified in the regulation. Namely, the following is assured.

Even if the package is subject to the pressure difference between inside and outside of the packaging and thermal loads under normal and accident conditions of transport, the package has sufficiently the containment and shielding performance required in the regulation, and there is no change of the configuration which affects the criticality and thermal analysis.

It was confirmed that there is no deformation affecting the configuration which is the base for criticality analysis and thermal analysis, except the basket for box type fuel which suffers a slight plastic deformation partially in 9 m horizontal drop of the package.

It was confirmed that even under test conditions for package containing fissile material, as the analytical results, there is no impact on the configuration which is the base for the evaluation of the subcriticality, except the basket for box type fuel.

(2) Thermal analysis

In the thermal analysis of the package, the temperature evaluation of each portion under normal and accident conditions of transport is performed by using ABAQUS code.

As the results, it was confirmed that the package satisfies the criteria specified in the regulation under normal and accident conditions of transport, and the temperature of each portion does not significantly affect the structural strength, the containment and shielding performance.

(3) Containment analysis

In the containment analysis of the package, the radioactive concentration in air inside the package is assumed to be 3.7×10^{-6}TBq/m^3 and the leakage value of radioactive gas is obtained by using the equation shown in ANSI - N 14.5 1997 edition.

As the results, it was confirmed that under normal and accident conditions of transport, the obtained leakage values satisfied the criteria of radioactive material leakage value specified in the regulation and notification.

(4) Shielding analysis

In the shielding analysis of the package, the source intensity of the package is calculated by using the ORNL isotope generation and depletion code ORIGEN or ORIGEN-JR. Also, the gamma and neutron shielding calculation are performed by using the point kernel code QAD-CGGP2R and two dimensional discrete ordinates transport code DOT 3.5, respectively.

As the results, it was confirmed that the dose equivalent ratios on the surface of the package and at points of 1 m from its surface are sufficiently small compared with the criteria of each case specified in the regulations under routine, normal and accident conditions of transport.

(5) Criticality analysis

The criticality analysis is performed by using the three dimensional multigroup Monte Carlo KENO-Va code.

As the results, it was demonstrated that there is no deformation, etc. of the structure affecting subcriticality evaluation under normal conditions of transport pertaining to package containing fissile material, and it was confirmed that the subcriticality is maintained for the nuclear fuel package under routine conditions of transport, for the nuclear fuel package in isolation, and for the package in isolation and in array under the normal and accident conditions of transport pertaining to package containing fissile material.

(6) Consideration of Aging of Nuclear Fuel Package

As a result of the evaluation of aging effects due to the factors such as heat, radiation, and chemical changes under the conditions of use expected during the planned period of use, it was confirmed that such effects need not be considered in confirming compliance with the technical criteria. For the lifting and containment devices, it is necessary to consider aging effects due to fatigue as stress will be generated repeatedly. For the lifting and containment devices, each fatigue was evaluated considering the conservative repeat count expected during the period of use, and it was confirmed that there is no impact on compliance with the technical criteria as fatigue failure does not occur.

The details of each analysis and the evaluations are described in Chapter A through Chapter F.

For the purpose of conservative evaluation, the safety analysis assumes the cases where following fuel elements are loaded, which will pose more severe conditions than the current contents.

A. Structural analysis

A.1 Structural design

This Chapter verifies that the package satisfies the requirements of the regulations and the structural integrities are maintained under all conditions.

A.1.1 General description

[redacted]

[redacted] A drain valve and a vent valve are provided with the body of the packaging and in the recess of the lid, respectively, and protection covers are mounted over these valves to protect them against damage.

Protection covers are also [redacted] to prevent inadvertent operation of the valves. Both of the body (the thickness of the shell is [redacted] mm and the minimum thickness of the bottom plate is [redacted] mm) and the lid ([redacted] mm in thickness) of the packaging are fabricated with stainless steel to provide the sufficient strength to withstand under various conditions such as pressure, vibration, heat and drop.

The basket, as shown in (I)-Fig. C.19 through (I)-Fig. C.22, is designed in two different types depending on the fuel element to be loaded in the packaging. The two types of the basket are designed so as to maintain the subcriticality under normal and accident conditions of transport.

The packaging is provided with the special lifting lugs on the side wall of the body and the lid to ensure safe lifting and lowering of the packaging. A special tie down device is used to securely attach the packaging to vehicles or vessels so that the packaging can withstand the acceleration and deceleration of the vehicle or vessel during transport.

The external surfaces of the body and the lid of the packaging are provided with fins being capable of heat dissipation and absorbing impact caused by drop. The external surface of the packaging is finished to eliminate unevenness as much as possible, including the fins, so as to facilitate water removal and decontamination.

In carrying out the structural analysis of the package, tests by models were not used but the numerical analysis was employed.

The packaging is characterized by its fins provided on the top, bottom, and corners of the packaging to absorb the energy generated upon drop.

A.1.2 Design

1. Fundamentals of design

The principle of the design is to satisfy the technical standard and other conditions shown below.

1.1 Conditions of the technical standard

A. Requirements of package

(a) There shall be no chemical and electrical actions between the structural materials of the packaging or between the structural material and the radioactive contents.

(b) The material shall not cause the low temperature brittleness at -40℃ of environmental temperature.

(c) The containment system must be constructed to prevent inadvertent opening.

(d) The lifting device must be able to withstand three times the lifting load.

(e) The tie down device must be able to withstand the acceleration in all direction, 10g in the travelling direction, 5g in the lateral direction, and 3g in the vertical direction.

(f) The package must be able to withstand the influence due to external pressure.

(g) Consideration shall be given to the acceleration and vibration during transport.

B. Normal conditions of transport

(a) The stress of the body and the lid under the operating pressure shall be less than the allowable stress.

(b) The packaging shall be capable of withstanding the water spray test.

(c) The packaging shall be capable of withstanding the free drop test from 0.3 meter high and a drop of a 6 kg mild steel bar.

(d) The packaging shall be capable of withstanding the compression test by a five times the normal load.

C. Accident conditions of transport

(a) The packaging shall be capable of withstanding the 9 meter drop test.

(b) The packaging shall be capable of withstanding the 1 meter drop test onto mild steel bar.

(c) The packaging shall be capable of withstanding the thermal test.

(d) The packaging shall be capable of withstanding the water immersion test of 0.15 MPa.

(e) The material used to fabricate the packaging shall not cause the low temperature brittleness at -40℃ of environmental temperature.

After the completion of the above tests, the packaging shall be capable of maintaining the soundness in terms of thermal performance, containment, shielding performance, and subcriticality.

1.2 Other conditions

(a) The packaging shall have the rigidity to withstand the external pressure equivalent to that of 200 meters deep in water and shall have the containment.

The following conditions were examined referring.

・The packaging shall comply with the ASME Code. (It is the condition of the package to obtain the approvals from U.S.A. and/or U.K. Competent Authority. For details, refer to the appendix (II)-A.10.4).)

- The packaging shall have the rigidity to withstand the external pressure equivalent to that of 5,000 meters deep in water. For details, refer to the appendix (II)-A.10.5).

2. Design conditions and analysis

In accordance with the fundamentals of the design, the analysis method was determined considering the design conditions for the analytical item such as the reference drawings, property of materials, temperature, loads, and safety factors. Design conditions, analysis method, and criteria are shown in (II)-Table A.1.

The criteria are used to evaluate the analytical result obtained from the applicable mathematical expression or elements, while the analytical result is evaluated by the safety margin (MS) shown below.

$$\text{Safety margin MS} = \frac{\text{Criteria}}{\text{Analytical result}} - 1$$

Therefore, if the safety margin is positive, the design of the packaging is to be considered as safe. For the part to which the safety margin cannot be used, the standard and other requirements are set forth where applicable.

The criteria is determined according to the mechanical property of the material shown in Chapter (II)-A.3 and the temperature and other conditions shown in Chapter (II) B. Tolerance in numerical value used for analysis shall conform to the standard such as JIS. For weld efficiency, 0.70 shall be used in conformance to the Codes for nuclear power generation facilities : rules on design and construction for nuclear power plants (2012).

The results of the analysis are shown in (II)-Table A.20.

(Ⅱ)-Table A.1 Structural design conditions and analysis method〔Requirements of package (No.1)〕

Item	Design condition						Analysis method		Remarks
	Reference figure	Material	Temperature	Design load			Applied formula or element	Criteria	
				Kinds	Loading factor	Element			
Chemical and galvanic Reaction									
Chemical reaction	(Ⅱ)-Table A.4	Stainless steel		Corrosion	–	Activation		nil	
Galvanic reaction		Aluminum [redacted]		〃	–	Difference of electric potential		〃	
Low-temperature strength									
Body, lid	(Ⅱ)-Fig A.8	SA-182 [redacted] [redacted]	−40 ℃	Material	1	Low temperature brittleness	Minimum of normal service temperature in use	−40 ℃	
Basket	〃	SA-240 [redacted] [redacted]							
Fuel element	(Ⅱ)-Fig A.9	Aluminum alloy	−40 ℃	Material	1	Low temperature brittleness	Minimum of normal service temperature in use	−40 ℃	
Packing	(Ⅱ)-Table A.5	[redacted]	−40 ℃	Material	1	Low temperature brittleness	Minimum of normal service temperature in use	−40 ℃	
Lid bolt	(Ⅱ)-Fig A.10	SA-564 [redacted]	−40 ℃	Drop energy	1	Toughness	$K = \sigma \cdot \left[\frac{D}{d}\right]^2 \cdot \sqrt{\pi \cdot D}\ F(d/D)$ $K_{id} = 15.87C_v^{0.375}$	−40 ℃ $K < K_{id}$	K :Fracture toughness K_{id}: Dynamic fracture toughness σ : Stress D : Diameter of bolt d : Minor diameter of bolt F(d/D):Coefficient due to D and d Cv : Charpy impact value

(Ⅱ)-Table A.1 Structural design conditions and analysis method〔Requirements of package (№2)〕

Item	Design condition						Analysis method		Remarks
	Reference figure	Material	Temperature	Design load			Applied formula or element	Criteria	
				Kinds	Loading factor	Element			
Gap between shell and basket	(Ⅱ)-Fig A.11 (Ⅱ)-Fig A.12 (Ⅱ)-Fig A.13	SA-182 [redacted]	−40 ℃	Temperature gradient	1	Thermal expansion	$\triangle r = 1.0 - \mu_{r=a} - \triangle r_b$ $\mu_{r=a} = \frac{2a\alpha \cdot H}{b^2 - a^2}$ $\triangle r_b = \alpha \sum_{i=1\sim n} (T_i - 20)\ \ell_i$	$\triangle r > 0$	$\triangle r$: Gap 1.0 : Initial gap 1.0mm at room temperature $\mu_{r=a}$: Expansion value at r=a of shell in radial direction a : Inner radius of shell b : Outer radius of shell α : Coefficient of linear thermal expansion of shell H : Coefficient due to temperature differences between internal & external surface and inner & outer radius of shell $\triangle r_b$: Expansion value of basket in radial direction α : Coefficient of linear thermal expansion of i-th element of basket Ti : Average temperature of i-th element of basket ℓ_i : Length of i-th element of basket in radial direction
Containment system									
Lid	(Ⅰ)-Fig. A.1	SA-182 [redacted]		Opening by false operation		Advisability of false operation	Presence of lock	yes	
Drain valve and vent valve		SA-240 [redacted]		〃		〃	Presence of protection cover lock	yes	
Lifting lug									
Body lifting lug	(Ⅰ)-Fig. C.12	SA-240 [redacted]							
1) Normal lifting of the package									
Weld zone	(Ⅱ)-Fig. A.14	〃	[redacted] ℃	Weight of package	3	Shear	$\tau = \frac{T_v}{\text{Bead cross-sectional area}}$	$0.6\sigma_y\eta$	τ : Stress T_v : Vertical load

Notes) σ_y : Yield stress of material, η : Weld efficiency (＝0.7)

(Ⅱ)-Table A.1　Structural design conditions and analysis method〔Requirements of package　(No.3)〕

Item	Design condition						Analysis method		Remarks
	Reference figure	Material	Temperature	Design load			Applied formula or element	Criteria	
				Kinds	Loading factor	Element			
Weld zone	(Ⅱ)-Fig. A.14	SA-240 [redacted]	[redacted] ℃	Weight of package	3	Tension	$\sigma_b = \frac{M \cdot y}{I}$	$\sigma_y \eta$	σ_b : Stress M : Bending moment y : Distance from neutral axis I : Moment of inertia of area
Hole	(Ⅱ)-Fig. A.15	〃	〃	〃	3	Shear	$\tau = \frac{W}{A}$	$0.6\sigma_y$	τ : Stress W : Lifting load A : Shearing area of top portion of hole
2) When one body lifting lug is used by mistake for lifting the package	(Ⅱ)-Fig. A.16								
Weld zone	(Ⅱ)-Fig. A.17	SA-240 [redacted]	[redacted] ℃	Weight of package	1	Shear	$\tau = \frac{T_v}{\text{Cross-sectional area of bead weld}}$	$0.6\sigma_u \eta$	τ : Stress T_v : Parallel load to the weld surface
Weld zone	〃	〃	〃	〃	1	Tension	$\sigma_t = \sigma_d + \sigma_b$	$\sigma_u \eta$	σ_t : Max. tensile stress σ_d : Tensile stress due to vertical load on weld surface σ_b : Tensile stress due to bending moment
Hole	(Ⅱ)-Fig. A.18	〃	〃	〃	1	Shear	$\tau = \frac{W}{A}$	$0.6\sigma_u$	τ : Stress W : Lifting load A : Shearing area of top portion of hole
3) Fatigue strength		〃	〃	〃	3	Fatigue	Design fatigue curve	N	N : Number of allowable cycles

Notes)　σ_y : Yield stress of material,　η : Weld efficiency (= 0.7),　σ_u : Tensile strength of material

(II)-Table A.1 Structural design conditions and analysis method〔Requirements of package (No.4)〕

Item	Design condition						Analysis method		Remarks
	Reference figure	Material	Temperature	Design load			Applied formula or element	Criteria	
				Kinds	Loading factor	Element			
Lid Lifting lug									
1) When two lid lifting lugs are used by mistake for lifting the package	(II)-Fig. A.19								
Weld Zone	(II)-Fig. A.20	SA-240 [redacted]	[redacted] ℃	Weight of package	1	Shear	$\tau = \frac{T_H}{\text{Cross-sectional area of weld bead}}$	$0.6\sigma_y\eta$	τ : Stress T_H : Parallel load to the weld surface
Weld Zone	〃	〃	〃	〃	1	Tension	$\sigma_t = \sigma_d + \sigma_b$	$\sigma_y\eta$	σ_t : Max. tensile stress σ_d : Tensile stress due to vertical load on weld surface σ_b : Tensile stress due to bending moment
Hole	(II)-Fig. A.21	〃	〃	〃	1	Shear	$\tau = \frac{T}{A}$	$0.6\sigma_y$	τ : Stress T : Tensile force of Lifting lug due to lifting load A : Shearing area of portion of hole
Lid bolt	(II)-Fig. A.23	SA-564 [redacted]	[redacted] ℃	Fastening force	1	Tension	$\sigma = \frac{W}{A}$	σ_y	σ : Stress W : Fastening force of bolt A : Cross-sectional area of bolt
Lid bolt	〃	〃	〃	Weight of package + Fastening force	3	Tension	σ = tension due to fastening force + tension due to lifting load	σ_y	σ : Stress

Notes) σ_y : Yield stress of material, η : Weld efficiency (= 0.7)

(Ⅱ)-Table A.1 Structural design conditions and analysis method〔Requirements of package (№5)〕

Item	Design condition						Analysis method		Remarks
	Reference figure	Material	Temperature	Design load			Applied formula or element	Criteria	
				Kinds	Loading factor	Element			
Thread of the body	(Ⅱ)-Fig. A.24	SA-182 [redacted]	[redacted] ℃	Weight of package + Fastening force	3	Shear	$\tau = \frac{W'+W}{S}$	0.6 σ_y	τ : Stress W' : Initial Fastening force of lid bolt W : Force to lid bolt due to lifting load S : Shearing area of lid bolt
2) When one lid lifting is used for lifting the lid by mistake	(Ⅱ)-Fig. A.25								
Weld Zone	(Ⅱ)-Fig. A.26	SA-240 [redacted]	[redacted] ℃	Weight of lid	1	Shear	$\tau = \frac{T}{A}$	0.6 $\sigma_u \eta$	τ : Stress T : Horizontal load due to lifting load A : Shearing area of bead weld
Weld Zone	〃	〃	〃	〃	1	Tension	$\sigma_t = \sigma_d + \sigma_b$	$\sigma_u \eta$	σ_t : Max. tensile stress σ_d : Tensile stress due to vertical load on weld surface σ_b : Tensile stress due to bending moment
Hole	〃	〃	〃	〃	1	Shear	$\tau = \frac{W_1}{A}$	0.6 σ_u	τ : Stress W : Lifting load A : Shearing area of top portion of hole
3) Fatigue strength		〃	〃	〃	1	Fatigue	Design fatigue curve	N	N : Number of allowable cycles
Tie down device	(Ⅰ)-Fig. C.3 (Ⅱ)-Fig. A.27								
Travelling direction				10 g of the mass of the package	1	Compression	Compressive force F_1		
Lateral direction				5 g of the mass of the package	1	〃	Compressive force F_2		
Vertical direction				3 g of the mass of the package	1	〃	Compressive force F_3		

Notes) σ_y : Yield stress of material, η : Weld efficiency (=0.7), σ_u : Tensile strength of material

(II)-Table A.1　Structural design conditions and analysis method〔Requirements of package (No.6)〕

Item	Design condition						Analysis method		Remarks
	Reference figure	Material	Temperature	Design load			Applied formula or element	Criteria	
				Kinds	Loading factor	Element			
Bottom fin contacted to fin bolt	(II)-Fig. A.28	SA-240 [redacted]	[redacted] ℃	Max. load F of F_1, F_2, F_3	1	Compression	$\sigma_c = \frac{F}{A}$	$1.5\sigma_y$	σ_c : Max. compressive stress F : Max. compressive load A : Area of contact between bottom fin and fin shoe
Bottom fin contacted to skid	(II)-Fig. A.29 (II)-Fig. A.30 (II)-Fig. A.31 (II)-Fig. A.32 (II)-Fig. A.33	〃	〃	〃	1	Buckling	$\sigma_c = \frac{F}{A}$ $\sigma_{cr} = K \cdot \frac{\pi^2 E}{12(1-\nu^2)} \cdot \left[\frac{t}{b}\right]^2$	σ_{cr}	σ_c : Stress F : Compressive load A : Cross-sectional area σ_{cr}: Critical buckling stress K : Buckling coefficient b : Plate width t : Plate thickness E : Modulus of Longitudinal elasticity ν : Poisson's ratio
Bottom fin contacted to skid	(II)-Fig. A.33	〃	〃	〃	1	Compression	$\sigma_c = \frac{F}{A}$	$1.5\sigma_y$	σ_c : Stress F : Compressive load A : Cross-sectional area
Pressure Packaging		SA-182 [redacted]	[redacted] ℃	Pressure	1	Combination stress	ABAQUS		
Vibration Package			[redacted] ℃	Resonance	1	Natural vibrations	$f_1 = \frac{K_1}{2\pi}\sqrt{\frac{EI}{M\ell^4}}$	Resonance zone	f_1 : Natural vibrations K_1 : Coefficient E : Modulus of longitudinal elasticity I : Moment of inertia of area ℓ : Length of packaging M : Mass per unit length

Note) σ_y : Yield stress of material

(Ⅱ)-Table A.1　Structural design conditions and analysis method〔Normal conditions of transport (№7)〕

Item	Design condition						Analysis method		Remarks
	Reference figure	Material	Temperature	Design load			Applied formula or element	Criteria	
				Kinds	Loading factor	Element			
Thermal test									
1) Thermal expansion	(Ⅱ)-Fig. A.34			Temperature gradient	1	Thermal Stress			
Body, lid (longitudinal direction)	(Ⅱ)-Fig. A.38 (Ⅱ)-Fig. A.39	SA-182 [redacted]	[redacted] ℃~[redacted] ℃	Initial fastening force + internal pressure + temperature gradient	1	Combination	ABAQUS		
Basket (longitudinal direction)									
For box type fuel	(Ⅱ)-Fig. A.35	SA-240 [redacted]	[redacted]℃~[redacted]℃	Temperature gradient	1	Thermal expansion	ABAQUS and $\triangle \ell_{b}=\dfrac{\sum_{i=1} A_i \cdot E_i \cdot (T_i-20)\,\alpha_i}{\sum_{i=1} \dfrac{A_i \cdot E_i}{\ell_o}}$	Gap	$\triangle \ell_b$: Elongation of basket A_i : Cross-sectional area of i-th element of basket E_i : Modulus of longitudinal elasticity of i-th element of basket T_i : Mean temperature of i-th element of basket α_i : Coefficient of linear thermal expansion of i-th element basket ℓ_o : Total length of each basket
For MNU type fuel	(Ⅱ)-Fig. A.36		[redacted] ℃~[redacted] ℃	〃	1	〃			
Body, lid (radial direction)	(Ⅱ)-Fig. A39	SA-182 [redacted]	[redacted] ℃~[redacted] ℃	Initial fastening force + internal pressure + temperature gradient	1	Combination	ABAQUS		

(II)-Table A.1 Structural design conditions and analysis method [Normal conditions of transport (No.8)]

Item	Design condition						Analysis method		Remarks
	Reference figure	Material	Temperature	Design load			Applied formula or element	Criteria	
				Kinds	Loading factor	Element			
Basket (radial direction)									
For box type fuel	(II)-Fig. A.35	SA-240 [redacted]	[redacted] ℃~[redacted] ℃	Temperature gradient	1	Thermal expansion	ABAQUS and $\triangle r_b = \sum_{i=1} \alpha_i (T_i - 20)\ \ell_i$	Gap	$\triangle r_b$: Expansion value of basket α_i : Coefficient of linear thermal expansion of i-th element of basket T_i : Mean temperature of i-th element of basket ℓ_i : Length in radial direction of i-th element of basket
For MNU type fuel	(II)-Fig. A.36		[redacted] ℃~[redacted] ℃	〃	1	〃			
2) Thermal stress									
Body, lid	(II)-Fig. A.37, 38	SA-182 [redacted]	[redacted] ℃ [redacted] ℃ *1	Initial fastening force + internal pressure + temperature gradient	1	Combination	ABAQUS	$3S_m$	
Basket									
For box type fuel	(II)-Fig. A.35	SA-240 [redacted]	[redacted] ℃~[redacted] ℃ [redacted] ℃ *1	Temperature gradient	1	Thermal Stress	$\sigma_i = \frac{E_i}{\ell_i} [\triangle \ell_b - (T-20) \cdot \alpha_i \cdot \ell_i]$	$3S_m$	σ_i : Stress of basket Ei : Modulus of longitudinal elasticity of i-th element of basket ℓ_i : Length of i-th element of basket ℓ_b : Elongation in axial direction α_i : Coefficient of linear thermal expansion
For MNU type fuel	(II)-Fig. A.36		[redacted] ℃~[redacted] ℃ [redacted] ℃ *1	〃	1	〃			

Notes) S_m : Design stress intensity of material *1 : Design temperature determined conservatively for allowable stress

(II)-Table A.1 Structural design conditions and analysis method〔Normal conditions of transport (No.9)〕

Item	Design condition						Analysis method		Remarks
	Reference figure	Material	Temperature	Design load			Applied formula or element	Criteria	
				Kinds	Loading factor	Element			
Containment of contact surfaces of body and lid	(II)-Fig. A.42	SA-182 [redacted]	[redacted] ℃~[redacted] ℃	Initial fastening force + internal pressure + temperature gradient	1	Thermal expansion	ABAQUS	Compressive condition	
Lid bolt	(II)-Fig. A.40	SA-564 [redacted]	[redacted] ℃	〃	1	Thermal Stress	ABAQUS	$2S_m$	
Fatigue strength of lid bolt		〃	〃	〃	1	Fatigue	Design fatigue curve	N	N : Number of allowable cycles
Water spray		SA-182 [redacted]	Normal temperature	Water spray		Brittleness by absorption Puddle Corrosion	Absorption Drainer Corrosion resistance	nil good existence	
Free drop	To be analyzed by using results of analysis of drop test I.								
Vertical									
Horizontal									
Corner									
Stacking test									
Shell of body	(II)-Fig. A.43	SA-182 [redacted]	[redacted] ℃	6 times load of tare	6	Compression	$\sigma = \frac{W_1}{A}$	σ_y	σ : Stress W_1: Load equivalent to 6 times load of tare A : Cross-sectional area of shell
Bottom fin of body	(II)-Fig. A.44	SA-240 [redacted]	[redacted] ℃	〃	6	Compression	$\sigma = \frac{W_1}{A_{min}}$	σ_y	σ : Stress W_1: Load equivalent to 6 times load of tare A_{min} : Minimum cross-sectional area

Notes) S_m : Design stress intensity of material, σ_y : Yield stress of material

(II)-Table A.1 Structural design conditions and analysis method〔Normal conditions of transport (№10)〕

Item	Design condition						Analysis method		Remarks
	Reference figure	Material	Temperature	Design load			Applied formula or element	Criteria	
				Kinds	Loading factor	Element			
Bottom plate of body, lid	(II)-Fig. A.45	SA-182 [redacted]	[redacted] ℃	6 times load of tare	6	Compression	$\sigma = \frac{6M}{t^2}$	σ_y	σ : Stress M : Bending moment due to load equivalent to 6 times load of tare t : Thickness of lid or bottom plate
Bottom plate of body, lid	(II)-Fig. A.45	〃	〃	〃	6	Shear	$\tau = \frac{3}{2} \cdot \frac{Q}{t}$	$0.6\sigma_y$	τ : Stress Q : Shearing force per unit length due to load equivalent to 6 times load of tare t : Thickness of lid or bottom plate
Contact surfaces of body and lid	(II)-Fig. A.46	〃	〃	〃	6	Compression	$\sigma = \frac{W_1}{A}$	σ_y	σ : Stress W_1: Load equivalent to 6 times load of tare A : Area of contact surface of body and lid
Penetration	To be analyzed by using results of analysis of drop test II.								

Note) σ_y : Yield stress of material

(Ⅱ)-Table A.1 Structural design conditions and analytical method〔Accident conditions of transport (№11)〕

Item	Design condition						Analysis method		Remarks
	Reference figure	Material	Temperature	Design load			Applied formula or element	Criteria	
				Kinds	Loading factor	Element			
Drop test I 1) Impact analysis									
Vertical Drop									
Top vertical drop	(Ⅱ)-Fig. A.47 ~(Ⅱ)-Fig. A.51	SA-240 [redacted]		Drop energy		Absorbed energy	LS-DYNA		
Bottom vertical drop	(Ⅱ)-Fig. A.52 ~(Ⅱ)-Fig. A.56	〃		〃		〃	〃		
Horizontal drop	(Ⅱ)-Fig. A.57 ~(Ⅱ)-Fig. A.61	〃		〃		〃	〃		
Corner drop									
Top corner drop	(Ⅱ)-Fig. A.62 ~(Ⅱ)-Fig. A.66	〃		〃		〃	〃		
Bottom corner drop	(Ⅱ)-Fig. A.67 ~(Ⅱ)-Fig. A.71	〃		〃		〃	〃		
2) Vertical drop Containment at contact surface of body and lid									
Top vertical drop Seal boundary on lid flange and body flange	(Ⅱ)-Fig. A.72 (Ⅱ)-Fig. A.73	SA-182 [redacted]	[redacted] ℃ [redacted] ℃	Drop energy	1	Compression	LS-DYNA	Elastic condition	
Lid bolt	(Ⅱ)-Fig. A.74	SA-564 [redacted]	[redacted] ℃	〃	1	Tensions	〃	σ_y	
Bottom vertical drop Seal boundary on lid flange and body flange	(Ⅱ)-Fig. A.75 (Ⅱ)-Fig. A.76	SA-182 [redacted]	[redacted] ℃ [redacted] ℃	〃	1	Compression	〃	Elastic condition	
Lid bolt	(Ⅱ)-Fig. A.77	SA-564 [redacted]	[redacted] ℃	〃	1	Tension	〃	σ_y	

Note) σ_y : Yield stress of material

(II)-Table A.1 Structural design conditions and analytical method〔Accident conditions of transport (No.12)〕

Item	Design condition						Analysis method		Remarks
	Reference figure	Material	Temperature	Design load			Applied formula or element	Criteria	
				Kinds	Loading factor	Element			
Valve main bolt	(II)-Fig. A.79	SA-564 [redacted] (equivalent to SUS [redacted])	[redacted] ℃	Drop energy	1	Shear	$\tau = \frac{W \cdot g \cdot G_v}{S}$	0.6 σ_y	τ : Stress W : Mass of vent valve G_v : Impact deceleration S : Total shearing area of bolt
Valve protection cover bolt	(II)-Fig. A.80	〃	〃	〃	1	〃	$\tau = \frac{W \cdot g \cdot G_v}{S}$	0.6 σ_y	τ : Stress W : Mass of valve protection cover G_v : Impact deceleration S : Total shearing area of bolt
Basket for box type fuel									
Compartment plate, partition plate		SA-240 [redacted]	[redacted] ℃	Drop energy	1	Compression	$\sigma_c = \frac{W_B \cdot g \cdot G_v}{A}$	1.5 σ_{dy}	σ_c: Stress W_B: Mass of basket for box type fuel G_v : Impact deceleration A : Pressure area to vertical direction
Compartment plate, partition plate		〃	〃	〃	1	Buckling	$\sigma_c = \frac{W_B \cdot g \cdot G_v}{A}$	σ_{cr}	σ_c: Stress K : Buckling coefficient E : Modulus of longitudinal elasticity ν : Poisson's ratio a : Side length of square section t : Thickness

Notes) σ_y : Yield stress of material, σ_{dy} : Dynamic yield stress of material (= 1.25 σ_y), σ_{cr} :Critical buckling stress, g : Gravitational acceleration

(Ⅱ)-Table A.1　Structural design conditions and analytical method〔Accident conditions of transport (No.13)〕

Item	Design condition						Analysis method		Remarks
	Reference figure	Material	Temperature	Design load			Applied formula or element	Criteria	
				Kinds	Loading factor	Element			
for MNU type fuel Guide plate	(Ⅱ)-Fig. A.82	SA-240 [redacted]	[redacted] ℃	Drop energy	1	Compression	$\sigma_c = \frac{W_B \cdot g \cdot G_v}{A}$	$1.5\sigma_{dy}$	σ_c: Stress W_B: Mass of basket for MNU type fuel G_v : Impact deceleration A : Pressure area to vertical direction
Weld zone between square shape pipe and guide plate	(Ⅱ)-Fig. A.82	SA-240 [redacted]	[redacted] ℃	Drop energy	1	Shear	$\tau = \frac{W_B \cdot g \cdot G_v}{\ell \cdot d}$	$0.6\sigma_u \cdot \eta$	τ : Stress W_B: Mass of square shape pipe G_v : Impact deceleration ℓ : Weld length d : Throat of weld zone

Notes) σ_y : Yield stress of material, σ_{dy} : Dynamic yield stress of material (= $1.25\sigma_y$), η : Weld efficiency (= 0.7), σ_u : Tensile strength of material, F_r : Roll-swage force (tensile fracture load)
g : Gravitational acceleration

(II)-Table A.1 Structural design conditions and analytical method [Accident conditions of transport (No.14)]

Item	Design condition						Analysis method		Remarks
	Reference figure	Material	Temperature	Design load			Applied formula or element	Criteria	
				Kinds	Loading factor	Element			
JRR-3 standard silicide type fuel Fuel side plate	(I)-Fig. D.1	A[redacted] or [redacted]	[redacted] ℃	Drop energy	1	Compression	$\sigma_c = \frac{W \cdot g \cdot G_v}{A}$	$1.5\sigma_y$	σ_c: Stress W : Mass of element G_v : Impact deceleration A : Pressure area of fuel side plate to vertical direction
Fuel plate	〃	〃	〃	〃	1	Falling	$F = W \cdot g \cdot G_v$	F_r	F : Inertia force W : Mass of a piece of fuel plate G_v : Impact deceleration
JRR-3 follower silicide type fuel Fuel side plate	(I)-Fig. D.2	A[redacted] or A[redacted]	[redacted] ℃	Drop energy	1	Compression	$\sigma_c = \frac{W \cdot g \cdot G_v}{A}$	$1.5\sigma_y$	σ_c: Stress W : Mass of element G_v : Impact deceleration A : Pressure area of fuel side plate to vertical direction
Fuel plate	〃	〃	〃	〃	1	Falling	$F = W \cdot g \cdot G_v$	F_r	F : Inertia force W : Mass of a piece of fuel plate G_v : Impact deceleration

Notes) σ_y : Yield stress of material , F_r : Roll-swage force (tensile fracture load) , g : Gravitational acceleration

(II)-Table A.1 Structural design conditions and analytical method〔Accident conditions of transport (№.15)〕

Item	Design condition						Analysis method		Remarks
	Reference figure	Material	Temperature	Design load			Applied formula or element	Criteria	
				Kinds	Loading factor	Element			
JRR-3 MNU type fuel	(Ⅰ)-Fig. D.3 (Ⅰ)-Fig. D.4 (Ⅱ)-Fig. A.83								
(A-direction drop)									
Aluminum cladding	(Ⅱ)-Fig. A.84 (Ⅱ)-Fig. A.85	A[redacted]	[redacted] ℃	Drop energy	1	Compression	ABAQUS	1.5 σ_y	
Stopper		A[redacted]							
Metallic natural uranium		Metallic natural uranium							
(B-direction drop)									
Aluminum cladding	(Ⅱ)-Fig. A.86 (Ⅱ)-Fig. A.87	A[redacted]	[redacted] ℃	Drop energy	1	Compression	ABAQUS	1.5 σ_y	
Stopper		A[redacted]							
Metallic natural uranium		Metallic natural uranium							

Notes) σ_y : Yield stress of material , F_r : Roll-swage force (tensile fracture load) , g : Gravitational acceleration

(II)-Table A.1 Structural design conditions and analytical method〔Accident conditions of transport (№.16)〕

Item	Design condition						Analysis method		Remarks
	Reference figure	Material	Temperature	Design load			Applied formula or element	Criteria	
				Kinds	Loading factor	Element			
3) Horizontal drop Containment at contact surface of body and lid									
Seal boundary on lid flange and body flange	(II)-Fig. A.88 (II)-Fig. A.89	SA-182 [redacted]	[redacted] ℃ [redacted] ℃	Drop energy	1	Compression	LS-DYNA	Elastic condition	
Lid bolt	(II)-Fig. A.90	SA-564 [redacted]	[redacted] ℃	〃	1	Tension	LS-DYNA	σ_y	
Valve main bolt	(II)-Fig. A.91	SA-564 [redacted]	[redacted] ℃	Drop energy	1	Shear	$\tau = \frac{W \cdot g \cdot G_H}{S}$	$0.6\sigma_y$	τ : Stress W : Mass of vent valve G_H: Impact deceleration S : Total shearing area of bolt

Notes) σ_y : Yield stress of material , F_r : Roll-swage force (tensile fracture load) , g : Gravitational acceleration

(Ⅱ)-Table A.1 Structural design conditions and analytical method〔Accident conditions of transport (No.17)〕

Item	Design condition						Analysis method		Remarks
	Reference figure	Material	Temperature	Design load			Applied formula or element	Criteria	
				Kinds	Loading factor	Element			
Valve protection cover bolt	(Ⅱ)-Fig. A.92	SA-564 [redacted]	[redacted] ℃	Drop energy	1	Shear	$\tau = \frac{W \cdot g \cdot G_H}{S}$	$0.6\sigma_y$	τ : Stress W : Mass of valve protection cover G_H: Impact deceleration S : Total shearing area of bolt
Basket									
for box type fuel	(Ⅱ)-Fig. A.93								
X-direction drop Compartment plate, partition plate	(Ⅱ)-Fig. A.94 ~(Ⅱ)-Fig. A.97	SA-240 [redacted]	[redacted] ℃	Drop energy	1	Bending	ABAQUS	ε_u	
Y-direction drop Compartment plate, partition plate	(Ⅱ)-Fig. A.98 (Ⅱ)-Fig. A.99	〃	〃	〃	1	Bending	ABAQUS	$1.5\sigma_{dy}$	
Weld zone between compartment plate and partition plate	(Ⅱ)-Fig. A.100	〃	〃	〃	1	Shear	$\tau = \frac{(W_1 + W_2) \cdot g \cdot G_H}{A}$	$0.6\sigma_{dy}\eta$	τ : Stress W_1: Mass of one fuel element W_2: Mass of one partition plate G_H: Impact deceleration A : Shearing area weld zone of partition plate
Weld zone of frame	(Ⅱ)-Fig. A.101	SA-182 [redacted]	[redacted] ℃	〃	1	Bending	$\sigma_{bmax} = \frac{9 \cdot f \cdot R^2}{t^2}$	$1.5\sigma_{dy}\eta$	σ_{bmax}: Stress f : Uniform load R : Radius t : Thickness
for MNU type fuel	(Ⅱ)-Fig. A.103								
Square shape pipe	(Ⅱ)-Fig. A.102	SA-240 [redacted]	[redacted] ℃	Drop energy	1	Bending	$\sigma_{max} = \frac{M_{max}}{I} \cdot \frac{h_2}{2}$	$1.5\sigma_{dy}$	σ_{max}: Stress M_{max}: Bending moment I : Moment of inertia of area h_2: Height of square shape pipe

Notes) σ_y : Yield stress of material, σ_{dy} : Dynamic yield stress of material ($= 1.25\sigma_y$), ε_u: Rupture strain of material, η : Weld efficiency ($= 0.7$), g : Gravitational acceleration

(Ⅱ)-Table A.1 Structural design conditions and analytical method〔Accident conditions of transport (№.18)〕

Item	Design condition						Analysis method		Remarks
	Reference figure	Material	Temperature	Design load			Applied formula or element	Criteria	
				Kinds	Loading factor	Element			
Square shape pipe	(Ⅱ)-Fig. A.102	SA-240 [redacted]	[redacted] ℃	Drop energy	1	Shear	$\tau = \frac{F}{A}$	0.6 σ_{dy}	τ : Stress F : Force of edge A : Shearing area
Support plate	(Ⅱ)-Fig. A.104 (Ⅱ)-Fig. A.105	SA-240 [redacted]	[redacted] ℃	Drop energy	1	Compression	$\sigma_c = \frac{W \cdot g \cdot G_H}{A}$	1.5 σ_{dy}	σ_c: Stress W : Mass of fuel element and basket G_H: Impact deceleration A : Cross-sectional area of fuel side plate
JRR-3 standard silicide type fuel	(Ⅱ)-Fig. A.106	〃	〃	〃	1	Compression	$\sigma_c = \frac{W \cdot g \cdot G_H}{A}$	1.5 σ_y	σ_c: Stress W : Mass of fuel element G_H: Impact deceleration A : Cross-sectional area of fuel side plate
JRR-3 follower silicide type fuel	(Ⅱ)-Fig. A.107	〃	〃	〃	1	Compression	$\sigma_c = \frac{W \cdot g \cdot G_H}{A}$	1.5 σ_y	σ_c: Stress W : Mass of fuel element G_H: Impact deceleration A : Cross-sectional area of fuel side plate

Notes) σ_y : Yield stress of material , σ_{dy} : Dynamic yield stress of material (= 1.25 σ_y) , g : Gravitational acceleration

(II)-Table A.1 Structural design conditions and analytical method [Accident conditions of transport (No.19)]

Item	Design condition						Analysis method		Remarks
	Reference figure	Material	Temperature	Design load			Applied formula or element	Criteria	
				Kinds	Loading factor	Element			
JRR-3 MNU type fuel									
Aluminum cladding	(II)-Fig. A.108	A[redacted]	[redacted] ℃	Drop energy	1	Compression	ABAQUS	$1.5\sigma_y$	
Metallic natural uranium	(II)-Fig. A.109	Metallic natural uranium	〃	〃	1	〃	ABAQUS	$1.5\sigma_y$	
4) Corner drop Containment at contact surface of body and lid									
Seal boundary on lid flange and body flange	(II)-Fig. A.110 (II)-Fig. A.111	SA-182 [redacted]	[redacted] ℃ [redacted] ℃	Drop energy	1	Compression	LS-DYNA	Elastic condition	
Lid bolt	(II)-Fig. A.112	SA-564 [redacted]	[redacted] ℃	〃	1	Compression	LS-DYNA	σ_y	
5) Oblique drop		To be analyzed by using results of analysis results of corner drop.							

Note) σ_y : Yield stress of material, g : Gravitational acceleration

(II)-Table A.1 Structural design conditions and analytical method〔Accident conditions of transport (No.20)〕

Item	Design condition						Analysis method		Remarks
	Reference figure	Material	Temperature	Design load			Applied formula or element	Criteria	
				Kinds	Loading factor	Element			
Drop test II									
Shell of body	(II)-Fig. A.113 (II)-Fig. A.114	SA-182 [redacted]	[redacted] ℃	Drop energy	1	Bending	$\sigma_{max} = \dfrac{\frac{1}{4} L \cdot W \cdot g \cdot \alpha_{max}}{Z}$	1.5 σ_y	σ_{max}: Stress W : Mass of body L : Length of body α_{max}: Impact deceleration Z : Section modules of shell
Bottom plate of body, lid	(II)-Fig. A.115	〃	〃	〃	1	Bending	$\sigma_{max} = \dfrac{6M_{max}}{t^2}$	1.5 σ_y	σ_{max}: Stress M_{max}: Bending moment t : Thickness
Valve protection cover									
A-cross section	(II)-Fig. A.116	SA-182 [redacted]	[redacted] ℃	〃	1	Shear	$\left.\begin{matrix} \\ \\ \end{matrix}\right\} \tau_A = \dfrac{\pi/4 \cdot D_2^2 \cdot q}{\pi \cdot D_1 \cdot t}$	0.6 σ_u	τ_A: Searing stress D_1 : Diameter of shearing portion q : Crushing stress
B-cross section	〃	〃	〃	〃	1	Shear		0.6 σ_u	D_2 : Diameter of mild steel t : Thickness
Valve protection cover	(II)-Fig. A.117	〃	〃	〃	1	Deflection	$y_{max} = \dfrac{-a^2 \cdot W}{16 \pi D}$	Gap from valve	Y_{max}: Deflection value a : Radius of cover W : Collapsing stress D : Flexural rigidity of plate
Thermal test									
1) Thermal expansion	(II)-Fig. A.118			Temperature gradient	1	Thermal stress			
2) Comparison with allowable stress									
Body, lid	(II)-Fig. A.119~ (II)-Fig. A.121	SA-182 [redacted]	[redacted] ℃～[redacted] ℃	Initial fastening force + internal pressure + temperature gradient	1	Combined stress	ABAQUS	ε_u	
Packing	(II)-Fig. A.122	[redacted]	[redacted] ℃	〃	1	Elongation	〃	Restoration value	
Lid bolt	(II)-Fig. A.121	SA-564 [redacted]	(Top)[redacted]℃/[redacted]℃*1 (Btm)[redacted]℃/[redacted]℃*1	〃	1	Tension	〃	σ_u	

Notes) σ_y : Yield stress of material, σ_u : Tensile strength of material, ε_u: Rupture strain of material, g : Gravitational acceleration *1 : Design temperature determined conservatively for allowable stress

(II)-Table A.1 Structural design conditions and analytical method〔Accident conditions of transport (No.21)〕

Item	Design condition						Analysis method		Remarks
	Reference figure	Material	Temperature	Design load			Applied formula or element	Criteria	
				Kinds	Loading factor	Element			
3) Thermal expansion of shell and basket	(II)-Fig. A.123 ～(II)-Fig. A.126	SA-182 [redacted] SA-240 [redacted]	[redacted] ℃～[redacted] ℃ [redacted] ℃～[redacted] ℃	Temperature gradient	1	Thermal expansion	$\triangle r = 1.0 + \mu_{r=a} - \triangle r_b$ $\mu_{r=a} = \frac{2 \cdot a \cdot \alpha \cdot H}{b^2 - a^2}$ $\triangle r_b = \alpha \sum_{i=1} (T_i - 20)\ \ell_i$	$\triangle r > 0$	$\triangle r$: Gap 1.0 : Initial gap 1.0mm at room temperature $\mu_{r=a}$: Expansion value at r=a of shell in radial direction a : Inner radius of shell b : Outer radius of shell α_i : Coefficient of linear thermal expansion of shell H : Coefficient due to temperature differences between internal & external surface, and inner & outer radius of shell $\triangle r_b$: Expansion value of basket in radial direction T_i : Mean temperature ℓ_i : Length in radial direction
Thermal stress of basket	—	SA-240 [redacted]	[redacted] ℃～[redacted] ℃ [redacted] ℃*1	Temperature gradient	1	Thermal stress	$\sigma_{max} = \frac{E_0}{\ell_0} [\triangle \ell_b - (T - 20) \alpha_0 \cdot \ell_0]$	$3S_m$	σ_{max} : Stress E_0 : Modulus of longitudinal elasticity ℓ_0 : Length of basket $\triangle \ell_b$: Elongation in axial direction T_{max}: Max. temperature α_0: Coefficient of linear thermal expansion
Low temperature strength	—	SA-182 [redacted] SA-564 [redacted] SA-240 [redacted] Aluminum alloy [redacted]	−40 ℃	Material	1	Low temperature brittleness	Minimum of normal service temperature	−40 ℃	

Notes) ε_u: Rupture strain of material, σ_u : Tensile strength of material, S_m : Design stress intensity of material *1 : Design temperature determined conservatively for allowable stress

(Ⅱ)-Table A.1　Structural design conditions and analytical method〔Accident conditions of transport（No.22）〕

Item	Design condition						Analysis method		Remarks
	Reference figure	Material	Temperature	Design load			Applied formula or element	Criteria	
				Kinds	Loading factor	Element			
Water immersion External pressure equivalent to water depth　15 m Enhanced water immersion test External pressure equivalent to water depth　200 m									
Shell of body	(Ⅱ)-Fig. A.127	SA-182 [redacted]	[redacted]	External pressure	1	Combined stress	$S=\sigma_3-\sigma_2$	σ_y	S : Stress σ_3 : Radial stress σ_2 : Circumferential stress
Bottom plate of body, lid	(Ⅱ)-Fig. A.128	〃	〃	〃	1	Bending	$\sigma_b=\frac{6\cdot M}{t^2}$	$1.5\sigma_y$	σ_b: Stress M : Bending moment in radial direction t : Thickness
Bottom plate of body, lid	〃	〃	〃	〃	1	Shear	$\tau=\frac{3}{2}\cdot\frac{Q}{t}$	$0.6\sigma_y$	τ : Stress Q :Shearing force t : Thickness
Lid bolt	－	SA-564 [redacted]	〃	〃	1	Compression	$\sigma=P$	σ_y	σ : Stress P : External pressure
Body, lid	－	SA-182 [redacted]	[redacted] ℃	Temperature decrease	1	Thermal Stress	$\sigma=\alpha\cdot\triangle T\cdot E$	σ_u	σ : Stress α_i : Coefficient of linear thermal expansion E : Modulus of linear Longitudinal elasticity △T : Temperature difference
Containment at contact surface of body and lid	(Ⅱ)-Fig. A.129	SA-182 [redacted]	[redacted]	Initial fastening force + external pressure	1	Compression	$\sigma=\frac{F}{A}$	$1.5\sigma_y$	σ : Stress F : Compressive stress A : Pressure area

Notes）　σ_y : Yield stress of material,　　σ_{dy} : Dynamic yield stress of material ($1.25\sigma_y$),　　σ_u : Tensile strength of material

A.2 Weight and center of gravity

(II)-Table A.2 shows the weight and the total weight of the components which compose the package. In the analysis of the drop test I under the accident conditions of transport, the maximum weight of the package 23.2 × 10^3 kg is used.

(II)-Fig.A.1 shows the location of the center of gravity of the package in which the fuel elements is contained.

[redacted]

(II)-Fig.A.1 Center of gravity of the package

(II)-Table A.2 Weight of nuclear fuel package

(Unit : x 10^3 kg)

Basket	Box type	Box type (with adapter) *2	MNU type
Fuel element	JRR-3	JRR-3	JRR-3
	Standard silicide type	Follower silicide type	MNU type
(1)Body	[redacted]	[redacted]	[redacted]
(2) Lid	[redacted]	[redacted]	[redacted]
(3) Lid Bolt	[redacted]	[redacted]	[redacted]
(4) Basket	[redacted]	[redacted]	[redacted]
(5) Fuel element *3 (Per package)	[redacted]	[redacted]	[redacted]
Weight of nuclear fuel packaging (1)+(2)+(3)+(4)	[redacted]	[redacted]	[redacted]
Weight of nuclear fuel package *1 (1)+(2)+(3)+(4)+(5)	23.2		23.0
(6) Tie down device	1.9		
(7) Lifting device	0.2		
Gross lifting weight (1)+(2)+(3)+(4)+(5)+(6)	25.1	25.1	24.9
Gross weight (1)+(2)+(3)+(4)+(5)+(6)+(7)	25.3	25.3	25.1

Note) *1: The numerical value having an underline shows the weight of nuclear fuel package

*2: When follower type fuel elements are contained, the adapters made of aluminum alloy are inserted in the basket lodgments.

*3: Includes the weight of the adapters (0.13 x 10^3 kg).

A.3 Mechanical property of material

The mechanical property of the main materials which are used for this packaging is shown in (II)-Table A.3.

Also, the temperature dependency of the mechanical property of each material is shown in (II)-Fig.A.2 through (II)-Fig.A.7, respectively.

These values are based on the Japanese Industrial Standards (JIS), and U.S. Standards (the ASME Code, SECTION III), etc. Comparison made for the yield stress and tensile strength of stainless steel with the values specified in the Standards for Nuclear Power Generation Equipment: Material Standards (the 2013 supplement versions) showed that the differences are extremely small, and their influences on the existing analysis results are minor.

(II)-Table A.3 Mechanical property of material

Component		Material	Modulus of longitudinal elasticity [MPa] ($\mathrm{kg\ f/mm^2}$)	Yield stress [MPa] ($\mathrm{kg\ f/mm^2}$)	Tensile strength [MPa] ($\mathrm{kg\ f/mm^2}$)
Body, Lid*3)		SA-182 [redacted] (equivalent to [redacted] *2)	[redacted]	[redacted]	[redacted]
Lid lifting lug Body lifting lug*3)		SA-240 [redacted] (equivalent to [redacted] *2)	[redacted]	[redacted]	[redacted]
Basket	Frame*3)	SA-182 [redacted] (equivalent to [redacted] *2)	[redacted]	[redacted]	[redacted]
	Compartment plate*3), Partition plate	SA-240 [redacted] (equivalent to [redacted] *2)	[redacted]	[redacted]	[redacted]
Lid bolt*3)		SA-564 [redacted] (equivalent to [redacted] *2)	[redacted]	[redacted]	[redacted]
Fuel element*1)	Cladding	A[redacted]	[redacted]	[redacted]	[redacted]
		A[redacted]	[redacted]	[redacted]	[redacted]
	Fuel side plate・Outer cylinder	A[redacted]	[redacted]	[redacted]	[redacted]
		A[redacted]	[redacted]	[redacted]	[redacted]
JRR-3 MNU type fuel element	Cladding	A[redacted]	[redacted]	[redacted]	[redacted]
		A[redacted]	[redacted]	[redacted]	[redacted]
	Fuel	Metallic natural uranium	[redacted]	[redacted]	[redacted]

(At a normal temperature.)

*1) Fuel elements except JRR-3 metallic natural uranium type.

*2) Materials in parentheses are equivalent to JIS.

*3) Mechanical properties according to ASME Code1).

*4) Standards for Nuclear Power Generation Equipment: Material Standards (the 2013 supplement versions)

[redacted]

(II)-Fig.A.2 Temperature dependency of mechanical property of SA-182 [redacted] and SA-240 [redacted] (equivalent to SUS[redacted])

[redacted]

(II)-Fig.A.3　Temperature dependency of mechanical property of SA[redacted]1)

[redacted]

(II)-Fig.A.4 Yield stress of A[redacted]2)

[redacted]

(II)-Fig.A.5 High temperature strength of A[redacted]3)

[redacted]

(II)-Fig.A.6 Proof stress of A[redacted] and A[redacted]

[redacted]

(II)-Fig.A.7　Yield stress of metallic natural uraium4)

A.4 Standard for package

A.4.1 Chemical and electrical reactions

(II)-Table A.4 shows dissimilar materials which come in contact each other inside the packaging.

(II)-Table A.4 Dissimilar materials contacting

Contacting material	Part of structure
Stainless steel – [redacted]	Sealed part - Packing
Aluminum – Stainless steel	Fuel element - Basket
〃	Neutron poison - Basket

These contacting materials listed in the table exist independently or together in water or in the air but will not react electrically or chemically under normal and accident conditions of transport and are very stable.

A.4.2 Low-temperature strength

This paragraph shows that the integrity is maintained even if the packaging is used at the environmental temperature of -40℃. The following discussion assumes that the temperature of each component of the packaging is equal to the ambient temperature -40℃.

This assumption correspond to the case where no heat is generated at all from the contained fuel element, but actually, heat will be generated from the fuel elements so that the temperature of each component of the package will naturally be higher than -40℃. Therefore, the above assumption can be said as being on the safe side.

1) As shown in (II)-Fig. A.8, [redacted] and [redacted] (both material are equivalent to SUS[redacted] [redacted]which is the material used for the packaging and the basket is capable of withstanding the use at the temperature of up to -190℃ and there is no problem concerning the failure due to low-temperature brittleness.

2) As shown in (II)-Fig.A.8 and described later in (II)-A.4.2-5), the stainless steel [redacted] (equivalent to SUS [redacted]) which is the material used for the lid bolt also has sufficient toughness at -40℃ or above and is capable of withstanding the use at low temperature.

3) Aluminum alloy which is the material of the fuel elements is different from the steel materials used at low temperature and does not show the brittle behaviour at low-temperature.

   Therefore, the covering material can withstand the use at low temperature. For reference, (II)-Fig.A.9 indicates the mechanical property at low temperature of the aluminum alloy A[redacted] which is the cladding of the JRR-3 MNU type fuel element.

4) As shown in (II)-Table A.5, the lowest standard working temperature of [redacted] O-ring used in the packing of the containment system (for the contact surface of the body, the lid and the valve) is [redacted]. Therefore, the containment of the packaging can be maintained at -40℃.

   In addition, since the package is dry, the cooling water does not exist inside. Therefore, there is no possibility of the packaging being damaged due to freezing.

   Now, the decay heat of the fuel element will be considered. In this case, for the thermal stress generated on the body, even if the temperature of the external surface of the body is equal to ambient temperature -40℃, there is no problem because the integrity can be maintained under accident conditions of transport (such as fire accident) where the maximum temperature gradient occurs between internal and external surfaces of the body. Regarding the thermal expansion, the body of the packaging contracts, but it will not restrict the basket as shown in later (II)-A.4.2-6).

   As the above, the package will have no problem in low temperature brittleness, containment, thermal stress even at ambient temperature -40℃.

[redacted]

(II)-Fig.A.8 Low temperature impact value of metallic materials [8,9]

[redacted]

(II)-Fig.A.9 Mechanical property of Aluminum alloy [redacted] due to temperature

(II)-Table A.5 Standard usage for respective material of packings [10)]

[redacted]

* By " New usage of O-ring", edited by JAPAN VALQU CO.

5) Strength of the lid bolt at ambient temperature of -40℃

The tensile strength, yield stress, etc. of metal material tend to normally increase as the temperature decreases, however, the elongation, etc. are liable to decrease.11)

This paragraph indicates that the lid bolt provides the rigidity, resistible from the view point of strength even if the maximum stress is generated in the lid bolt under the temperature condition of -40℃.

This evaluation is made by comparing the fracture toughness value (K-value)12) of the lid bolt with the dynamic fracture toughness value (K_{Id} value)13) at temperature of -40℃. If K is proved to be smaller than K_{Id}, it provides the sufficient strength (toughness).

The stress generated in the lid bolt is maximized at the time of corner drop (drop test-I). The value (σ_{max}) is [redacted] MPa. (The stress is calculated based on the minor diameter [redacted] mm.)

Now, the diameter D and the minor diameter of the bolt are [redacted] mm and [redacted] mm, respectively. The stress in the section of diameter [redacted] mm converted from the above stress is calculated as follows.

[redacted] /[redacted] = [redacted] MPa

The analysis is made on the model shown in (II)-Fig.A.10, where the tensile stress (σ_{max}) of [redacted] MPa is applied.

The minor diameter of the bolt is [redacted], however, the analysis is made on [redacted] from the safety side.

The fracture toughness (K-value) of the lid bolt is found from the following formula.

$$K = \sigma \times \left[\frac{D}{d} \right]^{2} \times \sqrt{\pi D} \times F_{(d/D)}$$

[redacted]

(II)-Fig.A.10 Analytical model for fracture toughness of lid bolt

where, σ : Stress applied to the bolt

$\sigma_{\max}$ = [redacted] MPa

D : Diameter of the bolt = [redacted]

d : Minor diameter = [redacted]

$$F(d/D) : \text{Coefficient} = \frac{1}{2} \times \frac{d}{D} \times \frac{1-d/D}{4-3.2d/D} = \text{[redacted]}$$

Consequently, the following is given.

K = [redacted]

= [redacted] $\mathrm{MPa}\sqrt{\mathrm{mm}}$

On the other hand, the dynamic fracture toughness of [redacted] at the temperature of -40℃ can be given from the following formula (experimental interrelation formula).

$$K_{Id} = 15.87\ C_v{}^{0.375}$$

where, Cv : Sharpy impact value at -40 ℃ is [redacted] ft-1b, however, conservatively, [redacted] ft-1b at -100 ℃ is used for the analysis.

Accordingly, the following is given ;

K_{Id} = 15.87 × [redacted] $^{0.375}$

= [redacted] $(K_{si}\sqrt{\mathrm{in}}\ )$ = [redacted] $\mathrm{MPa}\sqrt{\mathrm{mm}}$

Then, [redacted] < [redacted] : $K < K_{Id}$ $(MPa\sqrt{mm})$

The safety factor (RF) and the safety margin (MS) can be give as follows ;

RF = [redacted] = [redacted]

MS = [redacted] − 1 = [redacted]

Therefore, the lid bolt has the sufficient fracture toughness at the ambient temperature of -40℃, and is resistible against the use under low temperature condition.

6) Thermal expansion at ambient temperature of -40℃

In finding the thermal expansion value at the shell of the packaging, the hollow cylindrical model shown in (II)-Fig. A.11 is considered.

The value of displacement (value of expansion) is calculated as follows.

where, μ_r : Displacement at arbitrary radius "r"

a : Inner radius

b : Outer radius

r : Arbitrary radius $(a \leqq r \leqq b)$

t_a : Temperature at inner radius

t_b : Temperature at outer radius

t : Temperature at radius "r"

α : Coefficient of linear thermal expansion

ν : Poisson's ratio

[redacted]

(II)-Fig.A.11 Thermal expansion analytical model for hollow cylinder

The values "t_a", "t_b", and "t" are those given by subtracting the reference temperature (temperature not to cause any expansion: 20℃).

The expansion value "μ_r" in this case can be found from the following equation ;

$$\mu_r = \frac{1+\nu}{1-\nu} \times \frac{\alpha}{r} \int_a^b t\,r\,dr + C_1 r + \frac{C_2}{r} \quad \cdots\cdots ①$$

In this case, C_1 ,C_2 and K_2 are the followings respectively ;

$$C1 = \frac{(1+\nu)(1-2\nu)}{1-\nu} \times \frac{\alpha}{b^2-a^2} \int_a^b t\,r\,dr - \nu k_2 \quad \cdots\cdots ②$$

$$C_2 = \frac{1+\nu}{1-\nu} \times \frac{\alpha a^2}{b^2-a^2} \int_a^b t\,r\,dr \quad \cdots\cdots ③$$

$$k_2 = \frac{2\alpha}{b^2-a^2} \int_a^b t\,r\,dr \quad \cdots\cdots ④$$

i) The temperature at radius "r" for axial symmetrical temperature distribution "t" under steady condition is given as follows ;

$$t = t_a + (t_b - t_a) \frac{\ell n(r/a)}{\ell n(b/a)}$$

If the term of $\int_a^b t\,r\,dr$ is "H" in this case, the following is given as follows;

$$H = \int_a^b t\,r\,dr = \int_a^b [t_a + (t_b - t_a) \frac{\ell n(r/a)}{\ell n(b/a)}] r\,dr$$

$$= \frac{t_a}{2} (b_2 - a_2) + \frac{(t_b - t_a)}{\ell n(b/a)} (\frac{b^2}{2} \ell nb - \frac{b^2}{2} \ell na - \frac{b^2}{4} + \frac{a^2}{4})$$

If the displacement "$\mu_{r=a}$" is inner radius (r = a) is substituted for (r = a) in equation ①, ② and ③ will be given as follows ;

$$\mu_{r=a} = C_1 a + \frac{C_2}{a} \quad \cdots\cdots ⑤$$

$$C_1 = \frac{(1+\nu)(1-2\nu)}{1-\nu} \cdot \frac{\alpha}{b^2-a^2} \cdot H - \nu \cdot \frac{2\alpha}{b^2-a^2} \cdot H \quad \cdots\cdots ⑥$$

$$C_2 = \frac{1+\nu}{1-\nu} \times \frac{\alpha\ a^2}{b^2-a^2} \cdot H \cdots\cdots⑦$$

If the equations ⑥ and ⑦ are substituted for equation ⑤, "$\mu_{r=a}$" is given as follows ;

$$\mu_{r=a} = \frac{2a\alpha H}{b^2-a^2} \cdots\cdots⑧$$

Since a = [redacted] and b = [redacted] in this case, H is given as follows ;

$$H = \text{[redacted]} \times \{ \frac{t_a}{2} - \text{[redacted]}\}$$

$$+ \text{[redacted]} \times (t_b - t_a) \cdots\cdots⑨$$

ii) Now, consider the case when the temperature changes linearly within the range from the inner radius (r = a) to the outer radius (r = b).

The temperature at the radius "r" is given as follows ;

$$t = t_a - \frac{(t_b - t_a)}{b-a} (r-a)$$

Arranging $\int_a^b$ t r dr in the same manner as case i), it is given as follows ;

$$H = \int_a^b t\ r\ dr = \frac{1}{6} (b-a) \{t_a(2a+b) + t_b(a+2b)\}$$

Since a = [redacted] and b = [redacted], H can be given as follows ;

$$H = \frac{1}{6} \times \text{[redacted]} (\text{[redacted]}\, t_a + \text{[redacted]}\, t_b) \cdots\cdots⑩$$

Consequently, the displacement value "$\mu_{r=a}$" is given as follows :

$$\mu_{r=a} = \frac{2a\alpha H}{b^2-a^2} = \text{[redacted]} \cdots\cdots⑪$$

a) Clearance between the shell and the basket under the ambient temperature -40℃.

The temperature distribution obtained by thermal analysis under ambient temperature of -40℃ of the nuclear fuel package is applied. The temperature distribution of the inner and the outer surface of the shell is shown in (II)-Fig A.12, and the temperature distribution of the basket is shown in (II)-Fig A.13. Here, for the basket, in order to conduct a more conservative evaluation than in the case of the contents, it shows the temperature distribution of the basket for box type fuel containing a fuel element assumed to have the largest expansion amount under normal conditions (hereinafter referred to as fuel element A).

Therefore, the evaluation for the relation between the displacement (expansion) of the basket and the displacement (shrink) of the shell is made as follows.

i) Displacement (shrink) at inner radius (r = [redacted] mm) of the body

The minimum temperature at the outer and inner surface of the shell is as follows from (II)-Fig.A.12 :

at outer surface [redacted]℃
at inner surface ℃

Therefore,

t_a = [redacted] = [redacted] (℃)
t_b = [redacted] = [redacted] (℃)
α = [redacted] (1/℃)

The above value is substituted in equation ⑩,⑪. H and $\mu_{r=a}$ will be given as follows.

$H = \frac{1}{6} \times$ [redacted] [[redacted] × ([redacted]) + [redacted] × ([redacted])] = [redacted]

$\mu_{r=a}$ = [redacted] = [redacted] mm

Therefore, the inner surface of the shell shrinks [redacted] mm in the radial direction.

ⅱ) Thermal expansion value of the basket

In this case, the expansion value "$\triangle r_b$" in the radial direction due to thermal expansion is obtained by adding the expansion value of each element to the radial direction, locating on line passing through the center of the basket in (II)-Fig.A.13.

The radial expansion value "$\triangle r_b$" is found by using the following equation ;

$$\triangle rb = \alpha \sum_{i=1\sim n} (T_i - 20) \ell_i$$

where, T_i : Mean temperature of i-th element

α :Coefficient of linear thermal expansion at the maximum temperature of the basket [redacted]℃.

= [redacted]

ℓ_i : Length in radial direction of i-th element

Therefore, the radial expansion value "$\triangle r_b$" can be given as follows ;

$\triangle r_b$ = [redacted] = [redacted]

As a result of above calculation, the expansion value in radial direction $\triangle r_b$ is [redacted] mm.

ⅲ) Clearance in the radial direction $\triangle r$ between the shell and the basket

Accordingly, the clearance "$\triangle r$" between the body and the basket is given as follows ;

$\triangle r$ = 1－[redacted]－[redacted] = [redacted] (mm)

Therefore, a clearance between the body and the basket at the ambient temperature of -40 ℃ is [redacted] mm. And even when considering the expected ambient temperature change during transportation (from -40℃ to 38℃), since there will be no change in the temperature range for the same material, there is no difference in the expansion amount of the transport container body nor that of the fuel basket, and no change in the amount of gap either. No stress due to constraint will occur in each basket.

[redacted]

(II)-Fig.A.12　Temperature distribution of the inner and outer surface of the shell under ambient temperature -40℃

[redacted]

(II)-Fig.A.13 Temperature distribution in the basket for box type fuel under ambient temperature -40°C

A.4.3 Containment system

As the sealing boundary of the packaging, there are [the contact surface of the body and the lid] and [the drain valve and the vent valve which is provided with the body and the lid, respectively].

The contact surfaces of the body and the lid are sealed by tightening the lid installed with [redacted] O-rings using [redacted] lid bolts.

[redacted]. [redacted].

The drain valve and the vent valve are closed by the blind plug provided with O-rings, and are closed additionally by the protection covers equipped with O-rings.. The protection covers are provided for the protection of the valves against the drop accident of the packaging.

[redacted], the protection cover bolts cannot be [redacted].

A.4.4 Lifting device

1. General description

The lifting device of the packaging is consisted of body lifting lugs and lid lifting lugs. Therefore, the strength of the following cases is evaluated in this paragraph.

(1) The body lifting lug

1) The case where two lifting lugs are used to lift the packaging normally.

2) The case where one lifting lug is used by mistake for lifting the package.

(2) The lid lifting lug

1) The case where two lifting lugs are used to lift the lid normally.

2) The case where one lifting lug is used by mistake for lifting the lid.

3) The case where two lifting lugs are used by mistake for lifting the package.

If two lid lifting lugs are used by mistake for lifting the package, the stress applied to the lid bolts is evaluated.

The value of the weight of the package shown in (II)-Table A.2 is used as the force applied to this evaluation.

2. Strength of the lifting device

(II)-Table A.6 shows the load conditions, allowable stress and safety factor of the body lifting lug and the lid lifting lug. The weight of the package used for the analysis discussed in this paragraph is calculated by using the values on the safe side shown in (II)-Table A.2.

(II)-Table A.6 Loading condition, allowable stress and safety factor of lifting lug

	Loading condition		Allowable stress *5 [MPa]	Safety factor *6 [Design desired value]
	No. of points to lift up (pt.)	Lifting weight kN ($\times 10^3$ kgf)		
Body lifting lug	2	*2 3W=745(75.9)	σ_y = [redacted]	above[redacted]
	1	*2 W =249(25.3)	σ_u = [redacted]	above [redacted] *1
Lid lifting lug	2	*4 $3W_1$ = [redacted]	σ_y = [redacted]	above [redacted]
	2	*3 W' =228(23.2)	σ_y = σ_y = [redacted] (Lid bolt)	above [redacted]
	1	*4 W_1 = [redacted]	σ_u = [redacted]	above [redacted] *1

*1 The safety factor, 5 ~ 6, is based on the Labor Safety Law.

*2 W : Body + lid + lid bolt + basket + fuel element + tie down device
= 249 kN (25.3 $\times 10^3$ kgf)

*3 W': Body + lid + lid bolt + basket + fuel element
= 228 kN (23.2 $\times$ 10^3 kgf)

*4 W_1: Weight of the lid = [redacted]

*5 Allowable stress
Lifting lug: σ_y and σ_u are the yield stress and the tensile strength at the temperature of [redacted]°C, respectively.
Lid bolt: σ_y is the yield stress at [redacted]°C.

*6 The safety factor is considered depending on the combination of the lifting weight and the allowable stress.

2.1 Strength of the body lifting lug

2.1.1 Strength of the lifting lug when two lifting lugs are used for lifting the package normally.

As shown in (I)-Fig. A.1 and (I)-Fig. C.12, two lifting lugs are welded to the shell of the body. The vertical load applied to one lifting lug is 1/2 of the load (7.45×10^5 N shown in (II)-Table A.6), which is 3.73×10^5 N. Therefore, the stress, which is generated in components when this load of 3.73×10^5 N is applied to one lifting lug, is analyzed.

1) Force applied to the lifting lug

From (II)-Table A.6, the load is 7.45×10^5 N. As shown in (II)-Fig.A.14, the vertical load T_v on one lifting lug is 3.73×10^5 N.

[redacted]

(II)-Fig.A.14 Details of the body lifting lug for 2-point lifting

2) Stress calculation of the weld zone

The shearing stress τ due to the vertical load, which generated on the weld zone of the lifting lug, $T_v = 3.73 \times 10^5$ N, is as follows ;

$$\tau = \frac{T_v}{\text{Cross-sectional area of bead weld}}$$

where,

T_v : Vertical load = 3.73×10^5N

Cross-sectional area of the bead weld = $260 \times 30 \times 2 = 1.56 \times 10^4$ mm^2

Therefore,

$$\tau = \frac{3.73 \times 10^5}{1.56 \times 10^4} = 24.0 \text{ MPa}$$

The allowable shearing stress τ a of the weld zone of the lifting lug is ;

$\tau_a = 0.6 \times \sigma_y \times \eta = 0.6 \times$ [redacted] $\times 0.70 =$ [redacted] MPa

Therefore, the safety factor (RF) and the safety margin (MS) are as follows ;

RF = [redacted] = [redacted]

MS = [redacted] - 1 = [redacted]

Therefore, the strength of the weld zone of the body lifting lug can withstand the shearing stress sufficiently.

Also, the bending moment due to the vertical load 3.73×10^5N arises on the weld zone. The maximum tensile stress σ_b due to this moment is generated on point "A" shown in (II)-Fig.A.14.

$$\sigma_b = \frac{M \cdot y}{I}$$

where,

M : Bending moment

y : Distance from the neutral axis

I : Moment of inertia of area on the bead weld

The moment of inertia of area to the weld center of the bead weld, I, is as follows ;

$$I = \frac{30 \times 2 \times 260^3}{12} = 8.79 \times 10^7 \text{ mm}^4$$

The bending moment M is as follows :

$M = 3.73 \times 10^5 \times 115 = 4.29 \times 10^7$ N•mm

The distance from the neutral axis y is as follows :

$y = 130$ mm

Therefore, the maximum tensile stress σ_b which arises on point "A" is as follows ;

$$\sigma_b = \frac{4.29\times10^7\times130}{8.79\times10^7} = 63.5 \text{ MPa}$$

The allowable tensile stress σ_a on the weld zone of the lifting lug is as follows ;

$\sigma_a = \sigma_y \times \eta =$ [redacted] $\times 0.70 =$ [redacted] MPa

Therefore, the safety factor (RF) and the safety margin (MS) are as follows ;

RF = [redacted] = [redacted]

MS = [redacted] - 1 = [redacted]

Therefore, the strength of the weld zone of the body lifting lug can withstand the tensile stress sufficiently.

3) Shearing strength on the top portion of the hole of the body lifting lug (refer to (II)-Fig. A.15)

The shearing stress τ on the hole is as follows ;

$$\tau = \frac{W}{A}$$

where,

W : Lifting load = 3.73×10^5N

A : Shearing area of the top portion of the hole

$= 59.5 \times 30 \times 2 \times 2 = 7.14 \times 10^3$ mm^2

Therefore,

$$\tau = \frac{3.73\times10^5}{7.14\times10^3} = 52.3\text{MPa}$$

The allowable shearing stress τ_a on the top portion of hole of the body lifting lug is ;

$$\tau_a = 0.6 \times \sigma_y = 0.6 \times \text{[redacted]} = \text{[redacted]}\ \text{MPa}$$

Therefore, the safety factor (RF) and the safety margin (MS) are as follows ;

$$RF = \text{[redacted]} = \text{[redacted]}$$

$$MS = \text{[redacted]} - 1 = \text{[redacted]}$$

Therefore, the strength of the hole of the body lifting lug can withstand the shearing stress sufficiently.

[redacted]

(II)-Fig.A.15　Details of the hole of the body lifting lug for 2-point lifting

2.1.2 Strength of the body lifting lug when one body lifting lug is used by mistake for lifting the package.

When the package is lifted by one lifting lug, the packaging is tilted at an angle of 1.335rad. (76.5°) with respect to the central axis. From (II)-Table A.6, the load on the lifting lug is 2.49×10^5 N. The stress of the body lifting lug under the above condition is analyzed. (refer to (Ⅱ)-Fig.A.16)

[redacted]

(II)-Fig.A.16 Load on the package lifted by one body lifting lug

1) Force applied to the lifting lug

The load Tv, acting parallel to the welded surface as shown in (II)-Fig. A.17, is expressed as follows ;

$$T_v = W \times \cos\phi$$

where,

W : Lifting load = 2.49×10^5 N

ϕ: Lifting angle to the center axis of the packaging = 1.335 rad.(76.5°)

Therefore,

$$T_v = 2.49 \times 10^5 \times \cos 1.335 = 5.82 \times 10^4 \text{ N}$$

Also, the load T_H, acting vertical to the welded surface, is expressed as follows ;

$$T_H = W \times \sin \phi$$

where,

W : Lifting load= 2.49×10^5 N

ϕ: Lifting angle to center axis of the packaging =1.335 rad. (76.5°)

Therefore,

$$T_H = 2.49 \times 10^5 \times \sin 1.335 = 2.43 \times 10^5 \text{ N}$$

2) Stress calculation of the weld zone

The shearing stress τ, which arises due to the load that acts parallel to the welded surface, is as follows ;

$$\tau = \frac{T_v}{\text{Cross-sectional area of the bead weld}}$$

where,

$T_v = 5.82 \times 10^4$ N

Cross-sectional area of the bead weld = $260 \times 60 = 1.56 \times 10^4$ mm^2

Therefore,

$$\tau = \frac{5.82 \times 10^4 \text{ N}}{260 \times 60} = 3.8 \text{ MPa}$$

The allowable shearing stress of the weld zone of the body lifting lug is as follows ;

$$\tau_a = 0.6 \times \sigma_u \times \eta = 0.6 \times \text{[redacted]} \times 0.70 = \text{[redacted]}\ \text{MPa}$$

Therefore, the safety factor (RF) and the safety margin (MS) are as follows ;

$$\text{RF} = \text{[redacted]} = \text{[redacted]}$$

$$\text{MS} = \text{[redacted]} - 1 = \text{[redacted]}$$

Therefore, the strength of the weld zone of the body lifting lug can sufficiently withstand the shearing stress, since the safety factor is greater than [redacted].

[redacted]

(II)-Fig.A.17 Details of the body lifting lug for one point lifting

The tensile stress σ_d, generated on the weld zone due to the load which acts vertical to the welded surface is as follows ;

$$\sigma_a = \frac{T_H}{\text{Cross-sectional area of bead weld}}$$

where,

$T_H = 2.43 \times 10^5$ N

Cross-sectional area of the bead weld$=1.56 \times 10^4$ mm^2

$$\sigma_d = \frac{2.43 \times 10^5}{1.56 \times 10^4} = 15.6 \text{ MPa}$$

Also, the bending moment is generated on the weld zone due to the load 5.82×10^4N which acts parallel to the welded surface.

Due to this bending moment, the maximum tensile stress σ_b is generated on point "A" shown in (II)-Fig. A.17.

That is as follows ;

$$\sigma_b = \frac{My}{I}$$

where,

M : Bending moment

y : Distance from the neutral axis

I : Moment of inertia of the bead weld

$M = 5.82 \times 10^4 \times 115 = 6.70 \times 10^6$ N•mm

$I = 8.79 \times 10^7$ mm^4

$y = 130$ mm

Therefore,

$$\sigma_b = \frac{6.70 \times 10^6 \times 130}{8.79 \times 10^7} = 9.91 \text{ MPa}$$

The maximum tensile stress σ_t, which is generated on the weld zone, is as follows ;

$$\sigma_t = \sigma_d + \sigma_b = 15.6 + 9.91 = 25.6 \text{ MPa}$$

The allowable tensile stress σ_a of the weld zone of the body lifting lug is ;

$\sigma_a = \eta \times \sigma_u = 0.70 \times$ [redacted] = [redacted] MPa

The safety factor (RF) and the safety margin (MS) are as follows ;

RF = [redacted] / 25.6 = [redacted]

MS = [redacted] − 1 = [redacted]

Therefore, the weld zone of the body lifting lug can withstands sufficiently the shearing stress and the tensile stress, since the safety factor is greater than 6.

3) Shearing Stress on top portion of the hole of the lifting lug (refer to (II-Fig. A.18)

The shearing stress τ, which arises on top portion of the hole of the lifting lug, is as follows ;

$$\tau = \frac{W}{A}$$

where,

W : Lifting load = 2.49×10^5N

A : Shearing area of the top portion of the hole

= $52.7 \times 30 \times 2 \times 2 = 6.33 \times 10^3$ mm^2

Therefore,

$$\tau = \frac{2.49 \times 10^5}{6.33 \times 10^3} = 39.4\text{MPa}$$

The allowable shearing stress τ_a of the lifting lug is ;

$\tau_a = 0.6 \times \sigma_u = 0.6 \times$ [redacted] = [redacted] MPa

The safety factor (RF) and the safety margin (MS) are as follows ;

RF = [redacted] = [redacted]

MS = [redacted] − 1 = [redacted]

Therefore, the hole of the body lifting lug can withstand the shearing stress, since the safety factor is greater than [redacted].

[redacted]

(II)-Fig.A.18　Details of the body lifting lug for one-point lifting

2.1.3 Fatigue strength of the body lifting lug

The cyclic stress occurs in the body lifting lug during the handling of the package. The fatigue strength of the lifting lug is evaluated in this paragraph.

The analysis is performed on the weld zone where the maximum stress occurs when the package is lifted by two body lifting lugs.

As shown in paragraph 2.1.1 2), the bending stress σ_b and the shearing stress τ of the weld zone is as follows.

$$\sigma_b = 63.5 \text{ MPa}$$

$$\tau = 24.0 \text{ MPa}$$

The amplitude S_{alt} of the repeated stress intensity including the stress concentration used for the fatigue evaluation is expressed as follows.

$$S_{alt} = \frac{1}{2} \left| \sigma_1 - \sigma_2 \right|$$

Where,

$$\sigma_1 = \frac{K\sigma_b}{2} + \sqrt{\left[\frac{K\sigma_b}{2}\right]^2 + [K\tau]^2} \quad \text{(the maximum principal stress)}$$

$$\sigma_2 = \frac{K\sigma_b}{2} - \sqrt{\left[\frac{K\sigma_b}{2}\right]^2 + [K\tau]^2} \quad \text{(the minimum principal stress)}$$

$K = 5$ (stress concentration factor)

Thus,

$$\sigma_1 = \frac{5\times 63.5}{2} + \sqrt{\left[\frac{5\times 63.5}{2}\right]^2 + [5\times 24.0]^2}$$

$$= 159 + 199 = 358 \text{ MPa}$$

$$\sigma_2 = \frac{5\times 63.5}{2} - \sqrt{\left[\frac{5\times 63.5}{2}\right]^2 + [5\times 24.0]^2}$$

$$= 159 - 199 = -40 \text{ MPa}$$

Therefore,

$$S_{alt} = \frac{1}{2} \left| 358+40 \right| = 199 \text{ MPa}$$

The following expression is used to obtain the value S'_{alt} used to calculate the allowable number of cycles based on the design fatigue curve of Fig. I-9.2.1 of the reference [1].

$$S'_{alt} = S_{alt} \frac{E'}{E}$$

Where,

E' = Modulus of longitudinal elasticity of the design fatigue curve

[redacted]MPa

E = Modulus of longitudinal elasticity of the weld zone of body lifting lug

[redacted] MPa (at [redacted]℃)

Thus,

S'_{alt} = 199 [redacted]= [redacted] MPa

In the design fatigue curve, the allowable number of cycles N corresponding to the value S'_{alt} is as follows.

$N = 7.4 \times 10^5$ times

On the other hand, assuming that the expected service life is 70 years, the frequency of use is once a year, and the number of handling times per transportation is 100 times, the repeat count of lifting (n) will be n = 7000 times. Here, to conservatively consider the repeat count of lifting, the value to be used in the calculation will be

$n = 1 \times 10^4$ times

Therefore, the safety factor (RF) and the safety margin (MS) of the fatigue strength of the body lifting lug are as follows.

$$RF = \frac{7.4 \times 10^5}{1 \times 10^4} = 74$$

$MS = 74 - 1 = 73$

Therefore, The integrity of the body lifting lug can be assured, since the allowable number of cycles of the body lifting lug N is sufficiently greater than the number of cycles during the life of the packaging n. Based on the above, as a result of the fatigue evaluation by setting the repeat count conservatively, it was confirmed that fatigue failure did not occur.

2.2 Strength of the lid lifting lug

For strength analysis of the lid lifting lug, two cases can be considered: one is the case where two lid lifting lugs are used for lifting the lid normally and the other is the case where the lid lifting lug is used by mistake for lifting the package. As shown in (II)-Table A.6, the comparison of the conditions of the load applied to the lifting lug gives $3W_1$ [*1] < W'[*2] : [redacted]kN < 228kN. Therefore, the analysis will be made based on the severe conditions of the latter (228kN). An evaluation is also made to the stress caused by the lifting load applied to the lid bolt. An analysis is also made of the strength when one lid lifting lug is used by mistake for lifting the lid.

2.2.1 Strength of the lid lifting lug when two lid lifting lugs are used by mistake for lifting the package: (refer to <u>(II)-Fig.A.19)</u>

As shown in (I)-Fig.C.1 and (I)-Fig.C.18, two lid lifting lugs are welded to the top of the lid. From the (II)-Table A.6, the load applied vertically to one lifting lug is 1/2 of 2.28×10^5 N, that is, 1.14×10^5 N. Therefore, the stress, which generates in components when this load of 1.14×10^5 N is applied to one lifting lug, is analyzed.

1) Force applied to the lifting lug

From (II)-Table A.6, the load is 2.28×10^5 N. As shown in <u>(II)-Fig. A.20</u>, the vertical load applied to one lifting lug is 1.14×10^5 N. However, since the direction of the lifting lug during lifting forms an angle of (1.05 rad.) (60°) with respect to the horizontal line, the force T is expressed as follows.

Notes : [*1] $3W_1$ denotes three times the weight of lid (68.7 kN × 3 = 206 kN).

[*2] W' denotes the weight of the package (228 kN).

[redacted]

(II)-Fig.A.19　State lifting the package

[redacted]

(II)-Fig.A.20 Details of the lid lifting lug for 2-point lifting

$$T = \frac{W}{\sin\phi}$$

where, W : Load applied to one lifting lug

$= 1.14 \times 10^5$N

ϕ: Lifting angle to the packaging center axis = 1.05 rad.(60°)

Therefore,

$$T = \frac{1.14\times10^5}{\sin1.05} = 1.32\times10^5\,\mathrm{N}$$

Also, the load T_H which acts parallel to the welded surface is expressed as follows ;

$$T_H = T \times \cos\phi = 1.32 \times 10^5 \times \cos 1.05 = 6.60 \times 10^4\mathrm{N}$$

2) Stress calculation of the weld zone

2)-1 The shearing stress τ, which is generated due to the load that acts parallel to the welded surface, is expressed as follows ;

$$\tau = \frac{T_H}{\text{Cross-sectional area of bead weld}}$$

where,

$T_H = 6.60 \times 10^4 N$

Cross-sectional area of the bead weld = $200 \times 25 \times 2 = 1.0 \times 10^4$ mm^2

Therefore,

$$\tau = \frac{6.60 \times 10^4}{1.0 \times 10^4} = 6.60 \text{ MPa}$$

The allowable shearing stress τ_a of the weld zone of the lifting lug, is expressed as follows ;

$\tau_a = 0.6 \times \sigma_y \times \eta = 0.6 \times$ [redacted] $\times 0.70 =$ [redacted] MPa

Therefore, the safety factor (RF) and the safety margin (MS) are as follows ;

RF = [redacted] = [redacted]

MS = [redacted] - 1 = [redacted]

Therefore, the strength of the weld zone of the lid lifting lug can withstand sufficiently against the shearing stress.

2)-2 The tensile stress σ_d which arises on the weld zone due to the vertical load is expressed as follows ;

$$\sigma_d = \frac{W}{\text{Cross} - \text{section area of bead weld}}$$

where,

$W = 1.14 \times 10^5 N$ (11.6×10^3 kgf)

Cross-sectional area of the bead weld = 1.0×10^4 mm^2

$$\sigma_d = \frac{1.14 \times 10^5}{1.0 \times 10^4} = 11.4 \text{ MPa}$$

Also, the bending moment due to the horizontal load 6.60×10^4N is generated on the weld zone. The maximum tensile stress σ_b due to this moment is generated on point "A" shown in (II)-Fig. A.20. That is,

$$\sigma_b = \frac{M \cdot y}{I}$$

where,

M : Bending moment

y : Distance from the neutral axis

I : Moment of inertia of area on the bead weld

The moment of inertia of area to the weld center of the bead weld, I , is as follows ;

$$I = \frac{50 \times 200^3}{12} = 3.33 \times 10^7 \text{ mm}^4$$

The bending moment M is as follows :

$M = 6.60 \times 10^4 \times 105 = 6.93 \times 10^6$ N・mm

The distance from the neutral axis y is as follows :

$y = 100$ mm

Then, the maximum tensile stress σ_b generated on "A" portion is expressed as follows ;

$$\sigma_b = \frac{6.93 \times 10^6 \times 100}{3.33 \times 10^7} = 20.9 \text{ MPa}$$

Then, the maximum tensile stress σ_t is,

$\sigma_t = \sigma_b + \sigma_d = 11.4 + 20.9 = 32.3$ MPa

where, the allowable tensile stress σ a of the weld zone of the lifting lug is expressed as follows.

$\sigma_a = \sigma_y \times \eta =$ [redacted] × 0.70= [redacted] MPa

Therefore, the safety factor (RF) and the safety margin (MS) are as follows ;

RF = [redacted] = [redacted]

MS = [redacted] - 1 = [redacted]

Therefore, the strength of the weld zone of the body lifting lug can withstand sufficiently against the tensile strength.

3) Shearing stress on the top portion of the hole of the lifting lug (refer to (II)-Fig. A.21).

The shearing stress τ, which arises on the top portion of hole of the lifting lug, is expressed as follows ;

$$\tau = \frac{T}{A}$$

where,

$T = 1.32 \times 10^5 N$

A = Shearing area of the top portion of the hole

$$= \{25 \times 30 + \frac{1}{2} \times (25 + 5) \times 20\} \times 2 \times 2$$

$$= 4.2 \times 10^3 \text{ mm}^2$$

$$\tau = \frac{1.32 \times 10^5}{4.2 \times 10^3} = 31.4 \text{ MPa}$$

[redacted]

(II)-Fig.A.21 Details of the lid lifting lug for 2-point lifting

The allowable shearing stress τ_a of the lifting lug is expressed as follows,

$\tau_a = 0.6 \times \sigma_y = 0.6 \times$ [redacted] = [redacted] MPa

Therefore, the safety factor (RF) and the safety margin (MS) are as follows ;

RF = [redacted] = [redacted]

MS = [redacted] $- 1 =$ [redacted]

Therefore, the strength of the hole of the lid lifting lug can withstand sufficiently against the shearing stress.

2.2.2 Strength of the lid bolt when two lid lifting lugs are used by mistake for lifting the package:

When the lid lifting lug is used for lifting the package, the lid bolt is subjected to the tensile load due to weight obtained by subtracting the weight of the lid from the weight of the package, the initial bolt fastening force, and the load caused by the internal pressure and the thermal stress in the packaging.

In this paragraph, the strength of the lid bolt is analyzed when the initial fastening force and the load for lifting is applied to the bolt so as to indicate that the lid bolt has sufficient strength against the load applied while the package is suspended.

The internal pressure and the thermal stress is analyzed in paragraph A.5.1.4 3.

[redacted]

(II)-Fig.A.22 Geometry of the lid bolt

1) Stress calculation of the lid bolt

Dimensions of the lid bolt are shown in (II)-Fig.A.22.

1)-1 Standards of bolt ([redacted])

Number of bolts	[redacted]pieces
Size	[redacted] mm
Length L	[redacted] mm
Effective diameter D	[redacted] mm
Pitch P	[redacted] mm
Thread angle Q	[redacted]
Coefficient of friction μ_0	0.14
Effective diameter of contact surface	[redacted] mm
Minor diameter of external thread	[redacted] mm
Diameter of bolt head	[redacted] mm
Cross-sectional area A	[redacted] mm^2
Length of thread engagement	[redacted] mm
Effective length of thread	[redacted] mm

1)-2 Mechanical property of the lid bolt and the thread of the body

The material of the bolt which is used for the lid bolt is [redacted] (according to (II)-Table A.3). The temperature of the lid bolt is below [redacted] under the normal conditions of transport. This analysis is carried out by using the values of [redacted]MPa for the yield stress at the temperature of [redacted] conservatively.

Also, in this paragraph, the strength of thread of the body is analyzed, where the yield stress of [redacted]Pa at [redacted] is used for the criteria.

1)-3 Fastening Stress

The bolt is fastened with the torque P of about [redacted] N・m.

The lead angle, α ((II)-Fig. A.23), is as follows ;

$\tan\alpha = \dfrac{P}{\pi \cdot D}$ = [redacted] = [redacted]

α = [redacted]

[redacted]

(II)-Fig.A.23 Lead angle of the bolt

Apparent coefficient of friction = [redacted] = [redacted]

= [redacted] = [redacted]

When this apparent coefficient of friction is converted into angle, the angle ϕ is as follows.

$\phi = \tan^{-1}$ [redacted] = [redacted]

Also, the torque P_1 which is necessary for overcoming the friction of the thread groove is expressed as follows.

$P_1 = W \cdot R_1 \tan$ ([redacted])

where,

W : Fastening force of the bolt

R_1: Average radius of the friction zone = [redacted] mm

Therefore,

$P_1 = W \cdot R_1 \tan$ ([redacted])

$= W \times$ [redacted] $\times$ [redacted] = [redacted] W N·mm

The tongue P_2 which is necessary for overcoming the friction of the bolt head is expressed as follows.

$$P_2 = W \cdot R_2 \cdot \mu_0$$

where,

R_2: Average radius of the contact surface = [redacted] ÷ 2 = [redacted] mm

Therefore,

$P_2 = W \times$ [redacted] $\times$ [redacted] $=$ [redacted] $W \quad N \cdot mm$

The torque P which is necessary for overcoming the friction of total fastening torque (the thread groove and the bolt head) is as follows,

$P =$ [redacted] $N \cdot mm =$ [redacted] $W +$ [redacted] $W =$ [redacted] W

The fastening force W is as follows.

$W =$ [redacted] $=$ [redacted] N

Therefore, the stress σ which acts to the bolt is,

$$\sigma = \frac{W}{A}$$

where,

A : Cross-sectional area of bolt = [redacted] mm^2

Therefore,

$\sigma =$ [redacted] $=$ [redacted] MPa

Then, the allowable tensile stress σ_a of the bolt is [redacted] MPa at [redacted] ℃.

Therefore, the safety factor (RF) and the safety margin (MS) are as follows ;

RF = [redacted] = [redacted]

MS = [redacted] − 1 = [redacted]

Therefore, the bolt can withstand sufficiently against the fastening force due to the torque P about [redacted] N·m.

1)-4 Strength of the lid bolt and the thread of the body when the lid lifting lug is used for lifting the package.

When three times the load of the total weight, [redacted]N, of the package acts on the lid bolts, the load W' per one of the bolts is expressed as follows,

W' = [redacted] = [redacted] N/piece

The tensile stress of the bolt is the stress generated due to this load, plus the initial fastening stress [redacted]MPa.

Therefore, the tensile stress σ generated on the bolt in case of lifting is as follows;

σ = [redacted] + [redacted] = [redacted] MPa

Then, the allowable tensile stress σ_a of the bolt is [redacted]MPa at [redacted]°C. Therefore, the safety factor (RF) and the safety margin (MS) are as follows ;

RF = [redacted] = [redacted]

MS = [redacted] - 1 = [redacted]

Therefore, the strength of the lid bolt can withstand sufficient against the load if the package is lifted with the lid lifting lugs.

1)-5 Next, the shearing strength is examined when 3 times the load of the total weight, 2.28×10^5N, of the package and the load due to the initial fastening force of the lid bolt act. The analytical model is shown in (II)-Fig.A.24 . Due to 3 times the load of the package, the load W′ per one of the bolts is,

W' = [redacted] N/piece

From paragraph 1)-3, the load W due to the initial fastening force of the lid bolt is,

W = [redacted]N

Also, the length of the thread engagement is [redacted] mm, and the effective diameter is [redacted] mm. The shearing area S is expressed as follows;

$S = 3.14 \times$ [redacted] $\times$ [redacted] $=$ [redacted] mm^2

Therefore, the shearing stress τ which arises on the thread of the body is as follows;

[redacted]

(II)-Fig.A.24 Analytical model of the thread groove

$\tau = \dfrac{W'+W}{S} =$ [redacted] $=$ [redacted] MPa

The allowable shearing stress τ_a of the thread of the body is expressed as follows;

$\tau_a = 0.6 \times \sigma_y = 0.6 \times$ [redacted] $=$ [redacted] MPa

Therefore, the safety factor (RF) and the safety margin (MS) are as follows ;

RF $=$ [redacted] $=$ [redacted]

MS $=$ [redacted] $- 1 =$ [redacted]

Therefore, the strength of the thread of the body can withstand sufficiently against the load if the body is lifted with the lid lifting lug.

2.2.3 Strength of the lid lifting lug when one lid lifting lug is used by mistake for lifting the lid

The lid lifting lug is shown in (I)-Fig. C.1 and (I)-Fig. C.18.

The vertical applied load is the weight of the lid, [redacted]N, based on (II)- Table A.6, when one lid lifting lug is used by mistake for lifting the lid.

Therefore, when this load [redacted]N) acts to the lifting lug, the stress is generated on each part.

For this stress, the analysis is carried out.

1) Force which acts to the lifting lug

The load is the weight of the lid, [redacted]N.

The loading condition is shown in (II)-Fig. A.25 and (II)-Fig. A.26 .

The direction at the time of lifting is tilted at an angle of 0.855 rad.(49°) to the top surface of the lid, so the force T which acts in the direction along with the top surface of the lid is expressed as follows ;

$$T = W_1 \times \cos\phi$$

where,

W_1 : Weight of the lid = [redacted]N

ϕ : Lifting angle = 0.855rad. (49°)

Therefore,

T = [redacted] × cos 0.855 = [redacted]N

Also, the load Tv which acts normal to the welded surface is ;

Tv = $W_1 \times \sin\phi$ = [redacted] × sin 0.855 = [redacted]N

[redacted]

W_1 : [redacted]N

ϕ : 0.855rad.(49°)

T : [redacted]N

T_V : [redacted]N

(II)-Fig.A.25 State of lifting the lid by one lid lifting lug

[redacted]

W_1 : [redacted] N
ϕ : 0.855rad.(49°)
T : [redacted] N
T_V : [redacted] N

(Unit : mm)

(II)-Fig.A.26　Details of the lid lifting lug for one point lifting

2) Stress calculation of the weld zone

The shearing stress τ, which is generated due to the load T, is expressed as follows.

$$\tau = \frac{T}{A}$$

where,

T : Load = [redacted] N

A : Cross-sectional area of the bead weld = $200 \times 25 \times 2$

$= 1.00 \times 10^4$ mm^2

Therefore,

$\tau =$ [redacted] $=$ [redacted] MPa

Then the allowable shear stress τ_a of the weld zone of the lifting lug is expressed as follows.

$\tau_a = 0.6 \times \sigma_u \times \eta = 0.6 \times$ [redacted] $\times 0.70 =$ [redacted] MPa

Therefore, the safety factor (RF) and the safety margin (MS) are as follows ;

RF = [redacted] = [redacted]

MS = [redacted] $- 1 =$ [redacted]

Therefore, the weld zone of the lid lifting lug can withstand sufficiently against the shearing stress, since the safety factor is greater than 6.

Also, the tensile stress σ_d, generated on the weld zone due to the normal load, is expressed as follows.

$$\sigma_d = \frac{T_v}{A}$$

where,

T_v: [redacted]N

A : 1.0×10^4 mm^2

Therefore,

$$\sigma_d = \text{[redacted]} = \text{[redacted]} \text{ MPa}$$

Also, the bending moment due to the load [redacted]N is generated on the weld zone. The maximum tensile stress σ_b due to this moment is generated on point "A" shown in (Ⅱ)-Fig.A.26.

The maximum tensile stress σ_b is expressed as follows.

$$\sigma_b = \frac{M \cdot y}{I}$$

where,

M : Bending moment = [redacted] × 105 = [redacted]N・mm

y : Distance from the neutral axis = 100 mm

I : Moment of inertial of the bead weld = 3.33×10^7 mm^4

Therefore,

$$\sigma_b = \text{[redacted]} = \text{[redacted]} \text{ MPa}$$

Therefore, the maximum tensile stress σ_t, generated on the weld zone, is expressed as follows.

$$\sigma_t = \sigma_d + \sigma_b = \text{[redacted]} = \text{[redacted]} \text{MPa}$$

Then, the allowable tensile stress σ_a of the weld zone of the lifting lug is expressed as follows.

$$\sigma_a = \sigma_u \times \eta = \text{[redacted]} \times 0.70 = \text{[redacted]} \text{ MPa}$$

Therefore, the safety factor (RF) and the safety margin (MS) are as follows ;

$$RF = \text{[redacted]} = \text{[redacted]}$$

$$MS = \text{[redacted]} - 1 = \text{[redacted]}$$

Therefore, the weld zone of the lid lifting lug can withstands sufficiently against the tensile stress, since the safety factor is greater than 6.

3) Shearing strength of the top portion of the hole of the lifting lug (Refer to (II)-Fig. A.26)

The shearing stress τ , which is generated on the top portion of the hole of the lifting lug, is as follows ;

$$\tau = \frac{W_1}{A}$$

where,

W_1: Lifting Load (weight of the lid)=[redacted]N

A : Shearing area of top portion of the hole

$$= \{25 \times 30 + \frac{1}{2} \times (25 + 5) \times 20\} \times 2 \times 2$$

$$= 4.2 \times 10^3 \text{ mm}^2$$

Therefore,

$$\tau = \text{[redacted]} = \text{[redacted]} \text{ MPa}$$

The allowable shearing stress τ_a of the lifting lug is expressed as follows ;

$$\tau_a = 0.6 \times \sigma_u = 0.6 \times \text{[redacted]} = \text{[redacted]} \text{ MPa}$$

Therefore, the safety factor (RF) and the safety margin (MS) are as follows ;

$$RF = \text{[redacted]} = \text{[redacted]}$$

$$MS = \text{[redacted]} - 1 = \text{[redacted]}$$

Therefore, the top portion of the hole of the lid lifting lug withstands the shear stress sufficiently, since the safety factor is greater than [redacted].

2.2.4 Fatigue strength of the lid lifting lug

When two lid lifting lug is used by mistake for lifting the package, the maximum stress occurs in the weld zone where the fatigue strength is severe. Therefore, the fatigue evaluation of the weld zone is performed using the above stress on the safe side.

As shown in paragraph 2.2.1 2), the bending stress σ_b and the shearing stress τ of the weld zone are as follows ;

$$\sigma_b = 32.3 \text{ MPa}$$

$$\tau = 6.6 \text{ MPa}$$

The amplitude S_{alt} of the repeated stress intensity including the stress concentration used for the fatigue evaluation is expressed as follows ;

$$S_{alt} = \frac{1}{2} \left| \sigma_1 - \sigma_2 \right|$$

Where,

$$\sigma_1 = \frac{K\sigma_b}{2} + \sqrt{\left[\frac{K\sigma_b}{2}\right]^2 + \left[K\tau\right]^2}$$

(the maximum principal stress)

$$\sigma_2 = \frac{K\sigma_b}{2} - \sqrt{\left[\frac{K\sigma_b}{2}\right]^2 + \left[K\tau\right]^2}$$

(the minimum principal stress)

$K = 5$ (stress concentration factor)

Thus,

$$\sigma_1 = \frac{5 \times 32.3}{2} + \sqrt{\left[\frac{5 \times 32.3}{2}\right]^2 + (5 \times 6.6)^2}$$

$$= 81 + 88 = 169 \text{ MPa}$$

$$\sigma_2 = \frac{5 \times 32.3}{2} - \sqrt{\left[\frac{5 \times 32.3}{2}\right]^2 + (5 \times 6.6)^2}$$

$$= 81 - 88 = -7 \text{ MPa}$$

Therefore,

$$S_{alt} = \frac{1}{2} \mid 169 + 7 \mid = 88 \text{ MPa}$$

The following expression is used to obtain the value S'_{alt} used to calculate the allowable number of cycles from the design fatigue curve of Fig. I-9.2.2 of the reference 〔1〕.

$$S'_{alt} = S_{alt} \frac{E'}{E}$$

Where,

E' = Modulus of longitudinal elasticity of the design fatigue curve

[redacted] MPa

E = Modulus of longitudinal elasticity of the weld zone of body lifting lug

[redacted] MPa (at [redacted]℃)

Thus,

[redacted]

In the design fatigue curve, the allowable number of cycles N corresponding to the value S'_{alt} is as follows.

N = [redacted] times

On the other hand, the number of cycles n of the lifting lug used during the life of the packaging is as follows.

$n = 1 \times 10^4$ times

Therefore, the safety factor (RF) and the safety margin (MS) of the fatigue strength of the lid lifting lug are as follows.

RF = [redacted] $= 1 \times 10^7$

MS = [redacted] $- 1 \fallingdotseq$ [redacted]

Therefore, the integrity of the body lifting lug can be assured, since the allowable number of cycles of the lid lifting lug N is sufficiently greater than the number of cycles during the usage of the package n.

A.4.5 Tie-down device (influence of tie-down device upon package)

1. General description

This packaging is loaded onto the vehicle or the ship by the use of tie-down device, and tied down to the tie-down device through the bottom fin. (Refer (I) -Fig.A.1. and (I)-Fig.C.3).

The evaluation of tie-down device on the package is made by analyzing the strength of bottom fin under the severest acceleration (deceleration) conditions of 10g to the travelling direction, 5g to the lateral direction and 3g to the vertical direction respectively.

The integrity of structural strength for this tie-down device has been confirmed by the Road Transport Bureau of Ministry of Land, Infrastructure and Transport in accordance with the “Application guide of the technical standard concerning transportation of radioactive material by vehicle”.

2. Force acting on the bottom fin

The packaging is tied down by tightening the bottom fin with fin bolt.

The force due to acceleration is supported by 7 bottom fins at front and rear respectively to the travelling direction, 4 bottom fins at right and left respectively to the lateral direction, and by a total of 22 bottom fins to the vertical direction.

All these loads are supported by 4 bottom fins welded to the base plate, and by the shock absorbing stand of the tie down device.

The details of the fastening parts are as shown in (II)-Fig.A-27.

[redacted]

(II)-Fig.A.27 Details of fastening parts of the tie-down device

Therefore, when the acceleration is applied, the points of the force applied on the packaging are on the parts in contact with the fin bolt (fin shoe) and skid of the packaging. The maximum force applied to one fin at such force acting points is as shown in (II)-Table A.7.

This paragraph analyzes the strength of these points of the bottom fin.

(II)-Table.A.7 The maximum force applied to one bottom fin

	Force applied when the acceleration of 10g acts to the travelling direction [N]	Force applied when the acceleration of 5g acts to the lateral direction [N]	Force applied when the acceleration of 3g acts to the vertical direction [N]
Part in contact with the fin bolt	[redacted] 1)	[redacted] 1)	2)
Part in contact with the skid	[redacted]	[redacted]	

Note-1 : The maximum value found on the assumption that acting force is cosine-distributed

Note-2 : The force applied when the acceleration acts to the vertical direction is omitted, since it is uniformly distributed and is small as compared with that when the acceleration acts to the travelling direction and the lateral direction.

3. Strength of the bottom fin in contact with the fin bolt

The force acting on the bottom fin in contact with the fin bolt is maximized when the acceleration of 5g acts to the lateral direction, of which force is given as follows from the (II)-Table A.7.

$F =$ [redacted] N

There are fin shoes arranged between the fin bolt and bottom fin to disperse the force, therefore, the force “F” generated at the fin bolt is transmitted to the bottom fin through the fin shoe.

Accordingly, the area “A” of the part where the bottom fin makes contact with the fin shoe is expressed as shown in (II)-Fig.A.28.

$A =$ [redacted] $\times$ [redacted] $=$ [redacted] mm^2

Therefore, the compressive stress “σ_c” generated at the bottom fin is as follows ;

$\sigma_c = \frac{F}{A} =$ [redacted] $=$ [redacted] MPa

In this case, the allowable compressive stress "σ_a" on the contact surface of the bottom fin is as follows;

$\sigma_a = 1.5 \times \sigma_y = 1.5 \times$ [redacted] $=$ [redacted] MPa

[redacted]

(II)-Fig.A.28 Contact area of the fin shoe

Consequently, the safety factor (RF) and the safety margin (MS) are as follows;

RF = [redacted] = [redacted]

MS = [redacted] $- 1 =$ [redacted]

As a result of above, from these points of view, the part in contact with the fin bolt of the bottom fin is fully resistible even when the acceleration of 10g to the travelling direction, 5g to the lateral direction and 3g to the vertical direction is applied.

4. Strength of the bottom fin in contact with the skid

4.1 Compressive stress due to the acceleration of 10g to the travelling direction

When the acceleration of 10g to the travelling direction is applied, the force applied on the bottom fin in contact with the skid is given from (Ⅱ)-Table A.7 as follows;

$$F_{10} = \text{[redacted]} \text{ N}$$

The cross-sectional area (A) of the bottom fin in contact with the skid and the shock absorbing stand where the acting force applied are given as follows as shown in (II)- Fig.A.29, (II)-Fig.A.30 and (II)-Fig.A.31.

$$A = S_f + S_{10} = (30 \times 130) + \{30 \times (2 \times 170 + 100)\} = 17100 \text{ mm}^2$$

where, S_f : Cross-sectional area of bottom fin

S_{10}: Cross-sectional area of shock absorbing stand

When the acceleration of 10g acts to the travelling direction, therefore, the compressive stress "σ_{c10}" generated at the bottom fin in contact with the skid is given as follows;

$$\sigma_{c10} = \frac{F_{10}}{A} = \text{[redacted]} = \text{[redacted]} \text{ MPa}$$

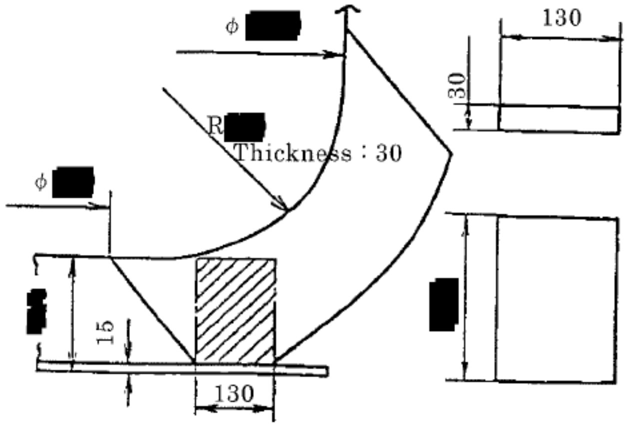

(Unit : mm)

Fig.(II)-A.29 Geometry and analytical model of the packaging supporting bottom fin

[redacted]

Fig.(II)-A.30 Shock absorbing stand of the tie-down device

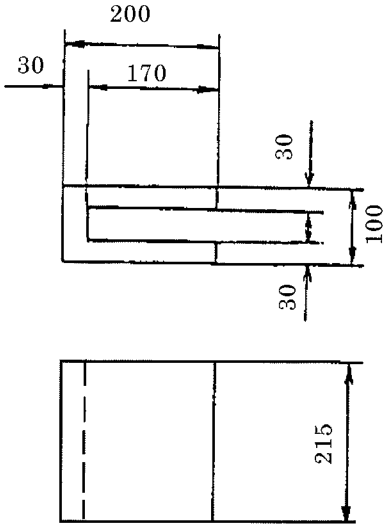

(Unit : mm)

(II)-Fig.A.31 Geometry of the shock absorbing stand to the travelling direction.

4.2 Compressive force generated when acceleration of 5g to the lateral direction is applied

When the acceleration of 5g is applied to the lateral direction, the force "F_5" applied on the bottom fin in contact with the skid is given as follows from (II)-Table A.7.

$F_5 =$ [redacted] N

The cross-sectional area (A) of the bottom fin in contact with the skid when acceleration of 5g applied to the lateral direction is given as follows as shown in (II)- Fig.A.29 and (II)-Fig.A.32.

$$A = S_f + S_5 = (30 \times 130) + (30 \times 2 \times 65) = 7800 \text{ mm}^2$$

where, S_f : Cross-sectional area of bottom fin

S_5 : Cross-sectional area of the shock absorbing stand

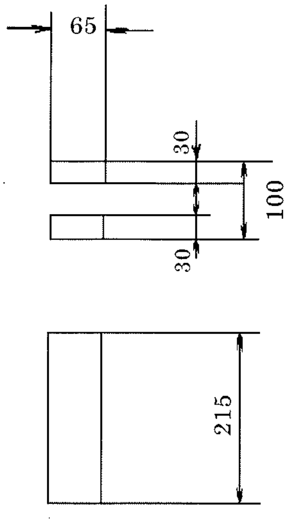

(Unit : mm)

(II)-Fig.A.32 Geometry of the shock absorbing stand to the lateral direction

When the acceleration of 5g is applied to the lateral direction, therefore, the compressive stress generated at the bottom fin in contact with the skid is given as follows ;

$\sigma_{c5} = \dfrac{F_5}{A} =$ [redacted] = [redacted] MPa

4.3 Strength of the bottom fin

The compressive stress generated at the bottom fin in contact with the skid is maximized in case when the acceleration of 5g is applied to the lateral direction.

The compressive stress "σ_{c5}" in this case is given as follows ;

$\sigma_{c5} =$ [redacted] MPa

If the analytical model of bottom fin in contact with the skid is designed on the safe side and the boundary condition is "simple support" as shown in (II)- Fig.A.33, the critical buckling stress σ_{cr} in this case will be expressed by the following formula;

[redacted]

(II)-Fig.A.33 Analytical model of the bottom fin

$$\sigma_{cr} = k \cdot \frac{\pi^2 E}{12(1-\nu^2)} \cdot \left[\frac{t}{b}\right]^2$$

where, k : a/b = 1.65

Buckling coefficient of single support = 4

b : Plate width ⋯⋯⋯⋯130 mm

t : Plate thickness ⋯⋯⋯30 mm

E : Modulus of longitudinal elasticity [redacted] MPa ([redacted]℃)

ν : Poisson's ratio (0.3)

Therefore, the following is given;

$\sigma_{cr} = 4 \times$ [redacted] = [redacted] MPa

Accordingly, the safety factor (RF) and the safety margin (MS) can be given as follows ;

RF = [redacted] = [redacted]

MS = [redacted] − 1 = [redacted]

The compressive stress is to be evaluated further on.

The allowable compressive stress "σ_a" on the bottom fin is given as follows;

$\sigma_a = 1.5 \times \sigma_y = 1.5 \times$ [redacted] = [redacted] MPa

Consequently, the safety factor (RF) and the safety margin (MS) against the compressive stress can be given as follows;

RF = [redacted] = [redacted]

MS = [redacted] - 1 = [redacted]

As described above, the bottom fin at the part in contact with the skid is free from plastic deformation even if the acceleration of 10g to the travelling direction, 5g to the lateral direction and 3g to the vertical direction is applied.

A.4.6 Pressure

If the ambient pressure of the packaging is reduced to 6.0×10^4 Pa, the stress in the packaging due to the change of the ambient pressure is obtained by means of correcting on the basis of the result shown in "Stress calculation" of paragraph A.5.1. The maximum internal pressure under normal conditions of transport is [redacted] PaG. However, [redacted] PaG is used as the internal pressure in the paragraph conservatively.

The pressure difference between inside and outside of the packaging is as follows.

[redacted] + ([redacted] $- 6.0 \times 10^4$) = [redacted] Pa

On the other hand, as the internal pressure under normal conditions of transport in paragraph (II)-A.5.1.3, [redacted] PaG is used conservatively in stead of [redacted] PaG.

In this case, since it is assumed that the ambient pressure is the atmosphere (0 PaG), the pressure difference between inside and outside of the packaging is [redacted] Pa.

Therefore, from the result of following equation, the stress due to the pressure difference [redacted] Pa between inside and outside of the packaging is [redacted] times that due to pressure difference [redacted] Pa.

[redacted] = [redacted]

The change on the stress corresponding to the increase in the internal pressure is obtained from the result of stress calculation due to only the internal pressure in paragraph A.5.1.3. The maximum stress (stress intensity) occurs in the inner surface at the center of the body bottom plate, and the value is [redacted] MPa (= [redacted]).

Therefore, if the ambient pressure is reduced to 6.0×10^4 Pa , the effect of the pressure reduction upon the packaging can be ignored.

In addition, in the evaluation of the strain level of the lid sealing boundary for the special test conditions shown in (II)-Table A.21, it was confirmed that the sealing property was maintained since the recovery of the initial clamping stress was confirmed and the mouth opening was less than [redacted] mm for an initial clamping allowance of [redacted] mm.

A.4.7 Vibration

The package will be transported in vertically upright state and the natural frequency (f_l) of the transport during its transport can be obtained by the following formula[14].

$$f_l = \frac{K_l}{2\pi}\sqrt{\frac{E\,I}{M\ell^4}}$$

where, K_l : Coefficient when vibration mode is 1 = 15.4

(one end is hinged and the other end is free)

E : Modulus of longitudinal elasticity [redacted] MPa

(at [redacted] ℃)

I : Moment of inertia

$$= \frac{\pi\,(d_2^{\,4}-d_1^{\,4})}{64} = \text{[redacted]}\ \mathrm{mm}^4$$

where, d_2 : Outer diameter of the shell = [redacted] mm

d_1 : Inner diameter of the shell = [redacted] mm

ℓ : Length of the packaging = [redacted] mm

g : Gravitational acceleration = 9.8×10^3mm/sec^2

M : Mass per unit length

$$= \frac{\text{Weight of package (maximum weight)}}{\ell \times g}$$

$$= \frac{23.2 \times 10^3 \times 9.8}{2100 \times 9800}$$

$$= 1.10 \times 10^{-2}\ \mathrm{N \cdot sec^2/mm^2}$$

Therefore,

f_1 = [redacted] Hz

Since the natural frequency of the package is about [redacted] Hz against the maximum effective frequency (approx. [redacted] Hz)[15] which is predicted during transportation, there will be no resonance during transportation.

The relationship[24] between the amplification factor and the ratio of frequencies is given by the curve shown in (II)-Fig. A.34. Here, since the expected frequency of vibrations during transportation is about [redacted] Hz, the amplification factor will be obtained as follows:

Ratio of frequencies = $f \,/\, f_n$

= [redacted]

Where, f_n : Natural frequency of the package

f: Frequency of vibrations during transportation

Therefore,

Amplification factor ≒ 1

Therefore, since there is no influence of load amplification due to vibrations during transportation, in addition, in the stacking evaluation ((II)-A.5.4) under the normal test conditions, considering the fact that the transport container will not be deformed even when it is subjected to five times its own weight + its own weight load, there is no risk of cracks, damages, etc. to the transport container due to vibrations during transportation.

Therefore,

$$f_1 \fallingdotseq 999 \text{ Hz}$$

Since the natural frequency of the package is about 999 Hz against the maximum effective frequency (approx. 50 Hz)[15] which is predicted during transport, there will be no resonance during transport.

Therefore, various bolts used for the packaging will not cause resonance, and they will not become loose because they are provided with antirotation keys.

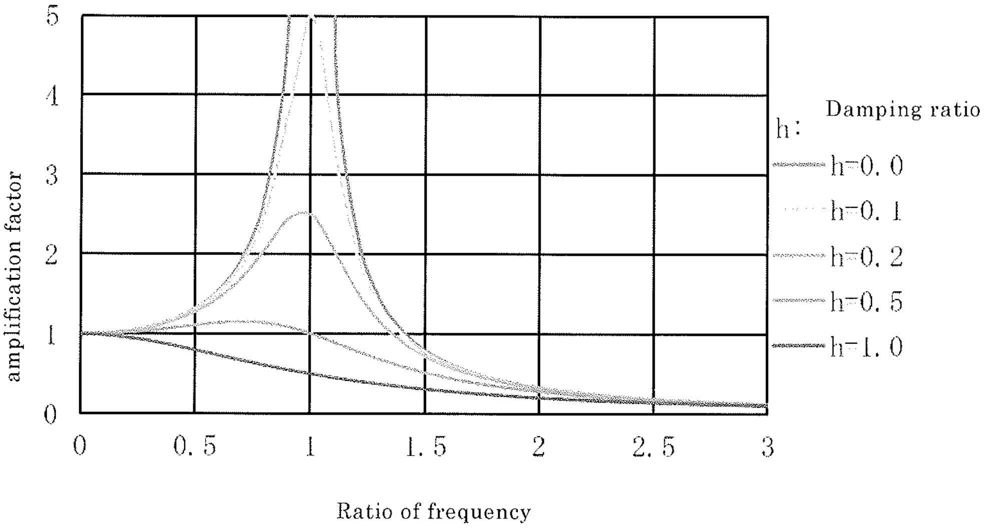

(II)-Fig. A.34 Relationship between amplification factor and ratio of frequencies

A.5 Normal conditions of transport

The packaging has a wall of substantial thickness which is determined by the requirement for shielding performance rather than that for strength. It has extremely high mechanical strength. Baskets are designed to withstand the use under accident conditions of transport. Therefore, as shown in paragraph (II)-A.5.1 through paragraph (II)-A.5.7, various stresses generated under normal conditions of transport are lower than the allowable stress.

A.5.1 Thermal test

The results of thermal analysis of the nuclear fuel package conducted under the normal test conditions are summarized as shown in (II)-B.4.

1) The maximum temperature and maximum internal pressure will occur, when considering conservatively, under the environment where the fuel element As which have the greatest decay heat are contained and are subjected to the solar radiation heat.
2) The maximum thermal stress is generated under the absence of insolation where the temperature difference between the internal and external surfaces of the packaging is maximum when the above fuel element is contained in the packaging.
3) The lowest temperature for all the package is -40℃.

Details of the thermal test are described below.

A.5.1.1 Summary of pressure and temperature

(II)-B.4.2 and (II)-B.4.4 describe the analysis of the temperature and pressure of the components of the package under the normal conditions of transport, while (II)-Table A.8 shows the summary of the pressure and temperature.

The temperature distribution of the packaging and basket is shown in (II)-Fig.A.35 through Fig.A.37. The temperature distribution of the components of the packaging shown in (II)-Fig.A.35 denotes the values of the maximum temperature gradient when fuel elements are contained in the packaging.

Level	Temperature (°C)
1	[redacted]
2	[redacted]
	[redacted]
3	[redacted]
4	[redacted]
5	[redacted]
6	[redacted]
7	[redacted]
8	[redacted]
9	[redacted]
0	[redacted]
A	[redacted]
B	[redacted]

[redacted]

(II)-Fig.A.35 Temperature distribution of the packaging

(Normal conditions of transport)

[redacted]

The number marked with ○ shows the element number of basket.

Fig.A.36 Temperature distribution in the basket for box type fuel

[redacted]

Fig.A.37 Temperature distribution in the basket for MNU type fuel

The contained fuel was the fuel element A which was thermally analyzed under the conditions in an environment at 38℃ without the solar insolation.

(II)-Table A.8 Summary of pressure and temperature (Normal conditions of transport)

Basket	Max. temperature of packaging (°C)	Max. temperature of basket (°C)	Max. internal Pressure(× 104PaG)
Basket for box type fuel	[redacted]	[redacted]	[redacted]
Basket for MNU type fuel	[redacted]	[redacted]	[redacted]

*1) As the calorific values and temperature gradient in the basket become maximum when the fuel element A is contained, the values of such fuel element contained are shown in this Table.

A.5.1.2 Thermal expansion

The thermal expansion and the thermal stress caused by the thermal expansion of the packaging and the basket is discussed when the package is placed in a shade of 38°C and each fuel element is contained in the packaging.

1. Thermal stress and deformation of the packaging

For analysis of the thermal stress and deformation of the packaging, the general-purpose finite element program ABAQUS [6)] was used for the case where the temperature distribution and the pressure obtained from [(II)-Chapter B. Thermal Analysis] acted upon the packaging.

(II)-Fig. A.38 shows the model used for the analysis.

This analytical model is assumed not to have fins, lifting lugs and support attached to the external surface of the packaging, and the body (shell and bottom plate) and lid of the packaging are divided by using the 8 nodes axisymmetric isoparametric element. The contact condition for the joint part of the body and the lid is considered.

Considering the cross-sectional areas, the lid bolt hole and lid bolt are replaced with those having equivalent rigidity.

The initial fastening force due to the tightening of the lid bolt to the specified load is given to the analytical model, then the internal pressure and the temperature distribution is also given to the model.

The maximum internal pressure of [redacted] PaG when the fuel element A is contained (the value of the basket for box type fuel shown in (II)-Table A.8) was rounded conservatively as [redacted] PaG. The temperature distribution in which the greatest thermal stress would be expected, that is, temperature gradient would be the greatest (under ambient temperature of 38°C, without solar insolation and containing fuel element A) was used.

The thermal stress and the deformation obtained from this analytical model are shown in (II)-Fig.A.39 through (II)-Fig.A.41.

The analytical method is shown in (II)-A.5.1.3.

2. Thermal stress and thermal expansion of the baskets

As it is apparent from (II)-Fig.A.36 and (II)-Fig.A.37 which denote the temperature distribution of each basket when each fuel element is contained, there is a temperature difference between the central part and the peripheral part of the basket and also a temperature difference between the basket and the body.

Therefore, it is forecasted that thermal stress is generated in the basket.

a) Thermal expansion and thermal stress in the longitudinal direction

Elongation ($\Delta \ell_b$) in the longitudinal direction due to thermal expansion of each basket is expressed by the following expression obtained due to the force equilibrium on the assumption that entire length of each basket is ℓ_o.

[redacted]

(II)-Fig.A.38 Analytical model of the packaging

[redacted]

(II)-Fig.A.39 Mises equivalent stress contours (Normal conditions of transport)

[redacted]

(II)-Fig.A.40 Deformation (Normal conditions of transport)

[redacted]

(II)-Fig.A.41　Longitudinal stress contours of the lid bolt

(Normal conditions of transport)

$$\Delta \ell_b = \frac{\sum\limits_{i=1} A_i E_i (T_i - 20)\, \alpha_i}{\sum\limits_{i=1} \frac{A_i E_i}{\ell_0}}$$

where, T_i : Mean temperature of the i-th element

A_i : Cross-sectional area of the i-th element

E_i : Modulus of longitudinal elasticity of the i-th element

α_i : Coefficient of thermal expansion of the i-th element

As a result of the calculation of the above expression, the elongation $\Delta \ell_b$ in the longitudinal direction of the basket is obtained as shown in (II)-Table A.9 , which includes the safety factor and the safety margin.

On the other hand, the value of the gap g_0 between the internal surface of the packaging and the basket at the room temperature (20°C) is conservatively considered as below.

g_0 = [redacted] mm

From (II)-Fig. A.40, elongation $\Delta \ell_{\text{body}}$ of the entire length in the packaging obtained from the preceding paragraph is expressed as follows;.

$\Delta \ell_{\text{body}} = \ell' - \ell$

where, ℓ : Entire length in the packaging before the deformation

= [redacted] mm

ℓ' : Entire length in the packaging after the deformation

= [redacted] mm

Therefore,

$\Delta \ell_{\text{body}}$ = [redacted] - [redacted] = [redacted] mm

The maximum value of thermal expansion in the longitudinal direction is 1.44 mm, in the basket for box type fuel as shown in (II)-Table A.9.

(II)-Table A.9 Thermal expansion in the longitudinal direction of each basket and the packaging, safety factor and safety margin

	Initial gap at the room temperature (g_0) *	Thermal expansion of the packaging ($\Delta\ell_{body}$) *	$g_0 + \Delta\ell_{body}$ *	Thermal expansion of basket ($\Delta\ell_b$) *	Safety factor (RF)	Safety margin (MS)
Basket for box type fuel	[redacted]	[redacted]	[redacted]	1.44	[redacted]	[redacted]
Basket for MNU type fuel	[redacted]	—	—	0.66	[redacted]	[redacted]

(* Unit: mm)

Note) The safety factor and the safety margin of the basket for MNU type fuel are the values calculated on the basis of the initial gap at the room temperature (20 °C).

The result of the analysis is as follows;.

$\Delta\ell_b < g_0 + \Delta\ell_{body}$ (1.44 mm < [redacted] mm)

Therefore, it becomes the following in any basket.

$\Delta\ell_b < g_0 + \Delta\ell_{body}$

And even when considering the expected ambient temperature changes during transportation (from -40℃ to 38℃), since there is no change in the temperature range of the same material, there is no difference in the expansion amount of the transport container body nor that of the fuel basket, and no change in the amount of gap either.

Therefore, the basket is not restricted between the bottom plate of the body and the internal surface of the lid. Therefore, the stress generated in the basket is caused by the temperature gradient of the basket itself.

This stress σ_i is expressed by the following equation.

$$\sigma_i = \frac{E_1}{\ell_1}\{\Delta\ell_b - (T_i - 20)\,\alpha_i \ell_i\}$$

where,

T_i : Mean temperature of the i-th element

E_i : Modulus of longitudinal elasticity of the i-th element

α_i : Coefficient of thermal expansion of the i-th element

$\Delta\ell_i$: Length of the i-th element

$\Delta\ell_b$: Value of elongation in the longitudinal direction

(II)-Table A.10 shows the stress generated in each basket obtained from the calculation of the above expression (The element number in the Table is based on (II)-Fig. A.36 and (II)-Fig.A.37).

Therefore, The maximum stress generated in each basket is expressed as follows;, from (II)-Table A.10.

Maximum stress of the basket for box type fuel:

[redacted] MPa (compressive stress)

Maximum stress of the basket for MNU type fuel:

[redacted] MPa (tensile stress)

If the allowable stress under this condition is 3 times Sm at respective maximum temperature, the safety factor (RF) and the safety margin (MS) of each basket are as shown in (II)-Table A.11.

(II)-Table.A.10 Stress in Basket

Element No.	Basket for box type fuel	Basket for MNU type fuel
[redacted]	[redacted]	[redacted]

(Unit : MPa)

Therefore, the thermal stress in the longitudinal direction generated in each basket under normal conditions of transport is less than the allowable stress so that the integrity of the fuel basket is maintained.

b) Thermal expansion in the radial direction

In (II)-Fig. A.36 and (II)-Fig. A.37, the value of the thermal expansion in the radial direction caused by the thermal expansion of each basket is obtained by adding the value of expansion in the radial direction of individual element located on the line passing through the center axis. In the calculation, the following expression is used.

$$\Delta r_b = \sum_{i=1} (T_i - 20)\ \ell_i$$

where,
T_i : Mean temperature of the i-th element
α_i : Coefficient of thermal expansion of the i-th element
ℓ_i : Length in the axial direction of the i-th element

As a result of the calculation obtained by the above expressions, the elongations Δr_b in the radial direction of the basket are shown in (II)-Table A.12. In the Table, the initial gap g_0 at the room temperature, the safety factor, and the safety margin are also shown.

Therefore, as apparent from the Table, there is still a gap between each basket and the internal surface of the packaging even after thermal expansion. For this reason, the stress due to restriction is not generated in each basket.

And even when considering the expected ambient temperature changes during transportation (from -40℃ to 38℃), since there is no change in the temperature range of the same material, there is no difference in the expansion amount of the transport container body nor that of the fuel basket, and no change in the amount of gap either.

(II)-Table A.11 Maximum thermal stress generated in each basket

	Maximum thermal stress [MPa]	Maximum temperature*1 (°C)	Allowable stress*2 [MP]	Safety factor (RF)	Safety margin (MS)
Basket for box type fuel	[redacted]	[redacted]	[redacted]	[redacted]	[redacted]
Basket for MNU type fuel	[redacted]	[redacted]	[redacted]	[redacted]	[redacted]

*1 The value is assumed to be more conservative than the temperature of the result of the thermal analysis.
*2 Three times Sm1) at the maximum temperature

(II)-Table A.12 Thermal expansion in the radial direction of each basket and the packaging, safety factor and safety margin

	Initial gap at the room temperature (g_o)*	Thermal expansion of the packaging (Δr_b)*	$g_0 + \Delta r_{body}$ *	Thermal expansion of basket (Δr_b)*	Safety factor (RF)	Safety margin (MS)
Basket for box type fuel	[redacted]	[redacted]	[redacted]	0.981	[redacted]	[redacted]
Basket for MNU type fuel	[redacted]	-	-	0.338	[redacted]	[redacted]

(*Unit: mm)

Note) The safety factor and the safety margin of the basket for MNU type fuel are the values calculated based on the initial gap at the room temperature (20°C).

A.5.1.3 Stress calculation

In this paragraph, the thermal stress which is generated by the temperature gradient, pressure and load of the packaging under normal conditions of transport, is calculated. An analytical model shown in (II)-Fig. A.38 is used, and the analysis is carried out in the order as follows;

The thermal stress generated in the basket has been described in the preceding paragraph [A.5.1.2 (Thermal expansion)].

Calculation sequences:

First : Apply the load of the initial fastening force of the lid bolt to the element of the bolt to cause the contact surface between the lid and the body to be in compressed state. The tensile load F_b to be given to the bolt per bolt is expressed by the following expression.

$F_b =$ [redacted] N

This fastening force is balanced to the internal pressure of [redacted] MPa.

Second : Apply the maximum internal pressure generated under normal conditions of transport to the internal wall of the packaging.

Third : Apply to each element the thermal distribution which generates the maximum thermal stress, that is, the thermal distribution having the maximum temperature gradient.

Based on the stress obtained through the above sequences (refer to (II)-Fig. A.39 through (II)-Fig. A.41), the stress of the components of the packaging is evaluated.

A.5.1.4 Comparison of allowable stress

In this paragraph, the limit of the reasonable allowable stress, which is different depending on respective stress, is provided. Differences in effect upon the damage of materials are considered according to the type of the stress. The stress obtained from (II)-A.5.1.2 and (II)-A.5.1.3 is evaluated according to the reference 1)-V-3220.

1. Strength of the body and the lid

1.1 Allowable stress

As a result of the thermal analysis, the maximum temperature at the bottom center part of the packaging is [redacted]°C under normal conditions of transport. However, the temperature is assumed to be conservatively [redacted]°C. Because the thermal stress is included, the allowable stress (σ_a) of the forged material SA-182 [redacted] (equivalent to SUS [redacted]) is as follows:.

$\sigma_a = 3\ S_m$1) = 3 × [redacted] = [redacted] MPa

1.2 Calculation of stress intensity on the stress classification line

From the shape and load conditions of the body and the lid of the packaging, it is forecasted that a large stress is generated in A ~ D lines shown in (II)-Fig. A.42.

The cross-section used for evaluation of the stress is hereafter called "stress classification line".

However, as apparent from (II)-Fig. A.39 showing Mises equivalent stress, the maximum large stress is observed in the stress classification line at the center of the bottom plate. Therefore, the stress generated on stress classification line "A" is compared with the allowable stress.

[redacted]

(II)-Fig.A.42 Location of stress classification lines

Stress classification line "A":

When the radial stress and the stress in the thickness direction are represented as σ_ℓ and σ_r respectively, these stresses on the internal surface which has the maximum stress are as follows;

σ_ℓ = [redacted] MPa

σ_r = [redacted] MPa

Since these stresses are principal stresses, the stress intensity on the stress classification line "A" is expressed as follows;

$S = | \sigma_\ell - \sigma_r |$

= [redacted] MPa

The stress intensity on the stress classification line "A" due to only inner pressure is as follows

σ_ℓ = [redacted] MPa

σ_r = [redacted] MPa

$S = | \sigma_\ell - \sigma_r |$

= [redacted] MPa

The allowable stress σ_a of the packaging is expressed as follows.

$\sigma_a = 3$ Sm = [redacted] MPa

Therefore, the safety factor (RF) and the safety margin (MS) on the stress classification line "A" of the body and the lid are as follows;

RF = [redacted] = [redacted]

MS = [redacted] – 1 = [redacted]

Therefore, the structural integrity of the packaging is maintained, because the stress which is generated on each part of the packaging is within the allowable stress.

In addition, the temperature change from room temperature (20℃) to [redacted]℃ was studied. When considering the lowest ambient temperature of -40℃ expected during transportation, the temperature difference between -40℃ and [redacted]℃ is [redacted]℃. The stress in this case will be

[redacted] × [redacted] = [redacted] ≒ [redacted] MPa

Therefore, the safety factor RF and the margin factor MS are as follows:

$$RF = [redacted] = [redacted]$$

$$MS = [redacted] - 1 = [redacted]$$

Then, there is no risk of cracks or failures, etc. even when ambient temperature changes expected during transportation are considered.

2. Containment of contact surfaces of the lid and the body

In this analysis, it is considered that the lid and the body contact through the flange part.

The containment of the contact surfaces of the lid and the body under the normal conditions of transport is evaluated from the deformed conditions of the flange part where [redacted] O-rings are located.

The deformation of the flange part is shown in (II)-Fig.A.43.

From this result, the flange part keeps contact condition so that the containment of the contact surface is maintained.

3. Strength of the lid bolt

3.1 Allowable stress

From the results of the thermal analysis, the maximum temperature of the lid bolt is [redacted]°C under the normal conditions of transport, however, the maximum temperature of that is conservatively [redacted]°C.

The allowable stress (σ)7) of the material SA-564 [redacted] (equivalent to SUS [redacted]) used for the lid bolt is as follows since the lid bolt is to be used under thermal stress.

$$\sigma = 2\ Sm = 2 \times [redacted] = [redacted]\ \text{MPa}$$

3.2 Stress of the lid bolt

The longitudinal stress at the center of the lid bolt was obtained in respective calculation stages shown in (II)-A.5.1.3.

The results are shown in (II)-Table A.13. (Refer to (II)-Fig.A.41.)

(II)-Table A.13 Stress of lid bolt

	Stress [MPa]
After initial fastening	[redacted]
When internal pressure is applied : 6.0×10^4 PaG	[redacted]
When internal pressure and temperature are applied:	[redacted]

*1 : The maximum pressure [redacted] PaG is conservatively applied in this analysis though the maximum pressure is shown in (II)-Table A.8 is [redacted] PaG.

[redacted]

(II)-Fig.A.43 Deformation of the contact surface of the lid and the body

From the above Table, it is known that the lid bolt has the maximum stress when the internal pressure and the temperature distribution are given as the load conditions.

The stress S (tensile stress) in this condition is as follows;

S = [redacted] MPa

Therefore, the safety factor (RF) and the safety margin (MS) are as follows;

RF = [redacted] = [redacted]

MS = [redacted] − 1 = [redacted]

Therefore, the stress generated in the lid bolt under the normal conditions of transport is less than the allowable stress so that the structural integrity of the lid bolt is maintained.

3.3 Fatigue strength of the lid bolt

When the internal pressure and the temperature distribution are given, the largest stress is generated in the lid bolt. Therefore, the fatigue strength of the lid bolt is examined in this paragraph.

As shown in (II)-Table A.13, the stress σ generated in the lid bolt is expressed as follows;

σ = [redacted] MPa

The stress of the thread is the greatest at the root of thread and the stress concentration factor K[18)] corresponding to the radius of curvature [redacted] mm (M [redacted] metric fine pitch thread) is as follows;

$K = 6$

Therefore, the amplitude Salt of the repeated stress intensity including the stress concentration used for the evaluation of fatigue is expressed as follows;

$$S_{alt} = \frac{1}{2}K\sigma \quad = \frac{1}{2} \times 6 \times \text{[redacted]} = \text{[redacted]}\ \text{MPa}$$

The following expression is used to obtain the value S'_{alt} used to calculate the allowable number of cycles from the design fatigue curve (Fig. I-9.4 of the ASME Code Sec. III Div. 1-Appendices).

$$S'_{alt} = S_{alt} \frac{E'}{E}$$

where, E' : Modulus of longitudinal elasticity of the design fatigue curve

[redacted] MPa

E : Modulus of longitudinal elasticity of the lid bolt

[redacted] MPa (at [redacted] °C)

Therefore,

$S'_{alt} =$ [redacted] × [redacted] = [redacted] MPa

In the design fatigue curve, the allowable number of cycles N corresponding to the value S'alt is as follows;

$N = 3.4 \times 10^3$ cycles

On the other hand, the number of operating cycles n during the life of the packaging is 300 cycles.

The safety factor (RF) and the safety margin (MS) of the fatigue strength of the lid bolt are as follows;

$$RF = \frac{3400}{300} = 11.3$$

$$MS = 11.3 - 1 = 10.3$$

Therefore, the allowable number of cycles of the lid bolt is sufficiently greater than the number of operating cycles during the life of the packaging, and the fatigue failure dose not occur in the lid bolt.

* Times of use N = 4/year×70 years×margin = 300 times

A.5.2 Water spray

Because the packaging is manufactured with stainless steel, the packaging has sufficient corrosion resistance. Also, since the containment of the packaging is maintained even in the water immersion test of accident conditions of transport, it is not possible that the containment is affected by the water spray.

Water removal is excellent because the external surface of the packaging is smoothed and structured to prevent water from staying over the external surface.

A.5.3 Free drop

As shown in (II)-Table A.2, the mass of the package is 23.2×10^3 kg. The height of the free drop set forth in the technical standard is 0.3 m for the package whose mass exceeds 15×10^3 kg. Therefore, the free drop height of the package is 0.3 m.

On the other hand, the package is structured to absorb the energy generated upon drop it in 9 m drop test, which is one of accident conditions of transport, by the deformation of the fin attached to the body and lid.

The integrity of the body, lid and contents of the packaging are assured with respect to the drop impact value due to deformation. Therefore, the integrity of the package is sufficiently maintained in 0.3 m drop test.

A.5.4 Stacking test

The package is transported in vertically upright condition. Therefore, this paragraph shows the effect upon the package which is compressed vertically upright. Because the weight of the package is 2.28×10^5 N (23.2×10^3 kgf), the load W1 which is (5 times the weight of the package) + package = (6 times the weight of the package) is expressed as follows;

$$W_1 = 6\times2.28\times10^5 = 1.37\times10^6\,\mathrm{N}$$

On the other hand, the load W_2 obtained by multiplying the vertically projected area by 13 kPa is expressed by the follow expression because the outside diameter of the body is [redacted] m.

$W_2 = 13\times10^3\times\frac{\pi}{4}\times$ [redacted] = [redacted] N

Therefore, the strength of each component is evaluated regarding the case in which the greater load of the above, that is, W_1, is applied to the packaging for 24 hours.

(1) Strength of the shell under compression

(2) Strength of the bottom fin of the body under compression

(3) Strength of the bottom plate of the body and the lid under compression

  1) Strength to bending stress of the bottom plate and the lid

  2) Strength to shearing force of the bottom plate and the lid

(4) Compressive strength of contact surfaces of the body and the lid.

1. Strength of the shell under compression

The analytical model of the shell of the body is shown in (II)-Fig.A.44.

The compressive stress σ of the shell of the packaging is expressed as follows.

$$\sigma = \frac{W_1}{A_1}$$

[redacted]

(II)-Fig.A.44 Analytical model of the shell

where, $W_1 = 1.37 \times 10^6$ N

$A_1 = \frac{\pi}{4}(\text{[redacted]} - \text{[redacted]}) = \text{[redacted]}$ mm^2

Therefore,

$$\sigma = \frac{1.37 \times 10^6}{\text{[redacted]}} = \text{[redacted]}\ \text{MPa}$$

The allowable compressive stress σ_a of the shell at [redacted]℃ is expressed as follows;

$$\sigma_a = \sigma_y = \text{[redacted]}\ \text{MPa}$$

Therefore, the safety factor (RF) and the safety margin (MS) are as follows;

$$RF = \text{[redacted]} = \text{[redacted]}$$

$$MS = \text{[redacted]} - 1 = \text{[redacted]}$$

Therefore, the shell of the packaging has the sufficient strength if it is subjected to the compressive load 6 times that of the package.

2. Strength of the bottom fin under compression

The packaging is supported by the four bottom fins (30 mm in thickness) of the body, and the compressive strength of the bottom fin is evaluated.

The shape and dimensions of the bottom fin are shown in (II)-Fig.A.45. The maximum compressive stress σ is expressed as follows;

$$\sigma = \frac{W_1}{A_{min}}$$

where, W_1 = 1.37×10^6 N

A_{min} = Minimum cross-sectional area = $130 \times 30 \times 4$

= 1.56×10^4 mm^2

Therefore,

$$\sigma = \frac{1.37 \times 10^6}{1.56 \times 10^4} = 87.9\,\mathrm{MPa}$$

The allowable compressive stress σ_a of the bottom fin at the temperature [redacted]°C is expressed as follows;

$\sigma_a = \sigma_y =$ [redacted] MPa

[redacted]

(II)-Fig.A.45 Shape and dimensions of bottom fin for supporting the packaging

Therefore, the safety factor (RF) and the safety margin (MS) are expressed as follows;

$$RF = \frac{\text{[redacted]}}{87.9} = \text{[redacted]}$$

$$MS = \text{[redacted]} - 1 = \text{[redacted]}$$

Therefore, the bottom fin for supporting the packaging is sufficiently resisted the load when it is subjected to the compressive load 6 times the package.

3. Strength of the bottom plate of the body and the lid

Since the bottom plate is [redacted] mm in thickness and the lid is [redacted] mm in thickness, this paragraph evaluates the strength of the bottom plate of the body which is less thickness in the case of 6 times the load of the weight of the package applied.

As shown in (II)-Fig.A.46, the analytical model of the bottom plate is a disk whose periphery is fixed under uniformly distributed load.

The uniformly distributed load q is expressed as follows;

$$q = \frac{W_1}{A_1}$$

where, $W_1 = 1.37 \times 10^6$ N

$D =$ [redacted] mm

$A_1 = \frac{\pi}{4} \times D^2 = \frac{\pi}{4} \times \text{[redacted]}^2 = \text{[redacted]}$ mm^2

Therefore,

$$q = \frac{1.37 \times 10^6}{\text{[redacted]}} = \text{[redacted]} \text{MPa}$$

The bending moment$^{14)}$ in the radial direction and circumferential direction per unit length generated at the fixed end of the periphery, is as follows;

[redacted]

(II)-Fig.A.46　Analytical model of the bottom plate under compression

The bending moment in the radial direction is expressed as follows;

$$M_r = \frac{\text{[redacted]}}{8} = \frac{\text{[redacted]}}{8} = \text{[redacted]}\ \text{N·mm/mm}$$

The bending moment Mt in the tangential direction is expressed as follows;

$$M_t = \nu M_r$$

If Poisson's rate ν is 0.3, the following is given.

$$M_t = \text{[redacted]} \times \text{[redacted]} \times \text{[redacted]}$$

$$= \text{[redacted]}\ \text{N·mm/mm}$$

The shearing force Q per unit length is obtained from the following expression.

$$Q = \frac{qb}{2} = \text{[redacted]} = \text{[redacted]}\ \text{N·mm/mm}$$

If the thickness of the bottom plate is t, the maximum stress is obtained by the following expression. The radial stress σ_r in the external surface of the bottom plate is expressed as follows;

$$\sigma_r = \frac{6 \times M_r}{t^2} = \frac{6 \times \text{[redacted]}}{\text{[redacted]}^2} = \text{[redacted]}\ \text{MPa}$$

where, t : Thickness of the bottom plate = [redacted] mm

Mr : 5[redacted] N·mm/mm

The circumferential stress σ_t is expressed as follows;

$$\sigma_t = \frac{6 \times M_t}{t^2}$$

where, M_t : Circumferential bending moment = [redacted] N·mm/mm

t : Thickness = [redacted] mm

Therefore,

$$\sigma_t = \frac{6 \times \text{[redacted]}}{\text{[redacted]}} = \text{[redacted]}\ \text{MPa}$$

The longitudinal stress σ_0 is given by the expression below;

$$\sigma_0 = -q = -\text{[redacted]}\ \text{MPa}$$

The shearing force τ at the center of the thickness is obtained by the following expression.

$$\tau = \frac{3}{2} \times \frac{Q}{t}$$

where, Q : Shearing force per unit length = [redacted] N/mm

t : Thickness = [redacted] mm

Therefore, the following expression is given.

$$\tau = \frac{3}{2} \times \frac{[redacted]}{[redacted]} = [redacted] \text{ MPa}$$

Therefore, the maximum stress σ_{max} and the maximum shearing stress τ_{max} is expressed as follows;

$\sigma_{max} = \sigma_r =$ [redacted] MPa

$\tau_{max} = \tau =$ [redacted] MPa

The allowable bending stress σ_{ab} and the allowable shear force τ_a at the operating temperature of [redacted] °C is expressed as follows.

$\sigma_{ab} = \sigma_y =$ [redacted] MPa

$\tau_a = 0.6 \times \sigma_y = 0.6 \times$ [redacted] = [redacted] MPa

Therefore, the safety factor (RF) and the safety margin (MS) for the maximum stress at the operating temperature of [redacted] °C are given by the following expressions.

RF = [redacted] = [redacted]

MS = [redacted] - 1 = [redacted]

The safety factor (RF) and the safety margin factor (MS) for the shear force at the operating temperature of 105°C are as follows;

RF = [redacted] = [redacted]

MS = [redacted]- 1 = [redacted]

Therefore, the lid and the bottom plate can withstand the load even if it is subjected to the compressive load 6 times that of the package.

4. Compressive strength of contact surfaces of the body and the lid (refer to (II)-Fig.A.47).

The compressive stress σ generated on the contact surface is expressed as follows;

$$\sigma = \frac{W_1}{A}$$

where, W_1 = 1.37×10^6 N

A : Entire area of the contact surface (excluding the O ring portion and the groove of leak tightness test)

$= \frac{\pi}{4}[$ [redacted] $) -$

$($ [redacted] $) - ($ [redacted] $)]$

= [redacted] mm²

Hence,

$\sigma = \frac{1.37 \times 10^6}{\text{[redacted]}} =$ [redacted] MPa

The allowable compressive stress σ_a of the contact surface of the body at the operating temperature of [redacted] °C, which is higher than the contact surface of the lid, is expressed as follows;

$\sigma_a = \sigma_y =$ [redacted] MPa

Therefore, the safety factor (RF) and the safety margin (MS) for the compressive stress of the contact surfaces of the body and lid are as follows;

RF = [redacted] = [redacted]

MS = [redacted] − 1 = [redacted]

Therefore, the contact surfaces of the body and the lid can sufficiently withstand the load if it is subjected to the compressive load 6 times that of the package.

[redacted]

(II)-Fig. A.47 Contact surfaces of the body and the lid

A.5.5 Penetration

If a mild steel bar of 3.2 cm in diameter and 6 kg in mass is drops on the package under normal conditions of transport, the energy E_1 upon impact is expressed as follows;

$E_1 = m_1 g h_1$

where, m_1 : Mass of the mild steel = 6 kg

g : Gravitational acceleration

h_1 : Drop height = 1 m

On the other hand, if the package drops on the mild steel bar of 15 cm in diameter in the drop test II shown in (II)- A.6.2, the energy E_2 of the impact is expressed as follows;

$E_2 = m_2\, g\, h_2$

where, m_2 : Mass of the package = 23.2×10^3 kg

g : Gravitational acceleration

h_2 : Drop height = 1 m

Since $h_1 = h_2$ from both expressions, the diameter of the mild steel bar is calculated as follows by comparing the energy of impact per unit area caused by drop of the bar on the package.

D_1 : Diameter of the mild steel bar = 32 mm

D_2 : Diameter of the mild steel bar = 150 mm

$$\frac{E_1}{\frac{\pi}{4} D_1^2} << \frac{E_2}{\frac{\pi}{4} D_2^2} \quad : \quad \frac{6 \times g \times h_1}{\frac{\pi}{4} 32^2} << \frac{23.2 \times 10^3 \times g \times h_2}{\frac{\pi}{4} 150^2}$$

that is, $7.46 \times 10^{-3} \cdot g \cdot h_1 << 1.31 \cdot g \cdot h_2$ $(h_1=h_2)$

As apparent from the above comparison, the drop test II shown in (II)-A.6.2 becomes severer than the drop test I. In the drop test II, since the packaging is not deformed nor penetrated by the mild steel bar, the external surface of the packaging is not penetrated by a 6 kg mild steel bar dropped under normal conditions of transport.

During transport, the valve is provided with the protection cover which is capable of withstanding the penetration test (refer to the drop test II of (II)-A.6.2-2).

The recess on the top of the lid is fitted with a plug of 20 mm in diameter for leak tightness test hole shown in (I)-Fig.C.16. If, however, a mild steel bar of 32 mm in diameter drops on, it hits on the top of the lid having sufficient strength against the drop test II and the plug in the recess is not hit directly. Upper part of this leak tightness test hole is covered and protected by the tie down device during transport.

As a result of the above, the package has sufficient strength against the penetration test.

A.5.6 Drop of square and edge

Not applicable.

A.5.7 Summary and evaluation of the results

The summary of the results and evaluation of the normal conditions of transport is as follows;

(1) Thermal test

As apparent from the results of the thermal stresses generated on the body and the basket shown in paragraph A.5.1.2 and A.5.1.3, the stresses which are generated on the shell, the bottom plate, the lid, the lid bolt and the basket are less than the allowable stress. Therefore, the integrity of the packaging is maintained.

(2) Water spray

It is assured that the containment is not affected by the water spray.

(3) Free drop

The package is structured to absorb the energy generated due to 9 m drop test, which is one of accident conditions of transport, by the deformation of the fin attached to the body and the lid.

The integrity of the body, the lid and the contents of the packaging are maintained against the drop impact value due to the deformation. Therefore, the integrity of the package is sufficiently maintained even in 0.3 m drop test.

(4) Stacking test

When the package is transported with horizontally and vertically upright condition, the analysis under the load of (5+1) times the weight of the package is made. The result of analysis is sufficient below the criteria. Therefore, the integrity of the package is maintained.

(5) Penetration

In the drop test II, since the packaging is not deformed nor penetrated by the mild steel bar, the external surface of the packaging is not penetrated by a 6 kg mild steel bar dropped under normal conditions of transport.

During transport, the valve is provided with the protection cover which is capable of withstanding the penetration test (refer to the drop test II of paragraph (II)-A.6.2 2).

(6) Evaluation of strain level

The evaluation of the elongation for the lid bolt, which is main containment system of the package, due to thermal stress and the pressure difference between the inside and the outside of the packaging under normal conditions of transport is made.

$$\Delta\ell = \frac{\sigma_b}{E} \cdot \ell$$

where, σ_b : Maximum tensile stress = [redacted] MPa

E : Modulus of longitudinal elasticity: [redacted] MPa([redacted] °C)

ℓ : Shank length of fastening ringflange bolt : [redacted] mm

Therefore,

$$\Delta\ell = \frac{\text{[redacted]}}{\text{[redacted]}} \times \text{[redacted]} = \text{[redacted]}\ \text{mm}$$

This value [redacted] mm is extremely small as compared with the restoration 3 mm of gasket (O-ring) of the lid. Therefore, the containment of the body is maintained.

As the evaluation of strain level is made under severer condition of the 9 m drop test under accident conditions of transport, that of the 0.3 m drop test is omitted.

As shown in 1 m penetration test where the external surface of the packaging is not penetrated by a mild steel bar of 6 kg, the package has sufficient strength against the penetration test.

A.6 Accident conditions of transport

This chapter shows by using the analysis that the package satisfies the structural requirements specified in the technical standard under accident conditions of transport set forth in the IAEA Regulations.

This package is a type B(U) package, and the special tests for the package are as shown below;

(1) Mechanical test
  1) Drop test- I (9 meters drop)
  2) Drop test- II (1 meter drop)
(2) Thermal test
(3) Immersion test
(4) Low-temperature strength

The tests under accident conditions of transport are performed in order of mechanical test, thermal test, immersion test and low-temperature strength test sequentially.

The test sequence for drop test-I and drop test-II is determined, taking the influence by thermal test to be performed in succession into consideration.

For the package of which mechanical test may fear to affect the thermal test, such tests are performed in order of the drop test-I and drop test-II as little difference is thought to exist due to sequence of such tests.

A.6.1 Mechanical test・drop test I (9 m drop)

This analysis is intended to drop the package from the height of 9 m onto the flat rigid target without any yield, so that the maximum damage and impact is generated on the package.

The package is so constructed that the drop energy is absorbed by the fins attached to the body and the lid when the package falls from 9 m height.

This paragraph investigates the influence on the package based on the calculation results, such as deformation of fins and impact deceleration at various drop posture.

1. Analysis Method

Drop impact analysis of the package is carried out using dynamic analysis code LS-DYNA19) to get deformation and impact deceleration of the package.

Containment at the contact surface of the lid and the body is directly evaluated based on the results of drop impact analysis.

On the other hand for the contents, that is, basket and fuel elements, there strength are estimated based on the assumption that the deceleration obtained from the drop impact analysis acts statically as inertia force.

In the advance of these drop impact analysis, it is confirmed that the dynamic analysis code LS-DYNA code be applicable to the impact behavior of fin.

Appendix A.10.2 describes the summary results.

2. Analysis conditions

(1) According to the regulation, the package should be dropped from the height of 9 m onto the flat rigid target without any yield, so that the maximum damage and impact is generated on the package. In order to meet the above regulation's requirement, in the drop analysis, initial velocity 13.3 m/s is given to the package with the rigid boundary condition, because this velocity is equivalent to the drop from 9 m height. And, the initial fastening stress, [redacted] MPa, is given to the lid bolt before drop.

(2) The total mass of the package will be a maximum when the basket for box type fuel (contents: JRR-3 standard Silicide type fuel element, etc.) is contained. The maximum total mass of 23.2×10^3 kg is used in the analysis.

(3) The operating temperature of the material in the drop analysis is assumed based on the result of normal conditions of transport in the thermal analysis ((II)-Table B.6), namely, [redacted]°C for the body, [redacted]°C for the lid and the lid bolts, [redacted]°C for the fins.

(4) The stress-strain curves depending on the strain rate are used for the fins that absorbs the drop impact of the package. On the other hand, static stress-strain curves are used for the body, the lid and the lid bolts.
Detail explanation is presented in Appendix A.10.1.

(5) Impact deceleration acting on the contents (basket and fuel elements) is assumed to be equal to that of package.

The analysis conditions are shown in <u>(II)-Table A.14</u>.

(II)-Table A.14 The analysis conditions of the drop analysis

Drop height		9m
Target		Flat rigid body
Mass of the package (kg)		
Packaging	Body (Stainless steel)	[redacted]
	Lid (Stainless steel)	[redacted]
	Lid bolt (Stainless steel)	[redacted]
Contents	Basket + fuel elements	[redacted] (when the basket for box type fuel such as JRR-3 standard silicide type fuel is contained)
Total mass of the package		23.2 × 10^3
Operating temperature of the materials		
Part		Temperature (°C)
Body		[redacted]
Lid、Lid bolt		[redacted]
Fin		[redacted]

3. Analysis

3.1 Drop direction to analyze

The following directions are considered for drop directions by which the package suffers the most damage.

(i) Vertical drop

- Top vertical drop
- Bottom vertical drop

(ii) Horizontal drop

(iii) Corner drop

(in case the drop point is situated on perpendicular line passing through the gravity center of the package)

- Top corner drop
- Bottom corner drop

(iv) Oblique drop

The oblique drop comes in case between the corner drop and the vertical drop and case between the corner drop and the horizontal drop.

In either case, a part of the drop energy works as rotation moment as the drop point is off the gravity center of package, which will provide mild condition as compared with corner drop, thereby the influence against the package is mitigated.

Therefore, the analysis on the oblique drop is omitted in this paragraph.

3.2 Vertical drop

3.2.1 Top vertical drop

(1) Analytical model

The analytical model for top vertical drop is shown in (II)-Fig.A.48.

Considering its structural symmetry of the package, the one-quarter part of the package is modeled. The content, that is, the basket and the fuel elements, is modeled as homogeneous body.

The total mass of the analytical model is 5.8×10^3 kg, the one-quarter part of the package is modeled.

(2) Results of the analysis

The results of the analysis of top vertical drop are shown in (II)-Fig.A.49 through (II)-Fig.A.52.

(II)-Fig.A.49 and (II)-Fig.A.50 show the deformation of the package and the time history of the displacement of top fins, respectively. As shown in (II)-Fig.A.50, the maximum displacement of the top fin is about [redacted] mm.

(II)-Fig.A.51 and (II)-Fig.A.52 show the time history of the velocity of the package in the drop direction and the deceleration of the package, respectively.

The time history of the deceleration of (II)-Fig.A.52 is a result of filtering with a low path filter of 320Hz according to the advisory material for the IAEA regulations[23]. As shown in this figure, the maximum deceleration (α) is [redacted] g.

$\alpha =$ [redacted] g

[redacted]

(II)-Fig.A.48 Analytical model for 9 m top vertical drop analysis

[redacted]

(II)-Fig.A.49 Deformation of the package when the maximum displacement occurs in 9 m top vertical drop (at 6.9 ms)

[redacted]

(II)-Fig.A.50　Time history of displacement in the drop direction in 9 m top vertical drop

[redacted]

(II)-Fig.A.51 Time history of velocity in the drop direction in 9 m top vertical drop

[redacted]

(II)-Fig.A.52　Time history of deceleration in the drop direction in 9 m top vertical drop

3.2.2 Bottom vertical drop

(1) Analytical model

The analytical model for bottom vertical drop is shown in (II)-Fig.A.53.

Considering its structural symmetry of the package, the one-quarter part of the package is modeled. The content, that is, the basket and the fuel elements, is modeled as homogeneous body.

The total mass of the analytical model is 5.8 × 10^3 kg, because the one-quarter part of the package is modeled.

(2) Results of the analysis

The results of the analysis of bottom vertical drop are shown in (II)-Fig.A.54 through (II)-Fig.A.57.

(II)-Fig.A.54 and (II)-Fig.A.55 show the deformation of the package, and the time history of the displacement of bottom fins, respectively. As shown in (II)-Fig.A.55, the maximum displacement of the bottom fin is about [redacted] mm.

(II)-Fig.A.56 and (II)-Fig.A.57 are the time history of the velocity of the package in the drop direction and the deceleration of the package respectively.

The time history of the deceleration of (II)-Fig.A.57 is a result of filtering with a low path filter (320Hz). As shown in this figure, the maximum deceleration (α) is [redacted] g.

$\alpha =$ [redacted] g

[redacted]

(II)-Fig.A.53 Analytical model for 9 m bottom vertical drop analysis

[redacted]

(II)-Fig.A.54　Deformation of the package when the maximum displacement occurs in 9 m bottom vertical drop (at 4.9ms)

[redacted]

(II)-Fig.A.55 Time history of displacement of top fin in the drop direction in 9 m bottom vertical drop

[redacted]

(II)-Fig.A.56 Time history of velocity in the drop direction in 9 m bottom vertical drop

[redacted]

(II)-Fig.A.57 Time history of deceleration in the drop direction in 9 m bottom vertical drop

3.3 Horizontal drop

(1) Analytical model

The analytical model for horizontal drop is shown in (II)-Fig.A.58.

As shown in the figure, the whole of the package is modeled. The total mass of the analytical model is 23.2 × 10^3 kg.

Initial velocity 13.3 m/s, which is equivalent to the drop from 9 m height, is given to the model in the analysis.

(2) Results of the analysis

The results of the analysis of horizontal drop are shown in (II)-Fig.A.59 through (II)-Fig.A.62.

(II)-Fig.A.59 and (II)-Fig.A.60 show the deformation of the package, and the time history of the displacement of fins, respectively. As shown in (II)-Fig.A.60, the maximum displacement of the top fin and the bottom fin are about [redacted] mm and [redacted] mm, respectively.

(II)-Fig.A.61 and (II)-Fig.A.62 show the time history of the velocity of the package in the drop direction and the deceleration of the package, respectively.

The time history of the deceleration of (II)-Fig.A.61 is a result of filtering with a low path filter (320Hz). As shown in this figure, the maximum deceleration (α) is [redacted] g.

α = [redacted] g

[redacted]

(II)-Fig.A.58　Analytical model for 9 m horizontal drop analysis

[redacted]

(II)-Fig.A.59　Deformation of the package when the maximum displacement occurs in 9 m horizontal drop analysis (at 15.2 ms)

[redacted]

(II)-Fig.A.60 Time history of displacement in the drop direction in 9 m horizontal drop

[redacted]

(II)-Fig.A.61　Time history of velocity in the drop direction in 9 m horizontal drop

[redacted]

(II)-Fig.A.62 Time history of deceleration in the drop direction in 9 m horizontal drop

3.4 Corner drop

3.4.1 Top corner drop

(1) Analytical model

The analytical model for top corner drop is shown in (II)-Fig.A.63.

As shown in the figure, the analytical model is modeled on the whole in the same manner as the analytical model of horizontal drop. The total mass of the analytical model is 23.2×10^3 kg.

Initial velocity 13.3 m/s, which is equivalent to the drop from 9 m height, is given to the model in the analysis.

(2) Results of the analysis

The results of the analysis of top corner drop are shown in (II)-Fig.A.64 through (II)-Fig.A.67.

(II)-Fig.A.64 and (II)-Fig.A.65 are the deformation of the package and the time history of the displacement, respectively. As shown in (II)-Fig.A.65, the maximum displacement of the top fin is [redacted] mm.

(II)-Fig.A.66 and (II)-Fig.A.67 are the time history of the velocity of the package in the drop direction and the deceleration of the package, respectively.

The time history of the deceleration of (II)-Fig.A.67 is a result of filtering with a low path filter (320Hz). As shown in this figure, the maximum deceleration (α) is [redacted] g.

$\alpha =$ [redacted] g

[redacted]

(II)-Fig.A.63 Analytical model for 9 m top corner drop analysis

[redacted]

(II)-Fig.A.64 Deformation of the package when the maximum displacement occurs in 9 m top corner drop analysis (at 20.4 ms)

[redacted]

(II)-Fig.A.65　Time history of displacement in the drop direction in 9 m top corner drop

[redacted]

(II)-Fig.A.66　Time history of velocity in the drop direction in 9 m top corner drop

[redacted]

(II)-Fig.A.67 Time history of deceleration in the drop direction in 9 m top corner drop

3.4.2 Bottom corner drop

(1) Analytical model

The analytical model for bottom corner drop is shown in (II)-Fig.A.68.

As shown in the figure, the analytical model is modeled on the whole in the same manner as the analytical model of horizontal drop. The total mass of the analytical model is 23.2×10^3 kg.

Initial velocity 13.3 m/s, which is equivalent to the drop from 9 m height, is given to the model in the analysis.

(2) Results of the analysis

The results of the analysis of bottom corner drop are shown in (II)-Fig.A.69 through (II)-Fig.A.70.

(II)-Fig.A.69 and (II)-Fig.A.70 are the deformation of the package, and the time history of the displacement, respectively. As shown in (II)-Fig.A.70, the maximum displacement of the bottom fin is [redacted] mm.

(II)-Fig.A.71 and (II)-Fig.A.21 are the time history of the velocity of the package in the drop direction and the deceleration of the package, respectively.

The time history of the deceleration of (II)-Fig.A.72 is a result of filtering with a low path filter (320Hz). As shown in this figure, the maximum deceleration (α) is [redacted] g.

$\alpha=$ [redacted] g

[redacted]

(II)-Fig.A.68　Analytical model for bottom corner drop analysis

[redacted]

(II)-Fig.A.69 Deformation of the package when the maximum displacement occurs in 9 m bottom corner drop analysis (at 17.7 ms)

[redacted]

(II)-Fig.A.70　Time history of displacement in the drop direction in 9 m bottom corner drop

[redacted]

(II)-Fig.A.71　Time history of velocity in the drop direction in 9 m bottom corner drop

[redacted]

(II)-Fig.A.72 Time history of deceleration in the drop direction in 9 m bottom corner drop

A.6.1.1 Vertical drop

This drop test is intended to confirm that the body, the lid and the valve of the packaging retain the sufficient strength and the sufficient containment against the impact force at 9 meters drop test, and further that the basket and fuel element contained in the packaging are clearly free from any deformation.

Two types of the vertical drop is considered. These are top vertical drop and bottom vertical drop. Each maximum deceleration is [redacted] g and [redacted] g, respectively.

As shown in paragraph A.6.1, containment at the contact surface of the lid and the body is directly evaluated based on the results of drop impact analysis. On the other hand, for the contents, that is, basket and fuel elements, these strength are estimated on the assumption that the maximum deceleration from the drop impact analysis acts statically as inertia force.

For the packaging, the strength of the contact surface of the lid and the body, where is the severest part, is evaluated based on the results of drop impact analysis.

On the other hand, for the basket for box type fuel and fuel elements, the strength of contents are evaluated under the bottom vertical drop, because the maximum drop deceleration of the bottom vertical drop is larger than that of the top vertical drop. However, for the basket for MNU type fuel, the strength of content is evaluated under the top vertical drop, which is severer than the bottom vertical drop.

Furthermore, the strength of the valve in the same manner as that of contents is estimated on the assumption that the maximum deceleration from the bottom vertical drop acts statically as inertia force.

Accordingly, this paragraph analyzes the strength of each part during the vertical drop, of which analysis items are shown below.

1. Containment at the contact surface of the lid and the body
    - 1.1 Top vertical drop
    - 1.2 Bottom vertical drop
2. Strength of the valve
3. Strength of the baskets
    - 3.1 Basket for box type fuel
    - 3.2 Basket for MNU type fuel
4. Strength of the fuel elements

4.1 JRR-3 standard silicide type fuel

4.2 JRR-3 follower silicide type fuel

4.3 JRR-3 MNU type fuel

1. Containment at the contact surface of the lid and the body

The inertia force acts on the lid flange where the lid has the groove of O-ring at the time of top vertical drop. There is a possibility that the groove of O-ring is crushed, and the containment may be damaged. Therefore, in this paragraph, the behavior of plastic displacement of the portion is calculated, and it examines that the containment is maintained.

1.1 Top vertical drop

(II)-Fig.A.73 and (II)-Fig.A.74 show the distribution of the equivalent plastic strain generated on the lid flange and on the body flange after top vertical drop, respectively. From these figures, it is clear that the plastic strain is not generated on the gasket portion of these flanges, where are in the state of elasticity.

(II)-Fig.A.75 shows the time history of axial stress on the lid bolt during top vertical drop. As shown in this figure, although the stress of the lid bolt is decreased from the initial fastening stress [redacted] MPa to about [redacted] MPa due to the displacement of the flanges during impact, and then increased to maximum [redacted]MPa, it is restored after impact to the initial fastening stress [redacted]MPa.

Therefore, the containment of the packaging is maintained at the time of top vertical drop.

[redacted]

(II)-Fig.A.73　Equivalent plastic strain generated in the lid flange after top vertical drop

[redacted]

(II)-Fig.A.74　Equivalent plastic strain generated in the body flange after top vertical drop

[redacted]

a

(II)-Fig.A.75　Time history of the axial stress in the lid bolt during 9 m top vertical drop

1.2 Bottom vertical drop

(II)-Fig.A.76 and (II)-Fig.A.77 show the distribution of the equivalent plastic strain generated on the lid flange and on the body flange after bottom vertical drop, respectively. From these figures, it is clear that the plastic strain is not generated on the gasket portion of these flanges, where are in the state of elasticity.

(II)-Fig.A.78 shows the time history of axial stress on the lid bolt during bottom vertical drop. As shown in this figure, although the stress of the lid bolt is decreased from the initial fastening stress [redacted] MPa to about [redacted] MPa due to the displacement of the flanges during impact and then increased to maximum [redacted] MPa, it is restored after impact to the initial fastening stress [redacted]MPa.

Therefore, the containment of the packaging is maintained at the time of bottom vertical drop.

[redacted]

(II)-Fig.A.76 Equivalent plastic strain generated in the lid flange after bottom vertical drop

[redacted]

(II)-Fig.A.77　Equivalent plastic strain generated in the body flange after bottom vertical drop

[redacted]

(II)-Fig.A.78　Time history of the axial stress in the lid bolt during 9 m bottom vertical drop

2. Strength of the valve

For the bottom vertical drop, of which the maximum deceleration is larger than that of the top vertical drop, the strength of the drain valve should be evaluated.

As shown in (II)-Fig.A.79, the drain valve is installed by 57 degree inclination to the vertical surface. Therefore, the maximum deceleration that acts in the direction of the axis of the bolt is less than the maximum deceleration ([redacted] g) at the time of the bottom vertical drop. Hereafter, the strength of the drain valve is evaluated conservatively as that the [redacted] g of the maximum deceleration acts on the valve.

Deformation of the fin at the time of bottom vertical drop is as small as about [redacted]mm and the valve itself never contact with the target directly. However, the impact force may act on the main bolt of the drain valve and the valve protection cover bolt. In this paragraph, it is shown that the main bolt of the drain valve and the protection cover bolt have with the sufficient strength against the impact force.

At first, the examination is made on the valve main bolt. The valve main bolt is as shown in (II)-Fig.A.80.

[redacted]

(II)-Fig.A.79 Drain valve

The bolt constants ([redacted]) of the main bolt are as follows;

- Average diameter ………………………………………………[redacted] mm
- Minor diameter …………………………………………………[redacted]mm
- Cross-sectional area ……………………………………………[redacted] mm²
- Engagement length of thread with the body ……………[redacted] mm

The mass of the vent valve (excluding the valve protection cover) is [redacted] kg and the deceleration is [redacted] g.

Since the number of valve main bolts is [redacted], the total area (S) subjected to the shearing force is given as follows;

$$S = (\pi \times [redacted] \times [redacted]) \times [redacted] = [redacted] \ (\mathrm{mm}^2)$$

Consequently, the shearing stress (τ) is as follows;

$$\tau = [redacted] = [redacted] \ \mathrm{MPa}$$

In this case, the bolt temperature is [redacted]°C, however, the allowable shearing stress (τ_a) at 70°C is used conservatively as follows;

$$\tau_a = 0.6 \times \sigma_y = 0.6 \times [redacted] = [redacted] \ \mathrm{MPa}$$

[redacted]

II)-Fig.A.80 Valve main bolt

Consequently, the safety factor (RF) and the safety margin (MS) are as follows;

RF = [redacted] = [redacted]

M.S = [redacted] − 1 = [redacted]

As a result of the above, the valve main bolt has the sufficient shearing strength.

Then, the examination is made on the valve protection cover bolt. The valve protection cover bolt is shown in (II)-Fig.A.81.

The bolt constants ([redacted]) of the valve protection cover bolt are as follows;

- Mean diameter ······································ [redacted] mm
- Minor diameter ····································· [redacted] mm
- Cross-sectional area ······························ [redacted] mm^2
- Engagement length of thread with the body ··········· [redacted] mm

The mass of valve protection cover (including fin) is [redacted] kg, and the deceleration is [redacted] g.

Since the number of valve protection cover bolts is [redacted], the total area (S) subjected to the shearing force is given as follows;

S = (π × [redacted] × [redacted]) × [redacted] = [redacted] (mm^2)

Accordingly, the shearing force (τ) is given as follows;

τ= [redacted] = [redacted] MPa

The allowable shearing stress (τ_a) of bolt at the operating temperature at 70℃ is given as follows;

τ_a = 0.6 × [redacted] = [redacted] MPa

Therefore, the safety factor (RF) and the safety margin (MS) are given as follows;

RF = [redacted] = [redacted]

M.S = [redacted] − 1 = [redacted]

Therefore, the valve protection cover bolt has the sufficient shearing strength.

[redacted]

(II)-Fig.A.81　Valve protection cover bolt

3. Strength of the baskets

When the package falls in the vertical attitude, the inertia force due to impact acts on the basket.

The calculation is made on the stress of the basket in this case to indicate that it is clearly free from any plastic deformation and elastic buckling, and further that the neutron poison is not crushed.

The inertia force of the basket is given by the following equation.

$$F = W_B \cdot g \cdot G_v$$

where, F : Inertia force of the basket (N)

W_B : Mass of the basket (kg)

g : Gravitational acceleration (m/sec^2)

G_v : Impact deceleration (g)

When the inertia force is applied to the vertical direction, the compressive force is generated in the basket.

The stress is expressed by the following equation;

$$\sigma_c = \frac{F}{A}$$

where, σ_c : Compressive stress : (MPa)

F : Inertia force on the basket : (N)

A : Pressure area of basket to the vertical direction : (mm^2)

Consequently, the following is given;

$$\sigma_c = \frac{W_B \cdot g \cdot Gv}{A}$$

Now, the critical buckling stress of the basket is shown further on.

The critical buckling stress on the thin tube having a square section is given by the following equation[16].

$$\sigma_{cr} = \frac{k \pi^2 E}{12(1 - \nu^2)} \cdot \left(\frac{t}{a}\right)^2$$

where, σ_{cr} : Critical buckling stress (MPa)

k : Buckling coefficient

E : Modulus of longitudinal elasticity (MPa)

ν : Poisson's ratio

a : Length of one side on square section (mm)

t : Thickness (mm)

3.1 Strength of the basket for box type fuel

3.1.1 Strength of the basket

When the package falls in the vertical attitude, the compressive force occurs in the basket due to inertia force of drop.

The compressive force (σ_c) is expressed by the following equation.

$$\sigma_c = \frac{F}{A} = \frac{W_B \cdot g \cdot Gv}{A}$$

where, σ_c : Compressive force (MPa)

A : Pressure area of the basket to the vertical direction =[redacted](mm^2)

F : Inertia force on the basket =$W_B \cdot g \cdot G_v$ (N)

W_B : Mass of the basket for box type fuel =[redacted] (kg) (See (II)-Table A.2)

g : Gravitational acceleration = 9.8 (m/sec^2)

G_v : Impact deceleration = [redacted] (g) (Refer to (II)-A.6.1, paragraph 3.2.2)

Therefore, the compressive force (σ_c) on the basket is given as follows;

$\sigma_c =$ [redacted] = [redacted] MPa

In this case, the allowable compressive stress (σ_{ca}) at the operating temperature ([redacted]℃) of the basket is as follows;

$\sigma_{ca} = 1.5 \times \sigma_{dy} = 1.5 \times$ [redacted] = [redacted] MPa

Consequently, the safety factor (RF) and the safety margin (MS) of the basket against plastic deformation due to the vertical drop are as follows;

RF = [redacted] = [redacted]

MS = [redacted] − 1 = [redacted]

Therefore, the plastic deformation never occur in the basket for box type fuel.

The critical buckling stress of the basket is to be then found.

k= 4

E= [redacted] MPa

ν = [redacted]

a = [redacted] mm

t = [redacted] mm (The smallest thickness ([redacted] mm) is used on the safe side.)

The critical buckling stress (σ_{cr}) is given as follows;

$$\sigma_{cr} = \frac{k \pi^2 E}{12(1-\nu^2)} \cdot \left[\frac{t}{a}\right]^2$$

= [redacted] × [redacted]^2 = [redacted] Mpa

In this case, the compressive stress (σ_c) of basket generated due to inertia force in this case is as follows;

σ_c = [redacted] MPa

Accordingly, the safety factor (RF) and the safety margin (MS) against buckling are as follows;

RF = [redacted] = [redacted]

M.S = [redacted] − 1 = [redacted]

Therefore, no buckling will occur in the basket for box type fuel due to the vertical drop. In addition, as shown in "(I) C. Transport Container," the neutron absorber is surrounded by basket dividers, which means it will not be crushed and have no effect on subcriticality.

3.2 Strength of the basket for MNU type fuel

The basket for MNU fuel is constructed as shown (II)-Fig.A.82.

As is apparent from the figure, the support plate is welded to the square shape pipe with the throat of 2 mm, and the height of guide plate is higher than the square shape pipe. Therefore, the pressure to the vertical direction acts on the guide plate.

For the guide plate, and the weld zone between the square shape pipe and the support plate, these strength are evaluated on the assumption that the maximum deceleration from the top vertical drop impact analysis acts statically as inertia force because the top vertical drop is structurally severer than the bottom vertical drop in these parts.

3.2.1 Strength of the guide plate

When the package falls in the vertical direction, the compressive stress is generated in the guide plate due to inertia force resulting from total mass of basket.

The compressive stress (σ_c) is given by the following equation.

$$\sigma_c = \frac{F}{A} = \frac{W_B \cdot g \cdot Gv}{A}$$

where, σ_c : Compressive stress (MPa)

A : Pressure area of the guide plate to vertical direction = [redacted] (mm^2)

F : Inertia force on the basket= $W_B \cdot g \cdot G_v$ (N)

W_B : Mass of the basket for MNU type fuel= [redacted] (kg)

g : Gravitational acceleration (m/sec^2)= 9.8 (m/sec^2)

G_v : Impact deceleration= [redacted] (g)

Therefore, the compressive stress (σ_c) on the guide plate is given as follows;

σ_c = [redacted] = [redacted] MPa

In this case, the allowable compressive stress (σ_{ac}) of basket at operating temperature of [redacted]℃ is given as follows;

$\sigma_{ac} = 1.5 \times \sigma_{dy} = 1.5 \times$ [redacted] = [redacted] MPa

Therefore, the safety factor (RF) and the safety margin (MS) of the basket are as follows;

RF = [redacted] = [redacted]

MS= [redacted] − 1 = [redacted]

Consequently, no plastic deformation occurs in the guide plate of the basket for MNU type fuel due to the drop.

[redacted]

(II)-Fig.A.82 Basket for MNU fuel type

3.2.2 Strength of the weld zone between the square shape pipe and the support plate

When the package falls in the vertical direction, the shearing vertically stress occurs at the weld zone between the square shape pipe and the support plate of the basket.

For the analysis, the evaluation is made on the shearing stress at the welds of a-b-c-d-e which is generated due to the inertia force of the square shape pipe encircled by a, b, c, d, e and f, as shown in (II)-Fig.A.81.

This shearing stress (τ) is given by the following equation;

$$\tau = \frac{F}{A} = \frac{W_B \cdot g \cdot Gv}{\ell \cdot d}$$

where, τ : Shearing stress at the weld zone (MPa)

A : Cross-sectional area of the bead weld = $\ell \cdot d$ (mm^2)

ℓ : Weld length (welding upper/lower parts of box pipe)

= 46 × 14 × 2 = 1288(mm)

d : Throat (mm) = 2 (mm)

F : Inertia force (N) on the weld zone ($W_B \cdot g \cdot G_v$)

W_B : Mass of the square shape pipe encircled by a,b,c,d,e and f

= [redacted] = [redacted] (kg)

g : Gravitational acceleration = 9.8 (m/sec^2)

G_v : Impact deceleration = [redacted] (g)

Accordingly, the shearing stress (τ) on the weld zone is given as follows;

τ = [redacted] = [redacted] MPa

The allowable shearing stress (τ_a) of the basket at the operating temperature of [redacted]°C is given as follows;

$\tau_a = 0.6 \times \sigma_u \times \eta$ = 0.6 × [redacted] × 0.70 = [redacted] MPa

Therefore, the safety factor (RF) and the safety margin (MS) at weld are as follows;

RF = [redacted] = [redacted]

MS = [redacted] − 1 = [redacted]

Therefore, the weld zone between the square shape pipe and the support plate of the basket for MNU type fuel has the sufficient strength against the shearing stress due to vertical drop.

4.1 Strength of JRR-3 standard silicide type fuel

The inertia force due to the vertical drop acts on the fuel element. This paragraph shows that the fuel side plate has the sufficient strength enough to be resistible against the such inertia force, and further that the fuel plate never fall.

4.1.1 Strength of the fuel side plate

The compressive stress (σ_c) generated at the fuel side plate due to drop is given by the following equation.

$$\sigma_c = \frac{F}{A} = \frac{W \cdot g \cdot Gv}{A}$$

where, σ_c : Compressive stress (MPa)

A : Pressure area of the fuel side plate to the vertical direction

= [redacted] = [redacted] (mm^2)

F : Inertia force of the fuel element = $W \cdot g \cdot G_v$ (N)

W : Mass of the fuel element = [redacted] (kg)

g : Gravitational acceleration = 9.8 (m/sec^2)

G_v : Impact deceleration = [redacted] (g)

Consequently, the compressive stress (σ_c) on the fuel side plate is as follows;

$\sigma_c =$ [redacted] = [redacted] MPa

In this case, the yield stress (σ_y) of [redacted] MPa of material A[redacted] is used, since the yield stress of material A[redacted] at the temperature of [redacted]℃ is smaller than that of material A[redacted] as shown in (II)-Fig.A.6.

Therefore, the allowable compressive stress (σ_{ac}) of fuel element of the temperature of [redacted]℃ is given as follows;

$\sigma_{ac} = 1.5 \times \sigma_y = 1.5 \times$ [redacted] = [redacted] MPa

Therefore, the safety factor (RF) and the safety margin (MS) are as follows;

RF = [redacted] = [redacted]

MS= [redacted] − 1 = [redacted]

Therefore, the fuel side plate has the sufficient strength against the compressive stress due to the vertical drop.

4.1.2 Evaluation of the fuel plate for falling

The fuel plate is fixed to two fuel side plates by using "roll swage" method.

The impact force (F) applied to the fuel plate due to the vertical drop is given by the following equation;

$$F = W \times g \times G_v$$

where,

W : Mass of fuel element = [redacted] (kg)

G_v : Maximum deceleration at the time of vertical drop = [redacted] (g)

Consequently, the following is given;

F = [redacted] × 9.8 × [redacted] = [redacted] N

On the other hand, the anchoring force (F_r) of fuel plate fixed to the fuel side plate by using "roll swage" method is given as follows;

$$F_r = n \cdot L \cdot q$$

where,

n : Number of fuel plate = [redacted] (pieces)

L : Length of the fuel plate = [redacted] (mm)

q : Anchoring force of the fuel plate for each unit length in the fuel production specification = more than [redacted](N/mm)

Consequently, the following is given;

F_r = [redacted] = [redacted] N

Therefore, the safety factor (RF) and the safety margin (MS) against fixation of the fuel plate are as shown below;

$RF = \frac{F_r}{F}$ = [redacted] = [redacted]

MS= [redacted] − 1 = [redacted]

Therefore, the fuel plate is retained without falling.

4.2 Strength of JRR-3 follower silicide type fuel

The inertia force due to the vertical drop acts on the fuel element in the same manner as JRR-3 standard silicide type fuel element. This paragraph shows that the fuel side plate has the sufficient strength enough to be resistible against the such inertia force, and further that the fuel plate never fall.

4.2.1 Strength of the fuel side plate

The compressive stress (σ_c) generated at the fuel side plate due to drop is given by the following equation.

$$\sigma_c = \frac{F}{A} = \frac{W \cdot g \cdot Gv}{A}$$

where, σ_c : Compressive stress (MPa)

A : Pressure area of the fuel side plate to the vertical direction

= [redacted] = [redacted] (mm^2)

F : Inertia force of the fuel element = $W \cdot g \cdot G_v$ (N)

W : Mass of the fuel element = [redacted] (kg)

g : Gravitational acceleration = 9.8 (m/sec^2)

G_v : Impact deceleration = [redacted] (g)

Consequently, the compressive stress (σ_c) on the fuel side plate is as follows;

$\sigma_c =$ [redacted] = [redacted] MPa

In this case, the yield stress (σ_y) of [redacted] MPa of material A[redacted] is used, since the yield stress of material A[redacted] at the temperature of [redacted]℃ is smaller than that of material A[redacted] as shown in (II)-Fig.A.6.

Therefore, the allowable compressive stress (σ_{ac}) of fuel element of the temperature of [redacted]℃ is given as follows;

$\sigma_{ac} = 1.5 \times \sigma_y = 1.5 \times$ [redacted] = [redacted] MPa

Therefore, the safety factor (RF) and the safety margin (MS) are as follows;

RF = [redacted] = [redacted]

MS= [redacted] $-1=$ [redacted]

Therefore, the fuel side plate has the sufficient strength against the compressive stress due to the vertical drop.

4.2.2 Evaluation of the fuel plate for falling

The fuel plate is fixed to two fuel side plates by using "ro11 swage" method.

The impact force (F) applied to the fuel plate due to the vertical drop is given by the following equation;

$$F = W \times g \times G_v$$

where,

W : Mass of fuel element = [redacted] (kg)

G_v : Maximum deceleration at the time of vertical drop = [redacted] (g)

Consequently, the following is given;

F = [redacted] × 9.8 × [redacted] = [redacted] N

On the other hand, the anchoring force (F_r) of fuel plate fixed to the fuel side plate by using "roll swage" method is given as follows;

$$F_r = n \cdot L \cdot q$$

where,

n : Number of fuel plate = [redacted] (pieces)

L : Length of the fuel plate = [redacted] (mm)

q : Anchoring force of the fuel plate for each unit length in the fuel production specification = more than [redacted] (N/mm)

Consequently, the following is given;

F_r = [redacted] = [redacted] N

Therefore, the safety factor (RF) and the safety margin (MS) against fixation of the fuel plate are as shown below;

$RF = \frac{F_r}{F}$ = [redacted] = [redacted]

MS= [redacted] − 1 = [redacted]

Therefore, the fuel plate is retained without falling.

4.3 Strength of JRR-3 MNU type fuel

As the geometry of the JRR-3 MNU type fuel, there are two types of top/middle fuel element and bottom fuel element which are identical in shape as shown in (I)-Fig.D.3 and (I)-Fig.D.4. Since the top/middle fuel elements shown in (II)-Fig.A.83 are severe from the view point of stress as compared with the bottom fuel element, this paragraph shows the stress calculation on the top/middle fuel elements of this type.

In addition, the examination was made on the drop to two directions of A and B as shown in (II)-Fig.A.83.

The material characteristics used for calculation are shown in (II)-Table A.15.

The analysis was performed by using the structural analysis program ABAQUS.

The analytical model was handled as a symmetric problem with respect to the Z-axis.

(II)-Table A.15 Material characteristics of JRR-3 MNU type fuel

Material	Density (kg/m^3)	Modulus of longitudinal elasticity [MPa]	Poisson's ratio	Yield stress [MPa] [redacted]℃)
Aluminum alloy (A[redacted])	[redacted]	[redacted]	0.3	[redacted] *3
Aluminum alloy (A[redacted])	[redacted]	[redacted]	0.3	[redacted] *1
Metallic natural Uranium *2	[redacted]	[redacted]	0.23	[redacted]

Note : Based on JIS for items marked "＊"

＊1 ・・・ Based on "Aluminum handbook"

＊2 ・・・ Based on "Atomic energy handbook"

＊3 ・・・ Based on "SUMITOMO aluminum handbook"

[redacted]

(II)-Fig.A.83　Geometry of JRR-3 MNU type fuel

4.3.1 Drop to the A-direction

The boundary conditions for the drop to the A-direction and the stress at the drop impact deceleration of [redacted] g are shown in (II)-Fig.A.84 and (II)-Fig.A.85, respectively.

As a result of the analysis, the maximum stresses of aluminum cladding, end plug and metallic natural uranium are [redacted] MPa, [redacted] MPa, and [redacted] MPa, respectively.

As the allowable compressive stress in this case is 1.5 times the yield stress, the safety factor (RF) and the safety margin (MS) at each part of JRR-3 MNU type fuel are as shown in (II)-Table A.16.

As shown in the table, the JRR-3 MNU type fuel has the sufficient strength against the vertical drop to the A-direction.

(II)-Table A.16 Maximum stress, safety factor and safety margin of JRR-3 MNU type fuel for the drop to A-direction

	Maximum stress [MPa]	Allowable compressive stress [MPa]	Safety factor (RF)	Safety margin (MS)
Aluminum cladding	[redacted]	[redacted]	[redacted]	[redacted]
End plug	[redacted]	[redacted]	[redacted]	[redacted]
Metallic natural uranium	[redacted]	[redacted]	[redacted]	[redacted]

[redacted]

(II)-Fig. A.84　Boundary condition for drop to the A-direction

[redacted]

(II)-Fig.A.85 Stress for drop to the A-direction

4.3.2 Drop to the B-direction

The boundary conditions for the drop to the B-direction and the stress at drop impact acceleration of [redacted] g are shown in (II)-Fig.A.86 and (II)-Fig.A.87, respectively.

The maximum stresses of aluminum cladding, end plug and metallic natural uranium are [redacted] MPa, [redacted] MPa and [redacted] MPa, respectively.

As the allowable compressive stress in this case is 1.5 times of the yield stress, the safety factor (RF) and the safety margin(MS) at each part of the JRR-3 MNU type fuel are as shown in (II)-Table A.17.

As shown in the table, the JRR-3 MNU type fuel has the sufficient strength against the vertical drop to the B-direction.

(II)-Table A.17 Maximum stress, safety factor and safety margin of JRR-3 MNU type fuel for the drop to B-direction

	Maximum stress [MPa]	Allowable compressive stress [MPa]	Safety factor (RF)	Safety Margin (MS)
Aluminum cladding	[redacted]	[redacted]	[redacted]	[redacted]
End plug	[redacted]	[redacted]	[redacted]	[redacted]
Metallic natural uranium	[redacted]	[redacted]	[redacted]	[redacted]

[redacted]

(II)-Fig.A.86　Boundary condition for drop to the B-direction

[redacted]

(II)-Fig.A.87　Stress for drop to the B-direction

A.6.1.2 Horizontal drop

In this paragraph, it is shown that the body, the lid and the valve of the packaging retain the sufficient strength and the sufficient containment and further the basket and the fuel elements contained in the packaging have the sufficient strength against the impact force when the package drops in the horizontal attitude from 9 m in height.

These strengths are evaluated in the same manner as the vertical drop of the packaging. That is, the strength of the contact surface of the lid and the body, where is the severest part of the packaging, is directly evaluated based on the results of drop impact analysis. On the other hand, for the contents, that is, basket and fuel elements, these strengths are estimated on the assumption that the maximum deceleration from the drop impact analysis acts statically as inertia force.

Furthermore, the strength of the valve, in the same manner as that of contents, is estimated on the assumption that the maximum deceleration acts statically as inertia force.

The impact deceleration of [redacted] g (Refer to (II)-A.6.1 3.3) is used for the analysis, which is applied to each part of the package. The analysis items are as shown below;

1. Containment at the contact surface of the lid and the body
2. Strength of the valve
3. Strength of the baskets
    - 3.1 Basket for box type fuel
    - 3.2 Basket for MNU type fuel
4. Strength of the fuel elements
    - 4.1 JRR-3 standard silicide type fuel
    - 4.2 JRR-3 follower silicide type fuel
    - 4.3 JRR-3 MNU type fuel

1. Containment at the contact surface of the lid and the body

It is examined that the containment at the contact surface of the lid and the body is maintained during the horizontal drop.

(II)-Fig.A.88 and (II)-Fig.A.89 show the distribution of the equivalent plastic strain generated on the lid flange and on the body flange after horizontal drop, respectively. These figures show that the plastic strain is not generated on the gasket portion of these flanges, where are in the state of the elasticity.

(II)-Fig.A.90 shows the time history of axial stress in the lid bolt. As shown in (II)-Fig.A.90, the maximum stress of the lid bolt occurs in that of the vicinity where the package collides with target during impact. The value is [redacted] MPa, and is less than with the yield stress [redacted] MPa of the lid bolt. The stress becomes in the state of the initial fastening stress after impact.

Therefore, the containment of the packaging is maintained at the time of horizontal drop.

[redacted]

(II)-Fig.A.88　Equivalent plastic strain generated in the lid flange after horizontal drop

[redacted]

(II)-Fig.A.89 Equivalent plastic strain generated in the body flange after horizontal drop

[redacted]

(II)-Fig.A.90　Time history of axial stress in the lid bolt during 9 m horizontal drop

2. Strength of the valve

The vent valve and the drain valve are embedded in the body of packaging as shown in (I)-Fig.C.4.

Since they are covered with the protection cover and prepared at the groove among the fins, they do not make direct contact with the target when the package drops in the horizontal attitude. However, the impact force due to the drop will occurs in the main bolts and the valve protection cover bolt of the vent valve and the drain valve.

This paragraph shows that these bolts have the sufficient strength against the impact force.

The examination is made at first on the valve main bolt, which is shown in (II)-Fig.A.91.

The bolt constants ([redacted]) of the valve main bolt are as follows;

- Mean diameter .... [redacted] mm
- Minor diameter .... [redacted] mm
- Cross-sectional area .... [redacted] mm^2

The mass of the vent valve (excluding the valve protection cover) is [redacted]kg, and the impact deceleration is [redacted] g.

Since the number of valve main bolts is 6, the total area (S) to be subjected to shearing force is given as follows;

S = [redacted] × [redacted] = [redacted] (mm^2)

Consequently, the shearing stress (τ) is given as follows;

$$\tau = \frac{F}{S} =$$ [redacted] = [redacted] MPa

The bolt temperature is [redacted] ℃, however, the allowable shearing stress (τ_a) of bolt at [redacted] ℃ is conservatively given as follows ;

$\tau_a = 0.6 \times \sigma_y = 0.6 \times$ [redacted] = [redacted] MPa

Consequently, the safety factor (RF) and the safety margin (MS) are as follows;

RF = [redacted] = [redacted]

MS = [redacted] − 1 = [redacted]

[redacted]

(II)-Fig.A.91　Valve main bolt

Therefore, the valve main bolt has the sufficient strength against the shearing stress.

The examination is made then on the valve protection cover bolt.

The valve protection cover of the vent valve is provided with no fin, but the valve protection cover of the drain valve is provided with fins.

Therefore, the consideration is conservatively made on the valve protection cover bolts of the drain valve provided with the fins when considering the strength of valve protection cover bolt.

The valve protection cover bolt is shown in (II)-Fig.A.92.

The valve constants ([redacted]) of the valve protection cover bolt are as follows;

- Mean diameter ·· [redacted]mm
- Minor diameter ·· [redacted]mm
- Cross-sectional area ·································· [redacted] mm^2

The mass of the valve protection cover (including the fins) is [redacted]kg, and the impact deceleration is [redacted] g.

Since the number of valve protection cover bolts is 6, the total area (S) to be subjected to shearing stress is given as follows;

S = [redacted] = [redacted] (mm^2)

Consequently, the shearing stress (τ) is given as follows;

$$\tau = \frac{F}{S} = \text{[redacted]} = \text{[redacted]} \text{ MPa}$$

The bolt temperature is [redacted] ℃, however, the allowable shearing stress (τ_a) at [redacted] ℃ is conservatively given as follows;

$\tau_a = 0.6 \times \sigma_y = 0.6 \times$ [redacted] = [redacted] MPa

Consequently, the safety factor (RF) and the safety margin (MS) are given as follows;

RF = [redacted] = [redacted]

MS = [redacted] − 1 = [redacted]

Therefore, the valve protection cover bolt has the sufficient shearing strength.

[redacted]

(II)-Fig.A.92 Valve protection cover bolt

3. Strength of the baskets

When the package drop in the horizontal attitude, the basket is subjected to the inertia force due to the basket and the fuel elements contained in the basket. This paragraph shows the evaluation of the stress generated on the basket during horizontal drop.

To examine the strengths of the partition plate and the compartment plate of the basket for the box type fuel in the horizontal drop to the X-direction, which is sever case, the elastic-plastic stress analysis for the basket is performed using the general-purpose finite element code ABAQUS.

As the material property (SA-240 [redacted]) used in the analysis, in the same manner as that of the body and lid used in the drop analysis, the static stress-strain curve, which is obtained by means of equation ② shown in Appendix (II)-A.10.1, is used. Since the value in the equation ② is at room temperature, the stress in the stress-strain curve used in the analysis is modified as follows;

The stress used for analysis is equal to the stress in the equation ② multiplied by the ratio (=Yield stress at operating temperature / Yield stress at room temperature).

3.1 Basket for box type fuel

3.1.1 Strength of the compartment plate and the partition plate

The stress calculation for the horizontal drop of the basket for box type fuel is made for case when the basket drops to two directions of the X-direction and the Y-direction as shown in (II)-Fig.A.93.

The stress calculation for the basket is made by using the general-purpose finite element program ABAQUS.

The analysis is also made on the shearing strength at the weld zone between the compartment plate and the partition plate.

[redacted]

(II)-Fig.A.93 Horizontal drop direction of the basket for box type fuel

a) Strength for the drop to the X-direction

In the analysis, the inertia force of the basket itself, the fuel element and the neutron poisons generated by the deceleration are taken into.

The partition plate and the compartment plate are modeled with the shell element. As the mass of the fuel element in the analysis, the largest mass of standard type fuel element is used. JRR-3 standard silicide type fuel is assumed as a representative.

The partition plate and the compartment plate are modeled with the shell element. As the mass of the furl element in the analysis, the largest mass of standard type fuel element is used. It is assumed JRR-3 standard silicide type fuel as a representative. The fuel element, whose cross-sectional form is a rectangle [redacted]mm×[redacted]mm), is modeled with the solid element that has equivalent stiffness.

The equivalent stiffness E_{eq} is obtained by the following equation;

$$E_{eq} = E \times \frac{A_1}{A_2}$$

Where, E : Modulus of longitudinal elasticity of aluminum alloy ([redacted] at[redacted]C [redacted](MPa)

A_1 : Cross-sectional area of aluminum alloy in the cross-section of the fuel element [redacted](mm²)

A_2 : Rectangular cross-sectional area of the fuel element modeled 5.81×10^3 (mm²)

Consequently, the following is given;

E_{eq} =[redacted]×[redacted]

$= 1.74 \times 10^4$ MPa

The analytical model is shown in (II)-Fig.A.94.

The analysis results are shown in (II)-Fig.A.95 through (II)-Fig. A. 97.

(II)-Fig.A.95 and (II)-Fig.A.96 are the deformation in the state where deceleration[redacted]g is acting and after deceleration[redacted]g acting, respectively. The maximum displacement values in the state where deceleration is acting and after deceleration acting are[redacted]mm and[redacted]mm, respectively.

(II)-Fig.A.97 shows the equivalent plastic strain distribution in the state where deceleration [redacted] g is acting.

As shown in this figure, the maximum plastic strain occurs in portion A and the value is about [redacted]%. This value is smaller than the elongation of the material ([redacted]%).

Therefore, the partition plate and the compartment plate have the sufficient strength against horizontal drop.

[redacted]

(II)-Fig.A.94　Analytical model of the basket for box type fuel at the X-direction drop

[redacted]

(II)-Fig.A.95　Deformation of the basket for box type fuel when deceleration [redacted] g is acting

[redacted]

(II)-Fig.A.96 Deformation of the basket for box type fuel after deceleration [redacted] g acting

[redacted]

[redacted]

(Strain of lower surface)

(Strain of upper surface)

(II)-Fig.A.97 Equivalent plastic strain generated in the basket for box type fuel after deceleration [redacted] g acting

b) Strength for the drop to the Y-direction

Strength evaluation at the Y-direction drop is carried out. In the analysis, it is modeled in the same manner as the X-direction drop. Namely, the partition plate and the compartment plate are modeled with the shell element, and the fuel element, whose cross-sectional form is a rectangle ([redacted]), is modeled with the solid element that has equivalent stiffness. As the mass of the fuel element in the analysis, the largest mass of standard type fuel element is used. JRR-3 standard silicide type fuel is assumed as a representative.

The equivalent stiffness E_{eq} is also same as the X-direction drop.

The analytical model is shown in (II)-Fig.A.98.

The analysis results are shown in (II)-Fig.A.99.

All the generated stresses are in the state of the elasticity and the maximum compressive stress occurs on portion (a) in (II)-Fig.A.99.

The value is;

σ_{max} = [redacted] MPa

In this case, the allowable compressive stress (σ_{ac}) of the partition plate at the operating temperature of [redacted] ℃ is given as follows ;

$\sigma_{ac} = 1.5 \times \sigma_{dy} = 1.5 \times$ [redacted] = [redacted] MPa

Consequently, the safety factor (RF) and the safety margin (MS) of the partition plate are as follows;

RF = [redacted] = [redacted]

MS = [redacted] − 1 = [redacted]

Therefore, no plastic deformation occurs on the basket for the box type fuel in the horizontal drop to the Y-direction, and thus no influence is brought about to the subcriticality.

[redacted]

(II)-Fig.A.98　Analytical model of the basket for box type fuel at the Y-direction drop

[redacted]

(II)-Fig.A.99 Result of stress analysis of the basket for box type fuel at the Y-direction drop

c) Shearing strength at the weld zone between the compartment plate and the partition plate

As shown in (II)-Fig.A.100, the shearing stress at the weld zone due to the drop to the Y-direction is severe as compared with that to the X-direction. The examination is made on the weld zone at such part.

The shearing stress (τ) due to the dead weight of the fuel element and the partition plate is given as follows ;

$$\tau = \frac{(W_1+W_2)\cdot g\cdot G_H}{A}$$

where, τ : Shearing stress (MPa)

W_1 : Mass of one fuel element = 8(kg)

W_2 : Mass of one partition plate (Refer to (II)-Fig.A.100)

[redacted] = [redacted] (kg)

A : Welding cross-sectional area of the partition plate

= [redacted] = [redacted] (mm^2)

g : Gravitational acceleration = 9.8 (m/sec^2)

G_H : Impact deceleration = [redacted] (g)

Consequently, the following is given;

τ = [redacted] = [redacted] MPa

In this case, the allowable shearing stress (τ_a) of the partition plate at the operating temperature of [redacted]℃ is given as follows ;

$\tau_a = 0.6\times\sigma_{dy}\times\eta$ = 0.6× [redacted] ×0.70 = [redacted] MPa

Consequently, the safety factor (RF) and the safety margin (MS) of the partition plate are as follows;

RF = [redacted] = [redacted]

MS = [redacted] − 1 = [redacted]

Therefore, no significant deformation occurs at the weld zone and thus no influence is brought to the subcriticalty.

[redacted]

(II)-Fig.A.100 Analytical model at the weld zone of the basket for box type fuel

3.1.2 Strength of the weld zone in the basket frame

When the package drops in the horizontal attitude, the bending stress due to the impact force occurs at the weld zone of the basket.

This paragraph shows that no significant deformation due to bending stress occurs in the weld zone of the frame.

Since the basket frame is welded at the throat of [redacted] mm, the ring with thickness of [redacted] mm is to be considered as an analytical model for the weld zone of the basket frame as shown in (II)-Fig.A.101.

The maximum bending stress (σ_{bmax}) generated due to horizontal drop is given by the following equation;

$$\sigma_{bmax} = \frac{M_{max}}{1} \cdot \frac{t}{2}$$

where, σ_{bmax} : Maximum bending stress[14] (MPa)

Mmax: Maximum bending moment

(generated point (A) shown in (II)-Fig.A.101)

$$= \frac{3}{2} f R^2$$

f : Uniform load acting on the circumference of the basket frame (N/mm²) $= \dfrac{W \cdot g \cdot GH}{2\pi R}$

R : Radius of the basket frame = [redacted] (mm)

W : Mass per unit length of the basket plus the fuel element (kg/mm)

(Refer to (II)-Table A.2)

Mass of the basket plus the fuel element

= [redacted] = [redacted] kg

therefore,

W = [redacted] = [redacted] (kg/mm)

g : Gravitational acceleration = 9.8 (m/sec²)

GH : Impact deceleration = [redacted] (g)

I : Moment of inertia of area for the thickness per unit width of the basket frame (mm^4/mm) = $\frac{t^3}{12}$

t : Thickness = 20 (mm)

Consequently, the following is given;

$$f = \frac{W \cdot g \cdot G_H}{2\pi R} =$$ [redacted] = [redacted] N/mm/mm

$$\sigma_{bmax} = \frac{M_{max}}{I} \cdot \frac{t}{2} = \frac{\frac{3}{2} f R^2}{\frac{t^3}{12}} \times \frac{t}{2} = \frac{9 f R^2}{t^2}$$

= [redacted] = [redacted] MPa

The maximum displacement to the radial direction is obtained as follows.

The maximum displacement occurs at BC, of which value is given by the following equation;14)

$$w_{max} = 0.4292 \frac{f R^4}{EI} = \frac{0.4292 \times \text{[redacted]} \times f \times R^4}{E t^3}$$

where, E : Modulus of longitudinal elasticity (MPa)

Since E at the operating temperature of [redacted]C is [redacted] MPa, the maximum displacement (w_{max}) is given as follows ;

w_{max} = [redacted] = [redacted] (mm)

The actual bending stress (σ'_{bmax}) is given as follows, since the clearance between the basket frame and the shell is [redacted] mm.

σ'_{bmax} = [redacted] = [redacted] MPa

In this case, the allowable bending stress (σ_{ab}) of the basket frame at the operating temperature of [redacted]℃ is as follows;

$\sigma_{ab} = 1.5 \times \sigma_{dy} \times \eta = 1.5 \times$ [redacted] $\times 0.70 =$ [redacted] MPa

Consequently, the safety factor (RF) and the safety margin (MS) at the weld zone of the basket frame are as follows;

RF = [redacted] = [redacted]

MS = [redacted] − 1 = [redacted]

Therefore, the basket frame has the sufficient strength against 9m horizontal drop.

[redacted]

(II)-Fig.A.101 Analytical model at the weld zone in the frame of the basket for box type fuel

3.2 Basket for MNU type fuel

3.2.1 Strength of the square shape pipe

The severe stress due to the drop to X-direction and Y-direction is generated at the lowermost square shape pipes “a” and “b”, respectively as shown in (II)-Fig.A.103 when the basket for MNU type fuel drops horizontally.

Since these pipes are 1/4 symmetrical against the X-axis and the Y-axis, the strength is to be shown only for the lowermost square shape pipe at the drop to the X-direction.

As shown in (II)-Fig.A.103, the square shape pipe is supported by 7 support plates, therefore, the analytical model is assumed that the uniform load is acting on the square shape beam fixed at the both edges as shown in (II)-Fig.A.102.

[redacted]

(II)-Fig.A.102 Analytical model of the basket for MNU type fuel

The maximum bending stress (σ_{bmax}) and the maximum shearing stress τ are generated at the fixed edge due to the horizontal drop.

The maximum bending stress and the maximum shearing stress is given by the following formula;

[redacted]

(II)-Fig.A.103　Horizontal drop direction of the basket for MNU type fuel

$$\sigma_{bmax} = \frac{M_{max}}{I} \cdot \frac{h^2}{2} = \frac{\frac{w\ell^2}{12}}{\frac{(h_2^4 - h_1^4)}{12}} \cdot \frac{h^2}{2}$$

$$= \frac{w\ell^2}{(h_2^4 - h_1^4)} \cdot \frac{h^2}{2}$$

$$\tau = \frac{F}{A}$$

where, σ_{bmax} : Maximum bending stress (MPa)

M_{max} : Maximum bending moment (N・mm)

I : Moment of inertia of area (mm^4)

ℓ : Span length = [redacted] (mm)

w : Inertia force per unit length of the pipe and the fuel element piled up to X-direction (N/mm)

τ : Maximum shearing stress (MPa)

A : Cross-sectional area of one square shape pipe (mm^2)

F : Shearing force at the edge (N) $= \frac{w\ell}{2}$ (N)

h_1 : length of inner side of square shape pipe = [redacted] (mm)

h_2 : length of outer side of square shape pipe = [redacted] (mm)

a) In this case, the mass (W_1) of the square shape pipe per unit length is given as follows;

$W_1 = A \cdot \rho$

where, A : Cross-sectional area of one square shape pipe (mm^2)

= [redacted] = [redacted] (mm^2)

ρ : Density of the square shape pipe (kg/mm^3) = [redacted] ($kgmm^3$)

Therefore, the following is given;

W_1 = [redacted] = [redacted] (kg/mm)

b) The mass (W_2) of the fuel element per unit length is given as follows ;

$$W_2 = \frac{W_2'}{\ell_1}$$

where, W_2' : Mass of the fuel element = [redacted] (kg)

ℓ_1 : Length of the fuel element = [redacted] (mm)

Therefore, the following is given ;

W_2 = [redacted] = [redacted] (kg/mm)

c) [redacted] square shape pipes and [redacted] fuel elements are piled up to the X-direction.

The impact deceleration (G_H) is [redacted] (g).

Accordingly, the following is given ;

$W = (W_1 + W_2) \times$ [redacted] $\times g \times G_H$

= [redacted]$) \times$ [redacted] $\times 9.8 \times$ [redacted] = [redacted] N/mm

Therefore, the maximum bending stress (σ_{bmax}) is given as follows;

σ_{bmax} = [redacted] × [redacted] = [redacted] MPa

The shearing force (F) at the edge is given as follows ;

F = [redacted] = [redacted] N

Therefore, the shearing force (τ) is given as follows ;

τ = [redacted] = [redacted] MPa

In this case, the allowable bending stress (σ_{ab}) and the allowable shearing stress (τ_a) of the basket at the operating temperature of [redacted]℃ are as follows ;

$\sigma_{ab} = 1.5 \times \sigma_{dy} = 15 \times$ [redacted] = [redacted] MPa

$\tau_a = 0.6 \times \sigma_{dy} = 0.6 \times$ [redacted] = [redacted] MPa

Therefore, the safety factor (RF) and the safety margin (MS) against the bending stress and the shearing stress of the square shape pipe are as follows;

^ Against the bending stress of the square shape pipe

RF = [redacted] = [redacted]

MS = [redacted] − 1 = [redacted]

^ Against the shearing stress of the square shape pipe

RF = [redacted] = [redacted]

MS = [redacted] − 1 = [redacted]

According to the above result, the square shape pipe of the basket for MNU type fuel is not deformed when the package drops in the horizontal attitude, and thus no influence is brought about to the subcriticality.

3.3.2 Strength of the support plate

The basket is so constructed that the square shape pipe is supported by seven support plates of 10mm in thickness as shown in (II)-Fig.A.104.

The stress analysis is made on the part of the support plate where the fuel elements are loaded to the uppermost stage, and the analytical condition is the severest condition from the viewpoint of load.

The inertia force applied on one support plate is given by the following equation ;

$$F = \frac{W_1 \ell'_1}{\ell_1} + \frac{W_2 \ell'_2}{\ell_2} \quad g \cdot G_H$$

where, W_1 : Mass of the basket = [redacted] (kg)

W_2 : Mass of the fuel elements = [redacted] (kg)

g : Gravitational acceleration = 9.8 (m/sec^2)

G_H : Impact deceleration = [redacted] (g)

ℓ_1 : Total length of the basket (mm) = [redacted] (mm)

ℓ_2 : Total length of the fuel elements =[redacted] (mm)

ℓ'_1 : Extent of the basket supported by one support plate = [redacted] (mm)

ℓ'_2 : Extent of the fuel element supported by one support plate = [redacted] (mm)

Therefore, the following is given;

F = [redacted] ×9.8× [redacted] = [redacted] N

[redacted]

(II)-Fig.A.104 Extent of the square shape pipe supported by one support plate of the basket for MNU type fuel

Since the clearance between the support plate and the shell is a maximum of [redacted]mm, it is conservatively considered that the part is supported by "$\overset{\frown}{AB}$" and the inertia force acting on the support plate acts on "$\overline{CD}$" as shown in (II)-Fig.A.105.

The compression stress generated in this case is given by the following equation;

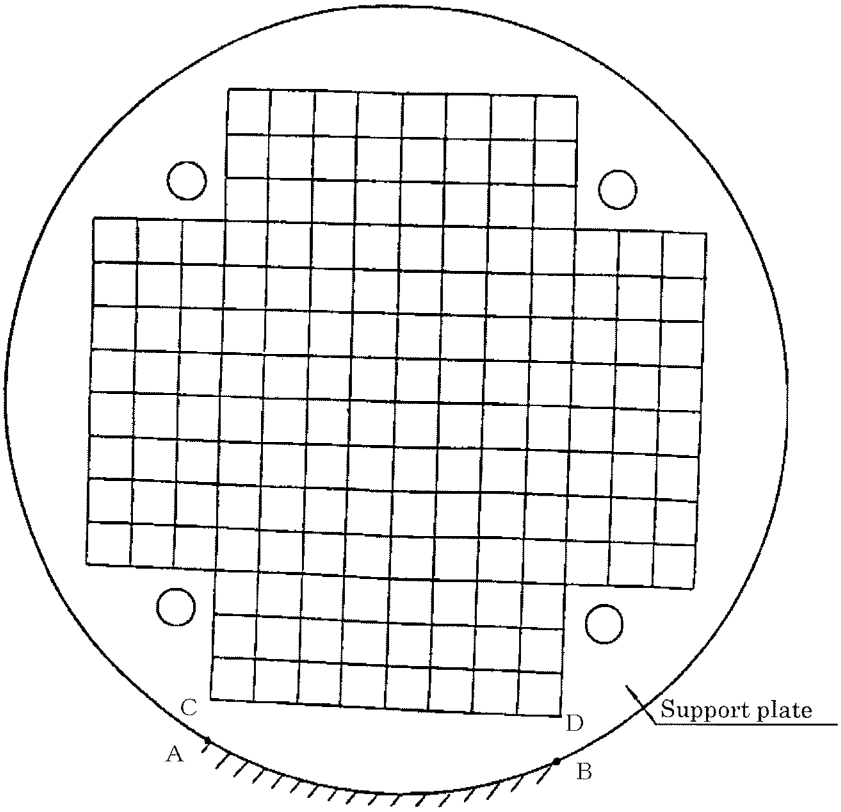

(II)-Fig.A.105 Analytical model of the support plate of the basket for MNU type fuel

$$\sigma_c = \frac{F}{A}$$

where, A: Cross-sectional area of CD = [redacted] × [redacted] × [redacted] = [redacted] (mm^2)

Therefore, the following is given;

σ_c = [redacted] = [redacted] MPa

In this case, the allowable compressive stress (σ_{ac}) of the basket at the operating temperature of [redacted]℃ is given as follows ;

σ_{ac}= 1.5× σ_{dy}= [redacted] = [redacted] MPa

Therefore, the safety ratio (RF) and the safety margin (MS) of the support plate are as given below;

RF = [redacted] = [redacted]

MS = [redacted] − 1 = [redacted]

According to the above result, the support plate has the sufficient strength against 9 m horizontal drop.

4. Strength of the fuel elements

Since each basket has the sufficient strength against the horizontal drop as described in (II)-A.6.1.2, 3, no significant deformation occurs in the fuel element due to deformation of the basket. This paragraph shows that each fuel element is never damaged due to the inertia force at the horizontal drop.

4.1 Strength of JRR-3 standard silicide type fuel

The horizontal drop direction of JRR-3 standard silicide type fuel is considered to the X-direction and the Y-direction as shown in (II)-Fig.A.106. The drop to the X-direction is severe, since the pressure area to the X-direction is smaller than that to the Y-direction.

Accordingly, this paragraph describes the compressive strength against the fuel side plate at the drop to the X-direction.

The compressive stress (σ_c) due to the inertia force is given by the following equation;

$$\sigma_c = \frac{W \cdot g \cdot G_H}{A}$$

where, W : Mass of the fuel element = [redacted] (kg)

g : Gravitational acceleration = 9.8 (m/sec^2)

G_H : Impact deceleration = [redacted] (g)

A : Cross-sectional area of the fuel side plate (mm^2)

= [redacted] × [redacted] × [redacted] = [redacted] (mm^2)

Therefore,

$\sigma_c =$ [redacted] = [redacted] MPa

In this case, since the yield stress of material A[redacted] at the temperature of [redacted] ℃ is less than that of material A[redacted] as shown in (II)-Fig.A.6, the yield stress (σ_y) of [redacted] MPa of material A[redacted] is used.

Consequently, the allowable compressive stress (σ_{ac}) at the temperature of [redacted] ℃ is given as follows ;

$\sigma_{ac} = 1.5 \times \sigma_y = 1.5 \times$ [redacted] = [redacted] MPa

Consequently, the safety factor (RF) and the safety margin (MS) is given as follows;

Consequently, the safety factor (RF) and the safety margin (MS) is given as follows;

RF = [redacted] = [redacted]

MS = [redacted] − 1 = [redacted]

As the above result, the fuel side plate has the sufficient strength against the compressive stress at the time of 9 m horizontal drop.

[redacted]

(II)-Fig.A.106 Horizontal drop direction of JRR-3 standard silicide type fuel

4.2 Strength of JRR-3 follower silicide type fuel

The inertia force due to the vertical drop acts on the fuel element in the same manner as JRR-3 standard silicide type fuel element. The horizontal drop direction of JRR-3 follower silicide type fuel element is considered to the X-direction and the Y-direction as shown in (II)-Fig.A.107 in the same manner as JRR-3 standard silicide type fuel element.

The drop to the X-direction is severe, since the pressure receiving area to the X-direction is smaller than that to the Y-direction in terms of compressive stress on fuel elements.

Accordingly, this paragraph describes the compressive strength against the fuel side plate at the drop to the X-direction.

The compressive stress (σ_c) due to inertia force is given by the following equation;

$$\sigma_c = \frac{W \cdot g \cdot G_H}{A}$$

where, W : Mass of the fuel element = [redacted] (kg)

g : Gravitational acceleration = 9.8 (m/sec^2)

G_H : Impact deceleration = [redacted] (g)

A : Cross-sectional area of the fuel side plate (mm^2)

= [redacted] × [redacted] × [redacted] = [redacted] (mm^2)

Therefore,

σ_c = [redacted] = [redacted] MPa

In this case, the yield stress (σ_y) of material A[redacted] at temperature of [redacted] ℃ is less than that of material A[redacted]. Therefore, the yield stress (σ_y) of [redacted] MPa of material A[redacted] is used.

Consequently, the allowable compressive stress (σ_{ac}) at the temperature of [redacted] ℃ is given as follows;

$\sigma_{ac} = 1.5 \times \sigma_y = 1.5 \times$ [redacted] = [redacted] MPa

Consequently, the safety factor (RF) and the safety margin (MS) are given as follows;

MS = [redacted] − 1 = [redacted]

As a result, the fuel side plate has the sufficient strength against the compressive stress at the time of 9 m horizontal drop.

[redacted]

(II)-Fig.A.107 Horizontal drop direction of JRR-3 follower silicide type fuel

4.3 Strength of JRR-3 MNU type fuel

The general-purpose finite element program ABAQUS is used for calculation of JRR-3 MNU type fuel at the 9 m horizontal drop. The analytical model is shown in (II)-Fig.A.108.

The inertia force (F) of each element is given by the following equation;

$$F = W \cdot g \cdot G_H$$

where, F : Inertia force per unit volume (N/mm^3)
W : Density (kg/mm^3)
g : Gravitational acceleration = 9.8 (m/sec^2)
G_H : Impact deceleration = [redacted] (g)

The valve shown in (II)-Table-A.15 was adopted as the material characteristic.

The inertia force (F_1) of the aluminum cladding per unit volume is given as follows;

F_1 = [redacted] × 9.8 × [redacted] = [redacted] N/mm^3

The inertia force (F_2) of the metallic natural uranium per unit volume is given as follows;

F_2 = [redacted] × 9.8 × [redacted] = [redacted] N/mm^3

The maximum stress generated on JRR-3 MNU type fuel when the above inertia forces act is shown in (II)-Fig.A.109.

The maximum stresses of the aluminum cladding and the metallic natural uranium are [redacted] MPa and [redacted] MPa, respectively.

According to (II)-Table A.16, allowable compressive stresses of the aluminum cladding and the metallic natural uranium are [redacted] MPa and [redacted] MPa, respectively.

Consequently, the safety factor (RF) and the safety margin (MS) of the aluminum cladding and the metallic natural uranium are as follows;

ﾍ Aluminum cladding

RF = [redacted] = [redacted]

MS = [redacted] − 1 = [redacted]

^ Metallic natural uranium

RF = [redacted] = [redacted]

MS = [redacted] − 1 = [redacted]

As the above result, JRR-3 MNU type fuel has the sufficient strength against 9 m horizontal drop.

[redacted]

(II)-Fig.A.108 Analytical model of JRR-3 MNU type fuel at the time of the horizontal drop

[redacted]

(II)-Fig.A.109　Stress in the Y-direction of JRR-3 MNU type fuel at the time of the horizontal drop

A.6.1.3 Corner drop

In this case, the package drops by inclining it in such a manner that the gravity center of the package is located on the vertical line of drop point, in which the package is subject to the greatest impact force among the oblique drop shown in (II)-A.6.1.4. Two types of the corner drop is considered, that is, top corner drop and bottom corner drop, in which the maximum impact deceleration to the vertical direction is [redacted] g and [redacted] g, respectively, as obtained from paragraph (II)-A.6.1, 3.4. The maximum impact deceleration is decomposed to the longitudinal component and the transverse component. These decomposed decelerations are [redacted] g, [redacted] g for the top corner drop and [redacted] g, [redacted] g for the bottom corner drop. Each of these components is less than [redacted] g for the top vertical drop, [redacted] g for the bottom vertical drop and [redacted] g for the horizontal drop. Therefore, the packaging is not deformed, nor the baskets and the fuel elements contained in the packaging are deformed.

However, in the case of top corner drop, large stresses occur on the gasket portion, that is, the contact surfaces of the lid and the body, and the lid bolt. Therefore, the strengths of those portions are evaluated in this paragraph.

(1) Containment at the contact surface of the lid and the body

(II)-Fig.A.110 and (II)-Fig.A.111 show the distribution of the equivalent plastic strain generated on the lid flange and on the body flange, respectively after 9 m top corner drop. These figures show that the plastic strain is not generated on the gasket portion of these flanges, where are in the elastic condition.

(II)-Fig.A.112 shows the time history of axial stress in the lid bolt during the drop.

As shown in the figure, the maximum stress of lid bolt occurs in the furthest lid bolt from the collision part of the package. The value is [redacted] MPa, which is less than the yield stress ([redacted] MPa). However, it is considered that the axial stress becomes in the state of the initial fastening stress after impact.

Therefore, the containment of the packaging is maintained at the time of top corner drop.

[redacted]

(II)-Fig.A.110　Equivalent plastic strain generated in the lid flange after 9 m top corner drop

[redacted]

(II)-Fig.A.111 Equivalent plastic strain generated in the body flange after 9 m top corner drop

[redacted]

(II)-Fig.A.112　Time history of axial stress in the lid bolt during 9 m top corner drop

A.6.1.4 Oblique drop

The oblique drop comes in between the corner drop and the vertical drop, or between the corner drop and the horizontal drop. In the case of the former drop, the absorption of drop energy is situated between the vertical drop and the corner drop. In the case of the latter drop, a part of drop energy acts as rotation moment, finally resulting in that the energy is absorbed in the same manner as the horizontal drop. Therefore, the condition for the oblique drop is mild as compared with these drop conditions.

Accordingly, the packaging is not deformed, nor the basket and the fuel elements contained in the packaging are deformed.

A.6.1.5 Summary of the results

1. Drop impact analysis of the package was carried out using dynamic analysis code LS-DYNA on the assumption that the target had the infinite rigidity.
   The result of calculation of the maximum impact is shown in (II)-Table A.18.

(II)-Table A.18 Maximum impact deceleration of drop test-I

Drop direction	Drop impact
	Impact deceleration (g)
Top vertical drop	[redacted]
Bottom vertical drop	[redacted]
Horizontal drop	[redacted]
Top corner drop	[redacted]
Bottom corner drop	[redacted]

2. Even in the severest drop condition for the lid and the body of packaging, that is, top vertical drop, the gasket part is still in the state of the elasticity. At this time, the lid bolt is also in the state of the elasticity and the initial fastening stress is maintained after drop. Therefore, the containment at the contact surface of the lid and the body is maintained and the shielding performance of packaging is maintained.
3. In any drop attitude, the remain fastening stress of the lid bolt is sufficient so that the containment at the contact surface of the lid and the body is maintained.
4. A slight plastic deformation has occurred partially on the basket for the box type fuel in the horizontal drop.
5. Each fuel elements has the sufficient strength against the impact force shown in (II)-Table A.18.

A.6.2 Strength test・drop test II (1m drop)

This paragraph describes the influence upon the package when it is drops onto the mild steel bar for the penetration from the height of 1m.

The condition becomes the severest when the package directly hit the mild steel bar through the center of gravity of the package.

Accordingly, the strength at each part under the above condition is to be examined in this paragraph.

The position of collision is to be the bottom plate in which the thickness is the thinnest in the packaging. (the thickness at the center and the circumference is [redacted] mm and [redacted] mm, respectively, therefore, [redacted] mm is used for the analysis for the sake of safety).

This paragraph shows that the containment of the valve is maintained by confirming the strength of the valve protection cover of each valve.

Since the integrity of the packaging is maintained in drop test I (9 m drop) which is severe for the basket, the lid bolt and the fuel elements as compared with this test, the analysis is omitted in this paragraph.

The analytical model for the case where the packaging hits the mild steel bar directly is shown in (II)-Fig.A.113.

When the bottom plate of the packaging directly hits the mild steel bar, a great shearing stress is generated at the part shown with oblique lines in the figure.

The compressive load (Fs) by which the part shown with oblique lines yields due to shearing stress is found as follows by using the Tresca's[17] yield condition.

$$Fs = A \times \sigma_y / 2$$

where, A : Shearing area

σ_y : Yield stress of the body of the packaging

= [redacted] MPa

Therefore, the following is given;

[redacted]

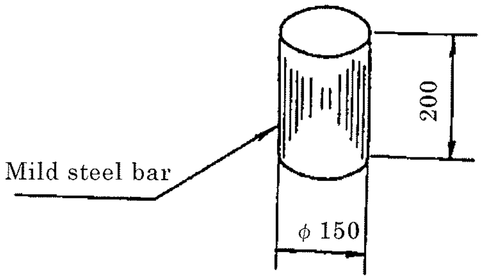

(Unit : mm)

(II)-Fig.A.113 Analytical model for case where the packaging directly hits the mild steel bar

$$F_S = \text{[redacted]} \times \pi \times \text{[redacted]} \times \text{[redacted]} / 2 = \text{[redacted]}\ \mathrm{N}$$

On the other hand, the load resistance (F_m) of the mild steel bar (150mm in diameter) is obtained as follows;

$$F_m = \frac{\pi}{4} \times 150^2 \times \sigma_B$$

where, σ_B : Tensile strength of the mild steel bar = 402 N

Therefore, (F_m) is given as follows;

$$F_m = \frac{\pi}{4} \times 150^2 \times 402 = 7.10 \times 10^6 \mathrm{N}$$

Accordingly, the following is given;

$$F_S > F_m$$

Therefore, the mild steel bar is crushed before the bottom plate, the thinnest part of the packaging, is damaged.

Accordingly, the integrity of the packaging is maintained in drop test II.

In this case, the maximum deceleration (α_{max}) to which the packaging is subjected can be given by the following equation;

$$\alpha_{max} = \frac{F_m}{W \times g} \quad (g)$$

where, W : The maximum mass of the package = 23.2×10^3 (kg)

g : Gravitational acceleration = 9.8 (m/sec^2)

Accordingly, the maximum deceleration (α_{max}) is given as follows ;

$$\alpha_{max} = \frac{7.10 \times 10^6}{23.2 \times 10^3 \times 9.8} = 31.3 \quad (g)$$

Therefore, the maximum deceleration of 31.3 g is applied to the package at the time of this drop test.

This paragraph shows that the integrity of the package is maintained when this maximum deceleration (31.3 g) is applied to the package.

1. Stress generated in the body of the packaging

The following is the evaluation of stress generated on the packaging when it directly hits the mild steel bar.

1.1 Horizontal drop

When the packaging makes contact with the mild steel bar, the packaging is bent as shown in (II)-Fig.A.114, by which the bending stress is generated at the shell of the packaging.

The maximum bending stress ($\sigma_{\max}$) generated at the shell of the packaging is given by the following equation ;

$$\alpha_{\max} = \frac{M_{\max}}{Z}$$

where, $M_{\max}$: The maximum bending moment generated on the vertical cross section passing through the center of gravity

Z : Section modulus

$$= \frac{\pi (D^4 - d^4)}{32D} = \text{[redacted]} \ (\mathrm{mm}^3)$$

[redacted]

(II)-Fig.A.114 Bending of the shell of the packaging

The maximum bending moment is given by using the maximum impact deceleration (α_{max}) obtained in the previous paragraph.

$$M_{max} = \frac{1}{2} L \frac{W \cdot g \cdot \alpha_{max}}{2}$$

where, L : Length of the body of the packaging = [redacted] (mm)

g : Gravitational acceleration = 9.8 (m/sec^2)

Therefore, the maximum bending stress is given as follows;

σ_{max} = [redacted] = [redacted] MPa

In this case, the allowable bending stress (σ_c) of the packaging at the operating temperature of [redacted]℃ is given as follows;

$\sigma_c = 1.5 \times \sigma_y = 1.5 \times$ [redacted] = [redacted] MPa

Therefore, the safety factor (RF) and the safety margin (MS) are as follows;

RF = [redacted] = [redacted]

MS = [redacted] − 1 = [redacted]

Therefore, the integrity of the shell is maintained under this drop test condition.

1.2 Vertical drop

The evaluation is made on the stress for the case when the bottom plate, the thinnest part of the packaging, is hit directly. It is said to be conservative, since the thickness of the lid is greater than that of the bottom plate.

The analytical model is shown in (II)-Fig.A.115 .

According to Table 24, case17 of the reference (14), the maximum bending moment (M_{max}) occurs at r = 0, and is given as follows;

$$M_{max} = \frac{W \cdot g \cdot \alpha_{max}}{4\pi} (1+\nu)\ \ell n \frac{a}{r_0'}$$

$$r_0' = \sqrt{1.6r_0^2 + t^2} - 0.675t \qquad (\text{for } r_0 < 0.5t)$$

where, $\alpha_{\max}$: Maximum impact deceleration = [redacted] (g)

W : Maximum mass of the package = 23.2 x 10^3 (kg)

g : Gravitational acceleration = 9.8 (m/sec^2)

a : Radius of the bottom plate = [redacted] (mm)

r_0 : Radius of the mild steel bar = 75 (mm)

ν : Poisson's ratio = 0.3

t : Thickness of the bottom plate = 300 (mm)

Therefore, the following is given;

$$r_0' = \sqrt{1.6 \times 75^2 + \text{[redacted]}} - 0.675t \times \text{[redacted]} = \text{[redacted]}$$

$$M_{\max} = \frac{23.2 \times 10^3 \times 9.8 \times \text{[redacted]}}{\text{[redacted]}} (1 + 0.3)\ \ell n \frac{\text{[redacted]}}{\text{[redacted]}}$$

$$= \text{[redacted]}\ \text{N} \cdot \text{mm}$$

[redacted]

(II)-Fig. A.115 Analytical model for the case when the bottom plate directly hits the mild steel bar

Accordingly, the maximum bending stress is given as follows;

$$\sigma_{\max} = \frac{6M_{\max}}{t^2} = \frac{6\times\text{[redacted]}}{\text{[redacted]}} = \text{[redacted]}\ \text{MPa}$$

In this case, the allowable bending stress (σ_c) of the packaging at the operating temperature of [redacted] ℃ is given as follows ;

$$\sigma_c = 1.5\times\sigma_y = 1.5\times\text{[redacted]} = \text{[redacted]}\ \text{MPa}$$

Therefore, the safety factor (RF) and the safety margin (MS) are given as follows ;

$$\text{RF} = \text{[redacted]} = \text{[redacted]}$$

$$\text{MS} = \text{[redacted]} - 1 = \text{[redacted]}$$

Accordingly, the integrity of the bottom plate can be maintained even under this drop test condition.

2. When the valve protection cover directly hits the mild steel bar.

This packaging is provided with a vent valve and a drain valve at the lid and the bottom corner part of the packaging.

The analysis is made for the case when the vent valve protection cover without the shock absorbing fin directly hits the mild steel bar, which is the severe condition, to show that the valve is protected and the containment is maintained. (See (II)-Fig.A.116).

The analysis is performed for the severest condition in which it passes through the center of the protection cover and the mild steel bar.

When the protection cover directly hits the mild steel bar, a great shearing stress is generated on the cross section of A and B shown in (II)-Fig.A.116.

The evaluation is made on both cross sections.

[redacted]

(II)-Fig.A.116 Situation for case where the valve protection cover directly hits the mild steel bar

The shearing stress (τ_A) acting on section-A is given by the following equation ;

$$\tau_A = \frac{A' \times q}{A} = \frac{\frac{\pi}{4} \times D_2{}^2 \times q}{\pi \times D_1 \times t}$$

where, A : Shearing area

D_1 : Diameter of section-A = [redacted] (mm)

t : Thickness of the protection cover at section-A = [redacted] (mm)

A' : Cross-sectional area of the mild steel bar on section-A

D_2 : Diameter of the mild steel bar on section-A = 110 (mm)

q : Crushing stress of the mild steel bar = 402 MPa

Therefore, the shearing stress is given as follows;

$$\tau_A = \frac{\frac{\pi}{4} \times 100^2 \times 402}{\pi \times 110 \times 40} = 277 \text{ MPa}$$

The shearing stress (τ_B) acting on section-B is given by the following equation ;

$$\tau_B = \frac{A' \times q}{A} = \frac{\frac{\pi}{4} \times D_2{}^2 \times q}{\pi \times D_1 \times t}$$

where, A : Shearing area

D_1 : Diameter of section-B = [redacted](mm)

t : Thickness of the protection cover at section-B

= [redacted] (mm)

A' : Cross-sectional area of the mild steel bar on section-B

D_2 : Diameter of the mild steel bar on section-B = 150 (mm)

q : Crushing stress of the mild steel bar = 402 MPa

Therefore, the shearing stress is given as follows;

$$\tau_B = \frac{\frac{\pi}{4} \times 150^2 \times 402}{\pi \times \text{[redacted]} \times \text{[redacted]}} = \text{[redacted] MPa}$$

In this case, the allowable shearing stress (τ_a) acting on the protection cover is given as follows;

$$\tau_a = 0.6 \times \sigma_u = 0.6 \times \text{[redacted]} = \text{[redacted] MPa}$$

Accordingly, the safety factor (RF) and the safety margin (MS) of each cross section are as follows;

Section – A

RF = [redacted] = [redacted]

MS = [redacted] − 1 = [redacted]

Section − B

RF = [redacted] = [redacted]

MS = [redacted] − 1 = [redacted]

Therefore, the shearing stress generated on section-A and section-B, where the greatest shear stress is generated, is less than the allowable stress when the protection cover directly hits the mild steel bar, and thus the protection cover has the sufficient strength.

Accordingly, the valve is protected and the containment is maintained.

The deflection of the protection cover is to be found further on. (Refer to (II)-Fig.A.117).

The protection cover has the thickness of [redacted] mm at the center and [redacted] mm at the circumference, however, the evaluation is made on the assumption that the thickness is all [redacted] mm.

The deflection value given under the above assumption is thought to be safety side assumption, since the value is greater than the actual value.

The maximum deflection (y_{max}) of the protection cover is generated at the center, and it is given by the following formula in accordance with Table 24, case 17 of the reference (14).

$$y_{max} = \frac{a^2 W}{16 \pi D}$$

where, D : Flexural rigidity of plate

$$= \frac{Et^3}{12(1-\nu^2)}$$

[redacted]

(II)-Fig.A.117 Analytical model of the valve protection valve

a : Radius of the valve protection cover = [redacted] (mm)

E : Modulus of longitudinal elasticity

= [redacted] MPa

t : Thickness of the valve protection cover = [redacted] (mm)

ν : Poisson's ratio = 0.3

W : Crushing load of the mild steel bar

$= \pi \times r_0^2 \times q$

where,

r_0 : Radius of the mild steel bar = 75 (mm)

q : Crushing stress of the mild steel bar = 402 MPa

Therefore,

$W = \pi \times 75^2 \times 402 = 7.10 \times 10^6$ N

The maximum deflection is given as follows;

y_{max} = [redacted] (mm)

In this case, the initial clearance between the valve and the protection cover is 5 mm, therefore, the safety factor (RF) and the safety margin (MS) are given as follows;

RF = [redacted] = [redacted]

MS = [redacted] − 1 = [redacted]

Accordingly, the valve is protected without any contact by the deflection of the protection cover, and thus the containment is maintained.

A.6.2.1 Summary of the result

When the packaging drops onto the mild steel bar of 15 cm in diameter from 1 m in height, the bottom plate, the smallest thickness part of the packaging, is not penetrated and the stress generated on the body and the lid is less than the allowable value.

The value protection cover is also provided with the sufficient strength allowable value even if the valve protection cover directly hits the mild steel bar.

Therefore, the integrity of the packaging is maintained, and its containment is certainly maintained.

A.6.3 Thermal test

A.6.3.1 Summary of temperature and pressure

The summary of temperature and pressure under accident conditions of transport (the fire accident) is shown in (II)-Table A.19.

The temperature distribution of the packaging at [redacted] minutes after the fire break-out, which shows the maximum temperature gradient as a result of thermal analysis, is shown in (II)-Fig.A.118.

A.6.3.2 Thermal expansion

This paragraph shows that the stress and thermal expansion at each part of the packaging shown below are calculated and are assured that those meet the requirement of the standard.

The analysis is made on the following items;

① The body and the lid
② Containment at the contact surfaces of the lid and the body
③ Strength of the lid bolt
④ Clearance between the shell and the basket
⑤ Thermal stress of the basket
⑥ Low-temperature strength under accident conditions of transport

Since the analytical model and procedure are the same as those described in (II)-A.5.1, they are omitted in this paragraph.

The initial fastening force of lid bolt, the internal pressure and the thermal load are inputted in these analyses. The internal pressure is [redacted] PaG, which is shown in (II)-Table A.19, however, the pressure of [redacted] PaG is given conservatively.

The thermal stress at each part of the packaging becomes to be the maximum value at [redacted] minutes after occurrence of the fire. Therefore, for the temperature distribution of fire accident, the temperature distribution at [redacted] minutes after fire break-out is given as input data for thermal stress analysis, and the elastic-plastic analysis is made for thermal stress analysis.

The results of the thermal stress analysis at [redacted] minutes after occurrence of the fire for a case where the JRR-3 MNU fuel elements, which would cause the maximum thermal stress, are installed are shown in (II)-Fig.A.119 through (II)-Fig.A.121.

Level	Temperature (°C)
1	[redacted]
2	[redacted]
3	[redacted]
4	[redacted]
5	[redacted]
6	[redacted]
7	[redacted]
8	[redacted]
9	[redacted]
0	[redacted]
A	[redacted]
B	[redacted]

[redacted]

(II)-Fig.A.118 Temperature distribution of the packing

([redacted] minutes after occurrence of the fire accident)

[redacted]

(II)-Fig.A.119 Deformation ([redacted]0 minutes after occurrence of the fire accident)

[redacted]

Level	Equivalent plastic strain (%)
1	[redacted]
2	[redacted]
3	[redacted]
4	[redacted]
5	[redacted]
6	[redacted]
7	[redacted]
8	[redacted]
9	[redacted]
0	[redacted]
A	[redacted]
B	[redacted]

(II)-Fig.A.120 Equivalent plastic strain distribution

([redacted] minutes after occurrence of the fire accident)

[redacted]

Level	Stress value (MPa)
1	[redacted]
2	[redacted]
3	[redacted]
4	[redacted]
5	[redacted]
6	[redacted]
7	[redacted]
8	[redacted]
9	[redacted]
0	[redacted]
A	[redacted]
B	[redacted]

(II)-Fig.A.121 Longitudinal stress contours of the lid bolt

([redacted] minutes after occurrence of the fire accident)

(II)-Table A.19 Summary of pressure and temperature(at fire accident)

Basket	Maximum temperature of the packaging (°C)	Maximum internal pressure [x 10^4 Pa]
Basket for box type fuel	[redacted]	[redacted]
Basket for MNU type fuel	[redacted]	[redacted]

A.6.3.3 Comparison of allowable stress

1. The body and the lid

As the result of the thermal stress analysis, the maximum plastic strainε_p during the fire accident occurs on the outer surface of bottom plate, which is shown in (II)-Fig.A.120.

That is;

ε_p = [redacted] %

On the other hand, the rupture strain of material is;

ε_u = [redacted] %

Accordingly, the safety factor (RF) and the safety margin (MS) are given as below;

RF = [redacted] = [redacted]

MS = [redacted] − 1 = [redacted]

Therefore, the strain generated at each part of the packaging at the time of fire accident is less than the rupture strain so that the integrity of the packaging is maintained.

2. Containment at the contact surfaces of the lid and the body

The following shows the containment at the contact surfaces of the lid and the body during the fire accident.

As the result of the elastic-plastic analysis, the distribution of the maximum deformation at the contact surfaces of the lid and the body is as shown in (II)-Fig.A.122. From this figure, it is known that the clearances at [redacted] O-ring and at [redacted] O-ring are [redacted] mm and [redacted] mm, respectively. These values are less than with the restoration value of the O-ring "about [redacted] mm".

In the evaluation, the larger clearance [redacted] mm at [redacted] O-ring is conservatively used.

The safety factor (RF) and the safety margin (MS) are as follows;

RF = [redacted] = [redacted]

MS = [redacted] − 1 = [redacted]

Accordingly, the containment at the contact surfaces of the lid and the body is maintained even if subjected to the severe temperature gradient during the fire accident.

[redacted]

(II)-Fig.A.122 Deformation of the contact surface of the lid and the body

3. Lid bolt

3.1 Allowable stress

At the time of [redacted] minutes after occurrence of the fire accident when the maximum temperature gradient is appeared, the axial temperature distribution of the lid bolt is greatly different in upper part and in lower part. The temperature of the lid bolt is [redacted]°C in the upper part and is [redacted]°C in the lower part, where JRR-3 MNU type fuel is stored.

Furthermore, the shape of the upper part of the bolt is different from that of the lower part. Namely, there are threads in the lower part where contact to the body flange, and the upper part is [redacted] mm in the diameter round bar.

Therefore, the allowable stress (σ_a) of the lid bolt sets another value respectively in the upper part and in the lower part.

Though the temperature of the lid bolt is [redacted]°C in the upper part and [redacted]°C in the lower part, [redacted]°C and [redacted]°C are used conservatively. When the tensile strength (σ_u) used for the allowable stress (σ_a) of the lid bolt, σ_a for each temperatures are as follows;

σ_a = [redacted] MPa at [redacted]°C

σ_a = [redacted] MPa at [redacted]°C

3.2 Stress of the lid bolt

This analysis is performed by using the analytical model and method described in (II)-A.5.1.3. The longitudinal stress contours of the lid bolt is shown in (II)-Fig.A.121.

The minor diameter of lid bolt (JIS-[redacted]) is modeled. The upper part of the model is [redacted] mm in the diameter round bar so that the maximum stress in the upper part of the bolt is converted in the ratio of the sectional areas. On the other hand, since there are threads in the lower part of the bolt, the result value of the analysis is used as it is for the maximum stress in the lower part of the bolt.

The maximum stress in the upper part of the lid bolt is given as follows;

$$\sigma_l = \sigma_m \times \frac{A_1}{A_2}$$

where, A_1 : Sectional area of minor diameter of external thread

= [redacted] (mm^2)

A_2 : Sectional area of diameter [redacted] mm = [redacted] (mm^2)

σ_m : Maximum stress of analysis result = [redacted] (MPa)

Therefore, the following is given;

σ_1 = [redacted] × [redacted] / [redacted]

= [redacted] MPa

On the other hand, the maximum stress in the lower part of the lid bolt is given as follow;

σ_2 = [redacted] MPa

Therefore, the safety factor (RF) and the safety margin (MS) are given as follows;

at the upper part;

RF = [redacted] = [redacted]

MS = [redacted] − 1 = [redacted]

at the lower part;

RF = [redacted] = [redacted]

MS = [redacted] − 1 = [redacted]

Therefore, the stress generated on the bolt during the fire accident is less than the allowable stress, and thus the integrity of the lid bolt is maintained.

4. Thermal expansion of the shell and the basket generated during the fire accident

The hollow cylindrical model shown in (II)-Fig.A.123 is considered to calculate the thermal expansion of the shell. The displacement value (expansion value) is to be found.

where,

μ_r : Displacement value at arbitrary radius (r)
a : Inside radius
b : Outside radius
r : Arbitrary radius $(a \leqq r \leqq b)$
t_a : Temperature at inside radius
t_b : Temperature at outside radius
t : Temperature at radius (r)
α : Coefficient of linear thermal expansion
ν : Poisson's ratio

[redacted]

(II)-Fig. A.123 Thermal expansion analytical model of the hollow cylinder

In this case, the values of t_a, t_b, and t are the values from which the reference temperature (the temperature at which no thermal expansion is generated ; 20°C) is subtracted.

The expansion value (μ_r) in this case is given by the following equation ;

$$\mu_r = \frac{1+\nu}{1-\nu} \times \frac{\alpha}{r} \int_a^r t\ r\ dr + C_1 r + \frac{C_2}{r} \cdots\cdots ①$$

In this case, C_1, C_2 and k_2 are given as follows ;

$$C_1 = \frac{(1+\nu)(1-2\nu)}{1-\nu} \times \frac{\alpha}{b^2 - a^2} \int_a^b t\ r\ dr - \nu k_2 \cdots\cdots ②$$

$$C_2 = \frac{1+\nu}{1-\nu} \times \frac{\alpha a^2}{b^2 - a^2} \int_a^b t\ r\ dr \cdots\cdots ③$$

$$k_2 = \frac{2\alpha}{b^2 - a^2} \int_a^b t\ r\ dr \cdots\cdots ④$$

i) In the case of axisymmetric temperature distribution (t) in the steady condition

The temperature at radius (r) is given as follows;

$$t = t_a + (t_b - t_a)\,\frac{\ell n(r/a)}{\ell n(b/a)}$$

If the term of $\int_a^b$ t r dr is substituted for (H), H is given as follows;

$$H = \int_a^b trdr \quad = \int_a^b \{t_a + (t_b - t_a)\,\frac{\ell n(r\ /a)}{\ell n(b\ /a)}\}r\ dr$$

$$= \frac{t_a}{2}(b^2 - a^2) + \frac{(t_b - t_a)}{\ell n(b\ /a)}\,(\frac{b^2}{2}\ell nb - \frac{b^2}{2}\ell na - \frac{b^2}{4} + \frac{a^2}{4})$$

$$= (b^2 - a^2)\left[\frac{t_a}{2} - \frac{t_b - t_a}{4\ell n(b\ /a)}\right] + \frac{b^2}{2}(t_b - t_a)$$

If r = a is substituted for equation ① to obtain the displacement at the inside radius (r = a), the equations ①, ② and ③ are as follows;

$$\mu_{r=a} = C_1 a + \frac{C_2}{a} \quad \cdots\cdots ⑤$$

$$C_1 = \frac{(1+v)(1-2v)}{1-v} \times \frac{\alpha}{b^2 - a^2} \cdot H - v \cdot \frac{2\alpha}{b^2 - a^2} \cdot H \quad \cdots\cdots ⑥$$

$$C_2 = \frac{1+v}{1-v} \times \frac{\alpha \cdot a^2}{b^2 - a^2} \cdot H \quad \cdots\cdots ⑦$$

If the equations ⑥ and ⑦ are substituted for equation ⑤, μ_r can be given as follows ;

$$\mu_{r=a} = \frac{2a\alpha \cdot H}{b^2 - a^2} \quad \cdots\cdots ⑧$$

Since a is [redacted]mm and b is [redacted]mm in this case, H is given as follows;

$$H = \text{[redacted]} \times \left[\frac{t_a}{2} - \frac{t_b - t_a}{\text{[redacted]}}\right] + \text{[redacted]} \times (t_b - t_a) \quad \cdots\cdots ⑨$$

ii) Now, consider the case when the temperature distribution changes from the inside radius (r = a) to the outside radius (r=b) linearly.

In this case, the temperature (t) at the radius (r) is given as follows;

$$t = t_a + \frac{(t_b - t_a)}{b - a} (r - a)$$

If $\int_a^b$ t r dr is arranged in the same manner as i), H is given as follows;

$$H = \int_a^b t\,r\,d\,r = \frac{1}{6} (b - a) \{t_a (2a + b) + t_b (a + 2b)\}$$

Since a is [redacted]mm and b is [redacted]mm in this case, H is given as follows;

$$H = \frac{1}{6} \times \text{[redacted]} (\text{[redacted]} t_a + \text{[redacted]} t_b) \cdots\cdots \text{⑩}$$

Accordingly, the displacement ($\mu_{r=a}$) at the inside radius (r=a) is given as follows:

$$\mu_{r=a} = \frac{2a\alpha \cdot H}{b^2 - a^2} = \frac{\text{[redacted]} \times H \times \alpha}{\text{[redacted]}} \cdots\cdots \text{⑪}$$

a) Clearance between the shell and the basket generated during the fire accident

This section examines the case of a basket for box type fuel, assuming that it is loaded with fuel elements that have a higher calorific value than the contents and a minimum gap between the container body and the fuel basket (hereinafter referred to as fuel element A) in order to make the analysis more conservative.

The temperature history of the basket for box type fuel is as shown in (II)-Fig.A.124 .

In this analysis, it is shown that a clearance between the shell and the basket further exists even under the severest condition.

The thermal expansion analysis is carried out using the temperature distribution at the time when the temperature of center of the basket becomes a maximum ([redacted] hours after fire occurrence). Because, it is expected to be the maximum deformation of the thermal expansion at that time. The deformation of the shell is smallest at the time before the fire, the thermal expansion analysis of the basket is conservatively made using that time.

i) Displacement (expansion) at the internal surface of the shell (r=[redacted]mm)

In the analysis, the temperature distribution between the internal surface and the external surface is assumed to change linearly as shown in (II)-Fig.A.125 .

t_a = [redacted] = [redacted] (°C)

t_b = [redacted] = [redacted] (°C)

α = [redacted] (1/°C)

If these equations are substituted for the equations ⑩ and ⑪, the following is given;

$$H=\frac{1}{6}\times \text{[redacted]}(\text{[redacted]}+\text{[redacted]})=\text{[redacted]}$$

$$\mu_{r=a}=\frac{\text{[redacted]}\times\text{[redacted]}\times\text{[redacted]}}{\text{[redacted]}}=\text{[redacted]}\ (\text{mm})$$

[redacted]

(II)-Fig.A.124 Temperature history of the basket for box type fuel contained JRR-3 standard aluminide type fuel

[redacted]

(II)-Fig.A.125 Temperature distribution model to thermal expansion analysis of the body at the time of fire accident

ii) Thermal expansion value of the basket

(II)-Fig.A.126 shows the temperature distribution of the basket for box type fuel at 35 hours after the fire occurrence.

In this case, the expansion value ($\triangle r_b$) to the radial direction due to thermal expansion is found by adding the expansion value of each element to the radial direction, locating on line passing through the center axis in (II)-Fig.A.126.

The radial expansion value ($\triangle r_b$) is found by using the following equation ;

$$\triangle r_b = \alpha \sum_{i=1\sim n} (T_i - 20)\ \ell_i$$

where, T_i : Average temperature of i-th element

ℓ_i : Length of radial direction of i-th element

α : Coefficient of thermal expansion

= [redacted] (1/°C)

Therefore, the radial expansion value ($\triangle r_b$) is given as follows ;

$$\triangle r_b = \text{[redacted]}[(\text{[redacted]} - 20) \times \text{[redacted]} + (\text{[redacted]} - 20) \times \text{[redacted]} + (\text{[redacted]} - 20) \times \text{[redacted]} + (\text{[redacted]} - 20) \times \text{[redacted]} + (\text{[redacted]} - 20) \times \text{[redacted]}] = \text{[redacted]} \text{ (mm)}$$

Accordingly, the clearance ($\triangle r$) between the body and the basket is given as follows ;

$\triangle r = 1 +$ [redacted] $=$ [redacted] (mm)

Therefore, the clearance between the body and the basket is [redacted] mm so that no stress is generated in each basket due to constraint.

[redacted]

(II)-Fig.A.126 Temperature distribution in the basket for box type fuel (35 hours after occurrence of the fire)

5. Thermal stress of the basket during the fire accident

This paragraph shows the analysis on the basket for box type fuel in which the amount of heat generated is the maximum and the temperature reaches the highest level during the fire accident.

Since there exists a clearance between the shell and the basket during the fire accident as described previously, no stress due to constraint is generated.

Accordingly, the stress generated within the basket will include only the thermal stress generated due to temperature gradient.

The maximum stress σ_i of the basket can be expressed by the following equation.

$$\sigma_{max} = \frac{E_0}{\ell_0} \{ \triangle\ell_b - (T_{Max} - 20)\ \alpha_0 \ell_0 \}$$

where, T_{max} : Maximum temperature of the basket element [redacted]°C

E_0 : Modulus of longitudinal elasticity at maximum temperature [redacted] MPa

α_0 : Coefficient of thermal expansion at maximum temperature for basket [redacted] 1/°C

ℓ_0 : Length of the basket [redacted]mm

$\triangle\ell_b$: Value of elongation in the longitudinal direction [redacted]mm (See the equation in Section 2 of paragraph A.5.1.2)

Therefore,

$$\sigma_{max} = \frac{\text{[redacted]}}{\text{[redacted]}} \{ \text{[redacted]} - (\text{[redacted]} - 20) \times \text{[redacted]} \times \text{[redacted]} \}$$

$$= \text{[redacted]}\ \text{MPa}$$

The maximum temperature of the basket at the fire accident is [redacted]°C.The temperature of the allowable compressive stress (σ_{ac}) is conservatively assumed to be [redacted]°C. Therefore, the allowable compressive stress is given as follows;

$$\sigma_{ac} = 3Sm^{1)} = 3 \times \text{[redacted]} = \text{[redacted]}\text{MPa}$$

Therefore, the safety factor (RF) and the safety margin factor (MS) are given respectively as follows ;

$$RF = \frac{\text{[redacted]}}{\text{[redacted]}} = \text{[redacted]}$$

MS=[redacted]－1=[redacted]

Therefore, the basket has the sufficient strength against the thermal stress during the fire accident.

6. Low-temperature strength under accident condition of transport

The package is subjected to the environment of －40°C after the fire test, however, the mechanical property of the structural material does not deteriorate due to the above test.*

Accordingly, the integrity of the packaging will not be damaged as described in (II)-A.4.2 "Low-temp. strength".

Note *：The maximum temperature of the lid bolt using [redacted] [redacted] at the time of fire accident is [redacted]°C, which is fully lower than the heat treatment temp. of [redacted]～[redacted]°C as described in (V)-I-A.2.3.

A.6.4 Water immersion

Since this nuclear fuel package is a package containing nuclear fuel material, etc. with an amount of radioactivity exceeding 100,000 times A2 value (the ratio of the radioactivity of the contents to be loaded to the 100,000 times A2 value is approximately [redacted] so exceeds 1), it will be evaluated whether the containment device is not damaged for the 200m immersion test.

It has been confirmed that permanent deformation does not occur and containment can be maintained at the water depth of 200 m (2.0MPa).

Therefore the packaging has enough strength and containment capacity at the water depth of 15m because the condition of immersion at the water depth of 200m is more severe than at the water depth of 15m.

Furthermore, in the appendix 5 of (II)-A.10.5, for reference, it is shown that the packaging has the sufficient strength even if the external pressure equivalent to the water depth of 5000 m is applied.

A.6.5 Summary and evaluation of the results

This paragraph shows summary and the evaluation of the results under accident condition of transport in accordance with each test item. (II)-Table A.20 shows the summary of the results of the structural analysis.

1. Drop test (9 m drop)

This item shows the summary of the result of the test.

(1) In the packaging, the gasket portion of the lid flange is the severest part, where is still in the state of the elasticity in any drop attitude, and the stress of the lid bolt is restored after drop to the initial fastening stress. Therefore, the containment at the contact surface of the lid and the body is maintained and the shielding performance is not lost.

(Refer to ⑦, ⑧, ⑩ and ⑫ of (II)-Table A.20.)

(2) In any drop attitude, the stress generated on the lid bolt is less than the yield stress of the material and the initial fastening stress is maintained after drop.

(Refer to ⑦, ⑧, ⑩ and ⑫ of (II)-Table A.20.)

(3) Among the baskets, though a slight plastic deformation occurs partially on the basket for the box type fuel in the horizontal drop, in a criticality analysis that considers that plastic deformation, no influence is brought about to the subcriticality as showing in appendix 3 of (II)-E.7.3.

(Refer to ⑧ and ⑪ of (II)-Table A.20.)

(4) Among the fuel elements, the severest stress is generated in JRR-3 MNU type fuel contained in the basket during the vertical drop. Even in this case, it has the sufficient strength, since the safety factor against the stress is [redacted].

(Refer to ⑨, ⑩, ⑪ and ⑫ of (II)-Table A.20.)

Consequently, no release of radioactive materials occurs, since neither basket nor fuel is damaged.

2. Drop test-II (penetration test)

The severest stress is generated when the mild steel bar directly hits the protection cover.

Since the safety factor against the stress is [redacted], the mild steel bar will not penetrate the packaging.

Accordingly, the containment of the packaging can be maintained.

(Refer to ⑬ of (II)-Table A.20.)

3. Thermal test

The severest stress due to the maximum temperature gradient is generated on lid bolt.

The safety factor against the stress is [redacted].

Therefore, the packaging will not be damaged, and the containment can be maintained.

(Refer to ⑬ and ⑭ of (II)-Table A.20.)

4. Water immersion test

The containment against the external pressure (0.15MP) equivalent to the water depth of 15 m can be sufficiently maintained.

(Refer to ⑭ of (II)-Table A.20.)

5. Evaluation of containment at the O-ring of the Lid (Evaluation of strain level)

The displacement located at the O-ring due to the load applied the lid at each test condition is found in each section. The comparison between the above displacement and the restoration value of the O-ring with initial fastening is shown in (II)-Table A.21. The displacement at each condition is less than the above restoration value so that the leaktightness is not lost.

(Ⅱ)-Table A.20 Result of structural analysis (Requirements of Package) (No.1)

Item	Analytical standard	Criteria	Analytical result	Safety factor	Safety margin	Remarks
• Chemical and galvanic reaction						These materials used in the packaging do not react electrically or chemically and are very stable.
Chemical reaction	—	—	—	—	—	
Galvanic reaction	—	—	—	—	—	
• Low temperature strength						
Body, Lid	Minimum temperature in use	−40℃	A material is capable of standing the use at −40℃	Good		
Basket Fuel element	〃	〃	〃	〃		
Packing	〃	〃	〃	〃		
Lid bolt	Toughness	[redacted] MPa・$\sqrt{\text{mm}}$	[redacted]MPa・$\sqrt{\text{mm}}$	[redacted]	[redacted]	
Gap between shell and basket	Gap	$0 < \Delta r$	[redacted] mm			Δr = Gap
• Containment system						[redacted] O-rings are used [redacted] and the fitting is controlled by [redacted].
Lid	—	—	—	—	—	
Drain valve and vent valve	—	—	—	—	—	

(Ⅱ)-Table A.20 Result of structural analysis (Requirements of Package) (No.2)

Item	Analytical standard	Criteria	Analytical result	Safety factor	Safety margin	Remarks
・Lifting lug Body lifting lug						
1) Normal lifting of the package						
Weld zone	$0.6\sigma_y \times \eta$	[redacted] MPa	[redacted] MPa	[redacted]	[redacted]	
〃	$\sigma_y \times \eta$	[redacted] MPa	[redacted] MPa	[redacted]	[redacted]	
Hole	$0.6\sigma_y$	[redacted] MPa	[redacted] MPa	[redacted]	[redacted]	
2) When one body lifting lug is used by mistake for lifting the package						
Weld zone	$0.6\sigma_u \times \eta$	[redacted] MPa	[redacted] MPa	[redacted]	[redacted]	
〃	$\sigma_u \times \eta$	[redacted] MPa	[redacted] MPa	[redacted]	[redacted]	
Hole	$0.6\sigma_u$	[redacted] MPa	[redacted] MPa	[redacted]	[redacted]	
3) Fatigue strength	N	7.4×10^5 cycles	1×10^4 cycles	74	73	
・Lid lifting lug						
1) When two lid lifting lugs are used by mistake for lifting the package						
Weld zone	$0.6\sigma_y \times \eta$	[redacted] MPa	[redacted] MPa	[redacted]	[redacted]	
〃	$\sigma_y \times \eta$	[redacted] MPa	[redacted] MPa	[redacted]	[redacted]	
Hole	$0.6\sigma_y$	[redacted] MPa	[redacted] MPa	[redacted]	[redacted]	
Lid bolt	σ_y	[redacted] MPa	[redacted] MPa	[redacted]	[redacted]	
〃	σ_y	[redacted] MPa	[redacted] MPa	[redacted]	[redacted]	
Thread of the body	$0.6\sigma_y$	[redacted] MPa	[redacted] MPa	[redacted]	[redacted]	

Notes) σ_y : Yield stress of material σ_u : Tensile strength of material η : Weld efficiency (=0.7) N : Number of allowable cycles

(II)-Table A.20 Result of structural analysis (Requirements of Package) (No.3)

Item	Analytical standard	Criteria	Analytical result	Safety factor	Safety margin	Remarks
2) When one lid lifting is used for lifting the lid by mistake						
Weld zone	$0.6\sigma_u \times \eta$	[redacted] MPa	[redacted] MPa	[redacted]	[redacted]	
〃	$\sigma_u \times \eta$	[redacted] MPa	[redacted] MPa	[redacted]	[redacted]	
Hole	$0.6\sigma_u$	[redacted] MPa	[redacted] MPa	[redacted]	[redacted]	
3) Fatigue strength	N	[redacted] cycles	1×10^4 cycles	[redacted]	[redacted]	
Influence on the package due to tie down device						
Travelling direction	10g of the mass of the package					
Lateral direction	5g of the mass of the package					
Vertical direction	3g of the mass of the package					
Bottom fin contacted to fin bolt	$1.5\sigma_y$	[redacted] MPa	[redacted] MPa	[redacted]	[redacted]	
Bottom fin contacted to skid	σ_{cr}	[redacted] MPa	[redacted] MPa	[redacted]	[redacted]	
〃	$1.5\sigma_y$	[redacted] MPa	[redacted] MPa	[redacted]	[redacted]	

Notes) σ_y : Yield stress of material σ_u : Tensile strength of material η : Weld efficiency (= 0.7) N : Number of allowable cycles
σ_{cr} : Critical buckling stress

(Ⅱ)-Table A.20 Result of structural analysis (Requirements of Package) (No.4)

Item	Analytical standard	Criteria	Analytical result	Safety factor	Safety margin	Remarks
• Pressure Packaging		6.0×10^4 Pa ; decrease of ambient pressure	The change in the stress is very small. The containment of the packaging can be secured.	Good		
• Vibration Package	Resonance zone	maximum of natural frequency ; [redacted] Hz	[redacted] Hz	Good		

(Ⅱ)-Table A.20　Result of structural analysis (Normal conditions of transport) (No.5)

Item	Analytical standard	Criteria	Analytical result	Safety factor	Safety margin	Remarks
^ Thermal test						
1) Thermal expansion						
Body, lid (longitudinal direction)		—	[redacted] mm	—	—	
Basket (longitudinal direction)						
For box type fuel	Gap	[redacted] mm	[redacted] mm	[redacted]	2.1	
For MNU type fuel	〃	[redacted] mm	[redacted] mm	[redacted]	5.0	
Body, lid (radial direction)		—	[redacted] mm	[redacted]	—	
Basket (radial direction)						
For box type fuel	Gap	[redacted] mm	[redacted] mm	[redacted]	[redacted]	
For MNU type fuel	〃	[redacted] mm	[redacted] mm	[redacted]	[redacted]	
2) Thermal stress						
Body, lid	3 S_m	[redacted] MPa	[redacted] MPa	[redacted]	[redacted]	
Basket						
For box type fuel	3 S_m	[redacted] MPa	[redacted] MPa	[redacted]	[redacted]	
For MNU type fuel	3 S_m	[redacted] MPa	[redacted] MPa	[redacted]	[redacted]	

Notes) S_m : Design stress intensity of material

(II)-Table A.20 Result of structural analysis (Normal conditions of transport) (No.6)

Item	Analytical standard	Criteria	Analytical result	Safety factor	Safety margin	Remarks
Containment of contact surface of body and lid	Compression		Compression			
Lid bolt	2 S_m	[redacted] MPa	[redacted] MPa	[redacted]	[redacted]	
Fatigue strength of lid bolt	N	[redacted] cycles	[redacted]cycles	[redacted]	[redacted]	
^ Water spray						
Non water trap	—	—	—	Good		The packaging is manufactured with stainless steel and the external surface is smoothed.
Cutwater	—	—	—	〃		
Anticorrosion	—	—	—	〃		
^ Free drop						
Vertical	The packaging satisfies the criteria even in the evaluation for the analytical results of drop test- I which is severer than this condition.					
Horizontal						
Corner						
• Penetration	The packaging is no penetration in the evaluation for the analytical results of drop test- II which is severer than this condition. Therefore, the package satisfies the criteria.					

Notes) S_m : Design stress intensity of material N : Number of allowable cycles

(II)-Table A.20 Result of structural analysis (Normal conditions of transport) (No.7)

Item	Analytical standard	Criteria	Analytical result	Safety factor	Safety margin	Remarks
・Compression (Stacking test)						
Shell of body	σ_y	[redacted]MPa	[redacted] MPa	[redacted]	[redacted]	
Bottom fin of body	σ_y	[redacted] MPa	[redacted] MPa	[redacted]	[redacted]	
Bottom plate of body, lid	σ_y	[redacted]MPa	[redacted] MPa	[redacted]	[redacted]	
〃	$0.6\sigma_y$	[redacted] MPa	[redacted] MPa	[redacted]	[redacted]	
Contact surfaces of body and lid	σ_y	[redacted] MPa	[redacted] MPa	[redacted]	[redacted]	

Note) σ_y : Yield stress of material

(II)-Table A.20　Result of structural analysis (Accident conditions of transport) (No.8)

Item	Analytical standard	Criteria	Analytical result	Safety factor	Safety margin	Remarks
Drop test I						
1) Impact analysis						
Vertical Drop						
Top vertical drop	Deceleration:	[redacted] (g)				
Bottom vertical drop	〃 :	[redacted] (g)				
Horizontal drop	〃 :	[redacted] (g)				
Corner drop			In the stress analysis of parts of the packaging at each drop, the impact deceleration (g)is used.			
Top corner drop	〃 :	[redacted] (g)				
Bottom corner drop	〃 :	[redacted] (g)				
Oblique drop	— :	—				
2) Vertical drop						
Containment at contact surface of body and flange						
Top vertical drop						
Seal boundary on lid flange and body flange	Elastic condition	Elastic condition	Elastic condition	Good		
Lid bolt	σ_y	[redacted] MPa	[redacted] MPa	[redacted]	[redacted]	

Note) σ_y : Yield stress of material

(II)-Table A.20 Result of structural analysis (Accident conditions of transport) (No.9)

Item	Analytical standard	Criteria	Analytical result	Safety factor	Safety margin	Remarks
Bottom vertical drop						
Seal boundary on lid flange and body flange	Elastic condition	Elastic condition	Elastic condition	Good		
Lid bolt	σ_y	[redacted] MPa	[redacted] MPa	[redacted]	[redacted]	
Valve						
Valve main bolt	$0.6\sigma_y$	[redacted] MPa	[redacted] MPa	[redacted]	[redacted]	
Valve protection cover bolt	$0.6\sigma_y$	[redacted] MPa	[redacted] MPa	[redacted]	[redacted]	
Basket						
‸ For box type fuel						
Compartment plate, partition plate	$1.5\sigma_{dy}$	[redacted] MPa	[redacted] MPa	[redacted]	[redacted]	
〃	σ_{cr}	[redacted] MPa	[redacted] MPa	[redacted]	[redacted]	
Neutron poison	$1.5\sigma_y$	[redacted] MPa	[redacted] MPa	[redacted]	[redacted]	
‸ For MNU type fuel						
Guide plate	$1.5\sigma_{dy}$	[redacted] MPa	[redacted] MPa	[redacted]	[redacted]	
Weld zone between square shape pipe and support plate	$0.6\sigma_u \times \eta$	[redacted] MPa	[redacted] MPa	[redacted]	[redacted]	

Notes) σ_y : Yield stress of material σ_{cr} : Critical buckling stress σ_{dy} : Dynamic yield stress of material (= $1.25\sigma_y$)
σ_u : Tensile strength of material η : Weld efficiency (= 0.7)

(Ⅱ)-Table A.20　Result of structural analysis (Accident conditions of transport) (No.10)

Item	Analytical standard	Criteria	Analytical result	Safety factor	Safety margin	Remarks
Fuel element						
• JRR-3 standard silicide type fuel						
Fuel side plate	1.5 σ_y	[redacted] MPa	[redacted] MPa	[redacted]	[redacted]	
Fuel plate	F_r	[redacted] N	[redacted] N	[redacted]	[redacted]	
• JRR-3 follower silicide type fuel						
Fuel side plate	1.5 σ_y	[redacted] MPa	[redacted] MPa	[redacted]	[redacted]	
Fuel plate	F_r	[redacted] N	[redacted] N	[redacted]	[redacted]	

Notes)　σ_y : Yield stress of material　　F_r : Roll-swage force (tensile fracture load)

(Ⅱ)-Table A.20 Result of structural analysis (Accident conditions of transport) (No.11)

Item	Analytical standard	Criteria	Analytical result	Safety factor	Safety margin	Remarks
^ JRR-3 MNU						
(A-direction drop)						
Aluminum cladding	$1.5\sigma_y$	[redacted] MPa	[redacted] MPa	[redacted]	[redacted]	
Stopper	$1.5\sigma_y$	[redacted] MPa	[redacted] MPa	[redacted]	[redacted]	
Metallic natural uranium	$1.5\sigma_y$	[redacted] MPa	[redacted] MPa	[redacted]	[redacted]	
(B-direction drop)						
Aluminum cladding	$1.5\sigma_y$	[redacted] MPa	[redacted] MPa	[redacted]	[redacted]	
Stopper	$1.5\sigma_y$	[redacted] MPa	[redacted] MPa	[redacted]	[redacted]	
Metallic natural uranium	$1.5\sigma_y$	[redacted] MPa	[redacted] MPa	[redacted]	[redacted]	

Notes) σ_y : Yield stress of material F_r : Roll-swage force (tensile fracture load)

(Ⅱ)-Table A.20 Result of structural analysis (Accident conditions of transport) (No.12)

Item	Analytical standard	Criteria	Analytical result	Safety factor	Safety margin	Remarks
3) Horizontal drop						
Containment at contact surface of body and flange						
Seal boundary on lid flange and body flange	Elastic condition	Elastic condition	Elastic condition	Good		
Lid bolt	σ_y	[redacted] MPa	[redacted] MPa	[redacted]	[redacted]	
Valve						
Valve main bolt	$0.6\sigma_y$	[redacted] MPa	[redacted] MPa	[redacted]	[redacted]	
Valve protection cover bolt	$0.6\sigma_y$	[redacted] MPa	[redacted] MPa	[redacted]	[redacted]	

Notes) σ_y : Yield stress of material F_r : Roll-swage force (tensile fracture load)

(II)-Table A.20 Result of structural analysis (Accident conditions of transport) (No.13)

Item	Analytical standard	Criteria	Analytical result	Safety factor	Safety margin	Remarks
Basket						
^ For box type fuel						
(X-direction drop)						
Compartment plate, partition plate	ε_u	[redacted] %	[redacted] %	[redacted]	[redacted]	
(Y-direction drop)						
Compartment plate, partition plate	$1.5\sigma_{dy}$	[redacted] MPa	[redacted] MPa	[redacted]	[redacted]	
Weld zone between compartment plate and partition plate	$0.6\sigma_{dy}\times\eta$	[redacted] MPa	[redacted] MPa	[redacted]	[redacted]	
Weld zone frame	$1.5\sigma_{dy}\times\eta$	[redacted] MPa	[redacted] MPa	[redacted]	[redacted]	
^ For MNU type fuel						
Square shape pipe	$1.5\sigma_{dy}$	[redacted] MPa	[redacted] MPa	[redacted]	[redacted]	
〃	$0.6\sigma_{dy}\times\eta$	[redacted] MPa	[redacted] MPa	[redacted]	[redacted]	
Support plate	$1.5\sigma_{dy}\times\eta$	[redacted] MPa	[redacted] MPa	[redacted]	[redacted]	

Notes) ε_u : Rupture strain of material σ_{dy} : Dynamic yield stress of material (= $1.25\sigma_y$) η : Weld efficiency (= 0.7)

(II)-Table A.20 Result of structural analysis (Accident conditions of transport) (No.14)

Item	Analytical standard	Criteria	Analytical result	Safety factor	Safety margin	Remarks
Fuel element						
^ JRR-3 standard silicide type fuel	$1.5\sigma_y$	[redacted] MPa	[redacted] MPa	[redacted]	[redacted]	
^ JRR-3 follower silicide type fuel	$1.5\sigma_y$	[redacted] MPa	[redacted] MPa	[redacted]	[redacted]	
^ JRR-3 MNU type fuel						
Aluminum cladding	$1.5\sigma_y$	[redacted] MPa	[redacted] MPa	[redacted]	[redacted]	
Metallic natural uranium	$1.5\sigma_y$	[redacted] MPa	[redacted] MPa	[redacted]	[redacted]	

Notes) σ_y : Yield stress of material

(II)-Table A.20 Result of structural analysis (Accident conditions of transport) (No.15)

Item	Analytical standard	Criteria	Analytical result	Safety factor	Safety margin	Remarks
4) Corner drop						
Containment at contact surface of body and flange						
Seal boundary on lid flange and body flange	Elastic condition	Elastic condition	Elastic condition	Good		
Lid bolt	σ_y	[redacted] MPa	[redacted] MPa	[redacted]	[redacted]	
5) Oblique drop	The packaging satisfies the criteria even in the evaluation for the analytical results of corner drop in the drop test I which is severer than oblique drop.					
^ Drop test II						
Shell of body	1.5 σ_y	[redacted] MPa	[redacted] MPa	[redacted]	[redacted]	
Bottom plate of body, lid	1.5 σ_y	[redacted] MPa	[redacted] MPa	[redacted]	[redacted]	
Valve protection cover						
A-cross section	0.6 σ_u	[redacted] MPa	[redacted] MPa	[redacted]	[redacted]	
B-cross section	0.6 σ_u	[redacted] MPa	[redacted] MPa	[redacted]	[redacted]	
Valve protection cover	Gap of valve	[redacted] mm	[redacted] mm	[redacted]	[redacted]	

Notes) σ_y : Yield stress of material σ_u : Tensile strength of material

(II)-Table A.20 Result of structural analysis (Accident conditions of transport) (No.16)

Item	Analytical standard	Criteria	Analytical result	Safety factor	Safety margin	Remarks
^ Thermal Test						
1) Thermal expansion						
2) Comparison with allowable stress						
Body, lid	ε_u	[redacted] %	[redacted] %	[redacted]	[redacted]	
Packing	Restoration value	[redacted] mm	[redacted] mm	[redacted]	[redacted]	
Lid bolt	σ_u	(Upper) [redacted] MPa (Lower) MPa	[redacted] MPa MPa	[redacted]	[redacted]	
Difference of thermal expansion between shell of body and basket		$0 < \Delta r$	[redacted] mm			
Thermal stress of basket	$3\ S_m$	[redacted] MPa	[redacted] MPa	[redacted]	[redacted]	
Low temperature strength under accident conditions of transport	Minimum temperature in use	-40℃	A material is capable of withstanding the use at -40℃.	Good		

Notes) S_m : Design stress intensity of material　σ_u : Tensile strength of material　ε_u : Rupture strain of material

(II)-Table A.20 Result of structural analysis (Accident conditions of transport) (No.17)

Item	Analytical standard	Criteria	Analytical result	Safety factor	Safety margin	Remarks
^ Water immersion test External pressure equivalent to water depth 15 m	The packaging has enough strength and containment capacity at the water depth of 15m because the condition of immersion at the water depth of 200m is more severe than at the water depth of 15m.					

(II)-Table A.21 Evaluation of the strain at the containment boundary between the lid and the shell flange under accident conditions of transport

Conditions		Relative opening displacement between the lid and the body flange at the position of the O-ring	Criteria
9 m drop	Top vertical drop	The lid gasket portion and the lid bolt keep elastic condition against the drop impact. Although the fastening stress of the lid bolt is decreased to about [redacted] MPa and then increased to maximum about [redacted] MPa during the impact, it is restored to the initial fastening stress [redacted] MPa after the impact.	The restoration value of O-ring = about [redacted] mm
	Bottom vertical drop	The lid gasket portion and the lid bolt keep elastic condition against the drop impacts. Although the fastening stress of the lid bolt is decreased to about [redacted] MPa and then increased to maximum about [redacted] MPa during the impact, it is restored to the initial fastening stress after the impact.	
	Horizontal drop	The lid gasket portion and the lid bolt keep elastic condition against the drop impacts. Although the fastening stress of the lid bolt is increased to maximum about [redacted] MPa during the impact, it is restored to the initial fastening stress after the impact.	
	Top corner drop	The lid gasket portion and the lid bolt keep elastic condition against the drop impacts. The maximum stress of lid bolt occurs in the furthest lid bolt from the collision part of the package. The value is [redacted] MPa, which is less than the yield stress ([redacted] MPa). However, the lid bolt is restored to the initial fastening stress after impact.	
1 m drop	Top vertical drop	The containment of the packaging is maintained in the 9 m drop test so that it is maintained in the 1 m drop test that is not severer than 9 m drop test.	
Thermal test	Thermal expansion (including pressure)	[redacted] mm or less	
15 m water immersion		No tensile stress occurs on the lid bolt since the external pressure acts in the direction where the lid is pressed against the shell.	

A.7 Enhanced water immersion test

Since this nuclear fuel package is a package containing nuclear fuel material, etc. with an amount of radioactivity exceeding 100,000 times A2 value (the ratio of the radioactivity of the contents to be loaded to the 100,000 times A2 value is approximately 4.5 so exceeds 1), it will be evaluated whether the containment device is not damaged for the 200m immersion test.

1. Strength of the packaging when the external pressure equivalent to the water depth of 200 m is applied

1.1 Strength of the shell

(II)-Fig.A.127 shows the analytical model of the shell to which the external pressure is applied.

As shown in Table-32, case-1c and case-1d of the literature (14), the principal stress generated at the shell under the external pressure equivalent to the water depth of 200 m is given as follows;

$$\sigma_1 = -\frac{qa^2}{a^2-b^2} \qquad \text{(longitudinal stress)}$$

$$\sigma_2 = -q\frac{a^2(r^2+b^2)}{r^2(a^2-b^2)} \qquad \text{(circumferential stress)}$$

$$\sigma_3 = -q\frac{a^2(r^2-b^2)}{r^2(a^2-b^2)} \qquad \text{(radial stress)}$$

[redacted]

In this case, the stress intensity (S) shows the maximum value on the inner surface of the shell.

Since a is [redacted] mm and b is [redacted] mm, σ_2 and σ_3 can be given as follows ;

$\sigma_2 = -$[redacted], $\sigma_3 =$ [redacted]

Accordingly, the stress intensity is given as below ;

$S = \sigma_3 - \sigma_2 =$ [redacted] $-$ [redacted] $=$ [redacted]

Since the external pressure (q) equivalent to the water depth of 200m is as follows ;

$q = 2.0$ MPa

the stress intensity (S) is given as follows ;

$S =$ [redacted] $\times 2.0 =$ [redacted] MPa

If the allowable stress (σ_a) at the shell is equal to the allowable stress (σ_y), σ_a is given as follows ;

$\sigma_a = \sigma_y =$ [redacted] MPa

Consequently, the safety factor (RF) and the safety margin factor (MS) are given as follows;

RF = [redacted] = [redacted]

MS = [redacted] $- 1 =$ [redacted]

Accordingly, the packaging has the sufficient strength against the external pressure equivalent to the water depth of 200 m.

1.2 Strength of the lid and the bottom plate

Since the bottom plate and the lid have [redacted] mm and [redacted] mm in thickness, respectively, the evaluation of the strength is made on the bottom plate having smaller thickness.

The analytical model is as shown in (II)-Fig.A.128, in which the disk fixed to the circumference is subjected to the uniform pressure.

According to the table-24, case-10b given in the reference (14), the maximum bending moment occurs at the fixed end of the circumference.

The bending moment per unit length is given as below;

$$M_r = \frac{qb^2}{8} = \frac{2.0\times\text{[redacted]}}{8} = \text{[redacted] N· mm/mm}$$

where, q : External pressure (2.0MPaG) equivalent to the water depth of 200m

b : Radius of the shell (= [redacted] mm)

Therefore, the circumferential bending moment is as follows;

$$Mt = \nu\, Mr = \text{[redacted] N·mm/mm}$$

where, ν : Poisson's ratio (=0.3)

The shearing force (Q) per unit length is given as follows;

$$Q = \frac{qb}{2} = \frac{2.0\times\text{[redacted]}}{2} = \text{[redacted] N·mm /mm}$$

[redacted]

(II)-Fig.A.128 Analytical model of the bottom plate

If the thickness of the bottom plate is t, the maximum stress is given as follows;

At the outer surface of the bottom plate

^ Radial stress

$$\sigma_r = \frac{6 \times M_r}{t^2} = \frac{6 \times \text{[redacted]}}{\text{[redacted]}^2} = \text{[redacted]}\,\text{MPa}$$

^ Circumferential stress

$$\sigma_t = \frac{6 \times M_t}{t^2} = \frac{6 \times \text{[redacted]}}{\text{[redacted]}^2} = \text{[redacted]}\,\text{MPa}$$

^ Longitudinal stress

$$\sigma_o = -q = -2.0\ \text{MPa}$$

At the center of the thickness

^ Shearing stress

$$\tau = \frac{3}{2} \times \frac{Q}{t} = \frac{3}{2} \times \frac{\text{[redacted]}}{\text{[redacted]}} = \text{[redacted]}\ \text{MPa}$$

Therefore, the maximum stress and the maximum shearing stress are given respectively as follows;

^ The maximum stress

$$\sigma_{max} = \sigma_r = \text{[redacted]}\ \text{MPa}$$

^ The maximum shearing stress

$$\tau_{max} = \tau = \text{[redacted]}\ \text{MPa}$$

Thus, the allowable bending stress (σ_{ab}) and the allowable shearing stress (τ_a) of the bottom plate are given respectively as follows ;

$$\sigma_{ab} = 1.5 \times \sigma_y = 1.5 \times \text{[redacted]} = \text{[redacted]}\ \text{MPa}$$

$$\tau_a = 0.6 \times \sigma_y = 0.6 \times \text{[redacted]} = \text{[redacted]}\ \text{MPa}$$

Accordingly, the safety factor (RF) and the safety margin (MS) against the bending stress are as follows;

$$RF = \frac{\text{[redacted]}}{\text{[redacted]}} = \text{[redacted]}$$

$$MS = \text{[redacted]} - 1 = \text{[redacted]}$$

The safety factor (RF) and safety margin (MS) of the bottom plate against the shearing stress are given as follows;

$$RF = \frac{\text{[redacted]}}{\text{[redacted]}} = \text{[redacted]}$$

$$MS = \text{[redacted]} - 1 = \text{[redacted]}$$

Therefore, the lid and the bottom plate have the sufficient strength against the external pressure equivalent to the water depth of 200 m.

1.3 Strength of the lid bolt

For the stress generated on the bolt when it is applied with the external pressure, it is assumed that no tensile stress by initial fastening force applies in the lid bolt and the packaging is subject to the external pressure 2.0 MPa. The longitudinal compressive stress 2.0 MPa is generated in the bolt when the packaging is subject to the external pressure 2.0 MPa.

The allowable compressive stress (σ_{ac}) of the lid bolt is as follows;

$\sigma_{ac} = \sigma_y =$ [redacted] MPa

Accordingly, the safety factor (RF) and the safety margin (MS) are respectively as follows;

$$RF = \frac{\text{[redacted]}}{2.0} = \text{[redacted]}$$

$$MS = \text{[redacted]} - 1 = \text{[redacted]}$$

Therefore, the lid bolt has the sufficient strength against the external pressure equivalent to the water depth of 200 m.

1.4 Thermal stress during drop in the sea

The outer surface of the package is quickly cooled (extremely thin surface layer) and the tensile stress arises immediately after it makes contact with seawater. This paragraph shows that no crack is generated on the surface of the packaging due to the stress.

Since the thermal capacity is great as shown in “accident condition of transport” of chapter-(II)-B “Thermal analysis”, the temperature gradient of the packaging is decreased and the packaging is cooled evenly as it is sinking into the sea. Thus there is no problem of thermal stress under such condition.

The analysis is made on the assumption that the surface of the packaging is cooled quickly down to the seawater temperature of approx. 0℃* to show that the thermal stress (tension stress) generated due to the temperature drop is less than the allowable tension stress (σ_u).

The thermal stress (σ) generated due to temperature drop under the above condition is given by the following equation;

$$\sigma = \alpha \triangle TE$$

where, α : Coefficient of thermal expansion = [redacted] 1/℃ (at [redacted]°C)

$\triangle T$: Temperature change = [redacted] = [redacted]℃

E : Modulus of longitudinal elasticity = [redacted] MPa (at average temperature 53℃)

Therefore, σ can be given as follows ;

σ = [redacted] × [redacted] × [redacted] = [redacted] MPa

Thus, the allowable tensile stress (σ_u) of the body is [redacted] MPa.

Accordingly, the safety factor (RF) and the safety margin (MS) are as follows;

RF = [redacted] = [redacted]

MS = [redacted] − 1 = [redacted]

The crack is not generated on the surface of the packaging by the thermal stress due to the rapid cooling in the sea while it sinks.

2. Containment at the contact surfaces of the lid and the body when it is subject to the external pressure equivalent to the water depth of 200 m.

This paragraph shows that the containment is assured at the contact surfaces of the lid and the body when it is subject to the external pressure (2.0 MPa) equivalent to the water depth of 200 m.

Note * : Seawater temperature in winter from "Table of science (2002)"

The analytical model is shown in (II)-Fig.A.129 .

At the contact surfaces, the external pressure is assumed conservatively to be applied to outside position “a” further from the outer O-ring.

In this case, the compressive stress (σ_c) is caused by the compressive force (F) on a-b contact surfaces of the lid and the body.

This compressive stress (σ_c) is given as follows;

$$\sigma_c = \frac{F}{A}$$

where, F :Compressive force on the a-b surface (N)

$$F = \frac{\pi}{4} \times \text{[redacted]}^2 \times 2$$

$$= \text{[redacted]} \text{ (N)}$$

A : Pressure area from which area of the O-ring and the leak tight test groove is subtracted (mm^2)

$$= \frac{\pi}{4} \times \{(\text{[redacted]}^2 - \text{[redacted]}^2) - (\text{[redacted]}^2 - \text{[redacted]}^2)$$

$$-(\text{[redacted]}^2 - \text{[redacted]}^2) + (\text{[redacted]}^2 - \text{[redacted]}^2)\}$$

$$= \text{[redacted]} \text{ (mm}^2\text{)}$$

Therefore, σ_c is given as follows ;

$$\sigma_c = \frac{\text{[redacted]}}{\text{[redacted]}} = \text{[redacted]} \text{ MPa}$$

In this case, the allowable compressive stress (σ_{ac}) of the lid at the operating temperature of 20℃ is as follows ;

$$\sigma_{ac} = 1.5 \times \sigma_y = 1.5 \times \text{[redacted]} = \text{[redacted]} \text{ MPa}$$

Therefore, the safety factor (RF) and the safety margin (MS) are given as follows;

$$RF = \frac{\text{[redacted]}}{\text{[redacted]}} = \text{[redacted]}$$

$$MS = \text{[redacted]} - 1 = \text{[redacted]}$$

Accordingly, the contact surface of the lid is under the compressive stress condition, and kept at the condition in which the O-ring is initially tightened to [redacted] mm, and no plastic deformation is generated, thus the containment is maintained.

[redacted]

(II)-Fig.A.129 The part of the O-ring and the leak tight test groove

A.8 Radioactive contents

The contents of the package are seven kinds as follows.

1) JRR-3 standard silicide type fuel
2) JRR-3 follower silicide type fuel
3) JRR-3 MNU type fuel

JRR-3 standard silicide type fuel and JRR-3 follower silicide type fuel are plate-type fuels where the fuel meats of uranium silicon aluminum dispersion type are covered with aluminum alloy.

Also, JRR-3 MNU type fuel is a cylindrical fuel which is the metallic natural uranium covered with aluminum alloy.

JRR-3 standard silicide type fuel are cut off its top and bottom portions, which do not contain uranium, before being loaded in the packaging.

The weight of those fuel elements are shown in paragraph (I)-C-5, (f), and the configurations are shown in (I)-Fig.D.1

The cladding of fuel is made of an aluminum alloy, which makes an extremely stable oxide film in water. It is stable in dry state in the packaging too. As shown in paragraph (II)-C.4.1, the aluminum cladding is not damaged due to corrosion during transport considering [redacted] mm of the minimum covering thickness. The change of the mechanical properties (yield stress, tensile strength, hardness and elongation) of material by irradiation is very small, and there is no problem in the analysis.

There is no problem concerning the blister generation under the temperature at the fire accident of the package as shown in paragraph (II)-C.4.1.

No damage of each fuel element occurs under the drop test of accident conditions of transport (refer to paragraph A.6.1). Also, no damage and no melting of each fuel elements occur under thermal test (refer to paragraph (II)-B.5.6).

From above, the integrity of the contents in the package is maintained under normal and accident conditions of transport and there is no problem for the integrity of the structural strength, the thermal performance, the containment and subcriticality.

A.9 Package containing fissile material

The package is corresponding to a package containing fissile material. Accordingly, in this paragraph, the damage state of the package assumed in "Criticality analysis" of Chapter (II)-E is evaluated under the following conditions.

A.9.1 Package containing fissile material normal conditions of transport

The test procedure for normal conditions of transport is as follows.

(1) Water spray that simulates exposure to rainfall of 50 mm per hour for one hour (water spray test)

(2) 0.3 m drop test (drop direction where the maximum damaged of the package occurs)

(3) Stacking test and 1 m penetration test

The following shows the state of the package after each test.

A.9.1.1 Water spray test

No influence is brought about to the integrity of the package.

A.9.1.2 0.3 m drop test

Assuming from the results of 9 m corner drop, the displacement value of the fins is only a few mm including the vertical, horizontal and corner drop. There is no change of the configuration of the package which affects the criticality analysis.

A.9.1.3 Stacking test and penetration due to a 6 kg mild steel bar

The stress generated by stacking test is very smaller than the allowable stress as shown in paragraph A.5.4. It is assured that the external surface of the packaging is not penetrated by dropping a 6 kg mild steel bar.

Accordingly, there is no change of the configuration of the package which affects the criticality analysis.

As the results, the state of the package under normal conditions of transport for packages containing fissile material is shown in (II)-Table A.22. The dent that includes a 10cm cube in a component of the package does not occur. And the fin deformation is limited to [redacted]mm as it is the largest accumulated displacement value under accident conditions of transport for the package which is approximately 1.9m outside diameter, 2.1m in height. It is obvious that each side of a circumscribed rectangular parallelepiped is more than 10cm under normal conditions of transport. Also, the integrity of the package is assured to be kept at ambient temperature of −40℃ as shown in paragraph A.4.2.

Accordingly, there is no change of the configuration of the package that affects the criticality analysis.

(II)-Table A.22 Damage state of the package under normal conditions of transport for packages containing fissile material

Test condition	Damage state of the package	Remarks
Water spray	No damage	—
0.3 m drop	Deformation of the fins	The fins are ignored in the criticality analysis conservatively. The drop impact deceleration and the stress of each part of the packaging are less than the results of 9 m drop test.
Stacking test	No damage	—
Penetration test of a 6 kg mild steel bar	No damage	—

A.9.2 Package containing fissile material accident conditions of transport

Since the test sequence shown in the following gives the maximum damage to the package among many test procedures for accident conditions of transport, the evaluation is performed according to the following test procedure.

(1) The package is exposed under normal conditions of transport of previous paragraph.

(2) 9 m drop test

(3) 1 m drop test

(4) Thermal test (800℃, 30 minutes)

(5) 0.9 m immersion test

A.9.2.1 Normal conditions of transport

As shown in previous paragraph, even if the package suffers the maximum damage under normal conditions of transport, the displacement of the fins is only a few mm. Accordingly, there is no significant change of the configuration so as to affect the criticality analysis. Also, since the impact deceleration caused under normal conditions of transport is less than that under the sequence test shown in 9 m drop test of later paragraph, the stress applied at each component of the basket is enough less than the criteria, and there is no deformation of the basket too.

A.9.2.2 9 m drop test

In 9 m drop test performed after normal conditions of transport shown in previous paragraph, the drop attitude and the test procedure assumed to suffer the maximum damage of the package are shown in (II)-Table A.23.

9.3 m (0.3 m + 9 m) drop impact analysis of the package is carried out using dynamic analysis code LS-DYNA in the same manner as the 9 m drop impact analysis. In this analysis, the package with the velocity 13.5 m/s, which is equivalent to the drop velocity from 9.3 m height, is made to crash with the flat rigid target without any yield. The initial fastening stress [redacted] MPa is given to the lid bolt before drop.

The analytical results for the case assumed to become the maximum deformation and impact deceleration are shown in (II)-Table A.24. The analytical results are as follows.

(II)-Table A.24 shows the relative values of the impact deceleration in 9 m drop test, which is evaluated in (II)-A.6.1. The amount of increases of both the deformation and the impact deceleration are very small.

In case of the horizontal drop, in which a slight plastic strain occurs on the basket for the box type fuel, the amount of increase of the impact deceleration is 1.02 times. It is confirmed that the shape deformation does not affect criticality analysis.

In case of the top corner drop, in which the safety margin of the lid bolt is smallest, the amount of increase of the impact deceleration is 1.01 times and the rate of increase is less than the safety margin [redacted]. Therefore, the lid bolt is in the state of the elasticity and satisfactory in sealing performance.

Since other parts of package have sufficiently safety margin, there is no problem on the strength.

From the above results, it is confirmed that the package satisfies the criteria against all the drop attitude.

(II)-Table A.23 Drop posture and procedure of sequence drop tests

	Remarks
Vertical drop	0.3 m vertical drop ↓ 9 m vertical drop
Horizontal drop	0.3 m horizontal drop ↓ 9 m horizontal drop
Corner drop	0.3 m corner drop ↓ 9 m corner drop

(II)-Table A.24 Accumulated displacement value and impact deceleration of 9 m drop test

Drop attitude		Accumulated displacement value (mm)	Impact deceleration (g)	Ratio of the impact deceleration generated due to drop test-I to that of this paragraph
		Fin		
Vertical	Top	[redacted]	[redacted]	[redacted]
	Bottom	[redacted]	[redacted]	[redacted]
Horizontal		[redacted]	[redacted]	[redacted]
Corner	Top	[redacted]	[redacted]	[redacted]
	Bottom	[redacted]	[redacted]	[redacted]

A.9.2.3 1 m drop test

In 9 m drop test performed before the 1 m drop test, the deformed portion is only a part of the fins, and further even if 1 m drop test is performed, all the deformation of the package is confined to only the outer surface. Thereby, as shown in paragraph A.6.2, a mild steel bar, 150 mm diameter and 200 mm length, does not affect the integrity of the package in each drop attitude, and there is no change of the configuration which affects the criticality analysis.

A.9.2.4 Thermal test

This thermal test does not affect the integrity of the package. Also, even if the sequence drop test described previously is performed before this test, each part of the package has a sufficient strength and satisfies the criteria as shown in paragraph A.6.3. Therefore, there is no change of the configuration which affects the criticality analysis.

A.9.2.5 0.9 m immersion

Even if 0.9 m immersion test is performed after thermal test, the integrity of the package is maintained and there is no change of the configuration which affects the criticality analysis as shown in “15 m immersion” of paragraph A.6.4.

A.9.2.6 Summary of the damage state of the package

(II)-Table A.25 shows the summary of the damage state of the package.

(II)-Table A.25 Damage state of the package under the accident conditions of transport for package containing fissile material

Test condition	Damage state of the package	Remarks
9 m drop	Deformation of the fins Deformation of the basket for the box type fuel	The fins are ignored in the criticality analysis. Though a slight plastic deformation occurs partially on the basket for the box type fuel in the horizontal drop, no influence is brought to the criticality analysis.
1 m penetration	Deformation of the fins	The fins are ignored in the criticality analysis.
Thermal test (Fire)	The temperature of each portion increases.	The fins are ignored in the criticality analysis. It is conservatively assumed in the criticality analysis that the water density is 1.0 g/cm^3 and the temperature of the fuel elements is 20℃.
0.9 m immersion	Not damaged (No water immersion)	It is assumed that there is water immersion into the package in array.

As shown in the above results and paragraph A.4.2, the integrity of the packaging is maintained at the ambient temperature of -40℃. Accordingly, even if the packaging is exposed under accident conditions of transport for package for fissile material, it is confirmed that there is no change of the configuration, which affects the criticality analysis.

A.10 Appendix

A.10.1 Appendix-1

Mechanical property of material used for drop impact analysis

A.10.2 Appendix-2

Drop impact analysis of fins using dynamic analysis code LS-DYNA and comparison with impact tests

A.10.3 Appendix-3

Strength analysis of lifting instrument

A.10.4 Appendix-4

Compatibility with the ASME Code under design conditions

A.10.5 Appendix-5

Strength of the packaging when the external pressure equivalent to the water depth of 5,000 m is applied

A.10.6 Appendix-6

References

A.10.1 Appendix-1

Mechanical property of material used for drop impact analysis

The stress-strain curves depending on the strain rate are used for the fins that absorb the drop impact of the package.

On the other hand, static stress-strain curve are used for the body, the lid, and the lid bolt. The material of the fin is SA-240 [redacted]. The material of the body and the lid is SA-182 [redacted]. These are [redacted] stainless steel.

The stress-strain curve of [redacted] stainless steel was estimated from reference 21. The constitutive equation of stress-strain curve for [redacted] stainless steel was expressed with the following equation from reference 21.

$$\sigma = (\sigma_0 + A\varepsilon_t^n)\cdot\left(\dot{\varepsilon} / \dot{\varepsilon}_c\right)^m \qquad \text{------------------------------①}$$

Where, $\dot{\varepsilon}$ and $\dot{\varepsilon}_c$ are strain rate, and the strain rate of $\dot{\varepsilon}_c$ is 10^{-2} s^{-1}.

In the case of $\dot{\varepsilon} < \dot{\varepsilon}_c$,

$m = 0$

Therefore, equation ①is shown as follows;

$$\sigma = (\sigma_0 + A\varepsilon_t^n) \qquad \text{------------------------------②}$$

In the case of $\dot{\varepsilon} > \dot{\varepsilon}_c$,

$m = 0.037$

Therefore, equation ①is shown as follows;

$$\sigma = (\sigma_0 + A\varepsilon_t^n)\cdot\left(\dot{\varepsilon} / \dot{\varepsilon}_c\right)^{0.037} \qquad \text{------------------------------③}$$

Where, σ_0, A, and n are shown as follows;

$\sigma_0 =$ [redacted] (MPa)

$A =$ [redacted] (MPa)

$n =$ [redacted]

For the stress-strain curve of the body and the lid, equation ② is used. The equation ③ is used to obtain the stress-strain curve depending on the strain rate for the fins.

Moreover, about the lid bolt (SA-564 [redacted]), it is assumed that the work hardening changes in a straight line to elongation ([redacted]% : standard value), corresponding to the tensile strength, from the yield stress.

As the operating temperatures of the body and the lid (SA-182 [redacted]), the lid bolt, and the fins (SA-240 [redacted]), the following values are used. These values obtained from the result of the normal conditions of transport in thermal analysis of the safety analysis report.

Body : [redacted]℃

Lid, and Lid Bolt : [redacted]℃

Fin : [redacted]℃

The modulus of longitudinal elasticity, the Poisson's ratio, and yield stress (static) of such material are used the following values.

- Body (SA-182 [redacted]) (at [redacted]℃)
  Modulus of longitudinal elasticity : 1[redacted] (MPa) (see reference 21)
  Poisson's ratio: 0.3
  Yield stress (static): [redacted] (MPa)
- Lid ([redacted]-182 [redacted]) (at [redacted]℃)
  Modulus of longitudinal elasticity : [redacted] (MPa) (see reference 21)
  Poisson's ratio: 0.3
  Yield stress (static): [redacted] (MPa)
- Lid Bolt (SA-564 [redacted]) (at [redacted]℃)
  Modulus of longitudinal elasticity : [redacted] (MPa) (see reference 21)
  Poisson's ratio: 0.3
  Yield stress (static): [redacted] (MPa)

- Fin (SA-240 Type 304)　(at 60℃)

  Modulus of longitudinal elasticity : 1.93×10^5 (MPa)　(see reference 21)

  Poisson's ratio: 0.3

  Yield stress (static): 193 (MPa)

Since the value of the stress-strain curves obtained by equation ② and ③ is a value of the room temperature, the stress in the stress-strain curve used in the analysis is the value which is $\sigma_{y,op} / \sigma_{y,room}$ times the stress in that obtained by the above equation as shown in (II)-Fig.A.10.1-1.

Here, $\sigma_{y,op}$ and $\sigma_{y,room}$ are the yield stress at operating temperature and at room temperature, respectively.

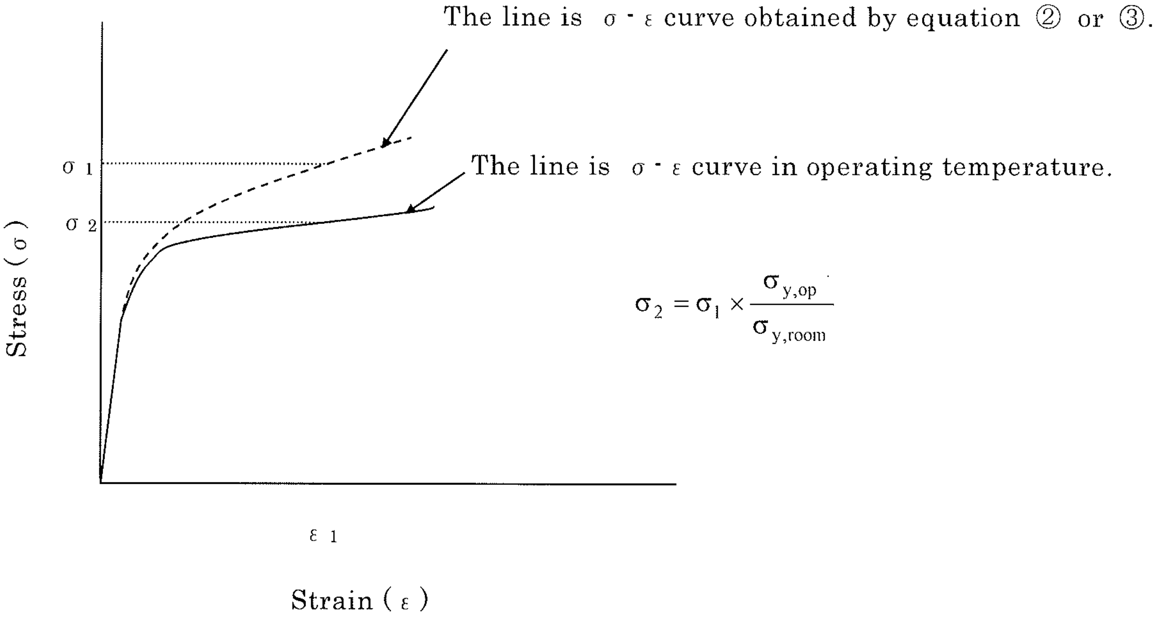

$$\sigma_2 = \sigma_1 \times \frac{\sigma_{y,op}}{\sigma_{y,room}}$$

(II)-Fig.A.10.1-1 Stress - strain curves

A.10.2 Appendix-2

Drop impact analysis of fins using dynamic analysis code LS-DYNA and comparison with impact tests

1. General

In order to confirm that the dynamic analysis code LS-DYNA is able to simulate the drop test of JRC-80Y-20T type package, dynamic analysis was performed for the test of reference 20 which describes about the impact test of fins.

2. Summary of results

From a comparison with a test and analytical results, it is concluded that the deformation mode, displacement value and peak load of a fin obtained by the dynamic analysis are considerably coincident with those of the test result.

3. Mechanical property of material

In this report, the test series 7384 of reference 1 is analyzed.

The Material of the test series 7384 is ASTM A285 Gr. C (carbon steel), and the thickness of the fin is 3/8 inch. From reference 21, it only describes 266 MPa as the yield stress about material property.

The following value is used as modulus of longitudinal elasticity, Poisson's ratio, and yield stress (static) of ASTM A285 Gr.C.

Modulus of longitudinal elasticity : 2.03×10^5 (MPa) (From reference 21)
Poisson's ratio : 0.3
Yield stress (static): 266 (MPa)

The stress-strain curve is determined using equation depending on the strain rate (reference 21).

The equation depending on the strain rate of the carbon steel is expressed as follows;

In the case of $\dot{\varepsilon} < \dot{\varepsilon}_0$ $(\fallingdotseq 10^{-2} \sim 10^{-1}\ \mathrm{s}^{-1})$

$$\sigma = \sigma_s$$ ①

In the case of $\dot{\varepsilon} > \dot{\varepsilon}_0$

$$\sigma = \sigma_s + \sigma_0 \cdot \log(\dot{\varepsilon} / \dot{\varepsilon}_0)$$ ②

Where, σ_s, $\dot{\varepsilon}_0$, $\dot{\varepsilon}$, and $\sigma_0 \cdot \log(\dot{\varepsilon} / \dot{\varepsilon}_0)$ are as follows, respectively.

σ_s : Static stress independent of strain rate

$\dot{\varepsilon}_0$: Specific strain rate ($\fallingdotseq 10^{-2} \sim 10^{-1}\ s^{-1}$)

$\dot{\varepsilon}$: Arbitrary strain rate

$\sigma_0 \cdot \log(\dot{\varepsilon} / \dot{\varepsilon}_0)$: Term depending on strain rate

σ_s is as follows;

$\sigma_s = A$ for at $\varepsilon < \varepsilon_{sy}$

$\sigma_s = B \cdot \varepsilon^{\ell}$ for at $\varepsilon > \varepsilon_{sy}$ ③

σ_0, $\dot{\varepsilon}_0$ are shown as follows;

$$\sigma_0 = C \bullet \varepsilon^m$$
$$\dot{\varepsilon}_0 = D \bullet \varepsilon^n$$ ④

The yield strain, ε_{sy}, which is constant strain, can be expressed with the following equation;

$$\varepsilon_{sy} = \left(\frac{A}{B}\right)^{\frac{1}{\ell}}$$ ⑤

Where, the value of A, B, C, D, ℓ, m and n are constants decided from carbon content.

Yield stress is shown by the following equation;

$$\sigma_y = \sigma_s + \sigma_0 \cdot \log(\dot{\varepsilon} / \dot{\varepsilon}_0)$$ ⑥

In the analysis, the values of 0.19% of carbon content are used. In this case, the value of A, B, C, D, ℓ, m and n are as follows, respectively;

$A = 228$ (MPa)

$B = 889$ (MPa)

$\ell = 0.3038$

$C = 26.1$ (MPa)

$m = -0.2155$

$D = 0.00126$

$n = -0.8172$

The yield stress, σ_y, independent of strain rate is 228 MPa based on reference 21.

On the other hand, the yield stress used in reference 20 is 266 MPa.

Therefore, the stress in the stress-strain curve used in the analysis is the value which is 266/228 times the stress in that obtained by the above equation as shown in (II)-Fig.A.10.2-1.

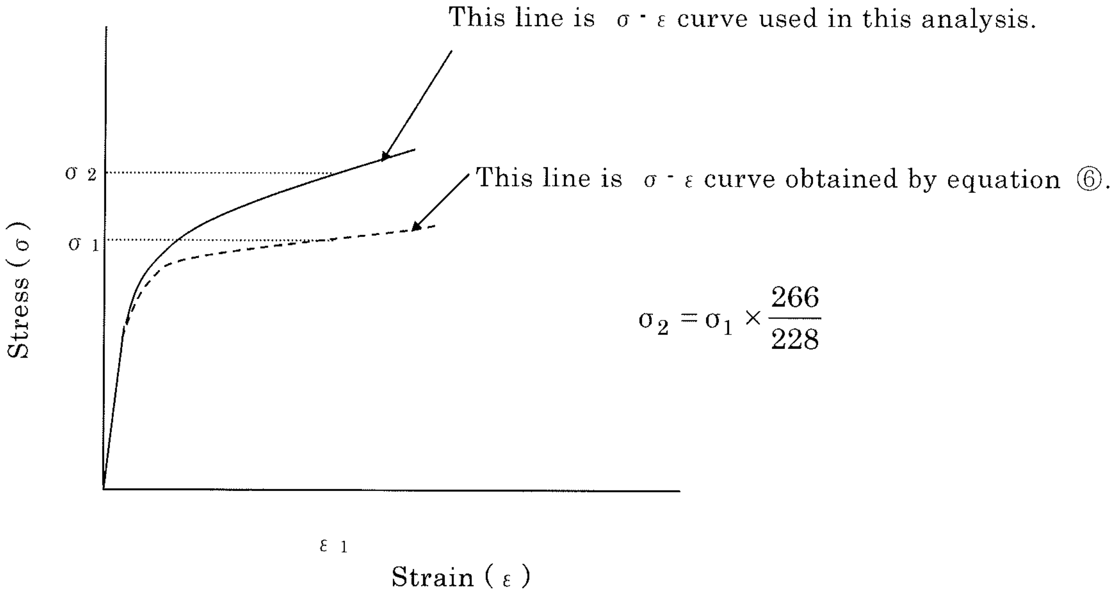

(II)-Fig.A.10.2-1 Stress - strain curves

4. Test pieces (fin) form, conditions and results of tests

The test piece of the test series 7384 shown in reference 20 is analyzed. The test piece form, conditions, and test result are shown below.

As shown in (II)-Fig.A.10.2-2, the test piece form is a fin of 8 inches in height, 3/8 inch in thickness, and it stands perpendicularly (Inclination is 0 degree.). The weight and the fall height of the drop hammer dropped to the fin are 60 pound (267 N) and 30 feet (9.1 m), respectively.

Six fins are tested and those test results are shown in (II)-Table A 10.2-1 and (II)-Fig.A.10.2-3.

(II)-Table A.10.2-1 and (II)-Fig.A.10.2-3 show the peak load, the deformation value and the deformation mode obtained from the test result, respectively.

As shown in (II)-Table A.10.2-1, the peak load and the deformation value of the fin obtained from the test result are in the range of 3.05×10^5 to 3.40×10^5 N, and 17.3 to 26.4 mm, respectively.

Moreover, as evident from (II)-Fig.A.10.2-3, the deformation mode of the fins is divided into two groups.

Therefore, about deformation mode 1, the bend occurs in the upper of the fin, and about deformation mode 2, the bend occurs in the center of the height of the fin.

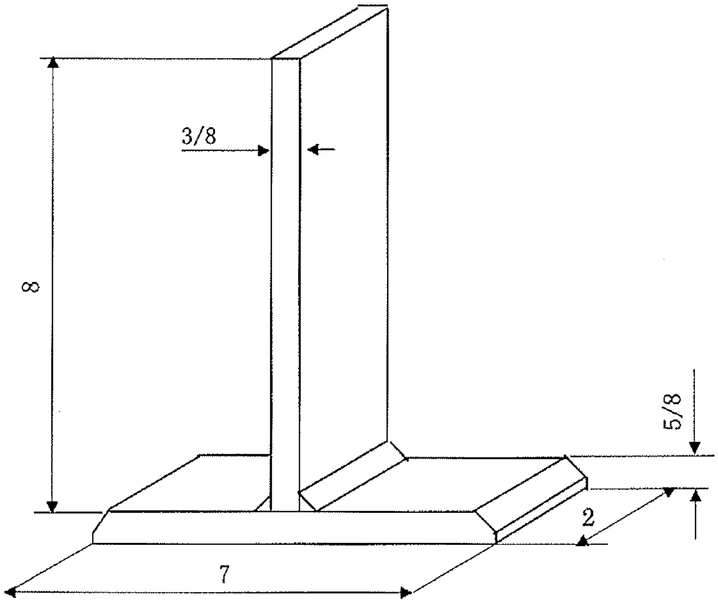

(Unit : inch)

(II)-Fig.A.10.2-2 Test piece form

(II)-Table A10.2-1 Peak load and deformation value of the fin (Test results)

*1 Fin ID No.	Load		Deformation	
	*1 Peak per unit fin width	Peak load	*1 Rate of deformation	Deformation value
	(lbs/in)	(×10⁵ N)	(%)	(mm)
73841	37636	3.35	8.5	17.3
73842	37636	3.35	13.0	26.4
73843	37082	3.30	9.0	18.3
73844	38189	3.40	12.5	25.4
73845	37636	3.35	11.0	22.3
73846	34315	3.05	13.0	26.4

*1 : The values shown in reference 20.

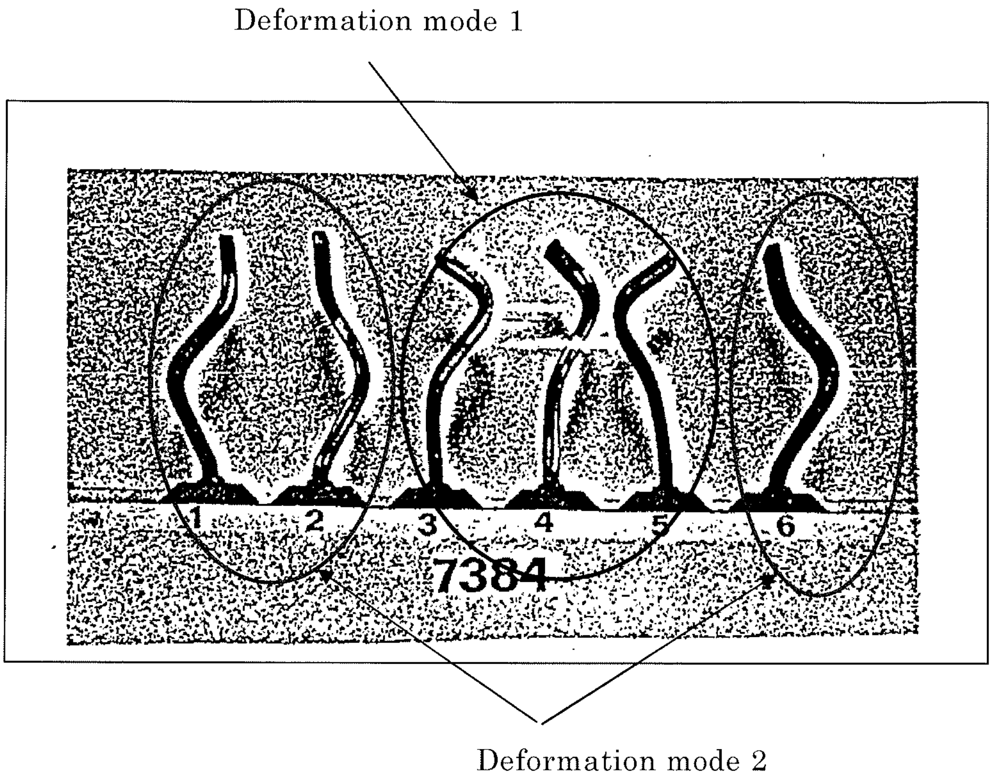

(II)-Fig.A.10.2-3 Deformation of test piece

5. Analytical model

Analytical model is shown in (II)-Fig.A.10.2-4 and analysis condition is shown in (II)-Fig.A.10.2-5.

In this report, in order to carry out the simulation of the different deformation mode and peak load of these fins, two kinds of pre-distortion are given to the analytical model.

For deformation mode 1, there is a possibility of having not collided in parallel between upper surface of the fin and the hammer. So, very small inclination is given to the surface of the top edge of the fin analytical model. The analytical model is defined as the analytical model 1.

For deformation mode 2, there is a possibility of having small bend of fin at initial condition. So, very small bend is given in the central region of the fin analytical model. The analytical model is defined as the analytical model 2.

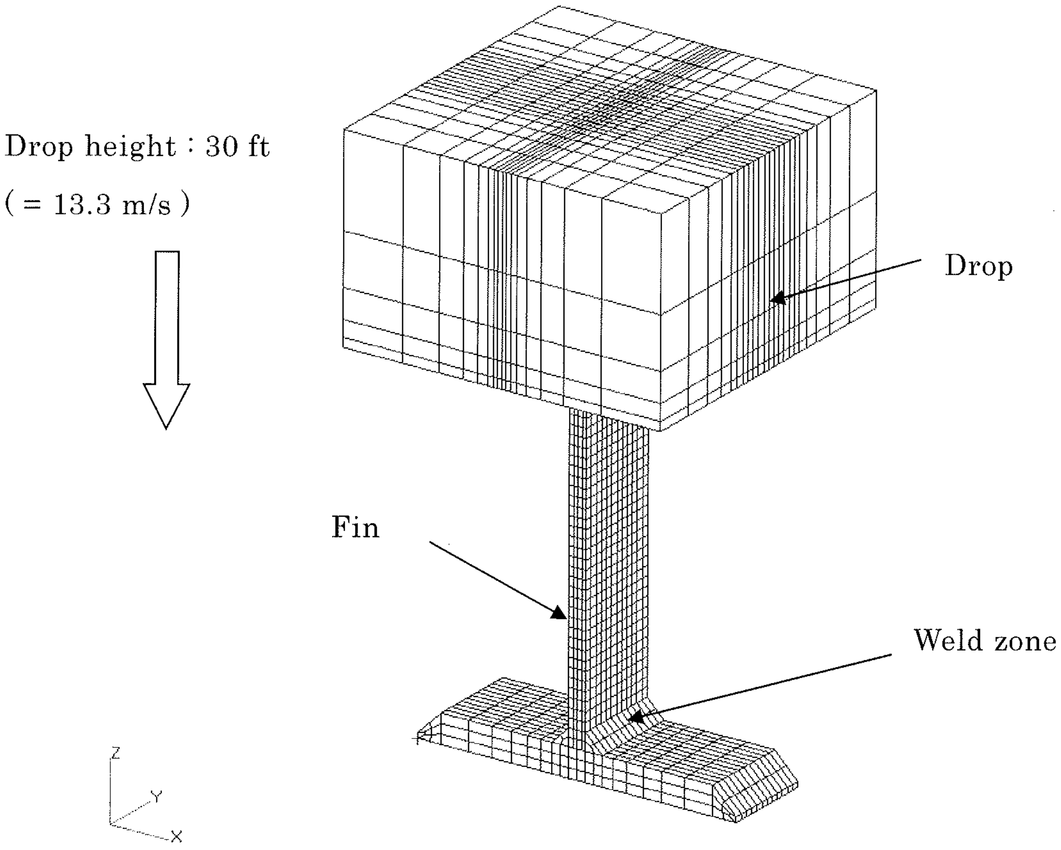

(II)-Fig.A.10.2-4 Analytical model

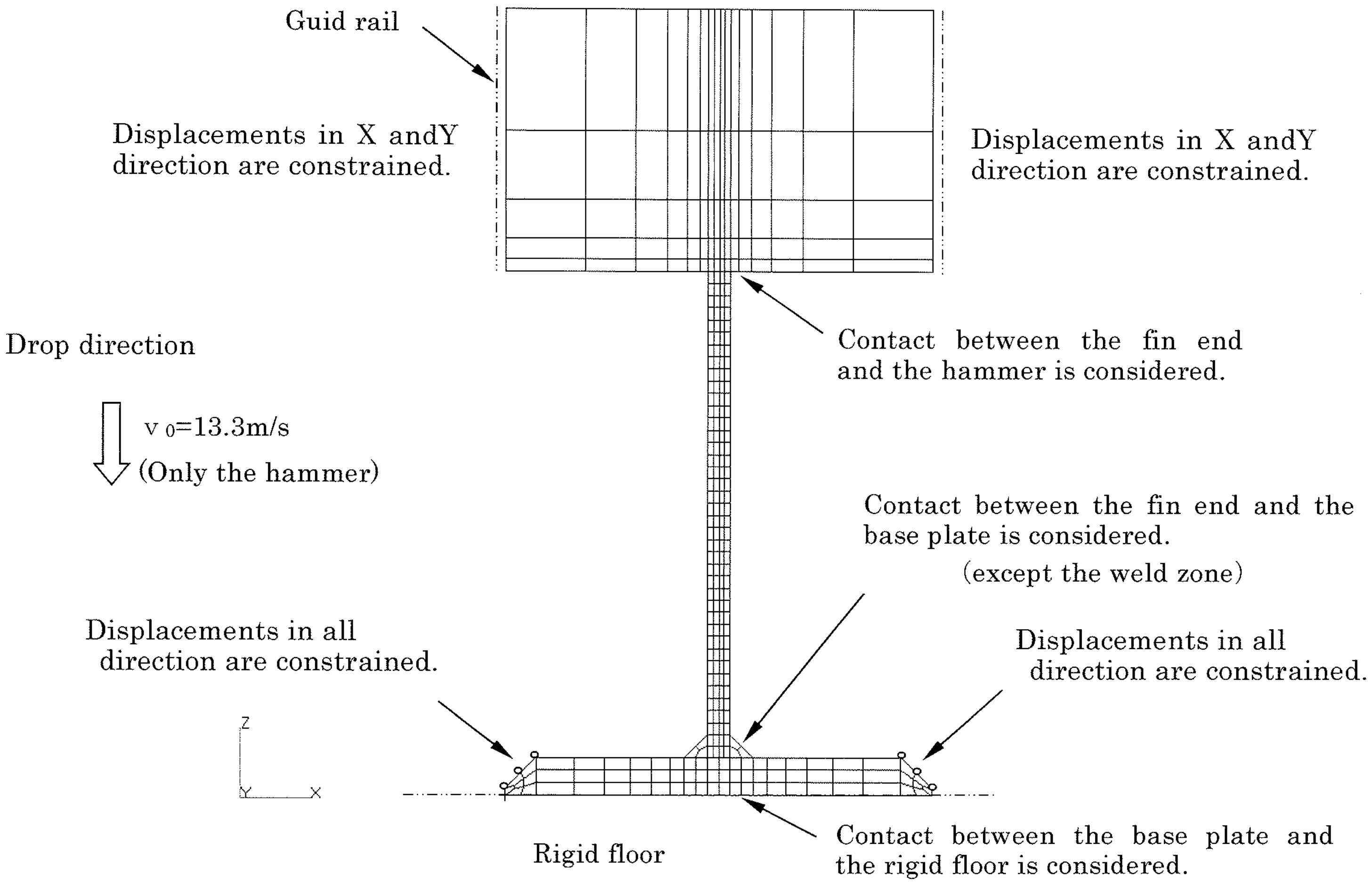

(II)-Fig.A.10.2-5 Analytical conditions

6. Analytical results and comparison with the test results

The analytical results about the analytical model 1 and 2 using LS-DYNA are shown below.

The analytical result of the analytical model 1 is shown in (II)-Fig.A.10.2-6 through (II)-Fig.A.10.2-8.

(II)-Fig.A.10.2-6 is the deformation of the fins. As shown in this figure, this deformation mode is the mode that a bend occurs in the upper part of the fin like the deformation mode 1 of the test result.

(II)-Fig.A.10.2-7 shows the time history of the displacement of the fin, and the deformation value after impact is 17.4 mm. The deformation value of the fin in the test result is within the range of 17.3 mm to 26.4 mm, and the analysis value is within the range.

Moreover, (II)-Fig.A.10.2-8 shows the time history of impact force generated on the fin. As shown in this figure, the maximum impact force is 3.20×10^5 N. This value is within the range of peak load, 3.05×10^5 N to 3.40×10^5 N, shown in (II)-Table A.10.2-1.

The analytical result of the analytical model 2 is shown in (II)-Fig.A.10.2-9 through (II)-Fig.A.10.2-11.

(II)-Fig.A.10.2-9 is the deformation of the fin. As shown in this figure, this deformation mode is the mode that a bend occurs in the central part of the height of a fin like the deformation mode 2 of a test result.

(II)-Fig.A.10.2-10 shows the time history of the displacement of the fin, and the deformation value after drop is 19.2 mm. This value is also within the range of 17.3 mm to 26.4 mm of the deformation value of the fin in the test result.

Moreover, (II)-Fig.A.10.2-11 shows the time history of impact force generated on the fin, and the maximum impact force is 3.26×10^5 N. This value is also within the range of peak load, 3.05×10^5 N to 3.40×10^5 N, of the test result.

Therefore, it is concluded that the deformation mode, the displacement value and the peak load of a fin obtained by the dynamic analysis are considerably coincident with those of the test results.

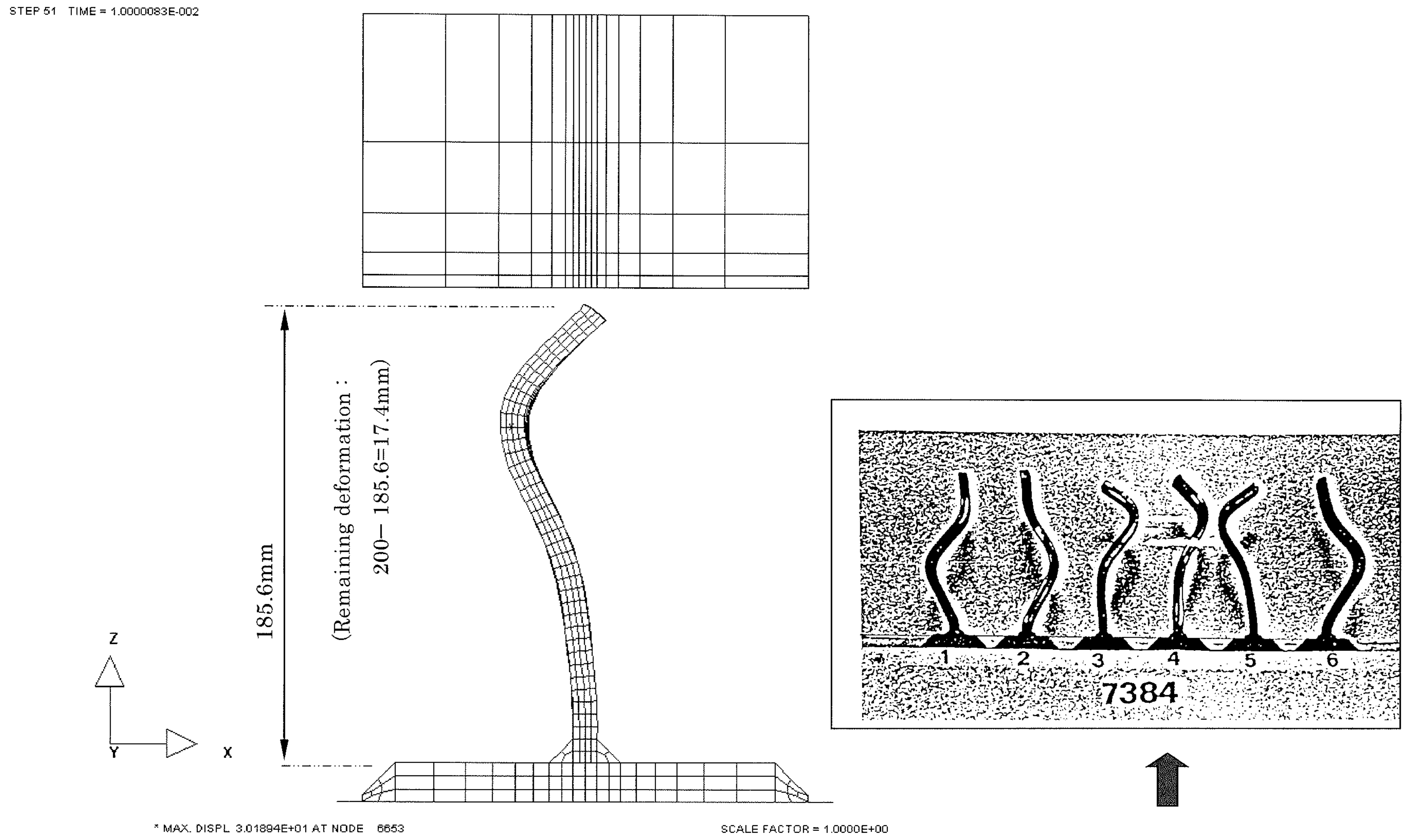

(II)-Fig.A.10.2-6 Deformation of analytical model 1

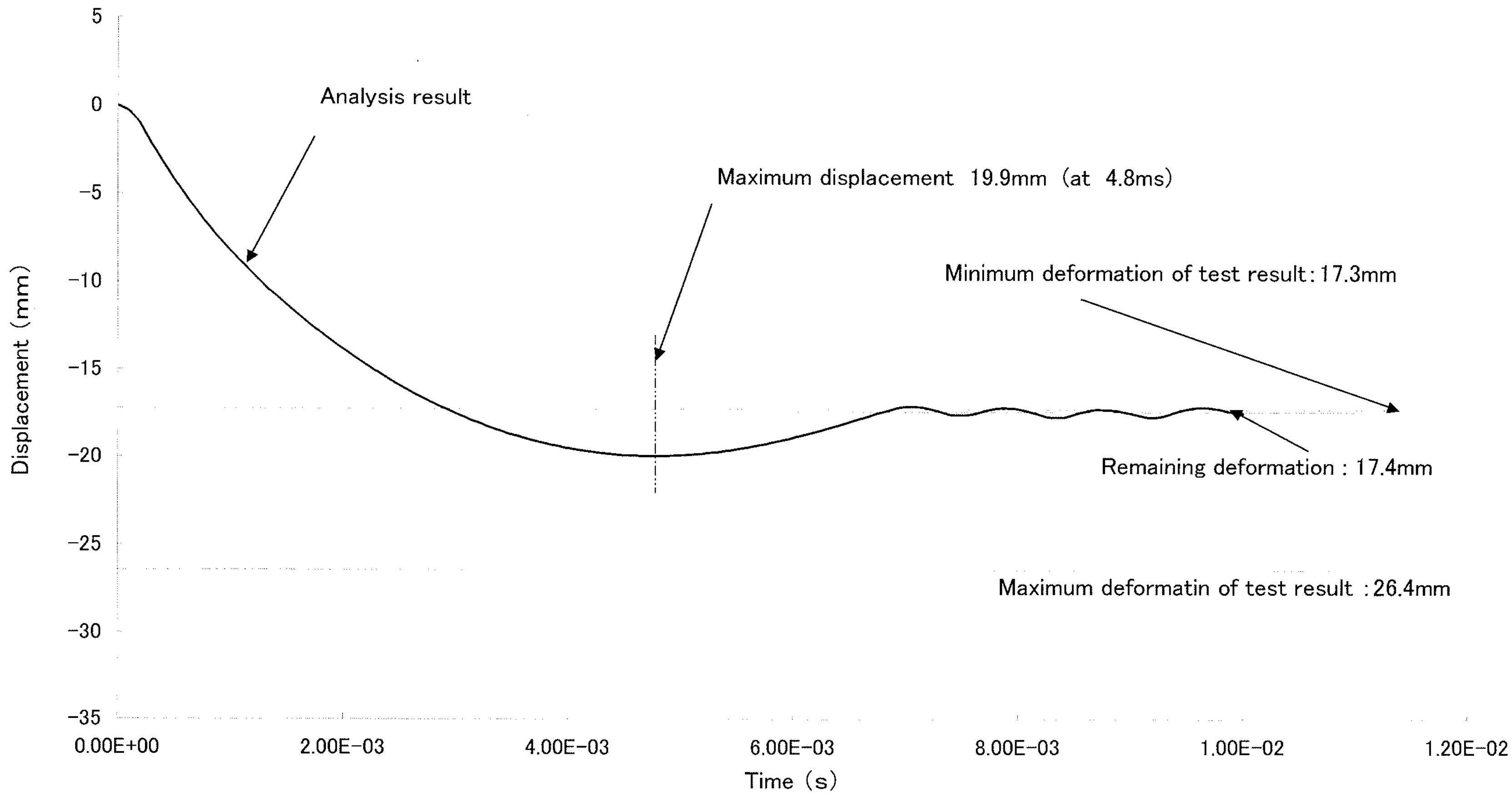

(II)-Fig.A.10.2-7 Time history of displacement of the fin

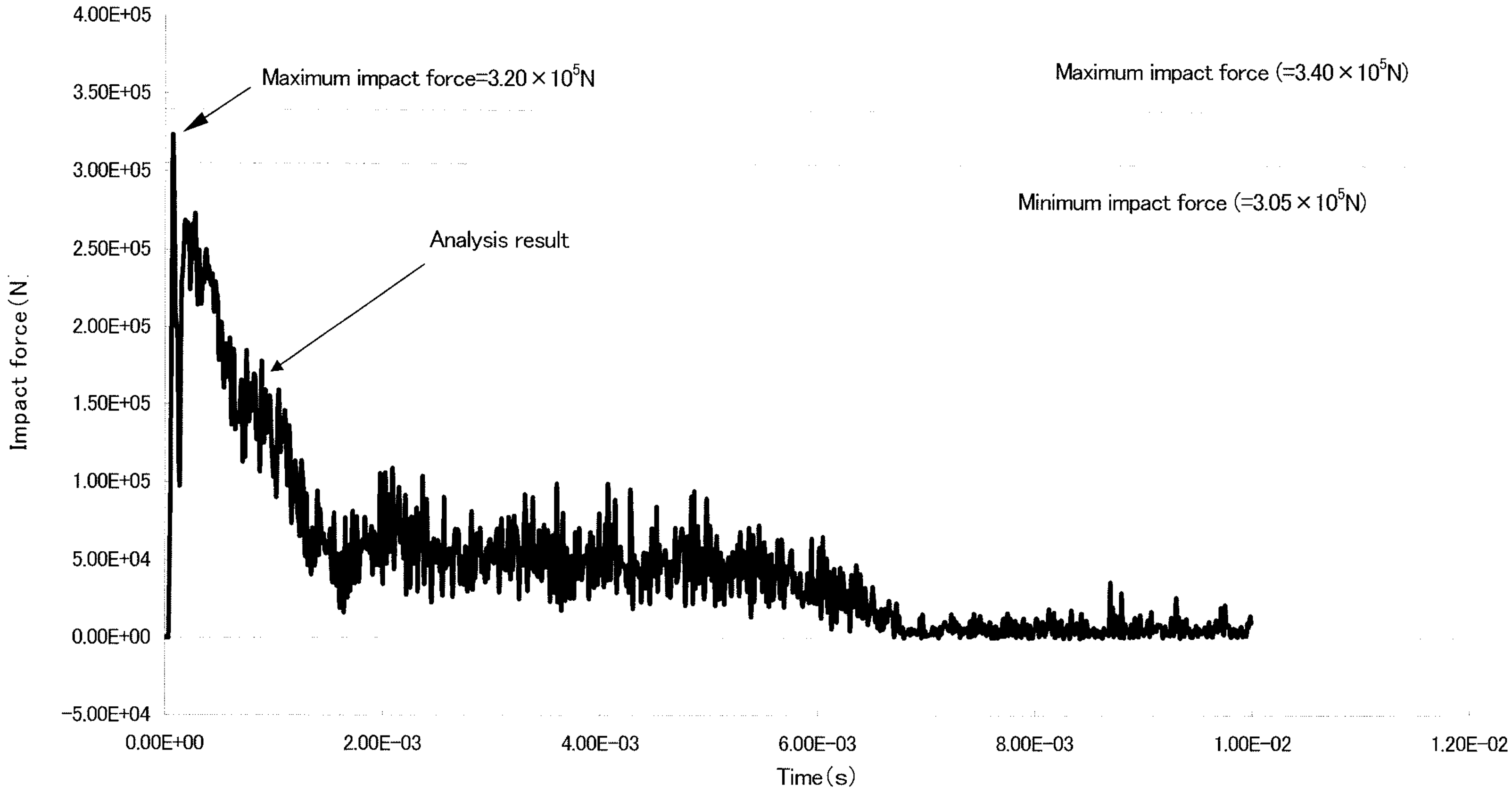

(II)-Fig.A.10.2-8 Time history of impact force generated on the fin

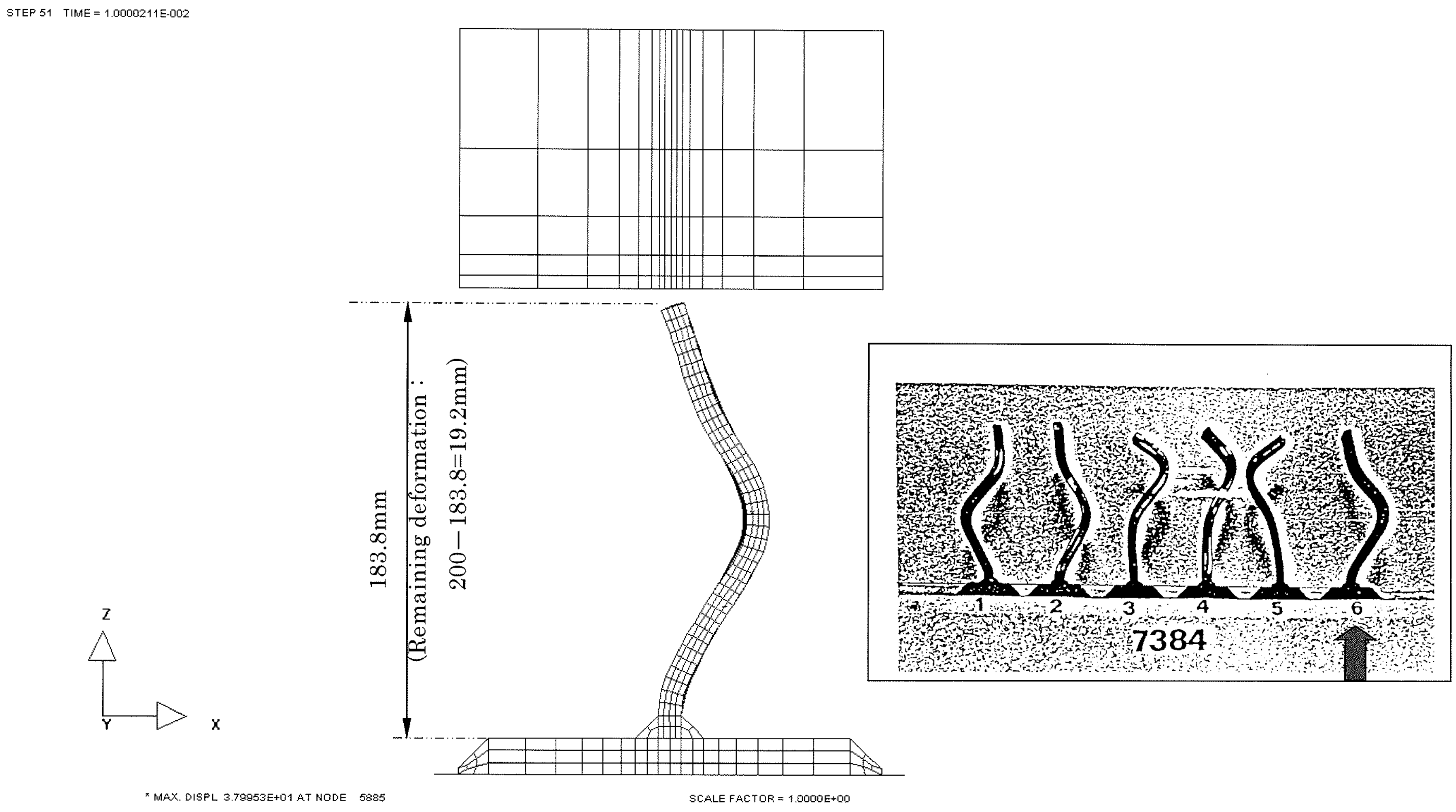

(II)-Fig.A.10.2-9　Deformation of analytical model 2

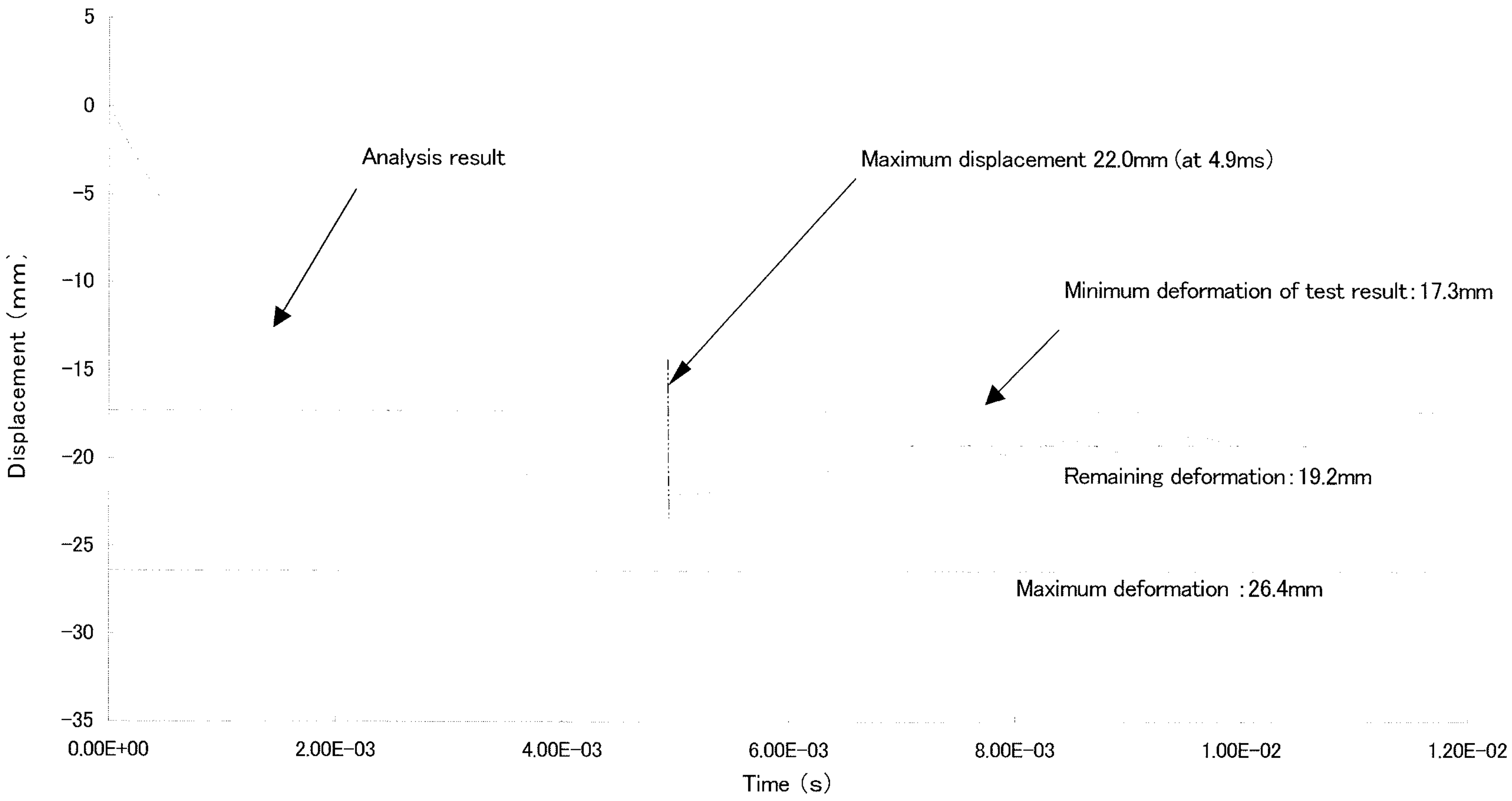

(II)-Fig.A.10.2-10 Time history of displacement of the fin

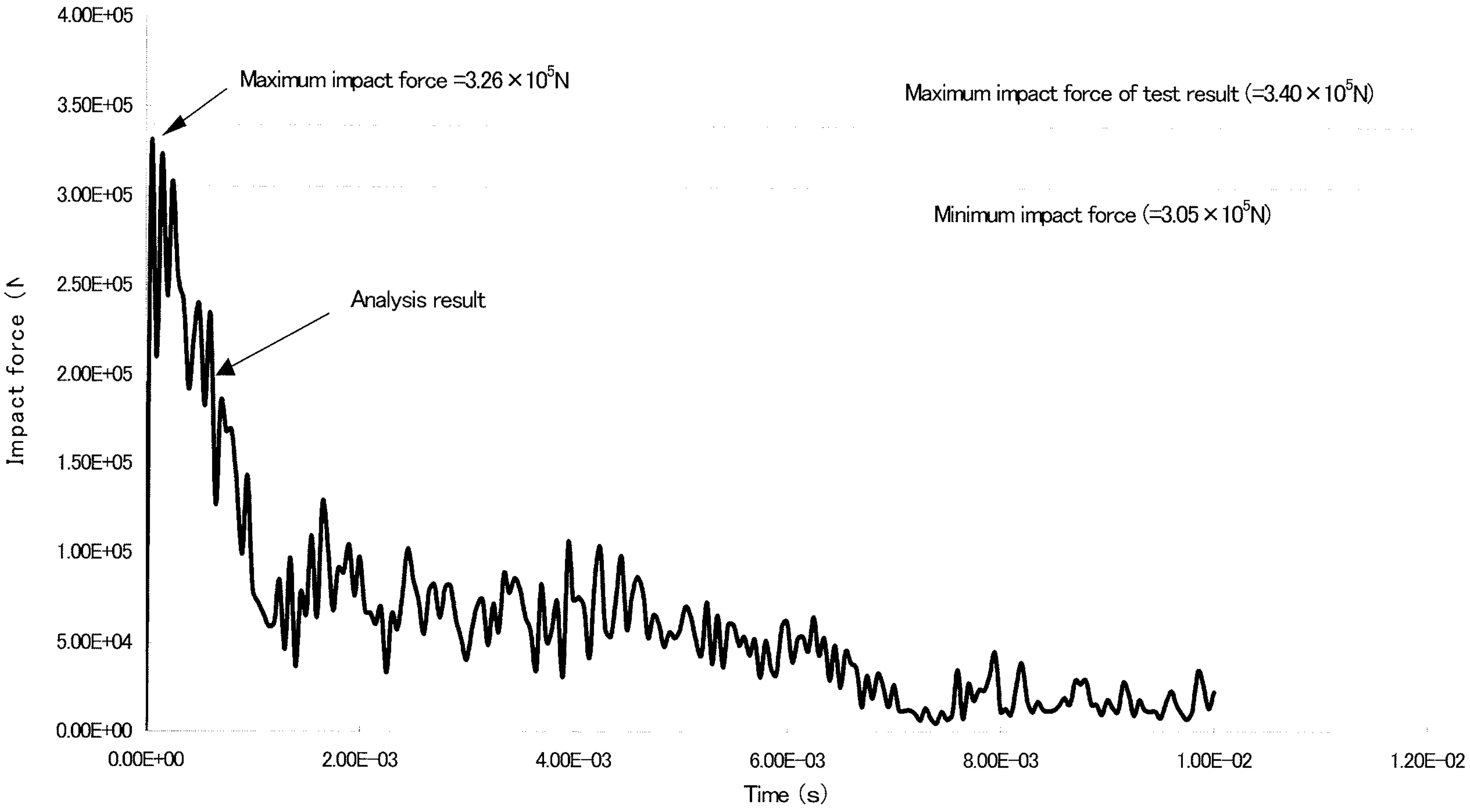

(II)-Fig.A.10.2-11　Time history of impact force generated on the fin

A.10.3 Appendix-3

Strength analysis of lifting instrument

The lifting instrument for this package includes a wire rope and a shackle.

They satisfy the following standard and have a sufficient strength.

(1) Wire rope

Standard: Core wire JIS B2801 SUS 304

Rope diameter :40 mm(7 x 19)

Tensile fracture load :844 × 10^3 N (86 × 10^3 kgf)

Operating load :140 × 10^3 N (14.3 × 10^3 kgf) (Safety factor = 6)

(2) Shackle

Standard: JIS B2801 SB65

Operating load : 294 × 10^3 N (30 × 10^3 kgf)

A.10.4 Appendix-4

Compatibility with the ASME Code under design conditions

1. Summary

This package is used to transport to the reprocessing facilities in foreign countries, such as U.S.A and U.K. etc, for reprocessing the spent fuels of JRR-3 standard silicide type, JRR-3 follower silicide type, JRR-3 MNU type, It is necessary to acquire the permission and approval of U.S.A and relevant countries as well as Japanese Government.

According to the U.S Government (the ASME Code), the performance of a pressure vessel is required for the body and the lid forming this package.

Therefore, for reference, the analysis is made on the following items.

- Minimum required thickness for the body and the lid
- Minimum required size for the lid bolt
- Minimum required thickness for the valve disc
- Minimum required sectional area for the valve main bolt
- Minimum required sectional area for the valve protection cover bolt
- Reinforcement of the valve hole
- Exclusions of fatigue analysis

As a result of the analysis, the dimensions of this packaging satisfy the requirements in the ASME code as shown in (II)-Fig.A.10.4-1.

2. Design conditions

Pressure : P = [redacted] KPa ([redacted] kgf/cm^{2}G)

Temperature : [redacted]℃

3. Allowable stress

3.1 Shell, bottom plate and lid

Material: SA-182 [redacted] forging (equivalent to [redacted])

From Table I-10.2 in the reference [1], the design stress intensity value Sm is as follows.

Sm = [redacted] MPa ([redacted] kgf/mm^2)

3.2 Lid bolt

Material: SA-564 [redacted] (equivalent to [redacted])

From Table I-1.3 in the reference [1], the design stress intensity value Sm is as follows.

Sm = [redacted] MPa ([redacted] kgf/mm^2)

4. Thickness of the shell (Refer to (II)-Fig.A.10.4-1)

4.1 Data

Material: SA-182 [redacted] forging (equivalent to [redacted])

Allowable stress : Sm = [redacted] MPa ([redacted] kgf/mm^2)

Inside radius : R = [redacted] mm

Thickness : t = [redacted] mm

4.2 Minimum required thickness (t_m)

According to NE 3324.3 in the reference [7], t_m is determined as follows ;

$$t_m = \frac{P \times R}{S_m - 0.6 \times P}$$

where,

$$t_m < \frac{R}{2} \text{ , and } P < 0.385\,S_m$$

Therefore, the minimum required thickness is as follow.

t_m = [redacted] mm

4.3 Conclusion

The thickness of the shell is greater than the minimum required thickness of the ASME Code.

5. Thickness of the bottom plate (Refer to (II)-Fig.A.10.4-1)

5.1 Data

Material : SA-182 [redacted] forging (equivalent to [redacted])

Allowable stress : Sm = [redacted] MPa ([redacted] kgf/ mm^2)

Inside diameter of the bottom plate : d = [redacted] mm

Thickness : t = [redacted] to [redacted] mm

5.2 Minimum required thickness (t_m)

According to NE 3325.2 in the reference [7], the minimum required thickness for the bottom plate is expressed by the following equation.

$$t_m = d\sqrt{C\ P/Sm}$$

Where, C is a constant determined according to NE 3325.3 in the reference [7].

C is 0.3 or $0.33 \times t_r$ / t_s which is larger.

t_r : Minimum required thickness for the shell = [redacted] mm

t_s : Actual thickness of the shell excluding the corrosion allowance = [redacted] mm

Therefore, $0.33 \times t_r$ / t_s = [redacted]

Consequently, C = 0.3 and t_m = [redacted] mm

Remark: Though the requirements in NE 3358.4 are not satisfied, it is confirmed in (II)-A.5.1.3 that there is no problem on strength in the weld-joint as a result of the structural analysis using the general-purpose finite element code ABAQUS.

5.3 Conclusion

From the above calculation, it is found that the thickness of the bottom plate is greater than the minimum required thickness in the ASME Code.

6. Thickness of the lid (Refer to (II)-Fig. A.10.4-1 and (II)-Fig.A.10.4-2)

6.1 Data

Material : SA-182 [redacted] forging (equivalent to [redacted])

Allowable stress : Sm = [redacted] MPa ([redacted] kgf/mm^2)

Outside diameter determined by Fig. 3325.1 (K) in the reference [7]

: d = [redacted] mm

Initial fastening load of the bolt

$$: W = \frac{\pi}{4} d^2 P = \frac{\pi}{4} \times \text{[redacted]}^2 \times \text{[redacted]}$$

$$= \text{[redacted] N ([redacted] kgf)}$$

(Internal pressure equivalent to claming load = [redacted] MPa ([redacted] kgf/mm^{2}G))

Distance between the contact circle of the gasket and the center circle of the bolthole. : h_G = [redacted] mm

Thickness of the lid : t = [redacted] mm

6.2 Thickness of the lid

The minimum required thickness is obtained by equation (2) shown in NE 3325.2 in the reference [7].

$$t_m = d\sqrt{C\ P/Sm + 1.27Wh_G/(Smd^3)}$$

From Fig. NE. 3325.1 (K) in the reference [7], C = 0.2

Therefore, t_m = [redacted] mm

Where, as P, the design pressure ([redacted] MPa ([redacted] kgf/mm^{2}G) or the internal pressure equivalent to the fastening load ([redacted] MPa ([redacted] kgf/mm^{2}G)) was used, which is larger.

6.3 Conclusion

The thickness of the lid is greater than the minimum required thickness of the ASME Code.

7. Size of the lid bolt (Refer to (II)-Fig.A.10.4-3)

7.1 Data

Material : SA-564 [redacted] (equivalent to [redacted])

Allowable stress	: Sm = [redacted] MPa ([redacted] kgf/mm^2)
Radius of contact circle of the gasket	: G = [redacted] mm
Cross-sectional area of one bolt	: [redacted] mm^2
Length of thread engagement	: L = [redacted] mm
Effective length of the thread	: [redacted] mm
Nominal diameter of the bolt	: d_s = [redacted] mm

7.2 Minimum required cross-sectional area (A_m)

According to XI-3221.1 and XI-3221.3 in the reference [1], the minimum required load for fastening of the bolt is as follows;

$$W = 0.785G^2P = \text{[redacted]}\ N\ (\text{[redacted]}\ kgf)$$

Where, as P, the internal pressure equivalent to the fastening load (= [redacted] MPa ([redacted] kgf/ mm^{2}G)) was used.

$$A_m = \frac{W}{16S_m} = \text{[redacted]} = \text{[redacted]}\ mm^2$$

7.3 Length of thread

According to NE 3362 (b) in the reference [7], the minimum required length for the bolt thread Lm is as follows;

$$L_m = 0.75 \times 48 \times \frac{S_m}{S_m{}'}$$

[redacted]

(II)-Fig.A.10.4-1　Geometry of the packaging

[redacted]

(II)-Fig.A.10.4-2　Geometry of the lid

[redacted]

(II)-Fig.A.10.4-3　Geometry of the lid bolt where, Sm and Sm′ are the allowable stresses of the bolt and the lid at [redacted] ℃ respectively.

$$L_m = 0.75 \text{ x } 48 \text{ x } \frac{\text{[redacted]}}{\text{[redacted]}} = \text{[redacted]} \text{ mm}$$

7.4 Conclusion

Both the cross-sectional area and the thread length of the lid bolt are greater than the minimum required value of the ASME Code.

8. Thickness of the valve disc

The geometry of the disc is shown in (II)-Fig.A.10.4-4.

[redacted]

(II)-Fig.A.10.4-4 Geometry of the valve disc

8.1 Data

Material : SA-182 [redacted] forging (equivalent to [redacted])

Allowable stress : S_m = [redacted] MPa ([redacted] kgf/ mm^2)

Mean diameter of the gasket : d = [redacted] mm

Thickness : t = [redacted] mm

8.2 Minimum required thickness

According to NE-3325.2 (b) in the Reference [7], the minimum required thickness t_m is found by the following equation:

$$t_m = d\sqrt{C\ P/Sm}$$

where, a constant C is 0.2 as shown in NE-3325-1 (n) in the reference [7].

Therefore, t_m = [redacted] mm.

8.3 Conclusion

The thickness of the disc is greater than the minimum required thickness of the ASME Code.

9. Valve main bolt

The geometry of the valve main bolt is shown in (II)-Fig.A.10.4-5.

9.1 Data

Material : SA-564 [redacted] (equivalent to [redacted])

Allowable stress : S_m = [redacted] MPa ([redacted] kgf/ mm^2)

Cross-sectional area : A = [redacted] mm^2

Internal pressure acting radius : d = [redacted] mm

Number of bolts : n = [redacted]

9.2 Minimum required cross-sectional area for the valve main bolt

The force F acting on one valve main bolt is determined by the following equation;

$$F = \frac{\frac{\pi}{4}\ d^2 P}{n} = \frac{\frac{\pi}{4} \times \text{[redacted]} \times \text{[redacted]}}{\text{[redacted]}} = \text{[redacted] N ([redacted] kgf)}$$

The minimum required cross-sectional area for the valve main bolt is as follows.

$$A_m = \frac{F}{S_m} = \text{[redacted]} = \text{[redacted] mm}^2$$

[redacted]

(II)-Fig.A.10.4-5　Geometry of the valve main bolt

9.3 Conclusion

The cross-sectional area of the valve main bolt is greater than the minimum required cross-sectional area of the ASME Code.

10. Valve protection cover bolt

(II)-Fig.A.10.4-6 shows the geometry of the cover bolt.

The force acting on the bolt will be balanced with the internal pressure acting on the disc, but for conservative evaluation here, on the assumption of leak from the disc seal, a greater force shall act on the bolt.

10.1 Data

Material : SA-564 [redacted] (equivalent to [redacted])

Allowable stress : S_m = [redacted] MPa ([redacted] kgf/ mm^2)

Cross-sectional area : A = [redacted] mm^2

Internal pressure acting radius : d = [redacted] mm

Number of bolts : n = [redacted]

10.2 Minimum required cross-sectional area for valve protection cover bolt

The force F acting on one bolt is found by the following equation.

$$F = \frac{\frac{\pi}{4}\ d^2 P}{n} = \frac{\frac{\pi}{4} \times \text{[redacted]}^2 \times \text{[redacted]}}{\text{[redacted]}} = \text{[redacted] N ([redacted] kgf)}$$

The minimum required cross-sectional area for the bolt is as follows.

$$A_m = \frac{F}{S_m} = \text{[redacted]} = \text{[redacted]}\ \text{mm}^2$$

10.3 Conclusion

The cross-sectional area of the value protection cover bolt is greater than the minimum required cross-sectional area of the ASME Code.

[redacted]

(II)-Fig.A.10.4-6 Geometry of the valve protection cover bolt

11. Reinforcement of the valve hole

Since the diameter of the drain and vent valves is both [redacted] mm, there is no need for reinforcing the hole according to NE-3332.1 (See NOTE below) in the reference [7].

NOTE: NE-3332.1 specifies the exclusions of reinforcement for a hole :

"If the hole diameter is less than 2-1/2" (64 mm), no reinforcement is required."

12. Cycle

As shown below, all requirements specified in NE 3221-5 (d) in the reference [7] are satisfied.

Consequently, no analysis is required.

12.1 Cycle between atmospheric pressure and operating pressure

$$Sa = 3 \times \text{[redacted]} = \text{[redacted]} \text{ MPa ([redacted] kgf/ mm}^2\text{)}$$

According to Fig. I-9.2.1 in the reference [1], the number of cycles corresponding to the above Sa value is about [redacted] cycles.

Since the maximum predicted number of cycles used is 300 cycles, it follows that the requirements in the ASME Code are satisfied.

12.2 Pressure fluctuations in normal operating pressure

The significant pressure fluctuation defined in the ASME Code is obtained by the following equation.

$$P_d = P \times \frac{1}{3} \times \frac{S_a}{S_m} = \text{[redacted]} \times \frac{1}{3} \times \text{[redacted]} = \text{[redacted]} \text{ MPa ([redacted] kgf/ mm}^2\text{)}$$

Where : P_d ; Design pressure

S_a ; Fatigue strength at 10^6 times

It is not expected that the pressure fluctuation during normal conditions of transport exceeds the above value.

Consequently, the requirements in the ASME Code are satisfied.

12.3 Temperature difference-startup and stop

The maximum distance d between two adjacent points is:

$$d = 2\sqrt{Rt}$$

where, R ; Average radius of the pressure vessel = [redacted] mm

t ; Thickness of the body = [redacted] mm

Therefore, d = [redacted] mm

The extreme occurring temperature in the body is [redacted] ℃ and [redacted] ℃.

The average temperature at that time is [redacted] ℃.

The modulus of longitudinal elasticity E and the coefficient of linear thermal expansion α of the material in this temperature are shown in Tables I-5.0 and I-6.0 in the reference [1] respectively :

E = [redacted] MPa

α = [redacted] 1/℃

Since the fatigue strength Sa is [redacted] MPa (cycles 100), the allowable temperature difference ΔT is determined by the following equation.

$$\Delta T = \frac{Sa}{2E\alpha} = \text{[redacted]} \ ℃$$

Since the maximum occurring temperature difference in the body is [redacted] ℃, the requirements in the ASME Code are satisfied.

12.4 Temperature difference-normal operating

The significant changes in temperature difference are found by the following equation;

$$\frac{Sa}{E\alpha} = \text{[redacted]} = \text{[redacted]} ℃$$

where, Sa ; Fatigue strength at 10^6 times = [redacted] MPa ([redacted] kgf/ mm^2)

It is not expected that such temperature difference changes as exceed the above value during normal conditions of transport are found.

Accordingly, the requirements in the ASME Code are satisfied.

12.5 Temperature difference-dissimilar material

Since the body is all of stainless steel, this paragraph does not apply.

12.6 Stress due to mechanical load

Since this packaging is fixed by the tie down devices during transport, no stress due to mechanical load as studied in this paragraph occurs.

13. Conclusion

The results of the requirements specified in the ASME Code for this packaging are shown in (II)-Table A.10.4-1.

As shown in this table, the requirements specified in the ASME Code for this packaging are satisfied.

(II)-Table A.10.4-1 Comparison between the allowable value and the actual size

	Minimum value required in the ASME Code	Actual size
Thickness of shell (mm)	[redacted]	[redacted]
Thickness of bottom plate (mm)	[redacted]	[redacted]
Thickness of lid (mm)	[redacted]	[redacted]
Cross-sectional area of lid bolt (mm)	[redacted]	[redacted]
Thickness of valve disc (mm)	[redacted]	[redacted]
Cross-sectional area of valve main bolt (mm^2)	[redacted]	[redacted]
Cross-sectional area of valve protection cover bolt (mm^2)	[redacted]	[redacted]

A.10.5 Appendix-5

Strength of the packaging when the external pressure equivalent to the water depth of 5,000 m acts.

In this paragraph, the stress generated when the external pressure equivalent to the water depth of 5,000 m acts on the packaging is calculated, and it is shown that the value is not exceed the yield stress.

1. Strength of the shell

(II)-Fig.A.10.5-1 shows the analytical model of the shell to which the external pressure (q) is applied. As shown in Table-32, case-1c and 1d of the reference (14), the principal stress generated at the shell under the external pressure equivalent to the water depth of 5,000 m is given as follows;

$$\sigma_1 = \frac{-qa^2}{a^2 - b^2} \qquad \text{(longitudinal stress)}$$

$$\sigma_2 = -q\,\frac{a^2(r^2 + b^2)}{r^2(a^2 - b^2)} \qquad \text{(circumferential stress)}$$

$$\sigma_3 = -q\,\frac{a^2(r^2 - b^2)}{r^2(a^2 - b^2)} \qquad \text{(radial stress)}$$

[redacted]

(II)-Fig.A.10.5-1 Analytical model of the shell

In this case, the stress intensity (S) shows the maximum value on the inner surface of the shell (r=b).

Since "a" is [redacted] mm and "b" is [redacted] mm, "σ_2" and "σ_3" can be given respectively as follows;

$\sigma_2 =$ [redacted], $\sigma_3 =$ [redacted]

Accordingly, the stress intensity is given as below;

$S = \sigma_3 - \sigma_2 =$ [redacted]

Since the external pressure "q" equivalent to the water depth of 5,000m is as follows;

q = 50 MPaG

The stress intensity "S" is given as follows ;

S = [redacted] × 50 = [redacted]MPa

If the allowable stress σ_a at the shell is equal to the yield stress σ_y, σ_a can be given as follows;

$\sigma_a = \sigma_y =$ [redacted] MPa

Consequently, the safety factor (RF) and the safety margin factor (MS) are given as follows;

RF = [redacted] = [redacted]

MS = [redacted] − 1 = [redacted]

Accordingly, the packaging has the sufficient strength against the external pressure equivalent to the water depth of 5,000 m.

2. Strength of the lid and the bottom plate

Since the bottom plate and the lid have [redacted] mm and [redacted] mm in thickness respectively, the evaluation of the strength is made on the bottom plate having smaller thickness.

The analytical model is as shown in (II)-Fig.A.10.5-2, in which the uniform pressure acts on the disk fixed to the circumference.

According to the table-24, case-10b given in the reference (14), the maximum bending moment occurs at the fixed end of the circumference.

The bending moment per unit length is given as follows;

$$M_r = \frac{q\,b^2}{8} = \frac{50 \times \text{[redacted]}^2}{8} = \text{[redacted]}\ \text{N}\cdot\text{mm/mm}$$

where, q : External pressure (50 MPaG) equivalent to the water depth of 5,000m

b : Radius of the shell (= [redacted] mm)

Therefore, the circumferential bending moment is as follows;

$$M_t = \nu M_r = \text{[redacted]}\ \text{N}\cdot\text{mm/mm}$$

where, ν : Poisson's ratio (=0.3)

The shearing force (Q) per unit length is given as follows;

$$Q = \frac{q\,b}{2} = \text{[redacted]} = \text{[redacted]}\ \text{N}$$

[redacted]

(II)-Fig.A.10.5-2 Analytical model of the bottom plate

If the thickness of the bottom plate is "t", the maximum stress can be given as follows;

On the outer surface of the bottom plate

- Radial stress

$$\sigma_r = \frac{6\times M_r}{t^2} = \frac{6\times\text{[redacted]}^{6}}{\text{[redacted]}^{2}} = \text{[redacted]}\ \text{MPa}$$

- Circumferential stress

$$\sigma_t = \frac{6\times M_t}{t^2} = \frac{6\times\text{[redacted]}}{\text{[redacted]}^{2}} = \text{[redacted]}\ \text{MPa}$$

- Longitudinal stress

$$\sigma_o = -q = -50\ \text{MPa}$$

At the center of the thickness

- Shearing stress

$$\tau = \frac{3}{2} \times \frac{Q}{t} = \frac{3}{2} \times \frac{\text{[redacted]}}{\text{[redacted]}} = \text{[redacted]} \text{MPa}$$

Therefore, the maximum stress and the maximum shearing stress are given respectively as follows;

- The maximum stress

$$\sigma_{\max} = \sigma_r = \text{[redacted]}\ \text{MPa}$$

- The maximum shear stress

$$\tau_{\max} = \tau = \text{[redacted]} \text{MPa}$$

Thus, the allowable bending stress (σ_{ab}) and the allowable shearing stress (τ_a) of the bottom plate are given respectively as follows ;

$$\sigma_{ab} = 1.5 \times \sigma_y = 1.5 \times \text{[redacted]} = \text{[redacted]}\ \text{MPa}$$

$$\tau_a = 0.6 \times \sigma_y = 0.6 \times \text{[redacted]} = \text{[redacted]}\ \text{MPa}$$

Accordingly, the safety factor (RF) and the safety margin (MS) against the bending stress are as follows;

$$RF = \frac{\text{[redacted]}}{\text{[redacted]}} = \text{[redacted]}$$

$$MS = \text{[redacted]} - 1 = \text{[redacted]}$$

The safety factor (RF) and safety margin (MS) against the shearing stress are given as follows.

$$RF = \frac{\text{[redacted]}}{\text{[redacted]}} = \text{[redacted]}$$

$$MS = \text{[redacted]} - 1 = \text{[redacted]}$$

Therefore, the lid and the bottom plate have the sufficient strength against the external pressure equivalent to the water depth of 5,000 m.

3. Strength of the lid bolt

For the stress generated on the bolt when it is applied with the external pressure, it is assumed that no tensile stress by initial fastening force applies in the lid bolt and the packaging is subject to the external pressure 50 MPaG. The longitudinal compressive stress 50 MPaG is generated in the bolt when the packaging is subject to the external pressure 50 MPaG.

The allowable compressive stress (σ_{ac}) of the lid bolt is as follows;

$\sigma_{ac} = \sigma_y =$ [redacted] MPa

Accordingly, the safety factor (RF) and the safety margin (MS) are as respectively as follows;

RF = [redacted] / [redacted] = [redacted]

MS = [redacted] − 1 = [redacted]

Therefore, the lid bolt has the sufficient strength against the external pressure equivalent to the water depth of 5,000 m.

A.10.6 Appendix-6

References

1) ASME Boiler and Pressure Vessel Code, Section Ⅲ, Division 1 Appendices, 1986 Edition including 1986 Addenda.
2) Aluminum Handbook, Japan Light Metal Association, 1973.
3) Sumitomo Aluminum Handbook, 1971.
4) Atomic Energy Handbook, Material Section, Shoko Publication.
5) Shinko Aluminum Handbook.
6) ABAQUS / STANDARD User Manual Version 6.3, Hibbitt, Karlsson&Sorensen, Inc. in USA.
7) ASME Boiler and Pressure Vessel Code, Section Ⅲ, Division 1, Subsection NE, 1986 Edition including 1986 Addenda.
8) Text of Technical Course of Stainless Steel, "About corrosion, heat treatment, welding and mechanical property at low-temperature". Japan Stainless Steel Association.
9) Aerospace Structural Metals Handbook, Vol.2, 1978.
10) New Usage of O-ring, Japan Valqua Co.
11) Mechanical Engineering Dictionary, Nikkan Kogyo Newspaper Co.
12) P.C. Paris, G.C. Sih : "Stress Alalysis of Crack" Fracture Toughness Testing and Its Application ASTM STP No.381.
13) R.H. Sailors and H.T. Corten : "Relationship between Material Fracture Toughness using Fracture Mechanics and Transition Temperature Tests".
14) R.J. Roark and W.C. Young, Formulas for Stress and Strain, MC Grow Hill Co., New York (1975).
15) IMV TECHNICAL REPORT, International Mechanical Vibration Laboratory, 1971.
16) Timoshenko, S., "Theory of Elastic Stability".
17) Ando, Okabayashi, "Structural Design of Atomic Energy Plant", Tokyo University Publication.
18) M.Nishida, "Stress Concentration", Morikita Publication.
19) LS-DYNA Version 970, USER'S MANUAL, LIVERMORE SOFTWARE TECHNOLOGY Co.
20) Verificxation of the performance of impact limiting fins for transportation containers,Part-II Monserco Limited, Sept. 5, 1986
21) Ikujima, Nagata, "Material data collection for impact calculation" (JARERI-M 88-191), p179
22) ASME Code, Sec. II-D, 2003 Addenda july 1, TABLE TM-1
23) IAEA ST-2 Para. 701.9

B. Thermal analysis

In this analysis, the thermal performance of the package is investigated under normal and accident conditions of transport.

B.1 Summary

The thermal analysis is performed to verify that thermal design of this package is satisfied with following conditions.

① Decay heat generated from contents is sufficiently dissipated to the outside of the package.

② Temperature rise-up of such important parts as fuel elements is sufficiently controlled even under accident conditions (the fire accident) of transport.

③ The package is maintained its integrity under an ambient temperature of -40 ℃.

This means that the thermal analysis is performed to verify the thermal design of this package to have enough thermal ability and to keep the integrity of structural strength, containment shielding ability and subcriticality of the package under normal and accident conditions of transport.

Thermal conditions and requirement under normal and accident conditions of transport specified in the IAEA Regulations are as follows.

(1) Normal conditions of transport

i) Surface temperature of the package shall not exceed 85 ℃ in the ambient temperature of 38 ℃.

ii) The package shall be insolated in the ambient temperature of 38 ℃.

iii) The integrity of the package shall be maintained under the ambient temperature of -40 ℃.

(2) Accident conditions of transport

i) The package is exposed to a 800 ℃ fire with the emissivity factor of an atmosphere of 0.9 for 30 minutes (evaluation at the fire accident). The package is insolated during fire.

ii) The package shall be insolated under the ambient temperature of 38 ℃ before and after a fire.

The summary of this package design is as follows.

This package is composed of the packaging with fins and the baskets contained. Each basket has the basket lodgement corresponding to the kinds of fuel elements, and the fuel elements are contained in the basket lodgement. Air is enclosed in the cavity of the package at atmospheric pressure when it is closed up. The cooling method of this package mainly depends on natural cooling. Namely, the decay heat generating from the spent fuel elements transfers to the body and the lid through the cavity air and the basket made of the neutron poison and stainless steel, and further is diffused from the outer surface of the package including the fins to ambient air by natural convection and radiation. Thermal analyses are carried out using above analytical models.

Each fuel element has different decay heat as shown in (II)-Table B.4. In the evaluation, assuming a case where 40 assemblies of more conservative fuel element (hereafter referred to as fuel element A) than the contents are loaded so as to maximize the decay heat per nuclear fuel package, the value was set to 2.25 kW. These decay heats are calculated by using ORIGEN and ORIGEN-JR code.

The results of thermal analysis are summarized as follows.

(1) Normal conditions of transport

The maximum temperature of the outer surface of this package without insolation is [redacted] ℃ at ambient temperature of 85 ℃ when Fuel element As are contained. The maximum surface temperature of this nuclear fuel package in the shade is [redacted] ℃ on the surface of the container body when fuel element A is contained, and will not exceed 85°C as specified in the technical criteria.

The maximum temperature of the contents in the solar insolation is 223 ℃ when Fuel element As are contained and this is less than melting point of Aluminum alloy, [redacted] ℃, that is used for fuel cladding. The maximum internal pressure is [redacted] MPaG*) under normal conditions of transports and this is less than the hydrostatic test pressure of the packaging, 0.98 MPaG (10 kgf/cm^{2}G). These results are shown in (II)-Table B.6. Furthermore the package under the ambient temperature of -40℃ is evaluated when the temperature of the package is -40℃ and the decay heat is considered.

(2) Accident conditions of transport

The temperatures rise up to[redacted] ℃ at the fuel element,[redacted] ℃ at the outer surface of the package,[redacted] ℃ at the containment boundary of the drain valve when Fuel element As are contained under the accident conditions of transport. The internal pressure rises up to[redacted]MPaG*) in this condition. These results are shown in (II)-Table B.8. Those temperature do not exceed the melting point of aluminum alloy of the fuel cladding,[redacted] ℃, that of stainless steel of the packaging, [redacted] ℃ and also the maximum permissible temperature of[redacted]for the packing,[redacted] ℃.

Under the above-mentioned normal and accident conditions of transport, the followings can be said about the package in the lowest temperature, in the highest temperature and in the maximum inner pressure.

① Stainless steel used for the main material of the packaging and aluminum alloy for the fuel cladding have enough toughness at low temperature, and the melting points of these material exceed the maximum temperature obtained by the thermal analysis.

② The normal service temperature[redacted]O-ring used for the contact portion of the body and the lid and each valve is from[redacted]C to[redacted]C, and the maximum permissible temperature of the[redacted]is 250℃. Therefore, the calculated temperatures of O-ring are within these conditions.

---

*) In the structural analysis, the values of increase pressure used in the normal conditions of transport and in the accident conditions of transport are assumed conservatively to be[redacted]MPaG and[redacted]MPaG respectively, and the obtained values of stress are rounded up for the stress calculations. In the containment analysis, the value of the pressure is assumed also conservatively to be[redacted]PaG [redacted]kgf/cm²G).

③ The maximum thermal stresses and thermal deformation of the package, occurring in the case of containing Fuel element A in the absence of insolation under normal conditions of transport and in the case of containing JRR-3 MNU type fuel under accident conditions of transport, are far less than the allowable values.

Therefore this package has enough thermal ability, and keeps the integrity of structural strength, containment, shielding ability, and subcriticality under normal and accident conditions of transport.

B.2 Thermal properties of material

The thermal properties of each material used for the thermal analysis are shown in (II)-Table B.1. These data are derived from reference 1) through 6). Since the heat transfer in each fuel element is evaluated and the heat source is assumed at the reasonable position in the thermal analytical model, the fuel meat (U-Al dispersion type, U-Si-Al dispersion type, metallic natural U type) is not used in the model. (Refer to paragraph. 1 of appendix (II)-B.6.1).

(Ⅱ)-Table B.1 Thermal properties

1. SUS [redacted] [1),2)]

Temperature t (℃)	Density ρ (kg/m³)	Specific heat Cp (J/gK)	Thermal conductivity k (W/mK)
-40	[redacted]	[redacted]	[redacted]
0	[redacted]	[redacted]	[redacted]
200	[redacted]	[redacted]	[redacted]
400	[redacted]	[redacted]	[redacted]
800	[redacted]	[redacted]	[redacted]

melting point = [redacted] ℃, emissivity ε = 0.15

2. Aluminum alloy [3),4),5)]

Temperature t (℃)	Density ρ (kg/m³)	Specific Heat Cp (J/gK)	Thermal Conductivity k (W/mK)
-40	[redacted]	[redacted]	[redacted]
20	[redacted]	[redacted]	[redacted]
100	[redacted]	[redacted]	[redacted]
300	[redacted]	[redacted]	[redacted]

melting point = [redacted] ℃, emissivity ε = 0.11

3. Neutron poison ([redacted]) [6)]

Temperature t (℃)	Density ρ (kg/m³)	Specific heat Cp (J/gK)	Thermal conductivity k (W/mK)
25	[redacted]	[redacted]	[redacted]

melting point = [redacted] ℃

(II)-Table B.1 Thermal properties (cont.)

4. Air3)

Temperature	Density	Specific heat		Coefficient of viscosity	Kinematic viscosity	Thermal conductivity		Thermal diffusivity
t (℃)	γ (kg/m^3)	C_P (J/gK)	〔(kcal/kg℃)〕	η ($kg\ s/m^2 \times 10^{-6}$)	ν ($m^2/s \times 10^{-4}$)	k (W/mK)	〔(kcal/mhr℃)〕	a (m^2/hr)
−50	1.533	1.005	〔0.240〕	1.49	0.095	0.0200	〔0.0172〕	0.0468
−20	1.348	1.005	〔0.240〕	1.65	0.120	0.0224	〔0.0193〕	0.0597
0	1.251	1.005	〔0.240〕	1.76	0.138	0.0241	〔0.0207〕	0.0689
20	1.166	1.005	〔0.240〕	1.86	0.156	0.0257	〔0.0221〕	0.0789
40	1.091	1.009	〔0.241〕	1.95	0.175	0.0272	〔0.0234〕	0.0892
60	1.026	1.009	〔0.241〕	2.05	0.196	0.0287	〔0.0247〕	0.100
80	0.968	1.009	〔0.241〕	2.14	0.217	0.0302	〔0.0260〕	0.111
100	0.916	1.013	〔0.242〕	2.23	0.239	0.0316	〔0.0272〕	0.123
120	0.869	1.013	〔0.242〕	2.32	0.262	0.0331	〔0.0285〕	0.135
140	0.827	1.017	〔0.243〕	2.40	0.285	0.0345	〔0.0297〕	0.148
160	0.789	1.017	〔0.243〕	2.48	0.308	0.0359	〔0.0309〕	0.161
180	0.754	1.022	〔0.244〕	2.56	0.333	0.0372	〔0.0320〕	0.174
200	0.722	1.026	〔0.245〕	2.64	0.358	0.0386	〔0.0332〕	0.188
250	0.652	1.034	〔0.247〕	2.83	0.426	0.0418	〔0.0359〕	0.223
300	0.596	1.047	〔0.250〕	3.01	0.495	0.0449	〔0.0386〕	0.259
350	0.548	1.059	〔0.253〕	3.18	0.569	0.0479	〔0.0412〕	0.298
400	0.508	1.068	〔0.255〕	3.34	0.645	0.0508	〔0.0437〕	0.337
500	0.442	1.093	〔0.261〕	3.65	0.810	0.0562	〔0.0483〕	0.419
600	0.391	1.118	〔0.267〕	3.94	0.989	0.0613	〔0.0527〕	0.506
800	0.319	1.156	〔0.276〕	4.47	1.37	0.0709	〔0.0610〕	0.693

Pressure : 1 kgf/cm^2 (0.098MPa) (except for saturated aqueous vaper)

B.3 Service equipments

Service equipments installed in the package are the vent valve, the drain valve and the leak test plug. The containment of those equipments are tested by pressure test and leaktightness test after the completion of packaging, and checked again by leaktightness test before the shipping of package. The normal service temperature range (normal use) of [redacted] for the packing is -[redacted] ℃ to [redacted] ℃, and the maximum permissible temperature is [redacted] ℃. The specification of those equipments are summarized in (Ⅱ)-Table B.2. Mechanical property of stainless steel is described in (Ⅱ)-A.3 and (Ⅱ)-A.4.2, and thermal property of [redacted] is described in (Ⅱ)-C.2.1. This package is not furnished with thermal insulation and not painted on its surface.

B.4 Normal conditions of transport

This package conforms to the requirements under the normal conditions of transports specified in the IAEA Regulations as follows.

B.4.1 Thermal analytical model

For the evaluation of temperature in each location of the package under the conditions of transport, the analytical model is used and the test model is not used.

The analytical procedures of the model are shown as follows.

The structure of the package is so complicated that the general-purpose finite element code ABAQUS 8) is used to obtain the whole detailed temperature distribution. ABAQUS code is used for both steady state and transient heat transfer of one, two or three dimensional model (rectangular co-ordinates, cylindrical co-ordinates or polar co-ordinates) and for any geometrical configuration and structure.

The calculation by theoretical equations is described in para. (Ⅱ)-B.6.1, para. (Ⅱ)-B.6.2 and para. (Ⅱ)-B.6.4.

(Ⅱ)-Table B.2 Specifications of service equipments

Item Equipment	Purpose	Figure	Materials (Body)	Materials (Gasket)	Materials (Plug)	Test temp.	Test pressure
Vent valve	Air ventilation	see (Ⅰ)-Fig.C.4 and (Ⅰ)-Fig.C.9	Stainless steel	Stem ; Stainless steel Gasket ; [redacted]	Stainless steel	Ambient temp.	Pressure test ; ・ 0.98MpaG or above ・ Hydropressure Leak test; ・ 0.42MpaG or above ・Pneumatic pressure (Air, Nitrogen)
Drain valve	Drain	see (Ⅰ)-Fig.C.4 and (Ⅰ)-Fig.C.9	Stainless steel	Stem ; Stainless steel Gasket ; [redacted]	Stainless steel		
Plug for leak test	Leak test	See (Ⅰ)-Fig.C.16	Stainless steel	O-ring ; [redacted]	Stainless steel		

B.4.1.1 Analytical model

The cooling of this package is natural convection and radiation.

The decay heat generated from the spent fuels transfers to the body and the lid through air inside the package, the neutron poison and the stainless steel of the basket components, and is dissipated to the ambient atmosphere by natural convection and radiation from the outer surface including the fins of the packaging.

Any deformation and damage of the package are not assumed in the analysis because the package after the tests under normal conditions of transport suffers little deformation and damage only in the local area of the fins of the packaging. The following contents are described in this section.

(1) Analytical item and analytical condition
(2) Decay heat
(3) Analytical model
(4) Heat transfer in the package
(5) Heat transfer outside the package

1. Analytical item and analytical conditions

The thermal analysis is carried out under the following conditions. The analytical conditions are shown in (Ⅱ)-Table B.3.

i) The thermal analysis under the absence of insolation is performed, and it is presented that the temperature of the outer surface of the packaging is less than the allowable value, 85 ℃, specified in the IAEA regulations.

ii) The maximum temperature of each part under normal conditions of transport is evaluated by performing the thermal analysis under the solar insolation.

iii) The temperature of the package under the ambient temperature of -40℃ is evaluated.

2 Decay heat

This package can contain seven kinds of fuel elements.

Total decay heat of each fuel element calculated with ORIGEN and

ORIGEN-JR code, which are shown in (Ⅱ)-Table B.4 collectively.

As the heat source per fuel element in the analytical model, the heat transfer in the fuel element is evaluated. It is assumed that the heat source of the standard type fuel elements and follower type fuel element, both of them are square shape, are the fuel side plate where the heat transfer into the basket is dominant, and the heat source of JRR-3 MNU type fuel of circular cross section is the fuel cladding of the outer cylinder. Decay heat is assumed to generate uniformly in its location and length of fuel elements.

(Ⅱ)-Table B.3 Thermal assumption under normal conditions of transport

(1) Ambient condition

Item / Condition	i) Evaluation in the absence of solar insolation	ii) Evaluation of the maximum temperature	iii) Evaluation of the minimum temperature
Ambient temperature	38℃	38℃	-40℃
Insolation	Not exist	Exist	Not exist
Ambient emissivity	1.0	1.0	1.0
Emissivity of outer surface	0.15	0.15	0.15

(2) Insolation data (the IAEA regulations, 2009 edition)

Form and location of surface	Insolation for 12 hours per day (Unit : W/m²)
(1) Flat surfaces transported horizontally	
a. downward facing	0
b. upward facing	800
(2) Surfaces transported vertically and other downward facing (not horizontal) surfaces	200
(3) All other surfaces	400

(Ⅱ)-Table B.4 Total decay heat

Basket	Basket for box type fuel	Basket for box type fuel (with adapter)	Basket for MNU type fuel	Basket for box type fuel
Reactor	JRR-3	JRR-3	JRR-3	-
Fuel element	Standard silicide type	Follower Silicide type	MNU type	Fuel type A
Number of fuel elements (piece)	40 or less	40 or less	160 or less	40 or less
Total decay heat (W/package)	2.24×10^3 or less	1.43×10^3 or less	7.24×10 or less	2.25×10^3 or less
Decay heat per piece (W/piece)	56.00 or less	35.75 or less	0.4525 or less	56.25 or less

3 Analytical model

This packaging can contain three kinds of fuel elements in three types of baskets. The basket for box type fuel is used to transport JRR-3 standard silicide type fuel and JRR-3 follower silicide type fuel. The basket for MNU type fuel is used to transport JRR-3 MNU type fuel. Namely, the package has two kinds of basket. Therefore, the thermal analysis is performed for two kinds of basket where the fuel elements of the maximum decay heat are contained.

3.1 Analytical model when the basket for box type fuel installed.

Two kinds of fuel elements, JRR-3 standard silicide type fuel and JRR-3 follower silicide type fuel, are contained in the basket for box type fuel.

The fuel elements, the basket and the packaging are handled together as an analytical model. Three-dimensional model of a sector at a center angle of 90° is adopted as the analytical model, since the basket is 1/4 symmetrical structure.

The general view, the longitudinal sectional view and the radial sectional view of the analytical model are shown in (Ⅱ)-Fig. B.1, (Ⅱ)-Fig. B.2 and (Ⅱ)-Fig.B.3, respectively.

The fuel element used for the analytical model is Fuel element A that has the maximum decay heat as the fuel elements contained in the basket for box type fuel.

The detailed heat transfer is shown in paragraph 4 of this section, appendix (Ⅱ)-B.6.1 and (Ⅱ)-B.6.2.

[redacted]

(Ⅱ)-Fig.B.1　The general view of the analytical model of the package containing the basket for box type fuel (In case of containing Fuel element A)

[redacted]

(Ⅱ)-Fig.B.2　The longitudinal sectional view of the analytical model containing the basket for box type fuel
(In case of containing Fuel element A)

[redacted]

(II)-Fig.B.3 The radial sectional view of the analytical model containing the basket for box type fuel
(In case of containing Fuel element A)

3.2 Analytical model when the basket for MNU type fuel installed

JRR-3 MNU type fuel is contained in the basket for MNU type fuel.

The shape of the basket is much different from the basket for box type fuel. The difference is the existence of a large air gap in the circumference of the basket, so the heat transfer through the side wall of the body is little and the decay heat transfers to the body mainly by way of the basket bottom plate through the fuel meat, the fuel cladding or the square shape pipe.

In the analytical model, the fuel cladding is handled as the heat source. The heat transfers to the body through the bottom plate of the basket.

As the analytical model, three-dimensional model of a sector at a center angle of 90° is adopted in the same way as the other baskets.

The general view, the longitudinal sectional view and the radial sectional view of the analytical model are shown in (Ⅱ)-Fig.B.4, (Ⅱ)-Fig.B.5 and (Ⅱ)-Fig.B.6 respectively.

The detailed heat transfer is shown in paragraph 4 of this section, appendix (Ⅱ)-B.6.1 and (Ⅱ)-B.6.2.

[redacted]

(Ⅱ)-Fig.B.4 The general view of the analytical model of the package containing the basket for MNU type fuel

(Incase of containing JRR-3 MNU type fuel)

[redacted]

(Ⅱ)-Fig.B.5 The longitudinal sectional view of the analytical model containing the basket for MNU type fuel
(In case of containing JRR-3 MNU type fuel)

[redacted]

(Ⅱ)-Fig.B.6　The radial sectional view of the analytical model containing the basket for MNU type fuel
(In case of containing JRR-3 MNU type fuel)

4 Heat transfer in the package

The heat transfers in the package when each basket installed are shown as follows.

4.1 Heat transfer in the package when the basket for box type fuel installed.

In solid material, heat transfer takes place by conduction.

For air gap in the package, heat transfer takes place by either convection or conduction and by radiation. For instance, for the basket containing Fuel element A, the convection is dominant in the lodgement for neutron source near center axis and the air gap above the fuel, and at other locations the conduction is superior to the convection. The heat transfer by the radiation is taken into account for the locations between the fuel side plate and the side surface of the basket lodgement, between the surface of the basket top end and the inner surface of the lid, between the side surface of the basket and the inner surface of the shell, between the upper basket bottom plate of the lodgement for neutron source and the inner surface of the lid, and between the top end surface of the fuel element and the inner surface of the lid.

For between the fuel side plate and the side surface of the basket lodgement, between the bottom end surface of the fuel element and the upper basket bottom plate, between the bottom end surface of the basket compositions such as frame, partition plate and compartment plate, and the upper basket bottom plate, between the upper basket bottom plate and the lower basket bottom plate, between the lower basket bottom plate and the body bottom plate, between the surface of the basket top end and the inner surface of the lid, between the side surface of the basket and the inner surface of the shell, and considering the structure of the basket, the air gaps between the neutron poison and the partition plate, these air gaps are assumed conservatively and the heat transfer is assumed to take place by the conduction of air. Concerning the heat transfer areas and the distances, the actual values are used for the evaluations.

The details of the heat transfer in the package are shown in appendix paragraph (Ⅱ)-B.6.1.

4.2 Heat transfer in the package when the basket for MNU type fuel installed.

In solid material, heat transfer takes place by conduction.

As shown in para. 3.2 of (Ⅱ)-B.4.1.1, the shape of this basket is much different from the basket for box type fuel, that is, the existence of a large air gap in the circumference of the basket. And the decay heat of JRR-3 MNU type fuel, which is stored in this basket, is small. Therefore, it is expected that the heat transfer by convection and radiation from the fuel element to the side wall of the body is little, and that most of the decay heat transfers to the body mainly by way of the basket bottom plate through the fuel meat, the fuel cladding or the square shape pipe.

In the analysis, since the cross section of JRR-3 MNU type fuel is almost a circle, the heat generation on the fuel cladding of the outer cylinder is assumed to be uniform in circumference and the internal fuel meat is considered to be insulation. Moreover, the square shape pipe is not modeled and it is assumed that the decay heat of fuel transfers only from the fuel cladding to the body bottom plate through the basket bottom plate.

In this case, for between the bottom end surface of the fuel element and the upper surface of the basket bottom plate, and for between the lower surface of the basket bottom plate and the body bottom plate, these air gaps are assumed conservatively and the heat transfer is assumed to take place by the conduction of air. Concerning the heat transfer areas and the distances, the actual values are used for the evaluations.

The details of the heat transfer in the package are shown in para. (Ⅱ)-B.6.1 of the appendix.

5. Heat transfer at the outer surface of the package

Heat transfer from the outer surface of the package to the ambient air is shown as follows.

The ambient condition around the package is shown in this section (Ⅱ)-Table B.3. It is considered that the heat transfer takes place by the natural convection and the radiation. As the heat transfer coefficient for convection, the empirical equation that is highly reliable at each location is applied. The applied equations are a natural convection equation of a vertical plate for the fin and the side of the body, a natural convection equation of an upward heating surface for the top surface of the body, and a natural convection equation of a downward heating surface for the bottom of the body, respectively. The geometrical factor of the outer surface of the package is calculated for the actual shape of each part. Namely, the geometrical factor is 1 for the part of the outer surface with no fin, and is calculated for that with fins considering radiation to surrounding air. The geometrical factor of the fins is 1 for the edge, and is calculated by means of ABAQUS code for the plane, assuming the closed cavity by modeling the outside ambient at each location. Radiation heat transfer between fins is also considered. The emissivity is considered to be 0.15 for both the outer surface of the body and the fins conservatively.

The shape of the fins is modeled in conformity with actual shape. Under normal conditions of transport, the package is assumed to be suffered no deformation and no damage in the analysis as shown previously. The solar insolation at each location is given in the outer surface of the packaging of the analytical model on the basis of (Ⅱ)-Table.B.3.

The details of the heat transfer at the outer surface of the package is shown in (Ⅱ)-B.6.2 of the appendix.

B.4.1.2 Test model

Not used.

B.4.2 Maximum temperature

This paragraph shows about i) the evaluation in the absence of insolation and ii) the evaluation of the maximum temperature.

1 Temperature evaluation in the absence of solar insolation.

In this evaluation, the steady-state thermal analysis when the package is exposed to ambient temperature of 38 ℃ in the absence of solar insolation is performed. The results obtained for the two kinds basket are shown in (Ⅱ)-Table B.5.

The temperature distributions on the main parts of the analytical model of the basket for the box type fuel containing Fuel element A and the basket for MNU type fuel containing JRR-3 MNU type fuel are shown in (Ⅱ)-Fig.B.7, (Ⅱ)-Fig.B.8 and (Ⅱ)-Fig.B.9, through (Ⅱ)-Fig.B.10 respectively.

As a result, the maximum temperature at the outer surface of the packaging is [redacted] ℃ at the center of the body bottom plate in case of containing Fuel element A which has the maximum decay heat. Therefore, it is assured that the temperature at the outer surface of this package does not exceed 85 ℃ in the absence of solar insolation of the ambient temperature 38 ℃ specified in the IAEA regulations.

(II)-Table B.5 Temperature in the absence of solar insolation

(Unit：℃)

Basket / Fuel element / Position		Basket for box type fuel	Basket for MNU type fuel
		Fuel element A	JRR-3 MNU type fuel
Inside of package	Fuel element	[redacted]	[redacted]
	Center of basket	[redacted]	[redacted]
	Outer surface of basket	[redacted]	[redacted]
Packaging	Inner surface (top)	[redacted]	[redacted]
	Inner surface (side)	[redacted]	[redacted]
	Inner surface (bottom)	[redacted]	[redacted]
	O-ring	[redacted]	[redacted]
	Lid bolt	[redacted]	[redacted]
	Vent valve	[redacted]	[redacted]
	Drain valve	[redacted]	[redacted]
	Outer surface (top)	[redacted]	[redacted]
	Outer surface (side)	[redacted]	[redacted]
	Outer surface (bottom)	[redacted]	[redacted]
	Top of top fin	[redacted]	[redacted]
	Top of lateral fin	[redacted]	[redacted]
	Top of bottom fin	[redacted]	[redacted]
Maximum pressure (MPaG)*1		[redacted]	[redacted]

*1 After the fuel elements are loaded in the packaging and the package reaches to the thermal equivalent, the package is sealed up.

[redacted]

(Ⅱ)-Fig.B.7　Temperature in the absence of solar insolation in case of containing Fuel element A (Longitudinal cross section)

[redacted]

(Ⅱ)-Fig.B.8　Temperature in the absence of solar insolation in case of containing Fuel element A
(Radial cross section)

[redacted]

(Ⅱ)-Fig.B.9　Temperature in the absence of solar insolation in case of containing JRR-3 MNU type fuel
(Longitudinal cross section)

[redacted]

(Ⅱ)-Fig.B.10　Temperature in the absence of solar insolation in case of containing JRR-3 MNU type fuel
(Radial cross section)

2 Evaluation of the maximum temperature

In this evaluation, the steady-state temperature distribution when the package is exposed to the ambient temperature of 38 ℃ under solar insolation is calculated.

The maximum temperature at each part of the package obtained by the analysis is summarized in (II)-Table B.6. The results in the absence of solar insolation are also shown in the Table.

The temperature distributions on the main parts of the analytical model of the basket for box type fuel containing Fuel element As are shown in (II)-Fig.B.11 and (II)-Fig.B.12. The temperature distributions on the main parts of the analytical model of the basket for MNU type fuel containing JRR-3 MNU type fuel are shown in (II)-Fig.B.13 and (II)-Fig.B.14.

Summarizing the results, the maximum temperature of the package is [redacted] ℃ at the fuel cladding when Fuel element A which is the maximum decay heat are contained. The value is lower than the melting point of the fuel cladding made of aluminum alloy, [redacted] ℃. And the maximum temperature of the containment boundary of the package is [redacted] ℃, at the [redacted] O-ring of the contact surface of the body and lid, which is below the maximum value of the normal service temperature of [redacted] ([redacted] ℃). Therefore, it is assured that this package maintains the containment under the ambient temperature of 38 ℃ under solar insolation when the packaging contains any kind of fuels.

(Ⅱ)-Table B.6 (No.1) Maximum temperature under normal conditions of transport in the solar insolation

・In case of the basket for box type fuel containing Fuel element A

Fuel element Position		Temperate in the absence of insolation (℃)	Maximum temperature (℃)	Maximum internal pressure (MPaG)
Inside of package	Fuel element	[redacted]	[redacted]	[redacted]
	Center of basket	[redacted]	[redacted]	[redacted]
	Outer surface of basket	[redacted]	[redacted]	[redacted]
Packaging	Inner surface (top)	[redacted]	[redacted]	
	Inner surface (side)	[redacted]	[redacted]	
	Inner surface (bottom)	[redacted]	[redacted]	
	O-ring	[redacted]	[redacted]	
	Lid bolt	[redacted]	[redacted]	
	Vent valve	[redacted]	[redacted]	
	Drain valve	[redacted]	[redacted]	
	Outer surface (top)	[redacted]	[redacted]	
	Outer surface (side)	[redacted]	[redacted]	
	Outer surface (bottom)	[redacted]	[redacted]	
	Top of top fin	[redacted]	[redacted]	
	Top of lateral fin	[redacted]	[redacted]	
	Top of bottom fin	[redacted]	[redacted]	

(Ⅱ)-Table B.6 (No.2) Maximum temperature under normal conditions of transport in the solar insolation

・In case of the basket for MNU type fuel containing JRR-3 MNU type fuel

Position	Fuel element	Temperate in the absence of insolation (℃)	Maximum temperature (℃)	Maximum internal pressure (MPaG)
Inside of package	Fuel element	[redacted]	[redacted]	[redacted]
	Center of basket	[redacted]	[redacted]	
	Outer surface of basket	[redacted]	[redacted]	
Packaging	Inner surface (top)	[redacted]	[redacted]	
	Inner surface (side)	[redacted]	[redacted]	
	Inner surface (bottom)	[redacted]	[redacted]	
	O-ring	[redacted]	[redacted]	
	Lid bolt	[redacted]	[redacted]	
	Vent valve	[redacted]	[redacted]	
	Drain valve	[redacted]	[redacted]	
	Outer surface (top)	[redacted]	[redacted]	
	Outer surface (side)	[redacted]	[redacted]	
	Outer surface (bottom)	[redacted]	[redacted]	
	Top of top fin	[redacted]	[redacted]	
	Top of lateral fin	[redacted]	[redacted]	
	Top of bottom fin	[redacted]	[redacted]	

[redacted]

(Ⅱ)-Fig.B.11 Temperature in solar insolation in case of containing Fuel element A
(Longitudinal cross section)

[redacted]

(Ⅱ)-Fig.B.12　Temperature in solar insolation in case of containing Fuel element A
(Radial cross section)

[redacted]

(Ⅱ)-Fig.B.13　Temperature in solar insolation in case of containing JRR-3 MNU type fuel
(Longitudinal cross section)

(Ⅱ)-Fig.B.14　Temperature in solar insolation in case of JRR-3 MNU type fuel
(Radial cross section)

[redacted]

B.4.3 Minimum temperature

The minimum temperature evaluation is carried out according to the case of the condition of ⅲ) evaluation of the minimum temperature shown in the preceding (Ⅱ)-Table B.3. In this case, assuming that neither the insolation nor decay heat exist, the low-temperature brittleness is studied. The temperature of the whole package becomes minimum, the value of which is equal to the ambient temperature, is at -40 ℃. This assumption is conservative, because the decay heat from the fuel actually exists and it is expected that the temperature of the package is greater than -40 ℃.

The integrity of the materials used for the package at -40 ℃ is shown in paragraph (Ⅱ)-A.4.2, which is summarized as follows.

(1) The main material of the packaging and the basket is stainless steel, which can be used at more than [redacted] ℃ without the brittle fracture.

(2) The stainless steel for lid bolts has sufficient toughness at -40 ℃ or more.

(3) The aluminum alloy of fuel cladding material doesn't have brittleness at the low temperature. So there is no problem of low temperature brittle fracture.

(4) No lowering of the mechanical properties, i.e. tensile strength and yield stress occurs at the low temperature.

(5) The permissible lowest temperature of [redacted] used the packing for the containment boundary is [redacted] ℃, therefore, it is certain that this package maintains the containment.

Furthermore, this package is the natural cooling type that does not contain the cooling water, therefore there is no possibility of the destruction of the package due to freezing.

Then the thermal stress etc. is investigated considering the decay heat of the fuel element. The thermal stress in the packaging under this condition is lower than that under the accident conditions of transport (the fire accident), in which the structural integrity has been assured to maintain. And also concerning the thermal expansions, the gap in the radial direction between the shell and the basket is [redacted] mm in the conservative assumption, so the basket is not restrained by the packaging.

Therefore, it is certain that there is no problem of brittle fracture, thermal stress and containment even if the packaging is used in the ambient temperature of -40 ℃.

B.4.4 Maximum internal pressure

This nuclear fuel package is sealed up after the verification that it is under the thermal equilibrium after containing the fuels.

Therefore, the maximum internal pressure of the package under the normal conditions of transport occurs by the internal temperature difference between at the time of sealing up under solar insolation. The details are shown in appendix paragraph (Ⅱ)-B.6.3. The results obtained are shown in (Ⅱ)-Table B.6. The maximum internal pressure occurs when Fuel element As are contained, and is [redacted] MPaG. In addition, even when considering the ambient temperature change expected during transportation (from -40℃ to 38℃), it is [redacted] MPaG. This value is sufficiently small compared to the pressure proof test pressure of 0.98 MPaG (10 kgf/cm^{2}G) or higher, then there is no problem due to pressure increase under general test conditions for this nuclear fuel package, and there is no risk of cracks or failures to the package..

B.4.5 Maximum thermal stress

The maximum temperature difference and thermal stress are summarized as described in paragraph (Ⅱ)-A.5.1 by temperature distribution shown in (Ⅱ)-Table B.5.

The maximum thermal stress of this package occur at the center of the body bottom plate under the normal conditions of transport in the absence of insolation when Fuel element As are contained, and the value of the stress is [redacted] MPa and the safety margin MS is [redacted]

The stress of the lid bolts (due to the initial fastning force + the maximum I nternal pressure + the thermal load) is [redacted] MPa, and the safety margin MS is [redacted] There is no problem of the containment for the contact surface between the body and the lid.

The maximum thermal expansion of the basket occurs when Fuel element As are contained in the same as the maximum thermal stress. In this case, the expansion of the basket in the longitudinal direction and the radial direction are [redacted] mm and [redacted] mm respectively. For the above values, the gap in the longitudinal direction is [redacted] mm and the gap in the radial direction is [redacted] mm, so that the basket is not restrained by the packaging.

Therefore, it is certain that there is no problem for the maximum thermal stress and the maximum thermal expansion.

B.4.6 Summary of the results and the evaluation under normal conditions of transport

This package has the thermal ability, satisfies the technical standard and maintains the integrity for the structural strength, the containment, the shielding ability and the subcriticality under the normal conditions of transport.

1. Surface temperature in the absence of solar insolation

The maximum surface temperature of the package in the absence of solar insolation is [redacted] ℃ when the packaging contains Fuel element A generating the maximum decay heat. The value is below 85 ℃ specified in the technical standard.

2. Maximum temperature (Melting)

The maximum temperature of each location of the package under the normal conditions of transport is [redacted] ℃ at the fuel element when the packaging contains Fuel element A. This value is much below [redacted] ℃, melting point of the fuel cladding, made of aluminum alloy, and also much below [redacted] ℃, melting point of main parts of the packaging made of stainless steel.

3 Maximum internal pressure, maximum thermal stress and thermal expansion (deformation)

i) The maximum internal pressure of this package under normal conditions of transports is [redacted] MPaG when the packaging contains Fuel element A. This value is much below the hydro test pressure of 0.98 MPaG (10 kgf/cm^{2}G).

ii) The maximum thermal stress under the normal conditions of transport is [redacted] MPa when the packaging contains the above fuels. The safety margin is [redacted]. The stress of the lid bolts is [redacted] MPa and the safety margin is [redacted].

iii) The maximum thermal expansion of the basket is [redacted] mm in the longitudinal direction and [redacted] mm in the radial direction when the above fuel elements are contained. For the above values, the gap between the basket and the body in the longitudinal direction is [redacted] mm and the gap in the radial direction is [redacted] mm.

Therefore, the stress of the package is much below the allowable stress and the fuel elements and the basket are not restrained.

4. Minimum temperature (Brittle fracture)

The minimum temperature of the package is -40℃. The stainless steel which the main material of the packaging, and the aluminum alloy of the fuel cladding can be used at more than [redacted] ℃ without the brittle fracture. The stainless steel used the lid bolts have sufficient toughness at more than -40℃. No lowering of the mechanical properties occurs at the above temperature and no problem for the thermal stress and thermal expansion occurs.

5. Containment

The temperature range of the packing for the containment boundary under the normal conditions of transport is from -40 ℃ to [redacted] ℃. For the above, the normal service temperature range (normal use) of [redacted] used as the packing is from [redacted] ℃ to [redacted]℃. Furthermore, the contact surfaces between the lid and the body keep the containment under this condition of transport even if the maximum stress works on the lid bolt.

B.5 Accident conditions of transport

This package satisfies the technical standard under the accident conditions of transport as follows.

B.5.1 Thermal analytical model

The evaluation of the thermal ability of the package under the accident conditions of transport is carried out by using the analytical model instead of the test model, namely by using the analytical code "ABAQUS".

The calculation of the maximum temperature of the fuel element when the packaging contains the basket for box type fuel installed is described later in paragraph (II)-B.6.5 of the appendix.

B.5.1.1 Analytical model

As the analytical model, following items are described in this report.

(1) Ambient condition

(2) Decay heat

(3) Analytical model

(4) Heat transfer in the package

(5) Heat transfer outside the package

The deformation of this package after the drop test under this condition is described in paragraph (II)-B.5.2, evaluation condition of the package, in detail.

1. Ambient condition

The ambient conditions before fire, on fire and after fire are shown in (II)-Table B.7 collectively.

(Ⅱ)-Table B.7　Ambient condition under accident conditions of transport

Situation Item	Before fire	On fire (30 min.)	After fire
Ambient temperature	38℃	800℃	38℃
Insolation	Exist	Exist	Exist
Ambient emissivity	1.0	0.9	1.0
Surface emissivity	0.15	0.8	0.15

The thermal analysis for the accident conditions of transport is performed under following assumed condition, namely the fire accident occurs after the drop test. Therefore, the temperature distribution of the package before fire is assumed to be that under the normal conditions of transports. The thermal conditions on fire as specified in the technical standard are as follows. The ambient temperature is 800 ℃ (30 min.), the ambient emissivity and the surface emissivity of the package are 0.9 and 0.8 respectively. It is assumed that the heat transfer from fire is performed by radiation and convection, and the solar insolation is also considered. The thermal conditions after fire are as follows. The ambient temperature is 38℃, the ambient emissivity and the surface emissivity of the package is 1.0 and 0.15 respectively. It is assumed that the thermal diffusion from the surface of the package is performed by natural convection and radiation. And the heat of insolation that is described in (Ⅱ)-Table B.3 is considered.

2. Decay heat

The decay heat of the fuel elements is shown in (Ⅱ)-Table B.4, which is the same as that used under the normal conditions of transport.

3. Analytical model

The analytical model is the same model as that used under normal conditions of transport.

The thermal analysis under this conditions is performed by using two kinds of analytical models, namely, the analytical models of the basket for box type fuel containing Fuel element A and the basket for MNU type fuel containing JRR-3 MNU type fuels.

As a fuel element to be analyzed in the evaluation of temperature distribution and maximum internal pressure, the JRR-3 standard silicide type fuel element has the largest decay heat among the three types, but more conservatively, we consider a fuel element A, which has the highest temperature distribution in the maximum temperature evaluation under normal conditions of transport. Fuel element A and JRR-3 MNU type fuel are used in the evaluation of the maximum thermal stress.

4. Heat transfer in the package

The heat transfer in the package is taken into account in the same way as mentioned in the proceeding paragraph (Ⅱ)-B.4.1.1 4.

5. Heat transfer outside the package

The heat transfer of the outer surface of the package is described as follows.

The ambient condition of the package is as shown in (Ⅱ)-Table B.7.

As the heat transfer, the convection and the radiation to the surrounding air are considered.

As the heat transfer coefficient of convection, the empirical equation that is highly reliable at each location is applied. Namely, the natural convection equation of a vertical plate for the fin and the side of the body, the natural convection equation of an upward heating surface for the top surface of the packaging before fire and after fire, the natural convection equation of an upward cool surface for the top surface of the body of the packaging on fire, the natural convection equation of a downward heating surface for the bottom surface of the body before fire and after fire, and the natural convection equation of a downward cool surface of the bottom surface of the body on fire are applied respectively.

Also, the emissivity for the surface of the packaging and the fin is 0.15 before and after fire, and 0.8 on fire.

Further, the treatment of the insolation, the geometrical factor, the heating surface area, the shape of the fin etc., is the same as the contents indicated in normal conditions of transport.

The detail of the outer heat transfer is described in paragraph (II)-B.6.4. of the appendix.

B.5.1.2 Test model

The analytical model is applied instead of the test model.

B.5.2 Evaluation condition of the package

The thermal analysis for the accident condition is performed under following assumed condition, namely the thermal test occurs after the drop test. The temperature change under this condition is influenced by the configuration change of the outer surface of the packaging and the posture after the drop test. However for this package the state of the package is scarcely changed after the drop test because the configuration of the package is almost spherical, the fins welded to the outside are symmetric and the thickness of the parts is large.

The main destruction of the package which occurs by the drop test is local and small deformation of the fins as shown in paragraph (II)-A.6. And the fins are not broken off, the effect of heating and cooling is considered to cancel each other. Therefore, the analytical model of which all fins are in perfect shapes is applied.

Also, there is practically no difference of the temperature history under this condition according to whether the package after the drop test stands in the normal state, or lays in the lateral state, or stands upside down. This is because the heat supply by radiation is more dominant than that by convection during fire. The factor (geometrical factor, emissivity) relating to the heat supply quantity by radiation is determined by the shape of the package surface, but does not depend on the position. The heat quantity by the insolation also before, after and during fire does not depend on the position. Therefore, for the analytical model, the package is considered to stand in the normal state.

B.5.3 Temperature of the package

The result of analysis under this condition, the values obtained for each portion of the package are shown in (Ⅱ)-Table B.8 collectively. Also the temperature history of the main portion (refer to (Ⅱ)-Fig.B.15) of the analytical model of the basket for box type fuel containing Fuel element A is shown in (Ⅱ)-Fig.B.16 through (Ⅱ)-Fig.B.18.

As a result of the analysis, the maximum temperature of each portion of the package occurs when the packaging contains Fuel element A generating the maximum decay heat. In this case, the maximum temperature of each portion of the package is [redacted] ℃ in the fuel, [redacted] ℃ in the basket, [redacted] ℃ in the edge of the fins, [redacted] ℃ in the outer surface of the body bottom plate and [redacted] ℃ in the packing of the containment boundary, drain valve.

B.5.4 Maximum internal pressure

The maximum internal pressure is considered in the same way as that of the normal conditions of transport. The calculation method of the maximum internal pressure is shown in paragraph (Ⅱ)-B.6.6. of the appendix. The maximum internal pressure occurs when the packaging contains Fuel element As, which is [redacted] MPaG. The result obtained is shown in (Ⅱ)-Table B.8 collectively.

(Ⅱ)-Table B.8 (No.1) Result under accident conditions of transport

・In case of the basket for box type fuel containing Fuel element A

Position		Temperature before fire (℃)	Maximum temperature (℃)	Maximum temperature (Lapse time) (hr)	Maximum internal pressure (MPaG)
Inside of package	Fuel element	[redacted]	[redacted]	[redacted]	[redacted]
	Center of basket	[redacted]	[redacted]	[redacted]	
	Outer surface of basket	[redacted]	[redacted]	[redacted]	
Packaging	Inner surface (top)	[redacted]	[redacted]	[redacted]	
	Inner surface (side)	[redacted]	[redacted]	[redacted]	
	Inner surface (bottom)	[redacted]	[redacted]	[redacted]	
	O-ring	[redacted]	[redacted]	[redacted]	
	Lid bolt	[redacted]	[redacted]	[redacted]	
	Vent valve	[redacted]	[redacted]	[redacted]	
	Drain valve	[redacted]	[redacted]	[redacted]	
	Outer surface (top)	[redacted]	[redacted]	[redacted]	
	Outer surface (side)	[redacted]	[redacted]	[redacted]	
	Outer surface (bottom)	[redacted]	[redacted]	[redacted]	
	Top of top fin	[redacted]	[redacted]	[redacted]	
	Top of lateral fin	[redacted]	[redacted]	[redacted]	
	Top of bottom fin	[redacted]	[redacted]	[redacted]	

(Ⅱ)-Table B.8 (No.2) Result under accident conditions of transport

・In case of the basket for MNU type fuel containing JRR-3 MNU type fuel

Position		Temperate before fire (℃)	Maximum temperature		Maximum internal pressure (MPaG)
			(℃)	(Lapse time (hr))	
Inside of package	Fuel element	[redacted]	[redacted]	[redacted]	[redacted]
	Center of basket	[redacted]	[redacted]	[redacted]	
	Outer surface of basket	[redacted]	[redacted]	[redacted]	
Packaging	Inner surface (top)	[redacted]	[redacted]	[redacted]	
	Inner surface (side)	[redacted]	[redacted]	[redacted]	
	Inner surface (bottom)	[redacted]	[redacted]	[redacted]	
	O-ring	[redacted]	[redacted]	[redacted]	
	Lid bolt	[redacted]	[redacted]	[redacted]	
	Vent valve	[redacted]	[redacted]	[redacted]	
	Drain valve	[redacted]	[redacted]	[redacted]	
	Outer surface (top)	[redacted]	[redacted]	[redacted]	
	Outer surface (side)	[redacted]	[redacted]	[redacted]	
	Outer surface (bottom)	[redacted]	[redacted]	[redacted]	
	Top of top fin	[redacted]	[redacted]	[redacted]	
	Top of lateral fin	[redacted]	[redacted]	[redacted]	
	Top of bottom fin	[redacted]	[redacted]	[redacted]	

[redacted]

(Ⅱ)-Fig.B.15　Points shown in temperature history figures

[redacted]

(Ⅱ)-Fig.B.16 Temperature history in case of containing Fuel element A

[redacted]

(Ⅱ)-Fig.B.17 Temperature history in case of containing Fuel element A

[redacted]

(Ⅱ)-Fig.B.18 Temperature history in case of containing Fuel element A

B.5.5 Maximum thermal stress

The maximum thermal stress occurs in [redacted] min, after fire breaks out. The maximum thermal stress is summarized as follows, which is described in paragraph (Ⅱ)-A.6.3.

The maximum thermal stress on the body occurs at the center of the outer surface of the body bottom plate when JRR-3 MNU type fuels are contained. The maximum plastic strain is [redacted] %, in which the safety margin is [redacted] since the rupture strain of the material is [redacted] %. The stress of the lid bolts (due to the initial fastening force + the maximum internal pressure + thermal load) is [redacted] MPa and the safety margin is [redacted] Thought [redacted] mm gap is caused on the contact surface between the lid and the body, the restoration value of the O-ring is [redacted] mm so that the safety margin is [redacted].

In the basket for box type fuel, which has the maximum thermal stress under the accident conditions of transport, the safety margin for the heat stress is [redacted] even if the conservative assumption is applied. The minimum gap of [redacted] mm between the shell body and the basket under the accident conditions of transport is caused in [redacted] hours after fire breakout when the packaging contains Fuel element A, which have the maximum heat decay. Therefore, the basket is not restrained.

Therefore, there is no problem with this package against the maximum thermal stress and the maximum thermal expansion.

B.5.6 Summary of the result and the evaluation under the accident conditions of transport

As described hereinafter, this package has the thermal ability, satisfies the technical standard and maintains the integrity for the structural strength, the containment, the shielding ability and the subcriticality under accident conditions of transport.

1. Effect of thermal ability by the drop test

As the effect of this package by the drop test under the accident conditions of transport, the local and small deformation of fins and the change of the posture of the package are considered. The effect of these on the thermal ability can be ignored.

2. Maximum temperature (Melting)

The maximum temperature of each location of the package under the accident conditions of transport occurs when the packaging contains Fuel element A. The value is [redacted] ℃ at the fuel element. It is much below [redacted] ℃, melting point of the fuel cladding made of aluminum alloy. Also, the maximum temperature of the packaging occurs at the top of the fin made of stainless steel which is the main material of the packaging, and the value is [redacted]℃, which is much below [redacted] ℃, melting point of the stainless steel.

3. Maximum internal pressure, maximum thermal stress and thermal expansion (deformation)

i) The maximum internal pressure of this package under the accident conditions of transport is [redacted] MPaG. This value is much below 0.98 MPaG (10 kg/cm^{2}G), pressure of the hydro test.

ii) The maximum thermal stress under accident conditions of transport occurs when the packaging contains JRR-3 MNU type fuels. In this case, the maximum plastic strain is [redacted] % and the safety margin is [redacted]. The stress caused on the lid bolt is [redacted] MPa and the safety margin is [redacted]. For the thermal expansion, the temperature of the basket does not increase abnormally and the packaging does not shrink rapidly because the heat capacity of the packaging is large.

As mentioned above, the stress caused on the package has enough margins compared with the allowable stress. Moreover, neither the fuel elements nor the basket are restrained by the packaging.

4. Containment

The temperature of the packing of the containment boundary of the package under the accident conditions of transport is from -40 ℃ to [redacted] ℃. For above, the normal service temperature range (normal use) of silicon rubber of the

the normal service temperature range (normal use) of [redacted] of the packing is from -[redacted] ℃ to [redacted] ℃, and the maximum permissible temperature is [redacted] ℃. And also when the maximum thermal stress is applied, the maximum gap of the contact surface between the body and the lid is [redacted] mm. This value is smaller than the restoration value of the O-ring of [redacted] mm.

B.6 Appendix

In this section following items are described.

B.6.1 Appendix-1

Details relating to heat transfer in the package

B.6.2 Appendix-2

Details with regard to heat transfer at the outer surface of the package under the normal conditions of transport

B.6.3 Appendix-3

Calculation of the maximum internal pressure under the normal conditions of transport

B.6.4 Appendix-4

Details with regard to heat transfer at the outer surface of the package under the accident conditions of transport

B.6.5 Appendix-5

Details with regard to calculation of the maximum temperature in the fuel element under the accident conditions of transport

B.6.6 Appendix-6

Calculation of the maximum internal pressure under the accident conditions of transport

B.6.7 Appendix-7

References

B.6.1 Details relating to heat transfer in the package

1. Heat transfer in the package when the packaging contains the basket for box type fuel

In solid material, heat transfer takes place by conduction. Then, it is examined which is dominant in the air layer of each portion, convection or conduction, and further the evaluation of the heat transfer is performed by taking account of the effectuality of radiation.

Therefore following items are described,

- Heat transfer in the fuel element
- Convection in the basket
- Emissivity factor of radiation in the basket

And also the treatment of the small gap between structural members is described. The locations where the above heat transfer is considered are shown in (II)-Fig.B.6.1.

[redacted]

(Ⅱ)-Fig.B.6.1　Heat transfer in the package

1.1 Heat transfer in the fuel elements

The standard type fuel element and the follower type fuel element have the sectional configuration, where more than ten thin fuel plates are put between two fuel side plates, and the heat transfer is not constant in circumference. The evaluation of the heat transfer in Fuel element A, which has the maximum decay heat, is performed

First of all, the heat transfer of the air layer in the fuel element is examined.

The thin air layers exist in the space of fuel plates in the fuel element. Therefore, it is examined which is dominant in the air layer, convection or conduction. (II)-Fig.B.6.2 shows the position of Fuel element A in the basket. This examination is judged by calculating Rayleigh number Ra for the air layer in each position. Namely, the convection is dominant in the region of Ra $>$ 10^3, and the conduction is dominant in the region of less than the above.

$$\mathrm{Nu} = \frac{hD}{k} \qquad \text{Nusselt number} \cdots\cdots\cdots ①$$

$$\mathrm{Ra} = \frac{g\beta \Delta t D^3}{a\nu} \qquad \text{Rayleigh number} \cdots\cdots\cdots ②$$

$$\mathrm{Gr} = \frac{g\beta \Delta t D^3}{\nu^2} \qquad \text{Grashof number} \cdots\cdots\cdots ③$$

where,
a	: Thermal diffusivity (m²/sec)
D	: Thickness of fluid layer (m)
g	: Gravitational acceleration (m/sec²)
h	: Heat transfer coefficient (w/m²K)
k	: Thermal conductivity of fluid (w/mK)
L	: Height of vertical fluid layer (m)
Δt	: Temperature difference between the parallel two planes (℃)
β	: Volumetric coefficient of thermal expansion of fluid (1/℃)
ν	: Kinematic viscosity (m²/sec)

The Rayleigh number of the air layer is obtained by assuming that the temperature of air is [redacted]℃ and substituting the following into the equation ② ;

$$Ra = \frac{g \beta \Delta t D^3}{a \nu}$$

g : 9.8 (m/sec^2)

β : Volumetric coefficient of thermal expansion of the air at [redacted] ℃

= [redacted] = [redacted] (1/℃)

a : Thermal diffusivity of the air at [redacted]℃= [redacted] (m^2/hr)

ν : Kinematic viscosity of the air at [redacted]℃

= [redacted] (m^2/sec)

then,

Ra = [redacted] = [redacted] $\cdot D^3 \cdot \Delta t$ ……………④

Therefore, the portion where the convection is dominant is the air layer which is in the condition of satisfying Ra > 10^3 (i.e.,$D^3 \cdot \Delta t$ > [redacted]). Nevertheless, the air layer thickness D is [redacted], and Rayleigh number Ra is as follows,

Ra = ([redacted]) · ([redacted])^3 · Δt = [redacted] · Δt < 10^3

It is assumed that Δt is the temperature difference ([redacted]℃) between the maximum temperature of fuel ([redacted]℃) and the minimum temperature (155℃) from (Ⅱ)-Fig.B.8. Therefore, the Rayleigh number Ra is as follows.

Ra = [redacted] × [redacted] = [redacted] < 10^3

So it can be concluded that the conduction is dominant than the convection in the air layer on the fuel element.

For other kinds of the fuel, the same conclusion is made, and the conduction is dominant in the air layer.

[redacted]

(Ⅱ)-Fig.B.6.2　Fuel element A in the basket

Secondly, the heat transfer in the fuel is examined.

It is examined whether the heat transfer of the decay heat to the basket is dominant in the direction of the fuel side plate ,or the fuel plate. The condition putting Fuel element A in the basket is shown in (II)-Fig.B.6.3.

The examination is performed by comparing the thermal resistance, R, in the direction ⓐ along the fuel plate with that in the direction ⓑ perpendicular to the fuel plate.

Generally speaking, the thermal resistance R on the condition that the conduction is dominant is given as follows;

$$R = \frac{L}{kA} \qquad \cdots\cdots\cdots\cdots\cdots\cdots\cdots\cdots ⑤$$

where, R : Thermal resistance (K/W)

L : Heat transfer distance (m)

k : Thermal conductivity (w/mK)

A : Heat transfer area (m^2)

Thermal resistance in the direction ⓐ along the fuel plate is obtained by substituting the following values into Equation ⑤ ;

$$R = \frac{L}{kA}$$

L: Maximum heat transfer distance

= ([redacted])($\frac{1}{2}$)= [redacted] (m)

k: Thermal conductivity of aluminum alloy at [redacted]℃

= [redacted] (w/mK)

A: Heat transfer area of the distance 1 mm in the direction of the axis

= ([redacted])([redacted])

= [redacted] (m^2)

[redacted]

(Ⅱ)-Fig.B.6.3 Direction of heat transfer in Fuel element A

Then, R is given as follows ;

R = [redacted] = [redacted] (K/W)

Since the conduction is dominant in the air layer between the fuel plates as above mentioned and the resistance of the air layer is compared with that of the fuel plate, the thermal resistance ⓑ perpendicular to the fuel plate is obtained as only the air layer.

Substitute the following values in Equation ⑤.

$$R = \frac{L}{k\,A}$$

L: Length of the air layer

= [redacted]

= [redacted] (m)

k : Thermal conductivity of the air at [redacted]℃

= [redacted](w/mK)

A: Heat transfer area to the distance 1 mm in the direction of the axis

= ([redacted])([redacted])

= [redacted] (m²)

then, R is obtained as follows ;

R = [redacted] = [redacted] (K/W)

Therefore, the thermal transfer resistance in the direction ⓑ perpendicular to the fuel palate is about [redacted] times of that of ⓐ, so it is assumed that the heat transfer in ⓐ the direction is dominant.

As the heat transfer in the fuel element that has a shape of box type, there are the one that flows into the basket from the fuel side plate and the other that flows into the basket through the external fuel plate. However, since it is difficult to estimate the rate of heat transfer quantity of the above two, it is assumed that the decay heat flows into the basket from the fuel side plate in the analysis. Namely, it is assumed that there is the heat source in only the fuel side plate, and the conduction between the two fuel side plates is performed through the fuel cladding except the fuel meat. By means of these assumptions, the heat transfer areas of the fuel and the basket are estimated smaller than actual areas and the fuel temperature is evaluated greater than the practical. Therefore, the assumption is conservative.

Furthermore, which direction the fuel side plate of each fuel faces in will scarcely affect the total temperature distribution, because the volume of the basket is large.

1.2 Air convection in the basket

Which is dominant, either convection or conduction, in the air layer which exists in the basket except for the portion of the fuel element is examined by the same way as mentioned in the previous paragraph, and the heat transfer coefficient is calculated for the air layer which the convection is dominant.

As the representation of the examination, the results for Fuel element As are presented.

As the air layer, the layer between the fuel side plate and the side surface of lodgement the basket, the space of the lodgment for neutron source and the space above the top of the fuel element, etc. are considered. The air layer thickness D between the fuel side plate and the side surface of the basket lodgement is [redacted] mm as shown in (Ⅱ)-Fig. B.6.2 and Rayleigh number Ra is given from Equation ④.

$$Ra = ([redacted]) \cdot ([redacted])^3 \cdot \Delta t$$

$$= [redacted] \cdot \Delta t < 10^3$$

For example from (Ⅱ)-Fig. B.8, it is assumed that Δt is temperature difference ([redacted] ℃) between the maximum temperature of fuel ([redacted] ℃) and the minimum temperature of the basket ([redacted] ℃). Rayleigh number Ra is as follows,

$$Ra = [redacted] \times [redacted] = [redacted] < 10^3$$

Therefore, the conduction is dominant in the air layer. The air layers where convection are dominant are the space in the lodgment for neutron source and above the top of the fuel element, and conduction is dominant in the others . The location where the convection is dominant is shown in (Ⅱ)-Fig.B.6.4.

The heat transfer coefficients of the convection for these locations are described as follows.

These air layers are in the shape that their surroundings are enclosed. Equation ⑥ 7) is used for the heat transfer with 2 pieces of the horizontal planes surrounding, and Equation ⑦ 3) is used for the heat transfer with the vertical flow of enclosed layer.

$$\left.\begin{array}{ll} Nu = 0.21 \cdot Ra^{1/4} & (10^4 < Gr < 3.2\times10^5) \\ Nu = 0.075 \cdot Ra^{1/3} & (3.2\times10^5 < Gr < 10^7) \end{array}\right\} \cdots\cdots\cdots\cdots ⑥$$

$$Nu = 0.28 \cdot Ra^{1/4} \quad (L/D)^{-1/4} \quad (10^3 < Ra < 10^7) \cdots\cdots\cdots\cdots ⑦$$

As one example, the evaluation for the upper and lower surface of the space of the lodgement for neutron source is described as follows, Rayleigh number Ra is obtained by substituting the following values into Equation ②.

$$Ra = \frac{g\beta\,\Delta t\,D^3}{a\nu}$$

g : 9.8 (m/sec^2)

β : Volumetric coefficient of thermal expansion of the air at [redacted] ℃

$= \dfrac{1}{\text{[redacted]} + 273} =$ [redacted] (1/℃)

a : Thermal diffusivity of the air at [redacted]℃

= [redacted] (m^2/hr)

ν : Kinematic viscosity of the air at [redacted]℃

= [redacted] (m^2/sec)

D : The thickness of the air layer (The height of the lodgement for neutron source)

= [redacted] m

[redacted]

(II)-Fig.B.6.4　Air area where convection is dominant in the basket for box type fuel then,

$$Ra = \frac{(9.8)(\text{[redacted]}^{2}(\text{[redacted]})(\text{[redacted]})^{3}\ \Delta t}{\text{[redacted]})} = \text{[redacted]}\ \Delta t$$

Grashof number is obtained from Equation ② and ③

$$Gr = \frac{Ra \ \cdot a}{\nu} = \frac{\text{[redacted]} \cdot \Delta t \times \text{[redacted]}}{\text{[redacted]}} = \text{[redacted]}\ \Delta t$$

Nusselt number is obtained from Equation ⑥

$$Nu = 0.075 \cdot Ra^{1/3} = 0.075 \cdot (\text{[redacted]} \cdot \Delta t)^{1/3} = \text{[redacted]} \cdot \Delta t^{1/3}$$

The heat transfer coefficient between the upper and the lower surface h is obtained from Equation ①.

$$h = \frac{Nu \ \cdot k}{D} = \text{[redacted]}$$

$$= \text{[redacted]}\ \Delta t^{1/3}\ (w/m^2K)$$

where, k : Thermal conductivity of the air at [redacted] ℃

= [redacted] (w/mK)

This value is natural convection heat transfer coefficient expressed by the relation between the temperature of the upper surface of the lodgement for neutron source (the lid bottom surface) and the lower surface (the upper surface of the basket bottom plate). The heat transfer coefficient between the upper or lower plane and the air is twice of h.

$$2h = 2 \times \text{[redacted]}\ \Delta t^{1/3} = \text{[redacted]}\ \Delta t^{1/3}\ (W/m^2k)$$

The heat transfer coefficient for the other air layer is obtained by the same procedure. The result obtained is shown in (Ⅱ)-Table B.6.1. These values are used as the input data of ABAQUS code.

(Ⅱ)-Table B.6.1 Heat transfer coefficient of convection (In case of containing Fuel element A)

Equation for heat transfer coefficient of convection

Upper and lower surface : Equation for 2 pieces of horizontal planes surrounding	$Nu = 0.21 \cdot Ra^{1/4}$ $Nu = 0.075 \cdot Ra^{1/3}$	$(10^4 < Gr < 3.2\times10^5)$ $(3.2\times10^5 < Gr < 10^7)$
Side : Equation for vertical flow of enclosed layer	$Nu = 0.28 \cdot Ra^{1/4}(L/D)^{-1/4}$	$(10^3 < Ra < 10^7)$
Rayleigh number	$Ra = g \cdot \beta \cdot \Delta t \cdot D^3 / (a \cdot \nu)$	
Grashof number	$Gr = g \cdot \beta \cdot \Delta t \cdot D^3 / \nu^2$	
Heat transfer coefficient	$h = Nu \cdot k / D$	
Temperature of air in the basket	[redacted]	
0℃	273K	
Gravitational acceleration	$9.8 m/s^2$	

Item			The space in the lodgement of neutron source		The space of the top of fuel element	
			Top,bottom surface	The side	Top,bottom surface	The side
Volumetric coefficient of thermal expansion of fluid	β	1/℃	[redacted]	[redacted]	[redacted]	[redacted]
Temputure difference between two parallel planes	Δt	℃	[redacted]	[redacted]	[redacted]	[redacted]
Thickness of fluid layer	D	m	[redacted]	[redacted]	[redacted]	[redacted]
Air layer height	L	m	[redacted]	[redacted]	[redacted]	[redacted]
Thermal diffusivity	a	m^2/s	[redacted]	[redacted]	[redacted]	[redacted]
Kinematic viscosity	ν	m^2/s	[redacted]	[redacted]	[redacted]	[redacted]
Rayleigh number	Ra	-	[redacted]	[redacted]	[redacted]	[redacted]
Grashof number	Gr	-	[redacted]	[redacted]	[redacted]	[redacted]
Nusselt number	Nu	$Nu = 0.21 \cdot Ra^{1/4}$ $Nu = 0.075 \cdot Ra^{1/3}$ $Nu = 0.28 \cdot Ra^{1/4}(L/D)^{-1/4}$	[redacted]	[redacted]	[redacted]	[redacted]
Thermal conductivity	k	W /(mK)	[redacted]	[redacted]	[redacted]	[redacted]
Heat transfer coeffiient	h	$W /(m^2K)$	[redacted]	[redacted]	[redacted]	[redacted]
	2h		[redacted]	[redacted]	[redacted]	[redacted]

1.3 Heat transfer of radiation in the packaging

The radiation is considered for following locations.

① Between the fuel side plate and the basket lodgement
(Aluminum alloy surface and stainless steel surface)

② Between the basket top end and the inner surface of the lid
(Stainless steel surface and stainless steel surface)

③ Between the side surface of the basket and the inner surface of the shell
(Stainless steel surface and stainless steel surface)

④ Between the upper basket bottom plate of the lodgement for neutron source and the inner surface of the lid
(Stainless steel surface and stainless steel surface)

⑤ Between the top end surface of the fuel element and the inner surface of the lid
(Stainless steel surface and stainless steel surface)

The emissivity factor of the radiation heat transfer is generally obtained from the following equation.

$$\mathcal{F}_{12} = \frac{F_{12}}{\frac{1}{\varepsilon_1} + \frac{1}{\varepsilon_2} - 1} \qquad \cdots\cdots ⑧$$

where, $\mathcal{F}_{12}$: Emissivity factor from surface 1 to surface 2

F_{12} : Geometrical factor from surface 1 to surface 2

ε_1 : Emissivity of surface 1

ε_2 : Emissivity of surface 2

The geometrical factor for each location is considered as 1.0. The emissivity of the aluminum alloy surface (ε1) and stainless steel surface (ε2) is 0.15 and 0.11 respectively as shown in (Ⅱ)-Table B.1.

Following values are used as the input data of ABAQUS code.

Emissivity of aluminum alloy surface: $\varepsilon_1 = 0.11$

Emissivity of stainless steel surface: $\varepsilon_2 = 0.15$

Stefan-Boltzmann's constant: $\sigma = 5.67032 \times 10^{-8}$ (W/m²K⁴)

1.4 Heat transfer between the bottom end surface of the fuel element and the upper basket bottom plate

A slight air layer exists between the fuel element and the upper basket bottom plate, which is evaluated as follows.

The heat transfer area is considered as only the sectional area of the fuel side plate. The thickness of the air layer is considered as the gap that occurs when the fuel element is inclined to the utmost physically possible limit in the basket lodgement. For instance, in case of Fuel element A, the inclination angle is [redacted] ° and the maximum air layer thickness is [redacted] mm, and the mean value is [redacted] mm. Therefore, as the air layer thickness, the mean value ([redacted] mm) is used.

1.5 Heat transfer between the bottom end surface of basket compositions (such as the frame, the partition plate and the compartment plate) and the upper basket bottom plate, between the upper basket bottom plate and the lower basket bottom plate, and between the lower basket bottom plate and the body bottom plate.

Between these stainless steel materials, the slightly thin air layer exists, which is evaluated as follows.

For the heat transfer area, the value which is taken into account of the reduction of the contact area with the groove for draining is used.

For the thickness of the air layer, assuming that each surface finishing is [redacted] *), the maximum gap becomes as follows.

[redacted] + [redacted] = [redacted] (mm)

This value is adopted.

---

*) JIS B 0601

The surface roughness shows the maximum height in micron ($1\mu = 0.001$mm) and the value of roughness (S) means the allowable maximum height.

1.6 Heat transfer between the surface of the basket top end and the inner surface of the lid, between the side surface of the basket and the inner surface of the shell

The air layer thickness 5 mm exists between the surface of the basket top end and the inner surface of the lid. And the air layer thickness 1 mm per radius exists between the side of the basket and the inner surface of the shell. The heat transfers of these air layers are considered.

1.7 Heat transfer between the neutron poison and the partition plate

The air layer thickness [redacted] mm exists in both side between the neutron poison and the partition plate. The heat transfers of these air layers are considered.

2. Heat transfer in the package when the packaging contains the basket for MNU type fuel

As shown in para. 4.2 of (Ⅱ)-B.4.1.1, heat transfer takes place by conduction in solid material. And it is expected that the heat transfer by convection and radiation from the fuel element to the side wall of the body is little, and that most of the decay heat transfers to the body mainly by way of the basket bottom plate through the fuel meat, the fuel cladding or the square shape pipe.

In the analysis, since the cross section of JRR-3 MNU type fuel is almost a circle, the heat generation on the fuel cladding of the outer cylinder is assumed to be uniform in circumference and the internal fuel meat is considered to be insulation. Moreover, the square shape pipe is not modeled and it is assumed that the decay heat of fuel transfers only from the fuel cladding to the body bottom plate through the basket bottom plate. By means of these assumptions, the heat transfer areas of the fuel element and the basket are estimated smaller than actual areas and the fuel temperature is evaluated greater than the practical. Therefore, the assumption is conservative.

In the condition of heat transfer between the fuel element and the body bottom plate, air gaps exist in the following locations. These widths are assumed conservatively and the heat transfer is assumed to take place by the conduction of air.

- Surfaces between the bottom end of the fuel element and the upper side of the basket bottom plate
- Surfaces between the lower side of the basket bottom plate and the body bottom plate

The locations, where the above heat transfers are considered, are shown in (II)-Fig.B.6.5.

2.1 Heat transfer between the bottom end surface of the fuel element and the upper surface of the basket bottom plate

A slight air layer exists between the fuel element and the basket bottom plate, which is evaluated as follows.

The heat transfer area is considered as only the sectional area of the stopper of the fuel element. The thickness of the air layer is considered as the gap that occurs when the fuel element is inclined to the utmost physically possible limit in the basket lodgement. The inclination angle is [redacted] ° and the maximum air layer thickness is [redacted] mm, and the mean value is [redacted] mm. Therefore, as the air layer thickness, the mean value ([redacted] mm) is used.

2.2 Heat transfer between the lower surface of the basket bottom plate and the body bottom plate

Between these stainless steel materials, the slightly thin air layer exists, which is evaluated as follows.

For the heat transfer area, the surface areas of the basket bottom plate is used since the basket for MNU type fuel has no groove for draining.

For the thickness of the air layer, assuming that each surface finishing is [redacted], the maximum gap becomes as follows.

[redacted] + [redacted] = [redacted] (mm)

This value is adopted.

[redacted]

(Ⅱ)-Fig.B.6.5　Heat transfer in the package

B.6.2 Details with regard to heat transfer at the outer surface of the package under the normal conditions of transport

The heat transfer between the outer surface of the packaging and ambient environment is performed by natural convection and radiation. The locations where natural convection and radiation for the outer surface of the package are considered are shown in (Ⅱ)-Fig.B.6.6. The heat transfer coefficient of the convection and the emissivity factor used in radiation are described as follows.

1. Heat transfer coefficient of convection

For the estimation of the heat transfer coefficient of the convection h, the highly reliable experimental equation according to each location is applied, i.e., the natural convection equation of the vertical plane ①$^{7)}$ is used for the fin and the side of the body.

$$\left\{\begin{array}{l} Nu = 0.555 \cdot Ra^{1/4}\ (10^4 < Ra < 10^8) \\ Nu = 0.129 \cdot Ra^{1/3}\ (10^8 < Ra < 10^{12}) \end{array}\right. \quad \cdots\cdots ①$$

The natural convection equation ②$^{7)}$ of the upward heating surface is used for the top surface of the body.

$$\left\{\begin{array}{l} Nu = 0.54 \cdot Ra^{1/4}\ (10^5 < Ra < 2\times10^7) \\ Nu = 0.14 \cdot Ra^{1/3}\ (2\times10^7 < Ra < 3\times10^{10}) \end{array}\right. \quad \cdots\cdots ②$$

And, the natural convection equation of the downward heating surface ③$^{7)}$ is used for the bottom surface of the body.

$$Nu = 0.27 \cdot Ra^{1/4}\ (3\times10^5 < Ra < 3\times10^{10}) \quad \cdots\cdots ③$$

where, $Nu = \frac{h\,D}{k}$ Nusselt number ⋯⋯④

$Ra = \frac{g\beta\,\Delta t\,D^3}{a\,\nu}$ Rayleigh number ⋯⋯⑤

a : Thermal diffusivity (m^2/sec)

D : Layer thickness of fluid (m)

g : Gravitational acceleration (m/sec2)

h : Heat transfer coefficient of convection (w/m^{2}k)

k : Thermal conductivity of fluid (w/mk)

L : Vertical layer height of fluid (m)

Δt: Temperature difference between two parallel planes (℃)

β : Volumetric coefficient of thermal expansion of fluid (1/℃)

ν : Kinematic viscosity (m^2/sec)

The Rayleigh number of the air layer is obtained by assuming that the temperature of air is 38 ℃ and substituting the above values into Equation ⑤

$$Ra = \frac{g\beta\ \Delta t\ D^3}{a\,\nu}$$

g : 9.8 (m/sec^2)

β : Volumetric coefficient of thermal expansion of the air at 38 ℃

$$= \frac{1}{38+273} = 0.00322 \quad (1/℃)$$

a : Thermal diffusivity of the air at 38 ℃

$= 0.0882$ (m^2/hr)

ν : Kinematic viscosity (at 38 ℃)

$= 0.173\times10^{-4}$ (m^2/sec)

in Equation ⑤, and

$$Ra = \frac{(9.8)(3,600)^2(0.00322)\ \Delta t\cdot D^3}{(0.0882)(0.173\times10^{-4})(3,600)} = 7.45\times10^7\cdot D^3\cdot\ \Delta t$$

The representative length D (m) corresponding to each location is substituted into the above equation, and the heat transfer coefficient of the convection at each location is obtained. As one example, the result of the upper surface of the lid is described. The representative length D is [redacted] m (outside diameter of the packaging).

Rayleigh number Ra is obtained.

$$Ra = 7.45 \times 10^7 \times (\text{[redacted]})^3 \cdot \Delta t$$

$$= \text{[redacted]} \ \Delta t$$

Nusselt number Nu is obtained from Equation ②

$$Nu = 0.14 \cdot Ra^{1/3}$$

$$= 0.14 \times (\text{[redacted]} \cdot \Delta t)^{1/3}$$

$$= \text{[redacted]} \cdot \Delta t^{1/3}$$

The heat transfer coefficient of the convection h is obtained

from Equation ④

$$h = \frac{Nu \cdot k}{D} = \frac{\text{[redacted]} \cdot \Delta t^{1/3} \cdot 0.0271}{\text{[redacted]}}$$

$$= \text{[redacted]} \cdot \Delta t^{1/3} \ (w/m^2k)$$

where, k : Thermal conductivity of the air at 38℃

= 0.0271 (w/mK)

The heat transfer coefficient of the convection for each location is shown in (Ⅱ)-Table B.6.2.

These values are used as the input data of ABAQUS code.

[redacted]

(Ⅱ)-Fig.B.6.6 Heat transfer at the outer surface of the package

(II)-Table B.6.2 Heat transfer coefficient of convection at the outer surface of the package

Equation for heat transfer coefficient of convection

The top surface of the packaging : Natural convection equation of upward heating surface	$Nu = 0.54 \cdot Ra^{1/4}$ $Nu = 0.14 \cdot Ra^{1/3}$	$(10^5 < Ra < 2\times10^7)$ $(2\times10^7 < Ra < 3\times10^{10})$
The fin and the side of the body : Natural convection equation of virtical plane	$Nu = 0.555 \cdot Ra^{1/4}$ $Nu = 0.129 \cdot Ra^{1/3}$	$(10^4 < Ra < 10^8)$ $(10^8 < Ra < 10^{12})$
The bottom surface of the packaging : Natural convection equation of downward heating surface	$Nu = 0.27 \cdot Ra^{1/4}$	$(3\times10^5 < Ra < 3\times10^{10})$
Rayleigh number	$Ra = g \cdot \beta \cdot \Delta t \cdot D^3 / (a \cdot \nu)$	
Heat transfer coefficient	$h = Nu \cdot k / D$	
Ambient temperature	38 ℃	
0℃	273 K	
Gravity acceleration	9.8 m/s^2	

Item			The outer surface of the packaging			Heat dissipating fin
			The upper surface	The bottom surface	The side	The outer surface
Volumetric coefficient of thermal expansion of fluid	β	1/℃	0.00321	0.00321	0.00321	0.00321
Temputure difference between two parallel planes	Δt	℃	-	-	-	-
Representative length	D	m	[redacted]	[redacted]	[redacted]	[redacted]
Thermal diffusivity	a	m^2/s	2.45E-05	2.45E-05	2.45E-05	2.45E-05
Kinematic viscosity	ν	m^2/s	1.73E-05	1.73E-05	1.73E-05	1.73E-05
Rayleigh number	Ra	-	[redacted]	[redacted]	[redacted]	[redacted]
Nusselt number	Nu	$Nu = 0.54 \cdot Ra^{1/4}$	[redacted]	-	-	-
		$Nu = 0.14 \cdot Ra^{1/3}$				
		$Nu = 0.555 \cdot Ra^{1/4}$	-	-	[redacted]	[redacted]
		$Nu = 0.129 \cdot Ra^{1/3}$				
		$Nu = 0.27 \cdot Ra^{1/4}$	-	[redacted] $\Delta t^{1/4}$	-	-
Thermal conductivity	k	W /(mK)	0.0271	0.0271	0.0271	0.0271
Heat transfer coeffiient	h	W /(m^2K)	[redacted]	[redacted]	[redacted]	[redacted]

2. Heat transfer by radiation

The geometrical factors for the surface of the body with no fins (the upper surface of the lid, the outer surface of the body bottom plate, the outer surface in the vicinity of the contact surface of the body and the lid) and the end surface of the fins are assumed to be 1. On the other hand, the geometrical factors for the surface of the body with fins and the fins themselves are calculated respectively by using ABAQUS code dividing the fins in the direction of longitudinal axis and the fins in the direction of the height of the fins.

The locations where the geometrical factor is 1 are shown in (II)-Fig.B.6.7.

Furthermore, the locations where the radiation for the surface of the body with the fins and the fins themselves is considered are, as shown in (II)-Fig.B.6.8, the top fin (Ⓐ), the lateral fin (Ⓑ) and the bottom fin (Ⓒ). The ambient air of the upper and side of these fins are considered, when the geometrical factors of these locations are calculated. The detail procedures of the radiation are described separately as follows.

1) The location where the geometrical factor is 1

2) The top fin (Ⓐ), the lateral fin (Ⓑ) and the bottom fin (Ⓒ)

1) The location where the geometrical factor is 1

For the surface of the body with no fins (the upper surface of the lid, the outer surface of the body bottom plate, the outer surface in the vicinity of the contact surface of the body and the lid) and the end surface of the fins, the geometrical factor is 1 so that the following values are used as the input data of ABAQUS code.

Geometrical factor: $F = 1$

Surface emissivity: $\varepsilon_1 = 0.15$
Ambient emissivity: $\varepsilon_2 = 1.0$
} (as shown in (II)-Table B.3)

Stefan-Boltzmann's constant: $\sigma = 5.67032 \times 10^{-8}$ (W/m²K⁴)

2) The top fin, the lateral fin and the bottom fin

For the top fin(Ⓐ), the lateral fin (Ⓑ) and the bottom fin (Ⓒ), the geometrical factor of each portion is obtained by making the closed cavity composed of the fin surface, the outer surface of the body between the fin and the ambient air surrounding them, in the analytical model of ABAQUS code. The emissivity factor of the portion is determined by the geometrical factor and the surface emissivity or the ambient emissivity.

[redacted]

(Ⅱ)-Fig.B.6.7　Surface where geometrical factor is 1.0

[redacted]

(II)-Fig.B.6.8　Explanation of fin and ambient air

3. Heating surface area of the outer surface of the packaging

The heating surface area of the outer surface of the packaging is evaluated as follows.

The heating surface area between the surface of the lid or the packaging and the ambient air is obtained by ignoring the lifting lug for the body and the lid, because the area is much small. The surface area of fin modeled is used as the heating surface area between the surface of fin and the ambient air.

The base plate is ignored because the effect of the heat transfer is small.

4. Solar insolation

The evaluation for the solar insolation based on (Ⅱ)-Table B.3 is performed as follows and the heat of the insolation q which is required for each location as shown in (Ⅲ)-Table B.3 is given for each outer surface in the analytical model. The heat absorption rate (surface emissivity) for the outer surface of the lid, the body and the fins is 0.15 and the geometrical factor is 1.0.

1) For the outer surface of the lid and the body

The insolations (q) on the surface of the package are obtained as follows.

① Flat surfaces transported horizontally (upward facing)

$q = 800 \times 0.15 = 120$ (W/m^2)

② Surfaces transported vertically and other downward facing (not horizontal) surfaces

$q = 200 \times 0.15 = 30$ (W/m^2)

③ All other surfaces

$q = 400 \times 0.15 = 60$ (W/m^2)

④ Flat surfaces transported horizontally (downward facing)

$q = 0$ (W/m^2)

2) For the surface of the fin

The insolations (q) on the surface of the fins are also obtained as follows.

① Flat surfaces transported horizontally (upward facing)

$q = 800 \times 0.15 = 120$ (W/m^2)

② Surfaces transported vertically and other downward facing (not horizontal) surfaces (each facing)

i) Side surfaces of fins

$q = 200 \times 0.15 = 30$ (W/m^2)

ii) End surfaces of fins

$q = 200 \times 0.15 = 30$ (W/m^2)

③ All other surfaces

$q = 400 \times 0.15 = 60$ (W/m^2)

④ The flat surfaces transported horizontally (downward facing)

$q = 0$ (W/m^2)

B.6.3. Calculation of the maximum internal pressure under the normal conditions of transport

This package is sealed after loading the fuel elements and achieving thermal equilibrium. Since there is only the air as the internal fluid in the package, the maximum internal pressure is obtained by calculating only the pressure increase due to the temperature increase between the temperature of the internal air in the packaging under the absence of insolation and that under solar insolation. For instance, when Fuel element A is contained, the minimum temperature of the internal air is considered to be equal to the temperature of the inner wall of the body in the results of "Temperature evaluation in the absence of solar insolation", [redacted] ℃ (refer to (Ⅱ)-Fig. B.7).

On the other hand, the maximum temperature of the inner air under solar insolation is considered to be equal to the maximum temperature of the fuel in the results of "The evaluation of the maximum temperature", [redacted]℃ (refer to (Ⅱ)-Table B.6). The actual air temperature is in between these two values, and the maximum internal pressure is lower than the value in case that the air temperature is assumed as [redacted]℃.

The maximum internal pressure in this case will be obtained by applying the state equation of the ideal gas as follows;

$$\frac{P_1 V_1}{T_1} = \frac{P_2 V_2}{T_2} \quad \cdots\cdots\cdots\cdots\cdots\cdots\cdots\cdots ①$$

where, P_1 : Internal pressure in sealed condition (atmospheric pressure) (MPa abs)

V_1 : Internal air volume in sealed condition (m^3)

T_1 : Internal air temperature in sealed condition (K)

P_2 : Internal pressure in the evaluation of the maximum temperature (MPa abs)

V_2 : Internal air volume in the evaluation of the maximum temperature (m^3)

T_2 : Internal air temperature in the evaluation of the maximum temperature(K)

From Equation ① ;

$$P_2 = \frac{P_1 V_1 T_2}{T_1 V_2} \quad \cdots\cdots\cdots\cdots\cdots\cdots\cdots\cdots\cdots\cdots\cdots\cdots ②$$

Substitute the following into the above equation;

$P_1 = 0.1013$ (MPa abs)

$V_1 = V_2$

$T_1 =$ [redacted] $+ 273 =$ [redacted] (K)

$T_2 =$ [redacted] $+ 273 =$ [redacted] (K)

then, the maximum internal pressure is,

$$P_2 = \frac{(0.1013) \times V_1 \times \text{[redacted]}}{\text{[redacted]} \times V_2}$$

$=$ [redacted] (MPa abs)

$=$ [redacted] (MPaG)

The maximum internal pressure for JRR-3 MNU type fuel is obtained by using the same procedure. The results is shown in (Ⅱ)-Table B.6.

In addition, when the ambient temperature change expected during transportation (-40°C to 38°C) is considered, it is assumed that the fuel is loaded in a -40°C environment and pressure is adjusted in a -40 °C environment. The internal temperature during pressure adjustment is determined by subtracting the ambient temperature change from the average temperature inside the container:

$$\frac{\text{[redacted]}}{2} - 78 = \text{[redacted]} \ (℃)$$

On the other hand, if the maximum temperature of internal air when subjected to the solar radiation heat in the same manner as in the maximum internal pressure calculation, is set to [redacted]°C assuming it is equal to the maximum temperature of the fuel element in the maximum temperature evaluation results, then the internal pressure at this time will be

$$P_2{}' = \frac{(0.1013) \times V_1 \times \text{[redacted]}}{\text{[redacted]} \times V_2}$$

= [redacted] (MPa abs)

= [redacted] (MPaG)

Since this is smaller than the calculated maximum internal pressure under normal conditions of transport, this will be covered by the above results, then even when considering the ambient temperature changes expected during transportation, this nuclear fuel package does not have a problem due to pressure increase under normal conditions of transport

B.6.4. Details with regard to heat transfer at the outer surface of the package under the accident conditions of transport

1. Heat transfer coefficient of convection

For the estimation of the heat transfer coefficient of convection, the reliable experimental equation corresponding to each location is adopted as the same as under the normal conditions of transport.

Namely, for the fin and the side of the body, the natural convection equation ①$^{7)}$ of the vertical plane is used.

$$\left\{\begin{array}{ll} Nu = 0.555 \cdot Ra^{1/4} & (10^4 < Ra < 10^8) \\ Nu = 0.129 \cdot Ra^{1/3} & (10^8 < Ra < 10^{12}) \end{array}\right. \cdots\cdots\cdots ①$$

For the top surface of the packaging before and after fire, the natural convection equation ②$^{7)}$ of the upward heating surface is used.

$$\left\{\begin{array}{ll} Nu = 0.54 \cdot Ra^{1/4} & (10^5 < Ra < 2\times10^7) \\ Nu = 0.14 \cdot Ra^{1/3} & (2\times10^7 < Ra < 3\times10^{10}) \end{array}\right. \cdots\cdots\cdots ②$$

For the top surface of the packaging on fire, the natural convection equation ③$^{7)}$ of the upward cool surface is used.

$$Nu = 0.27 \cdot Ra^{1/4} \quad (3\times10^5 < Ra < 3\times10^{10}) \cdots\cdots\cdots ③$$

For the bottom surface of the body before and after fire, the natural convection equation ④$^{7)}$ of the downward heating surface is used.

$$Nu = 0.27 \cdot Ra^{1/4} \quad (3\times10^5 < Ra < 3\times10^{10}) \cdots\cdots\cdots ④$$

For the bottom surface of the body on fire, the natural convection equation of the downward cool surface ⑤$^{7)}$ is used.

$$\left\{\begin{array}{ll} Nu = 0.54 \cdot Ra^{1/4} & (10^5 < Ra < 2\times10^7) \\ Nu = 0.14 \cdot Ra^{1/3} & (2\times10^7 < Ra < 3\times10^{10}) \end{array}\right. \cdots\cdots\cdots ⑤$$

where, $Nu = \frac{hD}{k}$ Nusselt number ……………………⑥

$Ra = \frac{g \beta \Delta t D^3}{a \nu}$ Rayleigh number ……………………⑦

where, a : Thermal diffusivity (m^2/sec)

D : Thickness of fluid layer (m)

g : Gravitational acceleration (m/sec^2)

h : Heat transfer coefficient (W/m^2K)

k : Thermal conductivity of fluid (W/mK)

L : Height of vertical fluid layer (m)

Δt : Temperature difference between two parallel planes (℃)

β : Volumetric coefficient of thermal expansion of fluid (1/℃)

ν : Kinematic viscosity (m^2/sec)

After and before fire, Rayleigh number is obtained by substituting the following into Equation ⑦ ;

$$Ra = \frac{g \beta \Delta t D^3}{a \nu}$$

$g = 9.8$ (m/sec^2)

β : Volumetric coefficient of thermal expansion of the air at 38 ℃

$$= \frac{1}{38+273} = 0.00322 \quad (1/℃)$$

a : Thermal diffusivity of the air at 38 ℃

$= 0.0882$ (m^2/hr)

ν : Kinematic viscosity of the air at 38 ℃

$= 0.173 \times 10^{-4}$ (m^2/sec)

, and then

$$Ra = \frac{(9.8)(3{,}600)^2(0.00322) \cdot \Delta t \cdot D^3}{(0.0882)(0.173 \times 10^{-4})(3{,}600)}$$

$= 7.45 \times 10^7 \cdot D^3 \cdot \Delta t$ ……………………………………………………⑧

Also, on fire, substitute the following into Equation ⑦ ;

$$Ra = \frac{g \beta \Delta t D^3}{a \nu}$$

$g = 9.8$ (m/sec^2)

β : Volumetric coefficient of thermal expansion of the air at 800 ℃

$$= \frac{1}{800+273} = 0.000932 \quad (1/℃)$$

a : thermal diffusivity of the air at 800 ℃

= 0.693 (m^2/hr)

ν : Kinematic viscosity of the air at 800 ℃

$= 1.37 \times 10^{-4}$ (m^2/sec)

then,

$$Ra = \frac{(9.8)(3{,}600)^2(0.000932) \cdot \Delta t \cdot D^3}{(0.693)(1.37 \times 10^{-4})(3{,}600)}$$

$$= 3.46 \times 10^5 \cdot D^3 \cdot \Delta t \cdots\cdots\cdots\cdots ⑨$$

Substituting the representative length D(m) corresponding to each location into the above two equations, the applicable natural convection equation is determined and the heat transfer coefficient is obtained.

As one example, the case applied to the top surface of the packaging is described.

The representative length D is considered to be outer diameter of the packaging of [redacted] m. The Rayleigh number Ra before and after fire is obtained from Equation ⑧ ;

Ra = 7.45×10^7 · ([redacted])^3 · Δt

= [redacted] · Δt

Also, the Rayleigh number Ra on fire is obtained from Equation ⑨ ;

$$Ra = 3.46\times10^5 \cdot ([redacted])^3 \cdot \Delta t$$

$$= [redacted] \cdot \Delta t$$

then, the Nusselt number Nu before and after fire is obtained from Equation ② ;

$$Nu = 0.14\times Ra^{1/3}$$

$$= [redacted] \cdot \Delta t^{1/3}$$

Also, the Nusselt number Nu on fire is obtained from Equation③ ;

$$Nu = 0.27\times Ra^{1/4}$$

$$= [redacted] \cdot \Delta t^{1/4}$$

Therefore, the heat transfer coefficient of convection h is obtained from Equation ⑥ ;

$$h = \frac{Nu \cdot k}{D} = \frac{0.14Ra^{1/3}\times0.0271}{[redacted]}$$

$$= [redacted] \cdot \Delta t^{1/3} \quad (W/m^2K)$$

where, k: Thermal conductivity of the air at 38 ℃

= 0.0271 (W/mK)

Also, the heat transfer coefficient of convection h is obtained from Equation ⑥ ;

$$h = \frac{0.27Ra^{1/4}\times0.0709}{[redacted]}$$

$$= [redacted] \cdot \Delta t^{1/4} \quad (W/m^2K)$$

where, k: Thermal conductivity of the air at 800 ℃

= 0.0709 (W/mK)

The heat transfer coefficient of convection for each location is shown in (Ⅱ)-Table B.6.3. These values are used as the input data of ABAQUS code.

2. Heat transfer coefficient of radiation

The emissivities ε_1, ε_2 are determined by the ambient condition as shown in (Ⅱ)-Table B.7. For the locations where the geometrical factor is assumed to be 1, the values of each surface emissivity (ε_1), each ambient emissivity (ε_2), geometrical factor (F=1) and Stefan-Boltzmann's constant (σ) are used as the input data of ABAQUS code.

For the top fin, the lateral fin and the bottom fin, the geometrical factor of each portion is obtained by making the closed cavity composed of the fin surface, the outer surface of the body between the fin and the ambient air surrounding them, in the analytical model of ABAQUS code. The input data of ABAQUS code are the geometrical factor, the surface emissivity, the ambient emissivity and Stefan-Boltzmann's constant.

3. Heating surface area of the outer surface of the packaging

The heating surface area of the outer surface of the packaging under the accident condition of transport is assumed to be same as that shown in paragraph (Ⅱ)-B.6.2.

4. Solar insolation

The solar insolation under the accident condition is considered before and after a fire and on fire. The solar insolation under the accident conditions of transport is treated as the same as that under the normal conditions of transport because the heating surface area and the outer surface configuration of the packaging are the same as those of the normal conditions of transport.

(II)-Table.B.6.3 Heat transfer coefficient of convection to ambient air under accident condition

Location Item		Upper surface of the packaging	Bottom surface of the packaging	Side of the packaging	Fin
D: Representative length(m)		[redacted]	[redacted]	[redacted]	[redacted]
Before and after a fire	R_a: Rayleigh number (−) N_u : Nusselt number (−) h : Heat transfer coefficient of convection (W/m^2K)	[redacted]	[redacted]	[redacted]	[redacted]
On fire	R_a: Rayleigh number (−) N_u : Nusselt number (−) h : Heat transfer coefficient of convection (W/m^2K)	[redacted]	[redacted]	[redacted]	[redacted]

B.6.5. Details with regard to calculation of the maximum temperature in the fuel element under the accident conditions of transport

The calculation of the maximum temperature evaluation of the fuel elements under the condition is shown for each kind of the baskets, as follows (refer to (Ⅱ)-Table B.8)

1. In case that the basket for box type fuel is contained (in case of containing Fuel element A in the packaging)

The temperature histories of each location under the accident conditions of transport are shown in (Ⅱ)-Fig.B.16 through (Ⅱ)-Fig.B.18, when the packaging contains Fuel element A. As shown in (Ⅱ)-Fig.B.16, the temperature increase of the fuel element contained in the packaging is very small. Therefore, the maximum temperature for the fuel element is obtained by adding the temperature difference Δ t of the portion in the inner surface of the packaging where the temperature difference between before and after fire has the maximum value to the maximum temperature of the fuel element under the normal conditions of transport shown in (Ⅱ)-Table B.6. It is expected that the actual temperature difference is smaller than the above calculated maximum temperature difference so that the calculation is conservative.

The maximum temperature difference of the inner surface of the packaging occurs in the inside of the body, and Δ t is as follows.

Δt = [redacted] − [redacted] = [redacted]℃

So, it is assumed that the maximum temperature difference of the fuel element between before and after a fire is [redacted] ℃. Therefore, the maximum temperature of the fuel element is [redacted] ℃, adding [redacted] ℃ to the maximum temperature of the fuel element under the normal conditions of transport [redacted] ℃.

2. In case that the basket for MNU type fuel is contained (in case of containing JRR-3 MNU type fuel in the packaging)

The shape of the basket for MNU type fuel is much different from the basket for box type fuel. The heat transfer into the inner surface (side wall) of the shell from the fuel element is very small, so the heat transfer between the fuel element and the body is mainly performed through the basket bottom plate. For this reason, the heat transfer to the fuel element in case of using this basket is faster than that in case of using the basket for box type fuel.

Therefore, the maximum temperature of the fuel element, when the packaging contains JRR-3 MNU type fuel, is directly obtained by the thermal analysis.

B.6.6. Calculation of the maximum internal pressure under the accident conditions of transport

The maximum internal pressure under the accident condition is evaluated in the same way as that under the normal conditions of transport.

The case that Fuel element As are contained is described. From Equation ② of paragraph B.6.4.

$$P_2 = \frac{P_1\ V_1\ T_2}{T_1\ V_2}$$

where, P_1 : The internal pressure in sealed condition (atmospheric pressure) 0.1013 (MPa abs)

P_2 : The maximum internal pressure (MPa abs)

$V_1 = V_2$: Internal air volume in sealed condition and in the maximum temperature condition (m^3)

T_1 : The internal air temperature in sealed condition

[redacted] $+273=$ [redacted] (K)

T_1 : The internal air temperature in the maximum temperature condition [redacted] $+273=$ [redacted] (K)

$$P_2 = \frac{(0.1013) \times V_1 \times \text{[redacted]}}{\text{[redacted]}\ V_2}$$

$=$ [redacted] (MPa abs) $=$ [redacted] (MPaG)

The maximum internal pressure for JRR-3 MNU type fuel is obtained by using the same procedure. The result is shown in (Ⅱ)-Table B.8.

B.6.7. References

1) Morishima and others : Property of Material necessary to Fuel Design and Calculation Chart, JAERI-M4881.

2) M. Hasegawa : Handbook of Stainless Steel

3) Japan Mechanics Engineering Society : Materials for Heat Transfer (3rd Ed.)

4) W. H. McAdams : Heat Transmission (3rd Ed.)

5) Alcoa : Aluminum the Cryogenic Metal (1971)

6) References supplied by Brooks & Perkins Inc. (Nov. 1975)

7) Chemical Engineering Society : Chemical Engineering Handbook (4th Ed.)

8) ABAQUS / STANDARD User Manual Version 6.3, Hibbitt, Karlsson & Sorensen, Inc. in USA.

C. Containment analysis

In this analysis, the leaktightness of this package under normal and accident conditions of transport is evaluated.

C.1 Summary

In this chapter, it is confirmed that leak rates of radioactive material from this package under normal and accident conditions of transport are less than the criteria of regulations, therefore this package has enough leaktightness.

C.2 Containment system

C.2.1 Containment system

In the following paragraphs, the containment system of this packaging shall be described in the following order: components, containment system, materials, pressure, temperature, seal, and inspection.

1. Components

The lid and the body of this packaging are of integral forged components, made of stainless steel having excellent leaktightness. This packaging itself constitutes a containment vessel, without using any special inner container.

The containment boundary is shown in (Ⅱ)-Fig.C.1.

Openings at containment boundary are:

① Lid/body joint (Containment boundary : [redacted] O-ring)

② Vent valve (Containment boundary : Gasket and [redacted] O-ring)

③ Drain valve (Containment boundary : Gasket and [redacted] O-ring)

[redacted]

(Ⅱ)-Fig.C.1　Containment boundary of packaging

This means that the containment boundary is composed of the inner wall of both the body and the lid, vent penetration hole, drain penetration hole, lid/body joint, vent valve, and drain valve. The lid/body joint is composed of [redacted] O-rings and the hole for leaktightness inspection (Refer to (Ⅱ)-Fig.C.2 and (Ⅱ)-Fig.C.3). The hole for leaktightness test is closed by the plug, having an O-ring. Both valves are of the same structure, composed of [redacted] (Refer to (Ⅱ)-Fig.C.4.).

2. Containment mechanism

[redacted] sealing method is adopted for the openings at the containment boundary mentioned in the preceding section. Note that the containment boundary is located on the inner side of closing. The details of the containment system are explained as follows.

The lid/body joint is sealed by the [redacted] O-rings provided on the lid, and the [redacted] O-ring constitutes the containment boundary. These O-rings are tightened by [redacted] lid bolts. Between [redacted] O-rings, a hole for leaktightness test is provided to test the leaktightness of this sealing part. The outlet of this hole is closed by the plug having an O-ring for leaktightness inspection. (Refer to (Ⅱ)-Fig.C.2 and Fig.C.3.)

The vent valve and drain valve are of the same dimensions and structure. Since they are of mounting type, they can be replaced easily. The valve is fitted to the body with [redacted] bolts, and leaktightness of the fitting part is maintained by the [redacted] O-rings provided in the valve body. Containment boundary is constituted by the [redacted] O-ring. Between these [redacted] O-rings, a hole for leaktightness test of the valve is provided to test the leaktightness of the fitting part. The outlet of the hole is closed by the plug for leaktightness test of the valve.

[redacted]

[redacted]

(Ⅱ)-Fig.C.3　Hole of leaktightness inspection and plug

[redacted]

(Ⅱ)-Fig.C.4　Vent and drain valve

[redacted]

The containment of [redacted] leading to the interior of the packaging is consisted of [redacted] (Containment boundary).

[redacted] using special tools, [redacted], then the containment is completed.

The outlet of the through hole is closed by [redacted]. The disk part is isolated [redacted]. The leaktightness inspection of the gasket is performed by the use of [redacted].

Furthermore, the valve is protected by the protection cover having an O-ring. The details of the protection cover are described in (Ⅱ)-C.2.4.-2. (Refer to (Ⅱ)-Fig.C.4, (Ⅱ)-Fig.C.5 and (Ⅱ)-Fig.C.6.)

3. Material

The body, lid, valve, and lid bolts constituting this containment system are all made of stainless steel having sufficient corrosion resistance and mechanical strength. Thermal and mechanical properties of this stainless steel are shown in (Ⅱ)-A.3 and (Ⅱ)-A.4.2.

All the packing used in the openings forming containment boundary are [redacted] O-rings or gaskets having strong resistance against heat and cold and excellent radiation resistance. Properties of [redacted] are shown in (Ⅱ)-Fig.C.7.

4. Pressure and temperature

The pressure and temperature of this nuclear fuel package, as shown in (II)-B Thermal Analysis, will be the severest conditions under normal and accident conditions of transport when 40 fuel assemblies which have higher pressure and temperature (hereinafter referred to as fuel element A) than the fuel elements to be loaded are loaded to make the evaluation more conservative. Even under these circumstances, the integrity of the containment system is maintained. Temperature and pressure of each part having any relation to the leaktightness of this package under both conditions are shown in

(Ⅱ)-Table C.1.

5. Seals

The lid is fitted to the body by the [redacted] lid bolts ([redacted]). For transport, [redacted].

The vent and drain valves are fitted to the lid and body with [redacted] bolts ([redacted]).

To cover the valve, protection cover is fixed with [redacted] bolts. This protection cover is [redacted] during transport. [redacted]. This [redacted], and even if [redacted] has occurred, it will be known immediately.

[redacted]

(Ⅱ)-Fig.C.5　Protection cover of drain valve

[redacted]

(Ⅱ)-Fig.C.6　Protection cover of vent valve

[redacted]

[redacted]

[redacted]

[redacted]

(Ⅱ)-Fig.C.7 (Notes)　Properties of [redacted]

(Ⅱ)-Table C.1 Temperature and pressure of nuclear fuel package under each conditions of transport

Condition Item	Normal conditions of transport			Accident conditions of transport	
	In the shade	Max.	Min.	Max.	Min.
Lid/Body joint temperature(℃)	[redacted]	[redacted]	-40	[redacted]	-40
Vent valve temperature (℃)	[redacted]	[redacted]	-40	[redacted]	-40
Drain valve temperature (℃)	[redacted]	[redacted]	-40	[redacted]	-40
Fuel element temperature (℃)	[redacted]	[redacted]	-40	[redacted]	-40
Inner gas temperature (℃)	[redacted]	[redacted]	-40	[redacted]	-40
Inner gas pressure (MPaG)	[redacted]				

(Note):The maximum temperatures in the above table are obtained in the case where fuel element A are contained. In this case, the temperature of each part shows the highest value, compared with the case where other fuel elements are contained. Heat power of the fuel element is 2.25kW. Under “the lowest” evaluation condition, it shall be 0 kW.

6. Inspection

When this packaging is completed, pressure inspection and leaktightness inspection shall be conducted. And, before each shipment, leaktightness inspection shall again be conducted. All of these inspections are to confirm that leakage of radioactive materials is less than the specified value in the Technical Standards under each test condition.

C.2.2 Penetration parts of containment system

In the following sections, the penetration parts of the containment system are described in the following order: Penetration Parts, functions of Penetration Parts, and Specifications of Penetration Parts.

1. Penetration part

As shown in (Ⅱ)-Fig.C.1 describing the containment system, a penetration hole leading to the vent valve is provided in the lid and another penetration hole leading to the drain valve is provided in the body. In addition, between the [redacted] O-rings at the lid/body joint, a hole for leaktightness test is provided.

2. Functions of penetration parts

This packaging is a dry cask that does not use cooling water. Loading and unloading of fuel elements into and out of this packaging are performed in pool water. For this purpose, the vent and drain penetration holes are used for injecting and draining water. Furthermore, the drain and vent penetration holes and the hole for leaktightness test are used for leaktightness test on the containment system.

As for the sealing of these penetration holes, the drain and vent penetration holes are sealed by the gasket provided in the midst of the through hole of the valve and the outlet plug with an O-ring. The hole for leaktightness test is sealed by another plug with an O-ring.

In consideration of gamma ray streaming, the penetration parts are so constructed not to allow direct observation of the interior of the packaging from outside. Therefore, the penetration parts shall never affect the shielding property of the package. (Refer to (Ⅱ)-Fig.C.1.)

3. Specifications of penetration parts

Specifications of the penetration parts are summarized in (Ⅱ)-Table C.2. Packing is [redacted], and, as stated in (Ⅱ)-C.2.1, there is no problem in its resistance to corrosion and heat.

(Ⅱ)-Table C.2 Specifications of penetration parts

Item Position	Purpose	Shape	Main material	Material of containment part	Material of plug	Test temperature	Test pressure
Vent valve	- Venting - Leaktightness test	See (II)-Fig .C.1	Stainless steel	Stem (valve seat): Stainless steel Gasket: [redacted]	Stainless steel	Room temperature	Pressure test: > 0.98MPaG (10kgf/cm²G) Hydrostatic Leaktightness test > 0.42 MPaG Pneumatic (air, nitrogen)
Drain valve	- Draining water - Leaktightness test	See (II)-Fig .C.1	Stainless steel	Stem (valve seat): Stainless steel Gasket: [redacted]	Stainless steel		
Plug of the hole for leaktightness test	- Leaktightness test	See (II)-Fig .C.3	Stainless steel	O-ring: [redacted]	Stainless steel		

C.2.3 Gasket of containment system and welded part

In the following section, the gasket and welded part of this containment system are described.

1. Gasket

The openings of this packaging are the lid/body joint, vent valve and drain valve. These openings are closed by the gaskets described below to maintain the leaktightness of the package. Thus leaktightness under normal and accident conditions of transport is made satisfactory.

1.1 Packing for lid/body joint

The leaktightness of the lid/body joint is ensured by the [redacted] O-rings made of [redacted]. [redacted] O-rings, a hole for leaktightness test is provided. When the packaging is completed and before shipment, the leaktightness inspection is performed to check the leaktightness of the packaging.

The shape of the lid/body joint is shown in (Ⅱ)-Fig.C.2 and C.3.

The standard applicable temperature range of [redacted] (normal use) is [redacted]C～[redacted]°C, and the [redacted] used in the position shown in (Ⅱ)-Table C.1 is never deteriorated in the applicable temperature range for the O-rings (−40°C～[redacted]°C). Although the same Table shows that the inner pressure is [redacted] MPaG ～ [redacted] MPaG, leakage of radioactive material is conservatively evaluated at [redacted] MPaG of inner pressure. And the containment of packaging is also confirmed by applying a pressure test (hydrostatic) of more than 0.98 MPaG (10 kg/cm^{2}G) and a leaktightness test of pneumatic (nitrogen) pressure of more than 0.42 MPaG, respectively.

1.2 Packing for vent valve and drain valve

The shape of the valve is shown in (Ⅱ)-Fig.C.4.

The through hole leading to the penetration hole is sealed by a [redacted] gasket and stainless steel bellows; the outlet is sealed by the outlet plug having a [redacted] O-ring; and the valve housing part is sealed by [redacted] O-rings made of [redacted].

When the packaging is completed and before shipment, the leaktightness test is performed on gaskets and bellows used for sealing the through hole, by the use of the outlet, and on the fitting part between the valve and valve housing by the use of the hole of leaktightness test between the [redacted] O-rings. Thus, the leaktightness of these parts can be checked.

The applicable temperature range for the packing used in this position is −40°C～[redacted]°C under the normal condition of transport and the maximum temperature of the packing reaches [redacted]°C for a short period under the accident condition of transport, as shown in (Ⅱ)-Table C.1. There is no possibility of the packing deterioration since the standard applicable temperature range of [redacted] (normal use) is [redacted]°C～[redacted]°C. There is no problem concerning pressure, as shown in the above paragraph.

2. Welded part

The face of the gasket that is containment boundary is fabricated with clad welding. For the welding, the liquid penetrant test are performed to check for absence of harmful defect such as crack, lack of fusion, etc. at the weld.

C.2.4 Lid

1. Lid (Refer to (Ⅱ)-Fig.C.2)

The lid is a [redacted] mm thick forged stainless steel plate of integral construction. The lid is fitted to the body by [redacted] bolts ([redacted]). The tightening torque is about [redacted] N·m ([redacted] kgf·m). Thus, the lid has a sufficient strength to withstand the pressures and temperatures under normal and accident conditions of transport. Since the lid is protected with a fin from external forces, it has sufficient strength to withstand drop test and penetration test.

During transport, [redacted] of the lid bolts are [redacted], which prevents loosening and inadvertent opening of the lid.

The sealing between the lid and body is provided by [redacted] O-rings made of [redacted] The openings of the lid are vent valve and hole for leaktightness inspection. As shown in the preceding section, the vent valve has a construction that ensures the leaktightness of the valve and housing.

The hole for leaktightness inspection is closed by the plug for leaktightness inspection equipped with a [redacted] O-ring.

2. Valve protection cover (Refer to (II)-Fig.C.5 and Fig.C.6.)

   There are two valve protection covers: one for the vent valve and the other for the drain valve. Each of these valves must not be operated carelessly. In order to protect the valve from accident, the cover with a [redacted] O-ring fitted inside of it is mounted to the body by [redacted] bolts, [redacted].

   Both valve protection covers have enough strength to protect the valves under normal and accident conditions of transport. (Refer to (II)-A.6.1.1-2, A.6.1.2-2 and A.6.2-2.) The structural difference between these two valve protection covers is that the drain valve protection cover has a buffer fin whereas the vent valve protection cover has not.

C.3 Normal conditions of transport

Since the leakage of radioactive materials from this package under normal conditions of transport must be evaluated conservatively, fuel element A that has maximum thermal condition is assumed to be contained in the package.

C.3.1 Leakage of radioactive materials

The leaktightness of this package is confirmed by the leaktightness inspection that is performed when the packaging is completed and also after loading of fuel elements and before shipping of the package.

Under the normal conditions of transport, the integrity of the containment system and fuel elements is maintained. In this section, analysis is made by assuming the hypothetical radioactive concentration in the gases inside the package, in order to verify that the package which has passed the leaktightness inspection before shipment has a leakage rate which is below the allowable radioactive material leakage rate for Type B(U) package as specified in the Technical Standards.

The analysis shall be made in accordance with the following sequence.

i) Assume the hypothetical radioactive concentration in air inside the package.

ii) Determine the acceptance criteria for the leaktightness inspection before shipment.

iii) Obtain the inner air leakage rate under standard condition (0.101 MPa, 298K) in the case where the acceptance criteria are met.

iv) Confirm that the radioactive material leakage rate is below the Technical Standards.

1. Radioactive concentration in air inside the package

1.1 For research reactors (JRR-3)

As described in (Ⅱ)-A.8 Radioactive Contents, under the normal conditions of transport, the integrity of the contents of this package is not damaged, therefore there are no leakage from fuel elements.

However, the evaluation is made by assuming radioactive concentration in air inside the package as follows.

- A source-term is determined as F.P. gasses leaked from fuel elements to inside packaging.
- There is no leakage of solid radioactive material from fuel elements to inside packaging.
- The radioactive concentration C in air inside the package is determined as 3.7 Bq/cm^3.

The radioactive concentration C in air inside the package is determined as follows;

Actual measurements of concentration have been made on another package which has similar specifications, and the measuring results were less than the detection sensitivity level (0.037 Bq/cm^3 (1×10^{-6} μCi/cm^3)).*

In this analysis, the radioactive concentration C is assumed conservatively to be 100 times larger than the detection sensitivity (C = 3.7 Bq/cm^3= 3.7×10^{-6} TBq/m^3).

And the criteria A$_2$ value in this analysis is defined by the above-mentioned assumption of the source-term, as follows;

- Although the radioactive concentration in air inside the package is determined in the above-mentioned assumption of the source-term, radionuclides are not identified.
- It is assumed that F.P. gasses as radioactive material leaked from fuel elements to inside the packaging, and no leakage of solid materials. Because radioactive materials emitting alpha ray are solid, they are not considered in this analysis.

A criteria A$_2$ value applying above mentioned conditions is 2×10^{-2} TBq, which is "A$_2$ value when radionuclides are unknown and only beta or gamma emitting nuclides are known to be present.", defined by Technical Standards.

---

*) Unifetch-L package

Radioactive concentration in air inside the package measured before shipment.

Results of measurement

1) Contents : 38 pieces of JRR-2 standard fuel elements
2) Date of measurement: May 8, 1978
3) Measuring instrument: Vibrating capacitor electrometer
   [Detection sensitivity: 0.037Bq/cm^3 (1×10^{-6} μCi/cm^3)]
   No.1< 0.037 Bq/cm^3 (1×10^{-6} μCi/cm^3)
   No.2 < 0.037 Bq/cm^3 (1×10^{-6} μCi/cm^3)
4) F. P. gas was not detected by the gamma ray spectrometer. (The Unifetch-L package (J/33/B(M)F) is of dry type, and is almost the same as this package.)

2. Acceptance criteria of leaktightness inspection before shipment

As mentioned in (Ⅱ)-C.6.1 Appendix, the leaktightness inspection before shipment shall be performed on the [redacted]-sealing part of the lid/body joint, vent valve, and drain valve.

The pressurization method is applied, and the pressure of nitrogen gas is greater than 0.42 MPaG in order to measure pressure change (decline) reliably.

The pressure change in each of the [redacted]-sealing parts is measured. The acceptance criteria shall be that the pressure change (decline) is 6.08×10^{-3} MPa per hour or less.

3. Radioactive material leakage rate

In the case where the acceptance criteria stated in the preceding section is met, the inner air volumetric leakage rate L_{STD} under standard condition shall be followings as shown in the attached document (Ⅱ)-C.6.

$$L_{STD} = \text{[redacted]} \left[\frac{m^3}{s}\right]$$

as shown in the attached document (Ⅱ)-C.6. Therefore, the radioactive material leakage rate R shall be obtained by the following equation.

$$R = L_{STD} \cdot C_{STD}$$

$$= (\text{[redacted]} \times 3600) \times \text{[redacted]}$$

$$= 9.77 \times 10^{-12} \text{ (TBq/h)}$$

where, C_{STD} : Inner air radioactivity concentration under standard condition.

The comparison with the technical standard is shown in (Ⅱ)-Table C.3. The radioactive material leakage rate under this condition is below the technical standard. For this analysis, the radioactive concentration and inner pressure rise of the air inside the package are assumed conservatively. It means that the safety of this package under the normal conditions of transport is assured.

(Ⅱ)-Table C.3 Radioactive material leakage rate under the normal conditions of transport.

Concentration*1 (TBq/m^3)	Leakage rate (TBq/h)	Technical standard [$10^{-6}A_2$] (TBq/h)	Comparison with the technical standard
[redacted]	9.77×10^{-12}	[redacted]	[redacted]

*) Under standard condition

C.3.2 Pressurizing the containment system

The factors for pressurizing the containment system are:

i) Temperature rise of the coolant and radiolysis

ii) Gasification of component materials by neutron irradiation

iii) Fission product gas released from fuel element

iv) Temperature rise of the air

The discussions on the above four factors as follows:

i) Temperature rise of the coolant and radiolysis

Pressure rise caused by the coolant does not affect this package, since no special coolant such as water is used in this dry-type packaging.

ii) Gasification of component materials by neutron irradiation

Radiation damage does not occur, since this package is made of stainless steel. The quantity of neutrons in the package is very small. Therefore, the generation of radioactive gases from the component materials caused by neutron irradiation is negligible.

iii) Fission product gas released from fuel element

The meat of fuel element to be contained in this package is clad with aluminum alloy. Since fuel element does not break under normal condition of transport, no fission product gas can be released from the fuel element.

iv) Temperature rise of the air temperature

This package shall be sealed hermetically after loading fuel elements and achieving thermal equilibrium. At this time, the temperature of inner gases is [redacted] °C (which shall be the lowest temperature of inner wall of packaging) when the packaging contains fuel element A generating maximum decay heat. Under the normal condition of transport, the inner gas temperature is raised to [redacted] °C (which shall be the maximum temperature of fuel element) due to solar heat. This temperature rise results in the pressurization of [redacted] MPaG.

To sum up, the maximum inner pressure of the package shall be [redacted] MPaG when the packaging contains fuel element A.

The inner pressure of [redacted] MPaG is assumed as [redacted] MPaG so that the radioactive material leakage evaluation is made conservatively.

C.3.3 Coolant contamination

Since this package is of dry type that does not require the use of cooling water, coolant contamination does not occur.

C.3.4 Loss of coolant

Since this package is of dry type which does not require the use of cooling water, a loss of coolant does not occur.

C.4 Accident conditions of transport

1. Drop test

1.1 Vertical drop

When the package is dropped upside down vertically, the severest force from the viewpoint of the maintenance of the leaktightness of the package is applied to the lid bolts. In this case, the maximum stress of [redacted] MPa generates in the lid bolt (Refer to (Ⅱ)-A.6.1.). Since this value is within the elasticity area of bolt material, and the stresses of the lid flange and the body flange are also within the elastic condition, the leaktightness can be maintained. In addition, the stresses applied in the lid and body are below the allowable stress, which eliminates the possibility of deteriorating the leaktightness of the package.

Moreover, since fuel element does not break as a result of vertical drop (Refer to (Ⅱ)-A.6.1), no release of radioactive materials from the fuel element occurs.

1.2 Horizontal drop

In the case of horizontal drop of the package, the maximum stress of [redacted] MPa generates in the lid bolt (Refer to (Ⅱ)-A.6.1.). Since this value is within the elastic condition of bolt material, and the stresses of the lid flange and the body flange are also within the elastic condition, the leaktightness can be maintained. In addition, stresses applied on the lid and the body are less than the allowable stress, which eliminates the possibility of deteriorating the leaktightness of the package.

Moreover, since fuel element does not break as a result of horizontal drop, no release of radioactive materials from the fuel element occurs.

1.3 Corner drop

As in the case of vertical drop, the maintenance of leaktightness is more severely affected by top corner drop than by bottom corner drop.

In the case of top corner drop of the package, the maximum stress of [redacted] MPa generates in the lid bolt (Refer to (Ⅱ)-A.6.1.). Since this value is within the elastic condition of bolt material, and the stresses of the lid flange and the body flange are also within the elastic condition, the leaktightness can be maintained. Besides, The stresses applied in the lid and the body do not affect the leaktightness.

Moreover, since the fuel element does not break as a result of corner drop, no release of radioactive materials from the fuel element occurs.

1.4 Valve and valve protection cover

The drop impact energy is received by the fin, so the valves will not be affected. Even if a mild steel bar directly hits the valve protection cover, the cover is so constructed that the bar does not touch the valve. Thus, leaktightness of the package is ensured. (Refer to (Ⅱ)-A.6.1.)

1.5 Plug of the hole for leaktightness inspection

The plug of the hole for the leaktightness inspection is mounted in a position surrounded by the fin as if buried in the lid. Therefore, the plug is not removed even when the package is dropped.

2. Fire resistant test

2.1 Fuel element temperature

The maximum temperature of the fuel element during fire resistant test is [redacted] ℃. (Refer to (Ⅱ)-B.5.3.)

This temperature is sufficiently lower than the melting point of aluminum used as a cladding material ([redacted] ℃). Therefore, the cladding material does not melt, and no release of radioactive materials from the fuel element occurs.

2.2 Packing

The highest packing temperature reaches [redacted] ℃ at the vent valve, among other gaskets used in the lid and valve sealing part. O-ring and gasket are made of [redacted], of which the standard applicable temperature range (normal use) is [redacted] ℃～[redacted] ℃. Therefore, there is no possibility of the packing deterioration.

C.4.1 Fission product gas

The gas produced by nuclear fission migrates inside the fuel meat by means of diffusion. However, since the fuel meat is clad with aluminum alloy, the fission product gas cannot be released unless the fuel cladding is broken.

The following cases of fuel cladding break are considered:

(i) Drop impact breaks the fuel cladding.

(ii) The temperature rise of fuel element causes the fuel cladding to melt.

(iii) Corrosion breaks the fuel cladding.

1. Discussion and results of the case when the fuel cladding is broken due to drop impact

The fuel elements don't break in the drop tests as shown in 1. Drop test of chapter C.4 Accident conditions of transport and there is no release of fission product gas.

2. Discussion and results of case when the temperature rise of fuel element causes the fuel cladding to melt.

The maximum temperature ([redacted] ℃) of the fuel element in fire condition occurs by the loading of fuel element A which generates maximum decay heat. Since the melting point of fuel cladding (aluminum alloy) is [redacted] ℃, the fuel cladding does not melt in this condition.

In manufacturing uranium aluminum dispersion type fuel such as fuel element A and so on, the element is held at [redacted] ℃ for [redacted] and its integrity is confirmed by the blister test. According to the data concerning the temperature at which blisters are formed on irradiated fuel elements, the blister generating temperature is about [redacted] ℃～ [redacted] ℃ even for the maximum local fission density of [redacted] fiss/cm^3, which corresponds to fuel element A. This is shown in (Ⅱ)-Fig.C.8.

In manufacturing uranium silicon aluminum dispersion type fuel such as JRR-3 standard silicide type fuel and so on, the element is held at [redacted] ℃ for [redacted] and its integrity is confirmed by the blister test. According to the data concerning the temperature at which blisters are formed on irradiated fuel elements, the blister generating temperature is [redacted] ℃ even for the maximum local density of [redacted] fiss/cm^3, which corresponds to JRR-3 standard silicide type fuel. This is shown in (Ⅱ)-Fig.C.9.

Therefore, fuel cladding cannot be broken by fire and no fission product gas is released.

3. Discussion and results of case when the fuel cladding is broken due to corrosion

Fuel cladding is made of aluminum alloy (contain more than [redacted] % Al), which has corrosion resistance.

For normal transport, coolant is not used in this package, which means that the fuel elements are put in air. The corrosion of aluminum in air is shown in (Ⅱ)-Fig.C.10. The figure shows that aluminum has good corrosion resistance in both coastal and industrial areas. The fact that fuel cladding is minimum [redacted] mm thick and the consideration of the atmosphere inside the package lead us to the conclusion that there is no possibility of fuel cladding corrosion during transport, and releasing fission product gas.

[redacted]

(Ⅱ)-Fig.C.8　Blister test on uranium aluminum dispersion type alloy

Blister test: This test is to examine the condition of boundary between fuel cladding and fuel meat, which is influenced by the change of the mechanical strength of fuel materials caused by irradiation, gas generated at the boundary, temperature, etc. In order to examine the correlation of these factors, method employed is optical observation of the presence or absence of “blisters” on the fuel plate surface that is exposed at a constant temperature for a predetermined period of time.

[redacted]

(Ⅱ)-Fig.C.9　Blister test on uranium silicon aluminum dispersion type alloy

[redacted]

(Ⅱ)-Fig.C.10　Corrosion of aluminum in air

C.4.2 Leakage of radioactive materials

As described in previous section C.4.1 Fission Product Gas, under the accident conditions of transport, [redacted] is not affected, therefore there are no leakage from fuel elements. However, in this analysis, the leakage rate of radioactive materials is evaluated by employing the same method as the normal conditions of transport. As well as the case under normal conditions of transport, the radioactive concentration C in air inside the package is as follows;

$$C = 3.7 \times 10^{-6}\ (\mathrm{TBq/m^3})$$

The acceptance criteria for leaktightness inspection before shipment requires the pressure change (decline) of the [redacted] sealing part per hour to be 6.08×10^{-3} MPa or less, which is the same as under the normal conditions of transport. Accordingly, the inner air volumetric leakage rate L_{STD} under standard condition when the above acceptance criteria is met will be followings as shown in attached document (Ⅱ)-C.6.5. The inner pressure of [redacted] MPaG is assumed as [redacted] MPaG so that the radioactive material leakage evaluation is made conservatively.

$$L_{STD} = \text{[redacted]} \left[\frac{\mathrm{m^3}}{\mathrm{s}}\right]$$

Therefore, the radioactive material leakage rate R is the following equation.

$$R = L_{STD} \cdot C_{STD}$$
$$= (\text{[redacted]} \times 3600 \times 24 \times 7) \times \text{[redacted]}$$
$$= \text{[redacted]}\ (\mathrm{TBq/week})$$

where, C_{STD} : Inner air radioactivity concentration under standard condition

The comparison with the technical standard is shown in (Ⅱ)-Table C.4.

The radioactive material leakage rate under this condition is well below the technical standard, which ensures the safety of the package.

(Ⅱ)-Table C.4 Radioactive material leakage rate under the accident conditions of transport.

Concentration*1 (TBq/m^3)	Leakage rate (TBq/week)	Technical standard [A_2 value] (TBq/week)	Comparison with the technical standard
[redacted]	[redacted]	2×10^{-2}	[redacted]

*1) Under standard condition

C.5 Summary and evaluation

As shown in the results of containment analysis below, it is confirmed that the leakage rates of radioactive material from the package is lower than the criteria of the technical standard. Therefore, this package satisfies the sealing performance.

(1) Containment system

This packaging itself constitutes a containment vessel. The sealing parts are the contact part between of flange of body and lid, and three orifices. These containment systems have enough strength for drop tests and fire test under normal and accident conditions of transport, and leaktightness of gaskets is maintained.

(2) Normal conditions of transport

(i) Containment system

Ratio of radioactive material leakage rate to the criteria under normal conditions of transport is 4.88×10^{-4}, which satisfies the criteria.

(ii) Pressurizing the containment system

The package is transported in dry condition, and does not include water which causes pressure increase by radiation and heat. Internal pressure of the package is less than atmospheric pressure under routine conditions of transport, and is not pressurized to damage leaktightness.

(iii) Coolant contamination

As the package is dry type that does not require the use of cooling water, coolant contamination does not occur.

(iv) Loss of coolant

As the package is dry type that does not require the use of cooling water, a loss of coolant does not occur.

(3) Accident conditions of transport

Ratio of radioactive material leakage rate to the criteria under accident conditions of transport is 6.77×10^{-8}, which satisfies the criteria.

C.6 Appendix

In this section, the following items are described.

C.6.1 Appendix-1 Method and acceptance criteria of leakage rate measurement inspection before shipment

The leakage rate measurement inspection before shipment is performed on O-rings and gaskets fitted to the lid/body joint, drain valve and vent valve. The pressure change method is employed.

First, increase of inner pressure caused by the temperature rise of inner gases due to decay heat is released into the atmosphere, and then the vent valve is closed. Then, it is confirmed that the drain valve is closed and the lid bolts are tightened with prescribed torque.

Under this condition, each [redacted] sealing part is pressurized with nitrogen gas to 0.42 MPaG (4.2 kgf/cm^{2}G) or over. The change in pressure in the [redacted] sealing part is measured. If the pressure decrease is 6.08×10^{-3} MPa per hour or less, it is considered acceptable.

C.6.2 Appendix-2 Inner air volumetric leakage rate at inspection before shipment

The leakage rate measured by the pressure change method in the leakage rate measurement inspection using compression gas can be expressed as follows[11]. Units in following equation are in accordance with the description in reference.

$$L_R = \frac{VT_s}{3600HP_s}\left|\frac{P_1}{T_1}-\frac{P_2}{T_2}\right| \cdots\cdots\cdots ①$$

where, L_R : Gas volumetric leakage rate measured during leaktightness testing (ref·m^3/s)

H : Test time (hr)

V : Volume of pressure change measuring part (m^3)

P_s : Standard pressure : 0.101 MPa

P_1 : Gas pressure at start of test (MPa)

P_2 : Gas pressure at end of test (MPa)

T_s : Standard temperature : 298K

T_1 : Temperature at start of test (K)

T_2 : Temperature at end of test (K)

It is considered that the package is in standard state, and T_1 and T_2 equal to T_s at inspection before shipment. Therefore, equation ① is expressed as follows;

$$L_R = \frac{V}{3600 \times H \times P_s}\,|P_1 - P_2| \cdots\cdots\cdots ②$$

C.6.3 Appendix-3 Leakage hole diameter of the containment system

Leakage hole diameter of the containment system is derived from the following equations based on the maximum permissible leakage rate (It is calculated by the maximum pressure drop at a leakage test before shipment). Because the containment of the package is maintained under normal conditions of transport, gas leakage rate corresponding to the criteria of leakage test before shipment is maintained.

$$La = (Fc + Fm)(Pu - Pd) \cdots\cdots\cdots\cdots\cdots\cdots\cdots\cdots \text{③}$$

where, La : leakage rate referred to average pressure (m^3/s)

$$Pa = \frac{1}{2}(Pu + Pd) \qquad \text{④}$$

Pu : Fluid upstream pressure (MPa)

Pd : Fluid downstream pressure (MPa)

Fc : Coefficient of laminar flow conductance per unit pressure ($m^3/ MPa \cdot s$)

$$Fc = \frac{\pi}{128}\,\frac{D^4}{a\,\mu} \qquad \text{⑤}$$

Fm : Coefficient of free molecular flow conductance per unit pressure (m^3/MPa)

$$Fm = \frac{\sqrt{2\pi R}}{6} \times \frac{D^3\sqrt{\frac{T}{M}}}{a \cdot P_a} \cdots\cdots\cdots\cdots\cdots\cdots \text{⑥}$$

where, D : Leakage hole diameter (m)

a : Leakage hole length (m)

μ: Fluid viscosity (MPa s)

T : Fluid absolute temperature (K)

M : Fluid molecular weight (kg/mol)

La is derived from the following equation.

$$La = L_R \times \frac{Ps}{Pa} \times \frac{Ta}{Ts} \cdots\cdots\cdots\cdots\cdots\cdots\cdots\cdots \text{⑦}$$

where, L_R : leakage rate referred to average pressure (ref m^3/s)

Ps : Standard pressure : 0.101 MPa)

Ts : standard temperature : 298 K

C.6.4 Appendix-4 Inner air volumetric leakage rate under normal conditions of transport

Because the containment of the package is maintained under normal conditions of transport, gas leakage rate corresponding to the criteria of leakage rate measurement inspection before shipment is maintained.

Therefore, inner air volumetric leakage rate under normal conditions of transport is evaluated by using the leakage hole diameter estimated in C.6.3, and pressure and temperature conditions under normal conditions of transport.

Following procedure is described in Reference 11): At first leakage hole diameter shall be calculated by equation ③ under the condition whose volumetric leakage rate is known, and then volumetric leakage rate shall be calculated by the same leakage hole under the required condition.

Since volumetric same leakage rate L_R of the leakage rate measurement inspection before shipment is known, leakage hole diameter shall be calculated by applying the values of the inspection before shipment and assuming $La = L_R$ in equation ③. Then, inner gas volumetric leakage rate under normal conditions of transport shall be obtained by using the calculated leakage hole diameter D and values under normal conditions of transport into the equation ③.

The results thus obtained are summarized in (Ⅱ)-Table C-Appendix 4.1.

(Ⅱ)-Table C-Appendix 4.1 Inner air leakage rate of package under the normal conditions of transport

Conditions	Items		Values
Leakage rate measurement inspection before shipment	H : Test time	(hr)	1
	V : Volume of pressure change measuring part	(m^3)	[redacted]
	$\lvert P_1\text{-}P_2 \rvert$: Pressure change during test	(MPa)	[redacted]
	L_R : Gas leakage rate at the test	($\frac{ref \cdot m^3}{s}$)	[redacted]
	a : Leakage hole length	(m)	[redacted]
	μ : Fluid viscosity	(MPa·s)	1.78×10^{-11}
	T : Fluid absolute temperature	(K)	298
	M : Fluid molecular weight	(kg/mol)	[redacted]
	Pu : Fluid upstream pressure(inner pressure)	(MPa)	[redacted]
	Pd : Fluid downstream pressure(external pressure)	(MPa)	[redacted]
	Pa : Fluid average pressure	(MPa)	[redacted]
	D : Leakage hole diameter	(m)	[redacted]
Normal conditions of transport	μ : Fluid viscosity	(MPa·s)	[redacted]
	T : Leakage gas temperature	(K)	[redacted]
	M : Leakage gas molecular weight	(kg/mol)	[redacted]
	Pu : Fluid upstream pressure	(MPa)	[redacted]
	Pd : Fluid downstream pressure	(MPa)	[redacted]
	Pa : Fluid average pressure	(MPa)	[redacted]
	La : Average volumetric leakage rate	(m^3/s)	[redacted]
	L_{STD} :Leakage rate under standard condition	(m^3/s)	[redacted]

C.6.5 Appendix-5 Inner air leakage rate under accident conditions of transport

Because the containment of the package is maintained under accident conditions of transport, gas leakage rate corresponding to the criteria of the leakage rate measurement inspection before shipment is maintained.

Therefore, inner air volumetric leakage rate under accident conditions of transport is evaluated by assuming that sealing parts have a leak hole which gives equivalent volumetric leakage rate to the criteria of leakage rate measurement inspection before shipment.

Since volumetric leakage rate L_R of the leaktightness test at inspection before shipment is known, leakage hole diameter shall be calculated by applying the values of inspection before shipment and assuming $La = L_R$ in equation ③. Then, inner gas volumetric leakage rate under accident conditions of transport shall be obtained by substituting calculated leakage hole diameter D and values under accident conditions of transport into the equation ③.

The results thus obtained are summarized in (II)-Table C-Appendix 5.1.

(Ⅱ)-Table C-Appendix 5.1 Inner air leakage rate of package under the accident conditions of transport

Conditions	Items		Values
Leakage rate measurement inspection before shipment	D : Leakage hole diameter	(m)	[redacted]
	a : Leakage hole length	(m)	[redacted]
Accident conditions of transport	μ : Fluid viscosity	(MPa·s)	[redacted]
	T : Leakage gas temperature	(K)	[redacted]
	M : Leakage gas molecular weight	(kg/mol)	[redacted]
	Pu : Fluid upstream pressure	(MPa)	[redacted]
	Pd : Fluid downstream pressure	(MPa)	[redacted]
	Pa : Fluid average pressure	(MPa)	[redacted]
	La : Average volumetric leakage rate	(m^3/s)	[redacted]
	L_{STD} :Upstream volumetric leakage rate	(m^3/s)	[redacted]

C.6.6 Appendix-6 References

1) “Valqua Review” Vol. 23 No. 10, Nippon Valqua Industries, Ltd.

2) “Valqua Review” Vol. 15 No. 10, Nippon Valqua Industries, Ltd.

3) J.M. Beeston, et al.:”Development and Irradiation performance of Uranium Alminide Fuels in Test Reactors”, Nucl.Technol., Vol.49, (June, 1980)

4) J.L.Snelgrove : “RERTR Program Progress in Qualifying Reduced Enrichment Fuels” RERTR meeting (1982)

5) J.L.Snelgrove, et al.: “Fuel Development Activities of the U.S.Program”, RERTR Meeting (1983)

6) G.L.Copeland,et al. : “Performance of Low-Enriched U3Si2-Aluminium Dispersion Fuels Elements in The Oak Ridge Research Reactor.” ,ANL/RERTR/TM-10,(1987)

7) W.Krug,et al. : “Final Results of Test-Irradiations with LEU-Plates at KFA Julich.”,RERTR Meeting,(1986)

8) H.Sakai,rt al. : “Post-Irradiation experiments of LEU Miniplates in the JMTR”, RERTR Meeting,(1986)

9) J.L.Snelgrove,et ai. :RERTR Program fuel testing and Demonstration an Update.”,ANL/RERTR/TM-6,(1984)

10) Aluminum Handbook (1963 edition) Light Metal Association

11) ANSI N14.5-1997 American National Standard for Radioactive Materials-Leakage Tests on Packages for Shipment

D. Shielding analysis

In this analysis, the shielding performance of the package is evaluated under routine, normal and accident conditions of transport.

D.1 Summary

The shielding material used in the package, the analytical standard and the influence on the shielding performance under the normal and the accident conditions of transport is shown as follows.

(1) Shielding materials

The shielding components for gamma rays and neutron released from the fuel elements in the packaging are provided mainly by its stainless steel of the body and the lid. The thickness of the body is [redacted]cm in the radial direction and [redacted]cm in the bottom direction. The thickness of the lid is [redacted]cm. Also, there is the shield effect due to the basket frame and the basket bottom plate made of stainless steel and the structural materials of the fuel meat and the fuel cladding.

The analytical models are nearly the same as the actual configurations except the following items.

- In the source region, the fuel meats, the fuel claddings, the structural materials of fuels and the structural materials of the basket are homogenized.
- The surface of the package is also assumed to be free from any fin.

(2) Standard

The analytical standards of shielding analysis under the normal and accident conditions of transport are as follows;

a. Dose equivalent rate shall not exceed 2.0 mSv/hr at any external surface of the package and 100 μSv/hr at a point of 1 m from its surface during normal conditions of transport.

b. Dose equivalent rate at any external surface of the package shall not increase remarkably, and shall not exceed 2.0 mSv/hr under the normal conditions of transport.

c. Dose equivalent rate shall not exceed 10.0 mSv/hr at a point of 1 m from the surface of the package under the accident conditions of transport.

(3) Influences of normal or accident conditions of transport on shielding analysis

According to the structural and thermal analysis, the damage or deformation of the package by the drop test under the normal and accident conditions of transport are limited to local deformation of the fins.

Even in the thermal test, no shielding material melts.

Since the surface of the packaging is assumed to be free from any fin in the analytical model, there is no reduction in the thickness of shield, even if there is deformation of fins.

Accordingly, the dose equivalent rate under the normal and accident conditions of transport is the same as that of routine conditions of transport.

(4) Shielding calculation

The source intensity of gamma ray and neutron emitted from the spent fuel elements is calculated by using the ORNL isotope generation and depletion code ORIGEN 1) or ORIGEN-JR 2). In addition, the neutron source intensity used in the analysis is evaluated by considering the effective multiplication coefficient (keff).

The secondary gamma ray induced by neutron is evaluated at the same time. The gamma shielding calculation is performed by using the point kernel code QAD-CGGP2R 3) and analytical method for gamma streaming calculation.

The neutron shielding calculation is performed by using two dimensional discrete ordinates transport code DOT3.5 4).

The calculation of each basket is performed with the fuel element which has the maximum source intensity.

(5) Calculation results

As the results of the shielding analysis, it can be concluded that the shielding performance of the package meets the criteria specified in the regulation under all conditions.

D.2 Source specifications

Three kinds of the fuel elements are contained in the packaging. The burnup, the power density and the cooling time of each fuel element are shown in (II)-Table D.1.

The specifications of the fuel element used for the shielding analysis are shown in (II)-Table D.2. In addition, in order to make the shielding analysis more conservative, the evaluation was performed assuming the case where the fuel elements with a higher source intensity (hereinafter referred to as fuel element B) than the fuel elements to be loaded are loaded. The values in the table are given, referring to the JAERI report 5), etc. The gamma ray and neutron source intensities are calculated by using ORIGEN code or ORIGEN-JR code.

The operation conditions assumed in the analysis, the cooling time and the number of fuel elements contained into the packaging are as follows;

○ In the JRR-3 (standard silicide type fuel and follower silicide type fuel), one cycle of operation time is 35 days (26 day of operation and 9 days of shutdown).
The packaging can contain 40 fuel elements of after burnup of 11 cycles at the maximum power 24.62MW. The cooling time is [redacted] days.

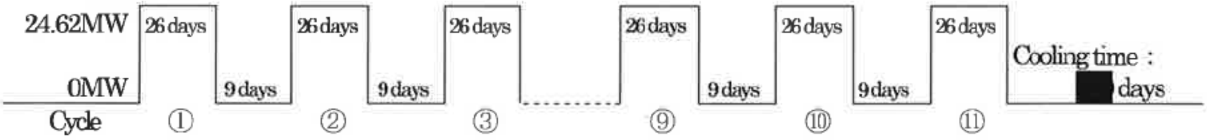

○ In the JRR-3 (MNU type fuel), one cycle of operation time is 21 days (12 days of operation and 9 days of shutdown). The packaging can contain 160 fuel elements of after burnup of 26 operation cycles at the maximum power 24.78MW. In the calculation, the 9-day shutdown period per one operation cycle is ignored. In other words, the calculation is performed with the assumption of continuous operation equal to 26 operation cycles, or 312 days (12 [day/cycle] × 26 [cycle]= 312 [days]). The cooling time is [redacted] years ([redacted] days) in all.

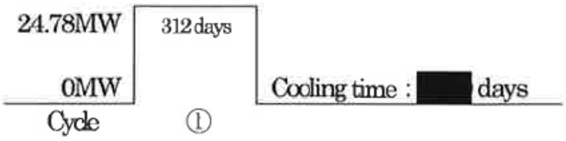

○ In the Fuel element B, the one cycle of operation time is 7 days (operation of 7 hours a day from Tuesday till Friday), and 42 cycles in a year. In the calculation, the one cycle of operation period is assumed to be 365 days (49 days of operation, 316 days of shutdown) by collecting the portion of 42 cycles. The packaging can contain 40 fuel elements of after burnup of 8 cycles at the maximum power 4.7355MW. The minimum cooling time is [redacted] days.

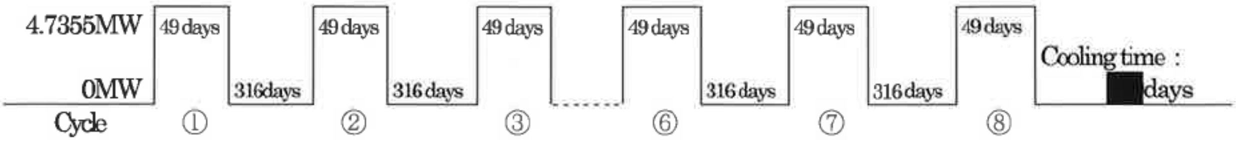

Since it is assumed that all fuel elements are irradiated at the maximum output position, the source intensity is evaluated conservatively.

Each fuel element is in the designated basket. For the basket to be used for containing two or three kinds of fuel elements, the calculation is performed with the fuel element which has the largest source intensity.

(Ⅱ)-Table D.1 Specification of fuel elements contained in the packaging

Basket	Box type	Box type (with Adapter)	MNU type
Reactor	JRR-3	JRR-3	JRR-3
Fuel element	Standard silicide type	Follower silicide type	MNU type
Total mass of ^{235}U (g/piece) 1)	[redacted]	[redacted]	[redacted]
Total mass of U (g/piece) 1)	[redacted]	[redacted]	[redacted]
Initial enrichment (%) 1)	[redacted]	[redacted]	[redacted]
Burnup (%) 2)	[redacted]	[redacted]	[redacted]
Cooling time(day) and Number of fuel elements (piece)	[redacted]	[redacted]	[redacted]

1) The value in the nuclear specification shows the upper limit that contains fabrication tolerance.

2) Burn up (%) = ((All depletion weight of ^{235}U)÷(Initial weight of ^{235}U))×100

(II)-Table D.2 Specification of fuel elements used in the shielding analysis

Basket			Box type	Box type (wi	MNU type	Box type
Reactor			JRR-3	JRR-3	JRR-3	—
Fuel element			Standard silicide type	Follower silicide type	MNU type	Fuel element B for evaluation
Fuel elements	Type		Plate fuel	Plate fuel	Rod fuel	Plate fuel
	Enrichment of ^{235}U (%)		[redacted]	[redacted]	[redacted]	[redacted]
	Mass of ^{235}U (g/piece)		[redacted]	[redacted]	[redacted]	[redacted]
	Mass of U (g/piece)		[redacted]	[redacted]	[redacted]	[redacted]
Core characteristics	Power (MW)		20	20	10	3.5
	Number of fuel elements (piece)		26 (standard type)+6 (follower type)	26 (standard type)+6 (follower type)	738	20
	Total mass of ^{235}U (g/core)		[redacted]	[redacted]	[redacted]	[redacted]
	Total mass of U (g/core)		[redacted]	[redacted]	[redacted]	[redacted]
	Maximum power (MW)		24.62	24.62	24.78	8
Operational characteristics	Irradiation cycle		11	11	1	49
	1 cycle	Days of operation (day)	26	26	312	316
		Days of shutdown (day)	9	9	0	0.852
	Neutron flux ratio	THERM	[redacted]	[redacted]	[redacted]	[redacted]
		RES	[redacted]	[redacted]	[redacted]	[redacted]
		FAST	[redacted]	[redacted]	[redacted]	[redacted]
Number of fuel elements (piece)			40	40	160	
Cooling time			〔[redacted] days cooling〕 ×40 (pieces)	〔[redacted] days cooling〕 ×40 (pieces)	〔[redacted] days cooling〕 ×160 (pieces)	〔[redacted] days cooling〕 ×40 (pieces)

D.2.1 Gamma source

The gamma source intensity is calculated by using ORIGEN code or ORIGEN-JR code together with the data such as irradiation, cooling condition, etc. shown in (Ⅱ)-Table D.2. The gamma source intensities per package are shown as a function of energy of gamma ray in (Ⅱ)-Table D.3.

Since the main nuclides and the radioactivity are a great kind because of the spent fuel being contained, those are not shown here.

ORIGEN code is the ORNL isotope generation and depletion code and one of the most effective means of evaluating gamma and neutron source of spent fuels. ORIGEN-JR code was developed on the basis of ORIGEN for calculating radiation sources of spent fuel cask and fuel reprocessing plant by Japan Atomic Energy Research Institute.

(II)-Table D.3 Gamma source intensity

(Unit : photons/sec/package)

Basket			Box type	Box type(with Adapter)	MNU type	Box type
Number of fuel elements (piece/package)			40	40	160	40
Reactor			JRR-3	JRR-3	JRR-3	—
Gamma group No.	Mean energy (MeV)	Energy range (MeV)	Standard silicide type	Follower silicide type	MNU type	Fuel element B for evaluation
1	[redacted]	[redacted]	[redacted]	[redacted]	[redacted]	[redacted]
2	[redacted]	[redacted]	[redacted]	[redacted]	[redacted]	[redacted]
3	[redacted]	[redacted]	[redacted]	[redacted]	[redacted]	[redacted]
4	[redacted]	[redacted]	[redacted]	[redacted]	[redacted]	[redacted]
5	[redacted]	[redacted]	[redacted]	[redacted]	[redacted]	[redacted]
6	[redacted]	[redacted]	[redacted]	[redacted]	[redacted]	[redacted]
7	[redacted]	[redacted]	[redacted]	[redacted]	[redacted]	[redacted]
8	[redacted]	[redacted]	[redacted]	[redacted]	[redacted]	[redacted]
Total		(photons/sec)	[redacted]	[redacted]	[redacted]	[redacted]
		(MeV/sec)	[redacted]	[redacted]	[redacted]	[redacted]
Length of source (cm)			[redacted]	[redacted]	[redacted]	[redacted]
Source intensity per unit length		(photons/sec/cm)	[redacted]	[redacted]	[redacted]	[redacted]
		(MeV/sec/cm)	[redacted]	[redacted]	[redacted]	[redacted]

D.2.2 Neutron source

Neutrons are generated by the reaction of spontaneous fission of transuranic elements which are made at burning in the nuclear reactor and (α,n) reaction for light elements in the fuels.

The neutron yields which are generated from the spontaneous fission are obtained by inputting the irradiation condition and the cooling condition shown in (II)-Table D.2 in ORIGEN code or ORIGEN-JR code in the same way as the gamma source intensity.

The neutron yields which are generated from the (α,n) reaction for the light elements in the fuels are obtained by means of the method shown in paragraph (II).D-6.1 of the appendix.

The effective multiplication coefficients obtained in the criticality analysis of chapter (II)-E for the neutrons due to the spontaneous fission and the (α,n) reaction respectively are taken into account for the evaluation of the neutron source intensity.

The effective multiplication coefficient used here is the value of routine conditions of transport obtained by criticality analysis code KENO-Va.

Neutron source intensities per package of each fuel element are shown in (II)-Table D.4.

The neutron source spectrum is derived from DLC-23 6). The spectrum is divided into 22 groups as shown in (II)-Table D.5.

(II)-Table D.4 Neutron source intensity

(Unit : neutron/sec/package)

Basket		Box type	Box type(with Adapter)	MNU type	Box type
Number of fuel elements (piece/package)		40	40	160	40
Reactor		JRR-3	JRR-3	JRR-3	—
Fuel element		Standard silicide type	Follower silicide type	MNU type	Fuel element B for evaluation
Neutron due to spontaneous fission	[redacted]	[redacted]	[redacted]	[redacted]	[redacted]
	Total	[redacted]	[redacted]	[redacted]	[redacted]
Neutron due to (α,n) reaction		[redacted]	[redacted]	[redacted]	[redacted]
Total neutron source So		[redacted]	[redacted]	[redacted]	[redacted]
Effective multiplication coefficient keff		0.176	0.124	0.234	0.101
Neutron source used in analysis So / (1-keff)		[redacted]	[redacted]	[redacted]	[redacted]
Length of source (cm)		[redacted]	[redacted]	[redacted]	[redacted]
Source intensity per unit length (neutron/sec/cm)		[redacted]	[redacted]	[redacted]	[redacted]

(Ⅱ)-Table D.5　Neutron source spectrum

Group No.	Energy range (eV)	Source Spectrum (n/sec)
1	[redacted]	[redacted]
2	[redacted]	[redacted]
3	[redacted]	[redacted]
4	[redacted]	[redacted]
5	[redacted]	[redacted]
6	[redacted]	[redacted]
7	[redacted]	[redacted]
8	[redacted]	[redacted]
9	[redacted]	[redacted]
10	[redacted]	[redacted]
11	[redacted]	[redacted]
12	[redacted]	[redacted]
13	[redacted]	[redacted]
14	[redacted]	[redacted]
15	[redacted]	[redacted]
16	[redacted]	[redacted]
17	[redacted]	[redacted]
18	[redacted]	[redacted]
19	[redacted]	[redacted]
20	[redacted]	[redacted]
21	[redacted]	[redacted]
22	[redacted]	[redacted]

D.3 Model specifications

D.3.1 Analytical model

This analytical model is prepared for the routine conditions of transport, and remains the same model even under normal or accident conditions of transport. This is because the package has no deformation which may cause the problem from the view point of shielding performance even under both normal and accident conditions of transport.

The gamma streaming calculation is described in (Ⅱ)-D.6.2 of the appendix.

(1) Basket for box type fuel

This basket can be loaded with 2 kinds of fuel elements.

For the gamma shielding calculation, JRR-3 standard silicide type fuel is used in the analysis because it has the maximum gamma source intensity per unit length.

And for the neutron shielding analysis, in order to make the evaluation more conservative, the case will be studied where the fuel element Bs, which are assumed to have a higher neutron source intensity per unit length than the contents, are loaded.

The fins arranged on the surface of the packaging are ignored and regarded as air, and the surface of the body is assumed to the surface of the packaging.

The following describes the analytical model for gamma shielding and neutron shielding respectively.

○ Analytical model of gamma shielding

The analytical model for gamma shielding is shown in (Ⅱ)-Fig.D.1.

The region of the fuel meat part is complicated. In this analysis, this region is treated as homogeneous region. Namely, the region of the fuel meat part, i.e. the fuel meat, the fuel cladding aluminum and the basket structural material made of stainless steel, is treated as homogeneous region by maintaining volumetrically the materials. In this region, the neutron absorber is ignored.

It is also assumed that the space at the lower part of the basket where no fuel meat is filled, the space provided with water drain groove at the bottom of the basket and the space between at the bottom of the basket and the body are all filled with air.

This assumption is conservative, as air provides the smaller shielding effect than the materials in such region.

The cavity length of the package is conservatively assumed as the same with fuel length.

○ Analytical model of neutron shielding

The analytical model for neutron shielding is treated as axisymmetric models as shown in (II)-Fig.D.2.

In the radial direction model, source region is assumed to be a cylindrical region circumscribed to the 40 basket lodgements. The composition of source region is determined by homogenizing volumetrically the fuel meat, the fuel cladding aluminum, the structural materials of fuels and the basket structural material made of stainless steel in the cylindrical region. The neutron poison is ignored.

Air region between the body and the basket are ignored in the model. The region of the lower or upper parts of the basket where no fuel meat exists, the region with water drain groove of the bottom of the basket and the space between the bottom of the basket and the body are assumed to be all filled with air. This assumption is conservative as air provides the smaller shielding effect than the materials in such region.

The cavity length of the package is conservatively assumed as the same with fuel length.

(2) Basket for MNU type fuel

This basket can be loaded with JRR-3 MNU type fuel. The gamma and neutron shielding analysis with these fuels is performed.

The fins arranged on the surface of the packaging are ignored and regarded as air, and the surface of the body is assumed to the surface of the packaging.

○ Analytical model of gamma shielding

The analytical model for gamma shielding is shown in (II)-Fig.D.3.

In this analysis, the source region is treated as homogeneous region. Namely, the region of the fuel meat, the fuel cladding aluminum and the basket structural material made of stainless steel is treated as homogeneous region by maintaining volumetrically the materials.

It is also assumed that the space at the lower part of the basket where no fuel meat is filled, the space provided with water drain groove at the bottom of the basket and the space between the bottom of the basket and the packaging body are all filled with air. This assumption is conservative, as air provides the smaller shielding effect than the materials in such region.

The cavity length of the package is conservatively assumed as the same with fuel length.

○ Analytical model of neutron shielding

The analytical model for neutron shielding is treated as a axisymmetric models as shown in (II)-Fig.D.4.

In the radial direction model, source region is assumed to be a cylindrical region circumscribed to the 160 basket lodgements. The composition of source region is determined by homogenizing volumetrically the fuel meat, the fuel cladding aluminum and the basket structural material made of stainless steel in the cylindrical region.

The region of the lower or upper parts of the basket where no fuel meat exists, the region with water drain groove of the bottom of the basket and the space between the bottom of the basket and the body are assumed to be all filled with air. This assumption is conservative as air provides the smaller shielding effect than the materials in such region.

The cavity length of the package is conservatively assumed as the same with fuel length.

[redacted]

(Ⅱ)-Fig.D.1 Gamma shielding analytical model with basket for box type fuel

(In case of containing JRR-3 standard silicide type fuel)

[redacted]

(II)-Fig.D.2 Neutron shielding analytical model with basket for box type fuel

(In case of containing fuel element B)

[redacted]

(Ⅱ)-Fig.D.3 Gamma shielding analytical model with basket for MNU type fuel

(In case of containing JRR-3 MNU type fuel)

[redacted]

(Ⅱ)-Fig.D.4　Neutron shielding analytical model with basket for MNU type fuel

(In case of containing JRR-3 MNU type fuel)

D.3.2 Atomic number density in each region of shielding analytical model

The volume ratio of materials in source region used for the analysis of gamma shielding is shown in (II)-Table D.6. The regional density of the analytical model is shown in (II)-Table D.7. The volume ratio of materials in source region and the atomic number densities in each region used in the neutron analysis are shown in (II)-Table D.8 and (II)-Table D.9, respectively.

The material density is shown in (II)-Table D.10.

The stainless steel is assumed to be [redacted]

These values are of the routine conditions of transport.

Since no deformation having problem in shielding performance under normal and accident conditions of transport occurs, these values are applied under these conditions. Besides, these values are at normal temperature, however, the change of density due to temperature change is very small and total mass of the package is always same and therefore the influence of temperature is ignored.

---

*) · This assumption that the density of stainless steel is [redacted]

· [redacted] these elements are ignored in the shielding analysis.

(II)-Table D.6 Volume ratio of materials in source region used in gamma shielding analysis

Basket Material	Box type	MNU type
Metallic natural uranium	—	1.82×10^{-1}
U_3Si_2	3.23×10^{-2}	—
Aluminum	2.48×10^{-1}	6.28×10^{-2}
Stainless steel	1.60×10^{-1}	9.88×10^{-2}
The others (Vacuum part)	5.60×10^{-1}	6.57×10^{-1}

(II)-Table D.7 Element density of each region used in gamma shielding analysis

(Unit : g/cm^3)

Basket Element		Box type	MNU type
Source region *)	[redacted]	[redacted]	[redacted]
Stainless steel	[redacted]	[redacted]	[redacted]
Air	N	9.27×10^{-4}	9.27×10^{-4}
	O	2.78×10^{-4}	2.78×10^{-4}

*) It is assumed that the air and the neutron poison in the source region are ignored and are vacuum condition.

(II)-Table D.8 Volume ratio of materials in source region used in gamma shielding analysis

Basket Material	Box type	MNU type
Metallic natural uranium	—	1.82×10^{-1}
U_3Si_2	1.40×10^{-2}	—
Aluminum	1.73×10^{-1}	6.28×10^{-2}
Stainless steel	3.30×10^{-1}	9.88×10^{-2}
The others (Vacuum part)	4.83×10^{-1}	6.57×10^{-1}

(II)-Table D.9 Atomic number density in each region used in neutron shielding analysis

(Unit : atoms/barn・cm)

Element \ Basket		Box type	MNU type
Source region *)	[redacted]	[redacted]	[redacted]
Stainless steel	[redacted]	[redacted]	[redacted]
Air	N	3.98×10-5	3.98×10-5
	O	1.05×10-5	1.05×10-5

*) It is assumed that the air and the neutron poison in the source region are ignored and are vacuum condition.

(II)-Table D.10 Density of materials used in shielding analysis

Material		Density (g/cm³)	
U_3Si_2		[redacted]	
Aluminum (Aℓ)		[redacted]	
Stainless steel	[redacted]	[redacted]	
Air	N O	1.21×10-3	9.27×10-4 2.78×10-4

D.4 Evaluation of shielding

(1) Evaluation of gamma shielding

The QAD-CGGP2R code was used for gamma shielding analysis.

QAD-CGGP2R code is a gamma shielding calculation code by means of point attenuation kernel method. The characteristic of QAD-CGGP2R code is that three dimensional shape can be treated.

There nuclear data used for the analysis are in the library of QAD-CGGP2R code. The air absorbed dose equivalent rate per gamma flux was obtained from ICRP Publ.74 7). These are shown in (II)-Table D.11.

The dose equivalent rates in various directions of the package are shown in (II)-Fig.D.5 through (II) -Fig.D.7.

The evaluation of gamma streaming is described in (II)-D.6.2 of the appendix.

(Ⅱ)-Table D.11 Conversion coefficient of unit gamma flux into air absorbed dose equivalent rate

Energy group	Mean energy (MeV)	Air absorbed dose per fluence	Effective multiplication coefficient (Fe) of air absorbed dose into gamma
1	[redacted]	[redacted]	[redacted]
2	[redacted]	[redacted]	[redacted]
3	[redacted]	[redacted]	[redacted]
4	[redacted]	[redacted]	[redacted]
5	[redacted]	[redacted]	[redacted]
6	[redacted]	[redacted]	[redacted]
7	[redacted]	[redacted]	[redacted]
8	[redacted]	[redacted]	[redacted]

[redacted]

(Ⅱ)-Fig.D.5　Gamma dose equivalent rate [Basket for box type fuel (Axial direction)]

(In case of containing JRR-3 standard silicide type fuel)

[redacted]

(Ⅱ)-Fig.D.6　Gamma dose equivalent rate [Basket for box type fuel (Radial direction)]

(In case of containing JRR-3 standard silicide type fuel)

[redacted]

(II)-Fig.D.7　Gamma dose equivalent rate [Basket for MNU type fuel (Axial direction)]

(In case of containing JRR-3 MNU type fuel)

(2) Evaluation of neutron shielding

DOT3.5 code was used for neutron shielding analysis. DOT3.5 code is two dimensional multi-group discrete ordinates transport code.

The neutron cross-section data used in the analysis are derived from DLC-23 cask library which has been widely used for neutron shielding analysis of packages in Japan. Also the conversion coefficient of neutron dose equivalent rate is shown in (II)-Table D.12. The conversion coefficient was obtained by interpolating the valves specified in ICRP Publ.74.

The neutron scattering is expressed with P_3S_8 approximation, and the space mesh in each region is taken smaller than the mean free path.

The dose equivalent rate in various directions of the package are shown in (II)-Fig.D.8 and (II)-Fig.D.9. These values were obtained by taking the effective multiplication coefficient obtained from (II)-E Criticality analysis.

The influence of secondary gamma rays upon the dose equivalent rate is extremely small enough to be ignored.

(II)-Table D.12 Conversion coefficient of neutron dose equivalent rate

Energy group	Upper limit energy (eV)	Conversion coefficient of dose equivalent rate (μSv/h) / (n/cm²·sec)
1	[redacted]	[redacted]
2	[redacted]	[redacted]
3	[redacted]	[redacted]
4	[redacted]	[redacted]
5	[redacted]	[redacted]
6	[redacted]	[redacted]
7	[redacted]	[redacted]
8	[redacted]	[redacted]
9	[redacted]	[redacted]
10	[redacted]	[redacted]
11	[redacted]	[redacted]
12	[redacted]	[redacted]
13	[redacted]	[redacted]
14	[redacted]	[redacted]
15	[redacted]	[redacted]
16	[redacted]	[redacted]
17	[redacted]	[redacted]
18	[redacted]	[redacted]
19	[redacted]	[redacted]
20	[redacted]	[redacted]
21	[redacted]	[redacted]
22	[redacted]	[redacted]

[redacted]

(Ⅱ)-Fig.D.8　Neutron dose equivalent rate [Basket for box type fuel (Axial direction)]
(In case of containing fuel element B)

[redacted]

(II)-Fig.D.9 Neutron dose equivalent rate [Basket for MNU type fuel (Axial direction)]

(In case of containing JRR-3 MNU type fuel)

D.5 Summary of the results and the evaluation

D.5.1 Characteristic of the shielding design

The shielding components for gamma rays and neutron released from the fuel elements in the packaging are provided mainly by its stainless steel of the body and the lid. The thickness of the body is [redacted]m in the radial direction and [redacted]cm in the bottom direction. The thickness of the lid is [redacted]cm.

Also, there is the shield effect due to the basket frame and the basket bottom plate made of stainless steel and the structural materials of the fuel meat and the fuel cladding.

D.5.2 Results and evaluation

The results are shown in (II)-Table D.13 and (II)-Table D.14 for each basket.

The maximum gamma dose equivalent rate of the nuclear fuel package occurs when JRR-3 standard silicide type fuels which has the maximum source intensity per unit length are contained in the basket for box type fuel.

The maximum neutron dose equivalent rate occurs when fuel element B which has the maximum source intensity per unit length. Even considered the summation of these maximum values, as shown below, this package satisfies the criteria under routine, normal and accident conditions of transport and thus there is no problem from the view point of shielding performance.

The maximum dose equivalent rate on the surface of package during routine conditions of transport is 0.218 mSv/hr and is 58 μSv/hr at a point of 1 m from the surface, each of which satisfies 2.0 mSv/hr or less and 100 μSv/hr or less, specified in the technical standard respectively. In addition, the maximum dose equivalent rate on the surface of the package under normal conditions of transport is 0.218 mSv/hr which also satisfies 2.0 mSv/hr or less specified in the technical standard.

The maximum dose equivalent rate at a point of 1 m from the surface under accident conditions of transport is 0.058 mSv/hr, which also satisfies 10.0 mSv/hr or less. Even when the above fuel is contained, the gamma streaming dose equivalent rate is 11 μSv/hr at the gap between the body and the lid showing the maximum value, and the dose equivalent rate on the surface is 0.175 mSv/hr even with the direct gamma/neutron dose equivalent rate 0.164 mSv/h taken into account, and thus there is no problem from the view point of shielding performance.

(II)-TableD.13 Maximum dose equivalent rate in transport of the package with basket for box type fuel

(Unit : μSv/h)

	Surface on the package			Point of 1m from the surface of the package		
	Side	Top	Bottom	Side	Top	Bottom
At routine conditions of transport						
Gamma rays	120	170	120	29	52	37
Neutron	44	48	44	5	6	6
Total	164	218	164	34	58	43
Under normal conditions of transport						
Gamma rays	120	170	120			
Neutron	44	48	44			
Total	164	218	164			
Under accident conditions of transport						
Gamma rays				29	52	37
Neutron				5	6	6
Total				34	58	43
Criteria: At routine conditions of transport	2,000			100		
Criteria: Under normal conditions of transport	2,000			—		
Criteria: Under accident conditions of transport	—			10,000		

Note) The dose equivalent rate at the point where gamma streaming is maximum is as follows. (The position is the gap between the body and the lid.)

(Unit : μSv/h)

	Surface on the package
Gamma ray streaming	11
Direct gamma rays	120
Neutron	44
Total	175

(II)-TableD.14 Maximum dose equivalent rate in transport of the package with basket for MNU type fuel

(Unit : μSv/h)

	Surface on the package			Point of 1m from the surface of the package		
	Side	Top	Bottom	Side	Top	Bottom
At routine conditions of transport						
Gamma rays	3	1	2	1	1	1
Neutron	1	1	1	1	1	1
Total	4	2	3	2	2	2
Under normal conditions of transport						
Gamma rays	3	1	2			
Neutron	1	1	1			
Total	4	2	3			
Under accident conditions of transport						
Gamma rays				1	1	1
Neutron				1	1	1
Total				2	2	2
Criteria						
At routine conditions of transport	2,000			100		
Under normal conditions of transport	2,000			——		
Under accident conditions of transport	——			10,000		

D.6 Appendix

D.6.1 Appendix-1 Neutron yields due to (α ,n) reaction

The number of neutrons which are generated from (α ,n) reaction for aluminum and silicon which are light nuclides in the fuel is obtained from the following equation [8].

$$\mathrm{Ymix} = \frac{\Sigma\,\mathrm{Ni}\cdot\mathrm{Ci}\cdot\mathrm{Yni}}{\Sigma\,\mathrm{Ni}\cdot\mathrm{Ci}} \qquad \text{——} \quad (1)$$

Where, Ymix : Neutron yield due to (α ,n) reaction for mixtures. (n/α /s)

Yni : Neutron yield due to (α ,n) reaction for unit element i. (n/α /s) Pu-238,Pu239,Pu-240,Am-241,Cm-242,Cm-244 are taken into account. The contribution of alpha particle of nuclides except those is ignored.

Element	Yni					
	Pu-238	Pu-239	Pu-240	Am-241	Cm-242	Cm-244
Aluminum	7.39×10^{-7}	3.74×10^{-7}	3.80×10^{-7}	7.28×10^{-7}	1.80×10^{-6}	1.14×10^{-6}
Silicon	1.22×10^{-7}	7.08×10^{-8}	7.17×10^{-8}	1.20×10^{-7}	2.79×10^{-7}	1.90×10^{-7}
Uranium	0	0	0	0	0	0

Ni : Atomic number density of unit element (1/cm^3)

Element	Ni			
	JRR-3	JRR-3	JRR-3	
	Standard silicide type	Follower silicide type	MNU type	Fuel element B
Aluminum	[redacted]	[redacted]	[redacted]	[redacted]
Silicon	[redacted]	[redacted]	[redacted]	[redacted]
Uranium	[redacted]	[redacted]	[redacted]	[redacted]

Ci : Ratio of stopping power of element i to that of oxygen

Element	Ci
Aluminum	1.434
Silicon	1.528
Uranium	4.803

The Ymix value of each emitter is obtained by substituting the above values for equation (1).

Alpha emitter	Ymix			
	JRR-3	JRR-3	JRR-3	
	Standard silicide type	Follower silicide type	MNU type	Fuel element B
Pu-238	[redacted]	[redacted]	[redacted]	[redacted]
Pu-239	[redacted]	[redacted]	[redacted]	[redacted]
Pu-240	[redacted]	[redacted]	[redacted]	[redacted]
Am-241	[redacted]	[redacted]	[redacted]	[redacted]
Cm-242	[redacted]	[redacted]	[redacted]	[redacted]
Cm-244	[redacted]	[redacted]	[redacted]	[redacted]

Since each alpha emitter releases an alpha particle per decay, the generation value of alpha particle per package is obtained from the radioactivity of each alpha emitter (from the results of ORIGEN code or ORIGEN-JR code).

Alpha emitter	Q (Bq= α /package)			
	JRR-3	JRR-3	JRR-3	
	Standard silicide type	Follower silicide type	MNU type	Fuel element B
Pu-238	[redacted]	[redacted]	[redacted]	[redacted]
Pu-239	[redacted]	[redacted]	[redacted]	[redacted]
Pu-240	[redacted]	[redacted]	[redacted]	[redacted]
Am-241	[redacted]	[redacted]	[redacted]	[redacted]
Cm-242	[redacted]	[redacted]	[redacted]	[redacted]
Cm-244	[redacted]	[redacted]	[redacted]	[redacted]

For the above, the number of neutrons Q・Ymix per package can be obtained.

Alpha emitter	Q·Ymix (n/s/ package)			
	JRR-3	JRR-3	JRR-3	
	Standard silicide type	Follower silicide type	MNU type	Fuel element B
Pu-238	[redacted]	[redacted]	[redacted]	[redacted]
Pu-239	[redacted]	[redacted]	[redacted]	[redacted]
Pu-240	[redacted]	[redacted]	[redacted]	[redacted]
Am-241	[redacted]	[redacted]	[redacted]	[redacted]
Cm-242	[redacted]	[redacted]	[redacted]	[redacted]
Cm-244	[redacted]	[redacted]	[redacted]	[redacted]
Total	[redacted]	[redacted]	[redacted]	[redacted]

D.6.2 Appendix-2 Gamma streaming calculation

The gamma streaming is evaluated for the case when the JRR-3 standard silicide type fuel is contained, which provides the maximum gamma source intensity per unit length.

6.2.1 Examination and results

The streaming will have influence on the dose equivalent rate at the following three positions;

(1) Drain hole

(2) Gap between the body and the lid

(3) Vent hole

These positions are as shown in (II)-Fig.D.2.1.

Since the neutron source intensity is very small the effect of neutron streaming is ignored. The effect of gamma streaming is examined in the calculation.

The surface dose equivalent rates at three positions of the package are summarized in (II)-Table D.2.1.

(II)-Table D.2.1 Dose equivalent rate at each point of packaging

Positions	Surface dose equivalent rate [μSv/h]
(1) Drain hole	1
(2) Gap between the body and the lid	11
(3) Vent hole	3

From the above result, the maximum dose equivalent rate of gamma streaming is 11 μSv/h at the gap between the body and the lid. The total surface dose equivalent rate on the surface of the package is 131 μSv/h even if adding the dose equivalent rate due to direct gamma rays at position ⑫ shown in (II)-Fig.D.6, 120 μSv/h.

[redacted]

(Ⅱ)-Fig.D.2.1　Evaluated Location of Gamma Streaming

Even when the neutron dose equivalent rate of 44 μ Sv/h is taken into consideration, total dose equivalent rate is 175 μ Sv/h. This value satisfies the criteria, and is smaller than the maximum surface dose equivalent rate of the package 218 μ Sv/h.

Therefore, there is no problem of gamma streaming. Also, there is no problem of the dose equivalent rate at 1m from the surface too.

6.2.2 Details of analysis

6.2.2.1 Drain hole

The drain hole is modeled as shown in (Ⅱ)-Fig.D.2.2 to perform the analysis in accordance with the following procedure.

- (i) Calculate gamma flux at drain hole inlet (point-P_1) by using QAD-CGGP2R code.
- (ii) Calculate attenuation from plane source of point-P_1 to point-P_2.
- (iii) Calculate gamma flux of scattering at point-P_2 and reaches point-P_3.
- (iv) Calculate attenuation of gamma flux by drain valve protection cover.

(1) Details of analysis

The gamma flux at point-P_1, calculated by using QAD-CGGP2R code, is shown in (Ⅱ)-Table D.2.2.

(Ⅱ)-Table D.2.2 Gamma flux at point P_1

Gamma flux group No.	Mean Energy (MeV)	Gamma flux at point P_1 Φ_{P1}(ph/cm^{2}sec)
1	[redacted]	[redacted]
2	[redacted]	[redacted]
3	[redacted]	[redacted]
4	[redacted]	[redacted]
5	[redacted]	[redacted]
6	[redacted]	[redacted]
7	[redacted]	[redacted]
8	[redacted]	[redacted]

[redacted]

(Ⅱ)-Fig.D.2.2　Streaming analytical model for the drain hole

The gamma flux of point-P$_2$ (ϕ_{P2}) can be obtained by the following equation with gamma flux at point P$_1$ (ϕ_{P1}).

$$\phi_{P2} = \frac{\phi_{P1}}{2} \ell n \left\{ 1 + \left(\frac{a}{r_1} \right)^2 \right\} \quad ^{9)}$$

where, a : Radius of hole [redacted]

r_1 : Distance from inlet of hole [redacted]

$\phi_{P2} = 4.98 \times 10^{-3} \cdot \phi_{P1}$

The result is as shown in (II)- Table D.2.3.

(II)-Table D.2.3 Gamma flux at point-P$_2$

Gamma flux group No.	Gamma flux at point-P$_2$ ϕ_{P2}(ph/cm^{2}sec)
1	[redacted]
2	[redacted]
3	[redacted]
4	[redacted]
5	[redacted]
6	[redacted]
7	[redacted]
8	[redacted]

The gamma flux at point-P$_3$ (Φ_{P3}) is evaluated by the following equation. Here, only single gamma scattering is considered.

$$\phi_{P3} = \phi_{P2} \times \frac{gS}{4\pi r_2^{\,2}} \times f \times s \times F^{9)}$$

g : Geometrical correction for the ratio of solid angle at scattering point

S : Area of scattering point ([redacted]

r_2 : Distance from P$_2$ to P$_3$ ([redacted]

f : Energy attenuation rate in scattering

s : Scattering ratio in the interaction of gamma ray with the shielding materials

F : Correction coefficient for the anisotropy of scattering

The result is as shown in (II)- Table D.2.4.

(II)-Table D.2.4 Gamma flux at point-P_3

Gamma flux group No.	Gamma flux at point-P_3 Φ_{P3}(ph/cm^{2}sec)
1	[redacted]
2	[redacted]
3	[redacted]
4	[redacted]
5	[redacted]
6	[redacted]
7	[redacted]
8	[redacted]

The gamma flux at point-P_4(Φ_{P4}) can be expressed by the following equation.

$$\Phi_{P4} = \Phi_{P3} \times e^{-\mu x}$$

where, " μ " means linear attenuation coefficient (1/cm) which is shown in (II)-Table D.2.5.

X: Thickness of shielding material ([redacted] cm)

(II)-Table D.2.5 Linear attenuation coefficient μ

Gamma flux group No.	μ (1/cm)
1	[redacted]
2	[redacted]
3	[redacted]
4	[redacted]
5	[redacted]
6	[redacted]
7	[redacted]
8	[redacted]

The result is as shown in (II)- Table D.2.6.

(II)-Table D.2.6 Gamma flux at point-P_4

Gamma flux group No.	Gamma flux at point-P_4 Φ_{P4}(ph/cm^{2}sec)
1	[redacted]
2	[redacted]
3	[redacted]
4	[redacted]
5	[redacted]
6	[redacted]
7	[redacted]
8	[redacted]

Accordingly, the dose equivalent rate of gamma ray streaming at point-P_4 (D_{P4}) is calculated as follows;

$$D_{P4} = \Phi_{P4} \cdot K$$

where, K means conversion coefficient of dose equivalent rate which is shown in (II)-Table D.11.

The result is shown in (II)-Table D.2.7.

(Ⅱ)-Table D.2.7 Dose equivalent rate at point-P_4

Gamma flux group No.	Dose equivalent rate [μ Sv/h]
1	[redacted]
2	[redacted]
3	[redacted]
4	[redacted]
5	[redacted]
6	[redacted]
7	[redacted]
8	[redacted]
Total	[redacted]

(2) Result

From the above result, the gamma streaming dose equivalent rate on the surface of the drain hole is less than 1 μ Sv/h and will not be any problem.

Similarly, there is no problem at 1m from the surface.

6.2.2.2 Gap between the body and the lid

The profile of gap between the body and the lid is shown in (Ⅱ)-Fig.D.2.3.

It is assumed that there are three routes (A), (B) and (C) shown in (Ⅱ)-Fig.D.2.4 as the route of leakage through the gap.

The following describes the calculation of these routes.

[redacted]

(Ⅱ)-Fig.D.2.3 Gap between the body and the lid

[redacted]

(Ⅱ)-Fig.D.2.4 Three routes of leakage

(1) Details of analysis

Three routes (A), (B) and (C) shown in (Ⅱ)-Fig.D.2.4 are examined.

Case (A)

There is no problem as the effective shielding thickness is increased [redacted]

Case (B)

There is no gap between the body and the lid, but the effective shielding thickness exclude gasket groove on this route is [redacted]m. The depth of gasket groove is less than [redacted]mm. The gamma streaming dose equivalent rate of the route is calculated by using the QAD-CGGP2R code.

The analytical model is shown in (Ⅱ)-Fig.D.2.5.

---

* [redacted]

[redacted]

(Ⅱ)-Fig.D.2.5　Gamma streaming analytical model for (B)

From the calculation, it appears that the gamma streaming dose equivalent rates of this route are as follows;

Surface of the package	1.1×10^{1} μSv/h
1m from the surface of the package	1.3×10^{0} μSv/h

Case (C)

As shown in (Ⅱ)-Fig.D.2.6, gamma ray is attenuated by the body and lid before it reaches the gap between the body and the lid, point-P_1. Furthermore, since the gap between the body and the lid is [redacted]mm thick and the gap bends at point-P_2, gamma streaming at point-P_3 is considered extremely small.

[redacted]

(Ⅱ)-Fig.D.2.6　Gamma streaming analytical model for (C)

(2) Result

The results of streaming calculation are summarized as shown in (II)-Table D.2.8.

(II)-Table D.2.8 Summary of streaming dose equivalent rate

	Dose equivalent rate on the surface of the package (μ Sv/h)
(A)	$\simeq 0$
(B)	11
(C)	$\simeq 0$

From the above results, the gamma streaming dose equivalent rate from the gap between the body and the lid is 11 μ Sv/h, which can be negligible.

It can be also ignored at 1m from the surface.

6.2.2.3 Vent hole

The profile of the vent hole is shown in (Ⅱ)-Fig.D.2.1. The analysis is performed using conservative model as shown in (Ⅱ)-Fig D.2.7.

The analysis is performed in accordance with the following procedure.

i) Calculate gamma flux at the vent hole inlet (point-P_1) by using QAD-CGGP2R code.

ii) Calculate the attenuation from the plane source of point-P_1 to point-P_2.

iii) Calculate gamma flux of scattering at point-P_2 and reaches point-P_3.

iv) Consider the attenuation of gamma flux by the vent valve protection cover.

(1) Details of analysis

The gamma fluxes at points P1, P2, P3 and P4 are shown in (Ⅱ)-Table D.2.9.

(Ⅱ)-Table D.2.9 Gamma flux at each point

Group NO.	Gamma flux [1] at point-P_1 Φ_{P1}(ph/cm^{2}sec)	Gamma flux [2] at point-P_2 Φ_{P2}(ph/ cm^{2}sec)	Gamma flux [3] at point-P_3 Φ_{P3}(ph/ cm^{2}sec)	Gamma flux [4] at point-P_4 Φ_{P4}(ph/ cm^{2}sec)
1	[redacted]	[redacted]	[redacted]	[redacted]
2	[redacted]	[redacted]	[redacted]	[redacted]
3	[redacted]	[redacted]	[redacted]	[redacted]
4	[redacted]	[redacted]	[redacted]	[redacted]
5	[redacted]	[redacted]	[redacted]	[redacted]
6	[redacted]	[redacted]	[redacted]	[redacted]
7	[redacted]	[redacted]	[redacted]	[redacted]
8	[redacted]	[redacted]	[redacted]	[redacted]

1) Calculated by QAD-CGGP2R code

2) $$\phi_{P2} = \frac{\phi_{P1}}{2} \ell n \left\{ 1 + \left(\frac{1.0}{26.0} \right)^2 \right\}$$

3) $$\phi_{P3} = \phi_{P2} \times \frac{3.14}{4\pi \times 26^2} \times f \times s \times F$$

4) $$\phi_{P4} = \phi_{P3} \times e^{-\mu X}$$

[redacted]

(Ⅱ)-Fig.D.2.7　Gamma streaming analytical model of the vent hole

Accordingly, the gamma streaming dose equivalent rate at point-P_4 is shown in (Ⅱ)-Table D.2.10.

(Ⅱ)-Table D.2.10 Dose equivalent rate on the surface of the vent hole

Group No.	Dose equivalent rate 〔μ Sv/h〕
1	5.60×10^{-2}
2	1.82×10^{0}
3	2.27×10^{-1}
4	1.47×10^{-1}
5	2.14×10^{-1}
6	6.79×10^{-3}
7	4.91×10^{-4}
8	1.60×10^{-5}
Total	2.47×10^{0}

(2) Result

According to the above result, the gamma streaming dose equivalent rate on the surface of the vent hole is 3 μ Sv/h, and will not be any problem.

Similarly, there is no problem at 1m from the surface.

D.6.3 Appendix-3 References

1) M.J.Bell, "ORIGEN – The ORNL Isotope Generation and Depletion Code", ORNL-4628 (1973)

2) K.Koyama, N.Yamano, S.Miyasaka, "ORIGEN-JR: A Computer Code for Calculating Radiation Sources and Analyzing Nuclide Transmutations", JAERI-M 8229 (1979)

3) Y.Sakamoto, S.Tanaka, "QAD-CGGP2 and G33-GP2 : Revised Versions of QAD-CGGP and G33-GP (Codes with the Conversion Factors from Exposure to Ambient and Maximum Dose Equivalents)", JAERI-M 90-110 (July 1990)

4) "DOT3.5-Two Dimensional Discrete Ordinates Radiation Transport Code", CCC-276, Oct.1976

   and

   W.A. Rhoades, "The DOT Ⅲ Two-Dimensional Discrete Ordinates Radiation Transport Code", ORNL-TM-4280,Sep.1973

5) JEARI-M 6245 (1975)

   JAERI-memo 5567 (1974)

   JAERI 1001 (1959)

   JAERI 1002 (1960)

   JAERI 1031 (1962)

   JAERI-memo 7376 (1977)

   JAERI-memo 7732 (1978)

   JAERI-M 6205 (1975)

   The other inside reports

6) ORNL RSIC "CASK ; 40 Group Coupled Neutron and Gamma-ray Cross Section Data" DLC-23 (1973)

7) ICRP, "Data for Use in Protection Against External Radiation", Publication 74

8) H. Matsunobu, and et al. "Data Book for Calculating Neutron Yields from (α,n) Reaction and Spontaneous Fission", JAERI 1324 (January 1992)

9) Atomic Energy Society of Japan, "A Handbook of Radiation Shielding –basics-", (March 2015).

E. Criticality analysis

In this analysis, it is investigated that any of packages during normal transportation, a package in isolation, and a package in isolation and array under general and special test conditions for packages containing fissile material would not reach criticality.

E.1 Summary

This section shows that subcriticality would be maintained under analysis conditions for isolation during normal transportation, and isolation and array under general and special test conditions for packages containing fissile material.

- The containment of the packaging is maintained, since there is no change of the configuration of the packaging which affects the criticality analysis under routine, normal and accident conditions of transport.
- The configuration of the basket is maintained under routine, normal and accident conditions of transport.
- The stuck parts of the fuel elements are maintained in the basket lodgement under routine, normal and accident conditions of transport.

From the above, the same criticality analysis model for the package shall be used during normal transportation, and under general and special test conditions for packages containing fissile material.

In the analysis, it is conservatively assumed that the enrichment of the fuel element contained is the same as the initial enrichment and [redacted] as a neutron poison is ignored. The three dimensional multigroup Monte Carlo KENO-Va code[1] is used to obtain the effective multiplication coefficient of the package.

From the result of the analysis, the maximum value of the effective multiplication coefficient ($k_{eff}+3\sigma$) is 0.873 when JRR-3 standard silicide type fuel are contained.

Therefore, the criticality safety for the package is confirmed.

E.2 Analytical object

E.2.1 Contents

Three kinds of the fuel elements, which are shown in (II)-Table E.1, are contained in the packaging. These fuel elements are contained in the two kinds of the baskets. These two baskets with the fuel elements are analyzed individually.

The fuel specifications used for the criticality analysis are shown in (II)-Table E.2.

With regard to the basket for box type fuel, the analyses are performed when JRR-3 standard silicide type fuel and JRR-3 follower silicide type fuel are contained in the packaging respectively. The maximum number of contained fuel elements is 40.

JRR-3 follower silicide type fuel are loaded with adapters.

With regard to the basket for MNU type fuel, the analysis is performed when JRR-3 MNU type fuels are contained in the packaging. The maximum number of contained fuel elements is 160.

The extremities of JRR-3 standard silicide type fuel where no fuel meat exists, are cut off before these fuel elements are contained into the packaging.

The configurations of the fuel elements after cut off are as follows. JRR-3 standard silicide type fuel element are [redacted] cm long and its extremities of [redacted]5 cm in length are fuel structural materials.

JRR-3 follower silicide type fuel are [redacted] cm long and its bottom extremity of [redacted] cm and its top extremity of [redacted] cm in length are fuel structural materials. JRR-3 MNU type fuel is [redacted] cm long and its bottom extremity of [redacted] cm and its top extremity of [redacted] cm in length are fuel structural materials.

(II)-Table E.1 Fuel element contained in the packaging

Basket	Box type	Box type (with adapters)	MNU type
Reactor	JRR-3	JRR-3	JRR-3
Fuel element	Standard silicide type	Follower silicide type	MNU type
Number of fuel elements*) (piece)	40	40	160
Enrichment*) (%)	[redacted]	[redacted]	[redacted]
Mass of ^{235}U (g/piece)	[redacted]	[redacted]	[redacted]

*) These values show the upper limits which include fabrication tolerance.

(Ⅱ)-Table E.2 Specification of fuel element used in the criticality analysis

Basket	Box type	Box type (with adapters)	MNU type	Box type
Reactor	JRR-3	JRR-3	JRR-3	—
Fuel element	Standard silicide type	Follower silicide type	MNU type	Fuel elements B for evaluation
Type	Plate fuel (dispersion type)	Plate fuel (dispersion type)	Metallic natural uranium	Plate fuel (dispersion type)
Enrichment of ^{235}U (%)	[redacted]	[redacted]	[redacted]	[redacted]
Mass of ^{235}U (g/piece)	[redacted]	[redacted]	[redacted]	[redacted]
Number of fuel elements (piece)	40	40	160	40
Mass of ^{235}U (kg/basket)	[redacted]	[redacted]	[redacted]	[redacted]
Burn up (MWD/tU)	[redacted]	[redacted]	[redacted]	[redacted]
Neutron poison	[redacted]	[redacted]	None	None

*) It is conservatively assumed that the cadmium wire is ignored in the criticality analysis.

E.2.2 Packaging

The body of the packaging consists of stainless steel of more than [redacted] mm thickness. No deformation of the packaging occurs under accident conditions of transport because of the packaging having a sufficient strength.

The fuel elements are hold at the position with the basket and the basket bottom plate. The basket is made of stainless steel and neutron poison, and the basket bottom plate is made of stainless steel. As described in (Ⅱ)-A.9.2, the deformation of the basket is [redacted] mm in maximum and no effect on the criticality analysis. Therefore, packages during normal transportation and under general and special test conditions for packages containing fissile material shall be treated as the same model. Also the fins welded on the external surface of the packaging are ignored conservatively.

E.2.3 Neutron poison

[redacted] is used as the neutron poison of the basket for box type fuel. [redacted] It is assumed that the amount of [redacted] of the minimum guarantee value conservatively.

As the neutron flux in the package is very small, the capture of these neutrons by boral plates will not significantly deplete the neutron poisons even after a long time.

The size and the positions to the basket lodgement are confirmed before installation. Therefore, the validity of the analytical models and the number densities shown in paragraph.E.3 is assured.

Furthermore, an evaluation will be made on the loss rate of ^{10}B in a hypothetical case of receiving neutron irradiation from the contents for 100 years to show that the [redacted] do not lose their efficacy.

^{10}B absorbs thermal neutrons and produces ^{10}B (n, α)^{7}Li reaction.

The neutron absorption loss rate of ^{10}B is expressed by the following equation:

(Neutron absorption loss rate) = (Neutron irradiation dose)

x (Absorption reaction cross-section of ^{10}B)

For the neutron irradiation dose for 100 years, using the value for fuel element B, which has the maximum source intensity per unit length, as shown in (II)-Table D.4, it will be:

[redacted]

Here, considering

Absorption cross-section of ^{10}B: 3837×10^{-24} (cm^2) Note 1

Then,

$$(3.25 \times 10^{14} \times 3837 \times 10^{-24}) \times 100 = 1.3 \times 10^{-4} \ (\%)$$

This means that the loss of ^{10}B is negligible and the neutron absorbing ability of [redacted] will not be lost.

[redacted] is used as the neutron poison for JRR-3 standard silicide type fuel, and JRR-3 follower silicide type fuel, but [redacted] is ignored in the analysis to evaluate conservatively.

Note 1: Radioisotope Pocket Data Book, 12th Edition (published by the Japan Radioisotope Association)

E.3 Model specification

E.3.1 Analytical model

E.3.1.1 Analytical model of package in isolation

The condition for a package in isolation specified in the regulation is that the inside of the package is filled with water and a reflection condition by means of water of 20 cm in thickness are assumed. Since the analytical model of the packages in array under the conditions that the package is filled with water is severer than that of the package in isolation, the evaluation is performed for the analytical model of the packages in array as described later.

E.3.1.2 Analytical model of packages in array

As described in (Ⅱ).9.2, the deformation of the package is [redacted] mm in maximum under normal and accident conditions of transport for packages containing fissile material and no effect on the criticality analysis. Therefore, packages under general and special test conditions for packages containing fissile material shall be treated as the same model.

As the boundary condition of the analytical model, the full reflection is adopted. It is assumed that the packages are in the infinite array, and the space between the packages is filled with water. This assumption is severer condition than that in isolation.

The analytical models of three baskets are as follows;

(1) Basket for box type fuel

The analytical models used in the criticality analysis are shown in (Ⅱ)-Fig.E.1 through (Ⅱ)-Fig.E.6. The model mainly consists of 3 parts.

① basket part

② space region (water)

③ stainless steel region

The basket part consists of the fuel meat regions, the fuel structure regions, the space regions (water), the neutron poison regions and the stainless steel regions.

The details of modeling method are as follows;

○ fuel meat region

The fuel meat region is composed of the fuel meats, the fuel cladding materials (Al) and the space.

○ fuel structure region

The fuel structure region is composed of the fuel side plates.

It is conservatively assumed that [redacted] of the neutron poison which is contained in fuel is ignored and all of that is aluminum.

○ extremities of the basket

These regions of the top and the bottom part of the basket which contain no fuel meat are composed of the basket structural materials (stainless steel), the neutron poisons, the fuel structural materials (Al) and space. This region is assumed to be water because almost of this area is void space.

○ adapter region (only for follower type fuel element)

Adapters made of alminium are inserted in the basket lodgement when the follower type fuel elements are loaded in the basket for box type fuel.

○ neutron poison [redacted] region

The neutron poison is made from [redacted] Its mean thickness is [redacted]mm and minimum thickness is [redacted]mm. The region is assumed to be [redacted]mm thick and placed in the center of the neutron poison hole ([redacted]mm wide). The side space of the neutron poison region is assumed to be stainless steel.

○ bottom of the basket

There are drain grooves and holes in the bottom of the basket. As this part is mostly occupied by stainless steel, the region is assumed to be stainless steel.

○ position of the fuel elements

The fuel elements are assumed to lean towards the center of the basket as shown in (Ⅱ)-Fig. E.2 and E.5. This assumption is conservative, since the critical size is assumed to be smaller.

○ packaging

Though the fins and the lifting lugs are attached on the outer surface of the packaging, it is assumed that those are conservatively ignored in the analysis as described previously. The length of the package cavity is assumed as the same with the length of fuel.

Therefore, the body of the packaging is assumed to be cylindrical ([redacted] in the model.

(2) Basket for MNU type fuel

The analytical models used in the criticality analysis are shown in (Ⅱ)-Fig.E.7 and (Ⅱ)-Fig.E.8. The model mainly consists of 3 parts.

① basket part

② space region (water)

③ stainless steel region

The basket part consists of the fuel meat regions and the space regions (water).

○ fuel meat region

The fuel meat region is composed of the fuel meats (metallic natural uranium), the fuel cladding materials (Al) and the space.

○ extremities of the basket

These regions of the top and the bottom part of the basket which contain no fuel meat are composed of the basket structural materials (stainless steel), the fuel structural materials (Al) and space. As this region is mostly occupied by space, it is assumed to be water.

○ bottom of the basket

There are drain grooves and holes in the bottom of the basket. As this part is mostly occupied by stainless steel, the region is assumed to be stainless steel.

○ packaging

Though the fins and the lifting lugs are attached on the outer surface of the packaging, it is assumed that those are conservatively ignored in the analysis as described previously. The cavity length of the package is assumed as the same with the length of fuel.

Therefore, the body of the packaging is assumed to be cylindrical ([redacted] cm in diameter× [redacted] cm in height) in the model.

[redacted]

(Ⅱ)-Fig.E.1 Analytical model of containing the basket for box type fuel
(Axial direction)
[In case of containing JRR-3 standard silicide type fuel]

[redacted]

(Ⅱ)-Fig.E.2　Analytical model of containing the basket for box type fuel
(Cross section of basket)
[In case of containing JRR-3 standard silicide type fuel]

[redacted]

(Ⅱ)-Fig.E.3　Cross section of JRR-3 standard silicide type fuel

[redacted]

(Ⅱ)-Fig.E.4 Analytical model of containing the basket for box type fuel
(Axial direction)
[In case of containing JRR-3 follower silicide type fuel]

[redacted]

(Ⅱ)-Fig.E.5 Analytical model of containing the basket for box type fuel
(Cross section of basket)
[In case of containing JRR-3 follower silicide type fuel]

[redacted]

(Ⅱ)-Fig.E.6　Cross section of JRR-3 follower silicide type fuel

[redacted]

(Ⅱ)-Fig.E.7　Analytical model of containing the basket for MNU type fuel

(Axial direction)

[In case of containing JRR-3 MNU type fuel]

[redacted]

(Ⅱ)-Fig.E.8 Analytical model of containing the basket for MNU type fuel
(Cross section of basket)
[In case of containing JRR-3 MNU type fuel]

E.3.2 Atomic number density in each region of analytical model

The atomic number densities of the elements in each region used in the analytical models are shown in (Ⅱ)-Table E.3.

[redacted] in the boral plate is conservatively assumed to be [redacted]

[redacted]

(II)-Table E.3　Atomic number density of each region

(Unit : atoms/b・cm)

Basket			Box type	Box type (with adapter)	MNU type
Reactor			JRR-3	JRR-3	JRR-3
Fuel element			Standard silicide type	Follower silicide type	MNU type
Fuel meat region	Fuel meat	U-235 U-238 Si Aℓ	[redacted]	[redacted]	[redacted]
	Fuel cladding material	Aℓ	[redacted]	[redacted]	[redacted]
	Space region	H O	6.69×10^{-2} 3.34×10^{-2}	6.69×10^{-2} 3.34×10^{-2}	6.69×10^{-2} 3.34×10^{-2}
Fuel structure region		Aℓ	[redacted]	[redacted]	[redacted]
Adapter region		Aℓ	[redacted]	[redacted]	[redacted]
Space region		H [redacted]	6.69×10^{-2} [redacted]	6.69×10^{-2} [redacted]	6.69×10^{-2} [redacted]
Neutron poison region		[redacted]	[redacted]	[redacted]	[redacted]
Stainless steel		[redacted]	[redacted]	[redacted]	[redacted]

E.4 Subcriticality evaluation

E.4.1 Analytical condition

The validity of the analytical model for the contents, the packaging and the neutron poison is shown as follows.

(1) Contents

The contents of the package are spent fuel elements. The enrichment of ^{235}U in the fuel elements is lower than the initial value by the irradiation in the reactors. In the analysis, the initial enrichment of the unirradiated fuel element is conservatively used.

Also, the fission products which serve as neutron poisons generated by the irradiation are conservatively ignored in the analytical model.

(2) Packaging

In the criticality analysis, the length of the packaging in the longitudinal direction is finite and the cavity length of the packaging has same length with fuels loaded in the package. It is conservatively assumed that there is no fin.

(3) Neutron poison

In the analysis, [redacted] content in [redacted] of neutron poison is conservatively assumed to be [redacted]

E.4.2 Water immersion into the package

Under the normal and accident conditions of transport of packages for fissile material, it is shown that the containment of the package is maintained (refer to chapter of (Ⅱ)-A). Therefore, water doesn't immerse into the package.

It is expected that the package will immerse in snow (water) in bad weather during transport. But water which immerses between the packages decreases the reactivity when each package is separated each other by the shell of the packaging made of thick steel. Therefore, there is no problem on the criticality safety.

The water density is assumed to be 1.0 g/cm^3 (at 4 ℃) in the calculation of the effective multiplication coefficient. Since the temperature change decreases the water density and lowers the reactivity, the expected temperature change is no problem on the criticality safety, too.

E.4.3 Calculation method

SCALE system developed in Oak Ridge National Laboratory in U.S.A. is used in the criticality analysis. Multigroup Monte Carlo calculation code KENO-Va is used in the calculation of the effective multiplication coefficient (k_{eff}). ENDF/B-V 238-groups library data which is one of the library data in SCALE system is used as nuclear data library.

E.4.4 Calculation results

The calculated effective multiplication coefficients (k_{eff}) are shown in (Ⅱ)-Table E.4. The standard deviation σ, and $k_{eff}+3\sigma$ are also shown in (Ⅱ)-Table E.4.

(Ⅱ)-Table E.4 Calculation results

Fuel element	Basket	Condition	k_{eff}	σ	$k_{eff}+3\sigma$
JRR-3 standard silicide type fuel	Box type	Undamaged and damaged packages in array	0.870	0.0008	0.873
JRR-3 follower silicide type fuel	Box type (with adapter)	Undamaged and damaged packages in array	0.697	0.0009	0.700
JRR-3 MNU type fuel	MNU type	Undamaged and damaged packages in array	0.619	0.0005	0.620

E.5 Benchmark experiments

The reliability of KENO-Va code used in the analysis is described as follows. Many benchmark calculations for KENO-Va code have been performed. The analysis on critical experiment 3) was made using JRR-4 (low enrichment silicide fuel) of Japan Atomic Energy Research Institute and the evaluation are performed in this paragraph.

JRR-4 is a swimming pool reactor for research which has the maximum power of 3.5 MW. The fuel element is low enrichment silicide fuel (Refer to (Ⅱ)-Table E.2). The fuel elements are arrayed in cells of 4×5. The fuel elements are surrounded by graphite reflectors (A large reflector of lid tank side is an aluminum reflector.), an irradiation pipe and a neutron source. Five control rods of plate shape and safety rods are between the fuel elements and between the fuel element and the reflector. The moderator and the coolant are light water. The arrangement plan of the core is shown in (Ⅱ)-Fig.E.9. The critical experiments of the minimum core and total core were performed in July 1998.

In the minimum core criticality, 12 pieces of the fuel elements were arrayed crosswise and the graphite reflectors were loaded around the fuel elements. C1, C2 and C3 of the control rods were withdrawn by full stroke. C4 and C5 of those were withdrawn to 369 mm and 292 mm in the longitudinal direction, respectively.

In the total core criticality, 20 pieces of the fuel elements (5×4) were arrayed in the core. C1 through C4 of the control rods were withdrawn to 255 mm and C5 292 mm in the longitudinal direction, respectively. The core temperature during the experiment was about 20℃.

The analyses of the minimum and total core criticality were performed by using ENDF/B-V 238-groups library and KENO-Va code.

As the results, the effective multiplication coefficient of the minimum core criticality is 1.013±0.0010. That of the total core criticality is 1.019±0.0009.

From the above, it can be concluded that the calculation method (ENDF/B-V 238-groups library and KENO-Va code) used in the analysis is conservative.

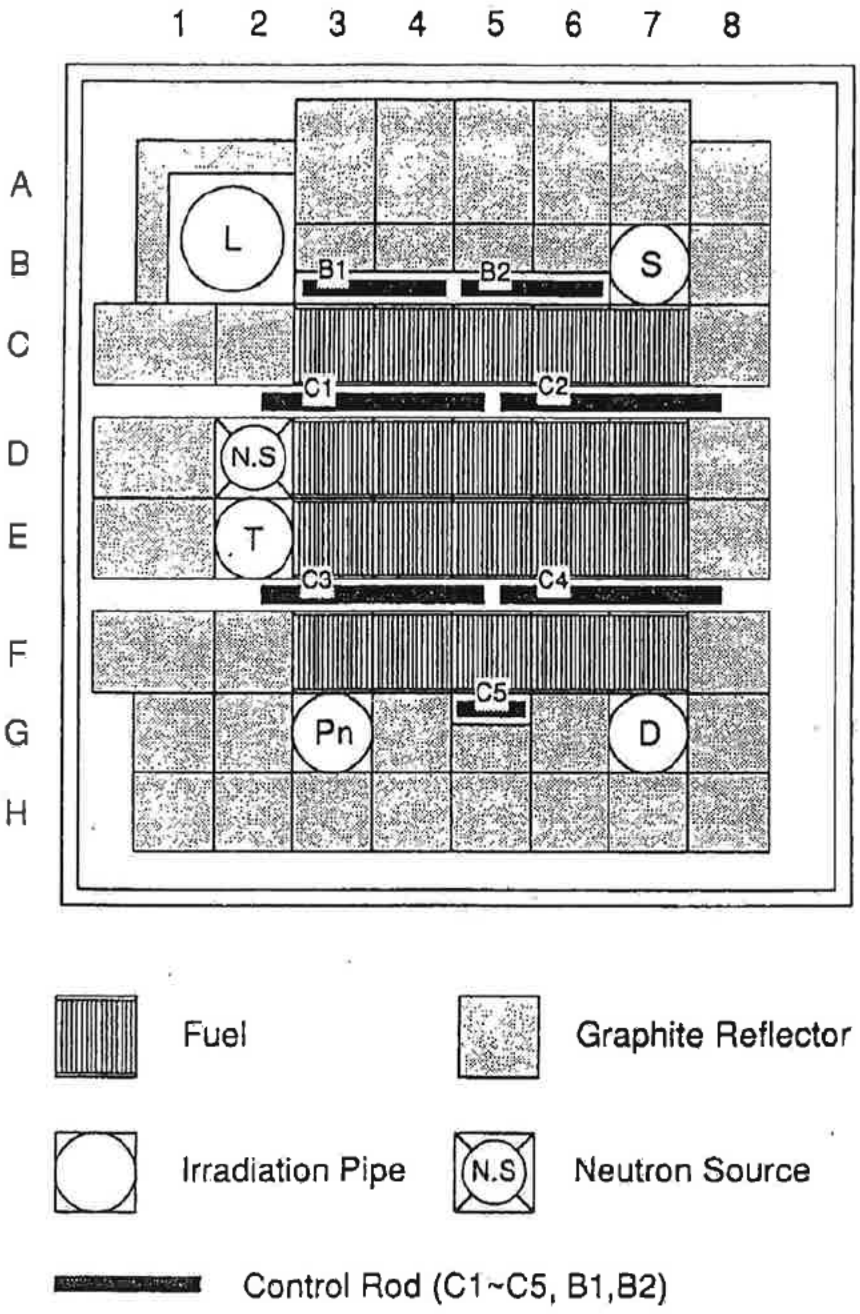

(II)-Fig.E.9 Arrangement plan of the core

E.6 Summary of the results and the evaluation

The stuck parts of the fuel elements are maintained in the basket lodgement under routine, normal and accident conditions of transport of packages for fissile material. There is no configuration change which affects the criticality analysis for the baskets, etc..

In the analysis, it is conservatively assumed that the enrichment of the contained fuel elements is the same as the initial enrichment and the [redacted] which is contained in some fuels as a neutron poison is ignored. Also, the amount of [redacted] contained in [redacted] used as a neutron poison in the basket is conservatively assumed to be [redacted] Further, it is assumed that the packages are filled with water and in infinite array.

From the results of the analysis using conservative assumption, the effective multiplication coefficient ($k_{eff}+3\sigma$) has a maximum value of 0.873, when JRR-3 standard silicide type fuel are contained in the packaging. Therefore, the criticality safety of the package is confirmed.

From the above results, it can be concluded that this package would not reach criticality for isolation during normal transportation, and isolation and array under general and special test conditions for packages containing fissile material even if any fuel element was installed.

E.7 Appendix

E.7.1 Appendix-1

Safety of the package under routine conditions of transport

The criticality safety is examined for the routine conditions of transport. Under the routine conditions of transport, the analysis is performed when there is no water inside and outside the packaging.

① Basket for box type fuel

The analytical models are the same as those shown in (Ⅱ)-Fig.E.1 through (Ⅱ)-Fig.E.14. The density of the space region shown in (Ⅱ)-Table E.3 is assumed to be that of air. The KENO-Va code is used for the analysis.

The results of the analysis are as follows;

JRR-3 standard silicide type fuel (in case of containing 40 fuel elements)

$$\begin{cases} k_{eff} & = 0.175 \\ \sigma & = 0.0002 \\ k_{eff} + 3\sigma & = 0.176 \end{cases}$$

fuel element B (in case of containing 40 fuel elements)

$$\begin{cases} k_{eff} & = 0.101 \\ \sigma & = 0.0002 \\ k_{eff} + 3\sigma & = 0.101 \end{cases}$$

JRR-3 follower silicide type fuel (in case of containing 40 fuel elements)

$$\begin{cases} k_{eff} & = 0.124 \\ \sigma & = 0.0002 \\ k_{eff} + 3\sigma & = 0.124 \end{cases}$$

From the above results, it can be concluded that the criticality safety is sufficiently kept.

② Basket for MNU type fuel

The analytical model is the same as that shown in (Ⅱ)-Fig.E.7 and

(Ⅱ)-Fig.E.8. The density of the space region shown in (Ⅱ)-Table E.3 is assumed to be that of air. The KENO-Va code is used for the analysis.

The result of the analysis is as follows;

JRR-3 MNU type fuel (in case of containing 160 fuel elements)

$$\begin{cases} k_{eff} & = 0.233 \\ \sigma & = 0.0003 \\ k_{eff} + 3\sigma & = 0.234 \end{cases}$$

From the above result, it can be concluded that the criticality safety is sufficiently kept.

E.7.2 Appendix-2

Safety of the package during the loading of the fuel elements

When the fuel element is being loaded in this packaging, the lid is opened and the fuel element is perfectly surrounded by the water. In this state, the criticality safety is examined for each fuel basket.

① Basket for box type fuel

The axial model of this basket is shown in (Ⅱ)-Fig.E.2.1 through (Ⅱ)-Fig.E.2.2.

The model of the fuel element region is the same as that shown in (Ⅱ)-Fig.E.2 ~E.5. Also, the model of the cross section of each fuel element is the same as that shown in (Ⅱ)-Fig.E.3 and E.6, respectively. The density of each component is the same as that shown in (Ⅱ)-Table E.3.

The thickness of surrounding water region is assumed to be 30 cm around the package, assuming the lid closed. The KENO-Va code is used for the analysis.

The results of the analysis are as follows;

JRR-3 standard silicide type fuel (in case of containing 40 fuel elements)

$$\begin{cases} k_{eff} & = 0.868 \\ \sigma & = 0.0010 \\ k_{eff} + 3\sigma & = 0.870 \end{cases}$$

JRR-3 follower silicide type fuel (in case of containing 40 fuel elements)

$$\begin{cases} k_{eff} & = 0.695 \\ \sigma & = 0.0008 \\ k_{eff} + 3\sigma & = 0.697 \end{cases}$$

From the above results, it can be concluded that the criticality safety is sufficiently kept.

② Basket for MNU type fuel

As the fuel elements are loaded in the MNU basket and stored in the pool, the criticality safety is examined for the basket without packaging.

The analytical model is shown in (II)-Fig.E.2.3. The unit cell is modeled with full reflection at the boundary surface. The density is shown in (II)-Table.E.2.1. The KENO-Va code is used for the analysis.

The results of the analysis are as follows;

JRR-3 MNU type fuel

$$\begin{cases} k_{eff} & = 0.720 \\ \sigma & = 0.0005 \\ k_{eff} + 3\sigma & = 0.722 \end{cases}$$

From the results, it can be concluded that the criticality safety is sufficiently kept.

[redacted]

(Ⅱ)-Fig.E.2.1 Analytical model in case of containing the basket for box type fuel (Axial direction)

[In case of containing JRR-3 standard silicide type fuel]

[redacted]

(Ⅱ)-Fig.E.2.2　Analytical model in case of containing the basket for box type fuel (Axial direction)
[In case of containing JRR-3 follower silicide type fuel]

[redacted]

(Ⅱ)-Fig.E.2.3　Analytical model in case of containing the basket for MNU type fuel

(Ⅱ)-Table E.2.1 Atomic number density used in the criticality analysis in case of containing the basket for MNU type fuel

Material		Atomic number density (atoms/barn·cm)
Fuel meat	U-235 U-238	[redacted]
Fuel cladding material	Aℓ	[redacted]
Water	H O	6.69×10^{-2} 3.34×10^{-2}
Stainless steel	[redacted]	[redacted]

E.7.3 Appendix-3

Safety of the package under accident conditions of transport

The basket for box type fuel of the package has very small deformation at 9 m drop test under accident condition of transport. The criticality safety of the package under this condition is confirmed.

As shown in (Ⅱ)-A.9.2, the basket for box type fuel deforms [redacted] mm in maximum under 9 m drop test. Fig. (Ⅱ)-E.3.1 shows the maximum displacement after having 9 m drop test, and the criticality calculation model of the basket for box type fuel after 9 m drop test is shown in Fig. (Ⅱ)-E.3.2. The model is same with the model shown in Fig. (Ⅱ)-E.1 through E.8 except the deformation of the basket. Calculations were performed by KENO-Va.

The results of the analysis are as follows;

JRR-3 standard silicide type fuel (in case of containing 40 fuel elements)

$$\begin{cases} k_{eff} = 0.869 \\ \sigma = 0.0009 \\ k_{eff} + 3\sigma = 0.872 \end{cases}$$

JRR-3 follower silicide type fuel (in case of containing 40 fuel elements)

$$\begin{cases} k_{eff} = 0.697 \\ \sigma = 0.0009 \\ k_{eff} + 3\sigma = 0.700 \end{cases}$$

From the results above, it can be concluded that the criticality safety is sufficiently kept.

[redacted]

(Ⅱ)-Fig.E.3.1 Maximum displacement of basket for box type fuel after 9 m drop test

[redacted]

(Ⅱ)-Fig.E.3.2　Analytical model of basket for box type fuel after 9 m drop test (Cross section of basket)

E.7.4 Appendix-4

Investigation of the optimum water density in the criticality evaluation

In order to confirm that the density of water moderator (ρ = 1.0 g/cm^3) used in criticality analysis in this package will result in the optimum condition, the effective multiplication coefficients are calculated with a parameter of water density.

The calculation model is the same as that described in paragraph E.3.1 and the atomic number density is the same as that described in paragraph E.3.2. The KENO-Va code is used. The results shows that the effective multiplication factor (keff) becomes the maximum value at water density ρ = 1.0 g/cm^3 for every basket. Accordingly, density (ρ = 1.0 g/cm^3) used in critical analysis of this package is confirmed to be a safe side for criticality.

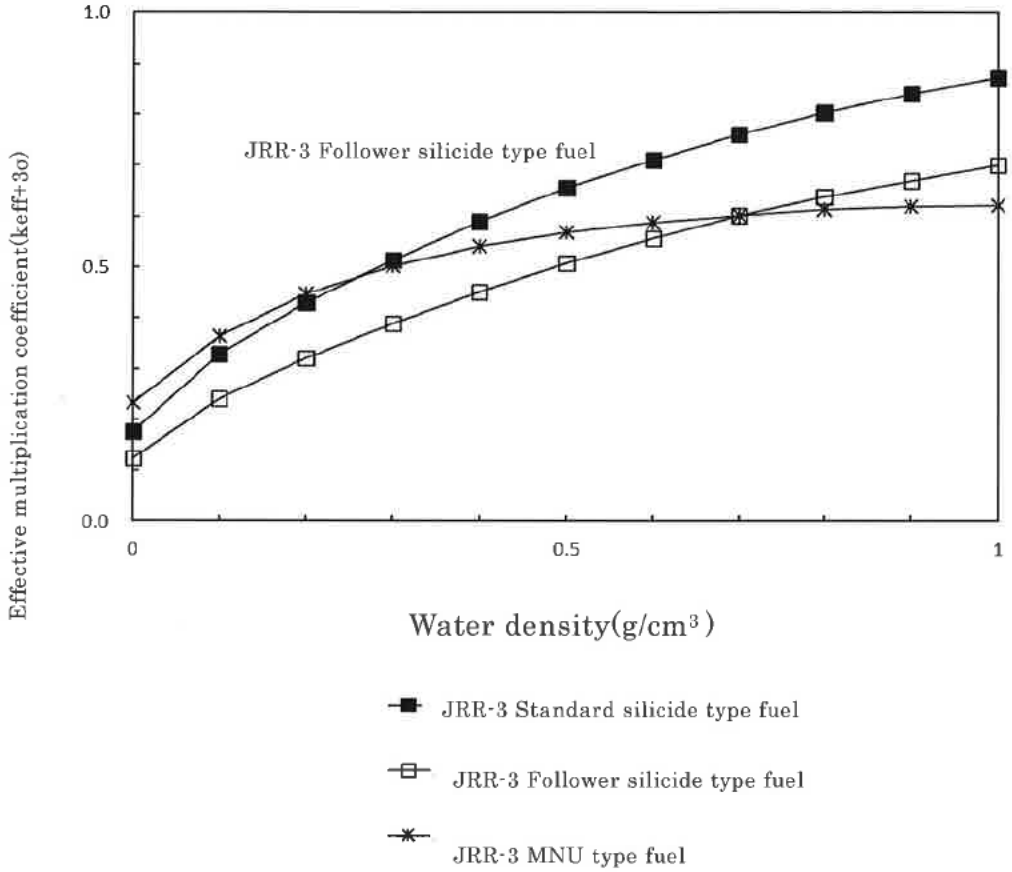

(II)-Fig.E.4.1 Influence of water density on effective multiplication coefficient (keff)

E.7.5 Appendix-5

References

(1) "SCALE:A Modular Code System for Performing Standardized Computer Analyses for Licensing Evaluation", ORNL/TM-2005/39, Version 6.0, Vols. I-III (January 2009)

(2) "Standard Review Plan for Transportation Packages for Spent Nuclear Fuel", NUREG-1617 (2000)

and

"The Radioactive Materials Packaging Handbook", ORNL/M-5003 (1998)

(3) Y. Nakano, et al.; "Neutronics Characteristics of JRR-4 Low Enriched Uranium Core", Proceedings of 21st International Meeting on RERTER (1998)

F. Consideration of Aging of Nuclear Fuel Package

This chapter describes the matters which are to be considered in the safety analysis in Chapter (II) with regard to aging of nuclear fuel package component materials during the planned period of use of the transport container.

F.1 Aging Factors to be Considered

For the nuclear fuel package, based on the anticipated conditions of use as shown in (II)-Table F.1, possible aging factors to be considered for the component materials of the transport container are thermal degradation, degradation due to irradiation, degradation due to chemical changes, and fatigue due to repeated stresses during container storage, before shipment, and during transportation.

The period of use of this package is 70 years from the time of manufacture, the frequency of use is once per year, and the number of days required for transport per transportation is conservatively 365 days. Assuming the number of handling times per transportation is 100 times, the total number of planned lifting times throughout the planned period of use is 7,000 times (100 times x 70 years) (A.4.4).

II)-Table F.1 Conditions of use anticipated during the planned period of use

Status	contents	Conditions of use
In storage	No	· Transport containers are stored indoors. · In order to confirm that the performance of the transport container is maintained, a periodic voluntary inspection based on "Chapter (III) Maintenance of transport containers and handling methods of nuclear fuel packages" described in the application for design approval of nuclear fuel packages (Appendix-1) is to be performed at least once a year.
Before transportation	Yes	· Nuclear fuel packages are to be stored indoors within the controlled area of the facility for up to three months

		from the time the contents are loaded to the time they are transported. ・Before shipment of the package, a pre-shipment inspection based on "Chapter (III) Maintenance of transport containers and handling methods of nuclear fuel packages" is to be conducted.
During transportation	Yes	・The package is to be transported by transport vehicle or vessel. ・The package is to be securely tied to the vehicle or vessel so that it can withstand the shock and vibration expected during transportation. ・The period of transportation is expected to be about 2 months.
After transportation	No	・After transportation, a visual inspection is to be conducted in controlled area (indoor) of the facility to confirm the integrity of the transport container. ・Transport containers are stored indoors.

F.2 Evaluation of Necessity of Considering Aging in Safety Analysis

Based on the aging factors shown in F.1, the necessity of considering the aging of each component material of the nuclear fuel package was evaluated with regard to thermal, radiation, and chemical changes that are expected during the planned period of use. Fatigue evaluation was also conducted for the lifting device, which is subjected to loads during handling, and for the sealing device, which is subjected to loads due to changes in internal pressure. The results of these evaluations are shown in (II)-Table F.2.

The component materials of this nuclear fuel package are shown in Chapter (I) C. Transport container, 3. Materials. Among these materials, those for which aging is to be considered are listed below.

・Stainless Steel

[redacted]

- Aluminum alloy (spacer)

Note that aging of O-rings is not considered because they are replaced with each transportation.

Also, that aging of contents is not consider because they changes with each transportation.

(II)-Table F.2 Evaluation of necessity of considering aging in safety analysis (1/3)

Component material	Aging factors	Evaluation
Stainless Steel	Heat	Although there may be mechanical property degradations such as creep, etc. (deformation) by high temperature embrittlement due to exposure to a high temperature environment, the results of thermal analysis indicate that the temperature near the fuel basket center axis is [redacted] (the highest temperature during transportation is [redacted] for the fuel elements) (B.4.2), which is below the temperature (425℃ or higher) (1) at which deformation due to creep, etc. may occur. Based on the above, there is no need to consider the effect of aging in confirming compliance with the technical criteria.
	Radiation	Although there may be effects on the mechanical properties due to microstructural changes (embrittlement, etc.) caused by neutron irradiation, the maximum neutron irradiation dose during the period of use is [redacted]/cm^2, which is less than the dose of 10^{16} n/cm$^{2(1)}$ that may cause microstructural changes (embrittlement, etc.). Based on the above, there is no need to consider the effect of aging in confirming compliance with the technical criteria.
	Chemical changes	Although there may be effects of corrosion on material strength, embrittlement, etc., stainless steel is a material that forms a passive film on its surface and is not susceptible to

		corrosion. The depth of corrosion in air is estimated to be 1μm (0.001mm)(2) per year with the maximum of 0.07mm during the period of use, which is a negligible amount of corrosion compared to the thicknesses of the component materials [redacted]mm for a transport container body). Based on the above, there is no need to consider the effect of aging in confirming compliance with the technical criteria.
	Fatigue	(1) Lifting device Assuming the frequency of handling of the lifting device is 100 times per year, the realistic assumed number of lifting times during the period of use will be 7,000 times. However, the number of lifting times in compliance with the technical criteria is conservatively assumed to be 10,000 times, and the repeat count of 10,000 times covers the assumed number of uses. Based on the above, fatigue is evaluated with the repeat count being conservatively set to confirm that fatigue failure does not occur (A.4.4). (2) Sealing device Assuming the frequency of handling of sealing devices is 4 times per year, the repeat count in 70 years will be 280 times. However, the repeat count in compliance with the technical criteria is conservatively assumed to be 300 times, and this repeat count of 300 times covers the assumed number of uses. Based on the above, fatigue is evaluated with the repeat count being conservatively set to confirm that fatigue failure does not occur (A.5.1.4).

(II)-Table F.2 Evaluation of necessity of considering aging in safety analysis (2/3)

Component material	Aging factors	Evaluation
[redacted]	Heat	Although there may be a functional degradation to maintain subcriticality due to microstructural changes caused by exposure to a high temperature environment, the results of the thermal analysis indicate that the maximum temperature during transportation is [redacted] (B.4.2), which is below the temperature at which this material melts (2450℃) (B.2). Based on the above, there is no need to consider the effect of aging in confirming compliance with the technical criteria.
	Radiation	Although there may be a functional degradation to maintain subcriticality due to loss of ^{10}B caused by neutron irradiation, the neutron irradiation dose is [redacted]/cm^2 assuming conservatively the period of use of 100 years, the loss of ^{10}B is estimated to be about 0.00013% (E.2.3), which means that the loss of ^{10}B due to neutron irradiation is negligible. Based on the above, there is no need to consider the effect of aging in confirming compliance with the technical criteria.
	Chemical changes	Although there may be a functional degradation to maintain subcriticality due to corrosion, corrosion does not occur because it is in a sealed space within the basket dividers (stainless steel), and does not come in contact with the outside air. Based on the above, there is no need to consider the effect of aging in confirming compliance with the technical criteria.

(II)-Table F.2 Evaluation of necessity of considering aging in safety analysis (3/3)

Component material	Aging factors	Evaluation
Aluminum alloy	Heat	Although there may be effects on the heat transfer performance due to the microstructural changes caused by exposure to a high temperature environment, the results of the thermal analysis indicate that the maximum temperature during transportation is [redacted]℃(B.4.2), which is below the temperature at which this material melts (660℃) (B.2). Based on the above, there is no need to consider the effect of aging in confirming compliance with the technical criteria.
	Radiation	Although there may be effects on the heat transfer performance due to microstructural changes (embrittlement, etc.) caused by neutron irradiation, the maximum neutron irradiation dose during the period of use is [redacted]cm^2, which is less than the dose of 10^{21} n/cm^2(1) that may cause microstructural changes (embrittlement, etc.). Based on the above, there is no need to consider the effect of aging in confirming compliance with the technical criteria.
	Chemical changes	Although there may be effects on the heat transfer performance due to corrosion, aluminum alloys form an oxide film on its surface and are not susceptible to corrosion (3). In addition, it is put to use after confirming that there are no abnormalities in its appearance before shipment. Based on the above, there is no need to consider the effect of aging in confirming compliance with the technical criteria.

F.3 Aging Considerations in Safety Analysis

As described in F.2, the necessity of considering aging effects was evaluated for the component materials of the nuclear fuel package. As a result of the evaluation of aging effects, with regard to the factors of heat, radiation, and chemical changes, under the conditions of use expected during the planned period of use, it was confirmed that there is no need to consider their effects in confirming compliance with the technical criteria. For the lifting device and sealing device, it is necessary to consider aging effects due to fatigue because of repeated stresses. As a result of the evaluations of fatigue of the lifting device and sealing device, considering the conservative repeat count expected during the period of use, it was confirmed that fatigue failure did not occur, and therefore, there was no effect on conformance to the technical criteria.

F.4 Appendix

F.4.1 Appendix-1 References

(1) Transportation Technology Advisory Board, "Measures to Ensure Safety of Post-Storage Transportation for Interim Storage of Spent Fuel" (2010).

(2) Nikkan Kogyo Shimbun, Ltd. "Stainless Steel Handbook" (1979).

(3) Sumitomo Light Metal Industries, Ltd., "Aluminum Handbook (3rd Edition)" (1985).

Chapter III：Maintenance conditions of transport packaging and handling method of package

With regard to the maintenance of transport containers and the handling methods of nuclear fuel packages that conform to the safety design of nuclear fuel packages (including consideration of aging), based on the results of the safety analysis ((II)-A to F), the pre-shipment inspection at each transportation to confirm the integrity of nuclear fuel packages and the periodic voluntary inspection to ensure the performance of transport containers for the planned period of use will be conducted. The details are shown below.

A. Handling method

A.1 Loading method

A typical procedure to load spent fuel elements in the packaging is shown as follows;

1. The packaging, which has been carried by the trailer, is moved in to the pool side as it is, and after the tie down device is removed, it is put on the pool side using the exclusive lifting instrument and the crane.
2. Inspect the conditions of the surface of the packaging, and confirm that there is no such damage as to interfere with the original function of the packaging.
3. From the view point of management of being exposed to the radioactive ray, confirm the radiation level of the surface, and decontaminate if necessary.
4. [redacted]
5. [redacted]
6. From the view point of management of being exposed to the radioactive ray, measure the radiation level of the air in the packaging.
7. Loosen the lid bolts ([redacted] pieces), and pull out them. [redacted]
8. From the view point of management of being exposed to radioactive ray, inspect the contamination of extraneous matter in the packaging, and decontaminate if necessary.

9. After checking the basket, [redacted]

(Except for the case of JRR-3 MNU type fuel, subcritical measurement may be performed according to needs.)

10. [redacted]
11. After checking conditions of the lid (especially the contact portion with the body of packaging, and O-ring), [redacted]
12. [redacted] put it on the pool side.
13. Inspect surface dose rate and radiation level of the packaging and decontaminate if necessary.
14. [redacted]
15. [redacted]
16. After it reaches the temperature equilibrium, measure temperature of the surface of packaging, and confirm to satisfy the technical standard.
17. After it reaches the temperature equilibrium (about [redacted] hours after draining), open the vent valve and drain valve, and let the internal pressure of packaging be atmospheric pressure.
18. [redacted]

    (Refer to (II)-C Containment Analysis for the test method.)
19. Measure surface dose equivalent ratio and surface radiation level, etc., and confirm that each succeed in the prior to shipping inspection.
20. After the leaktight inspection, [redacted]
21. Attach necessary marks.
22. Using the exclusive lifting instrument and the crane, put it on the skid which is

on the trailer, and install the tie down device.

A.2 Prior to shipping inspection of package

Whenever the package is shipped, carry out the prior to shipping inspection shown in (III)-Table A.1, and confirm to be suitable to the prior to shipping standard.

(III)-Table A.1 Prior to shipping inspection points (No.1)

Inspection item	Scope of Inspection	Inspection method	Successful standard	Remarks
1. Visual inspection	Package Spacer	Inspect visually outside appearance of package on condition that the fuel element is loaded.	To have no crack, abnormal flaw, deformation, or any defects.	
2. Lifting inspection	Lifting fittings Of container body	Inspect visually after lifting up, which shall be done when visual inspection is carried out for inspection of packaging.	To have no unusual deformation on lifting device of packaging.	
3. Weight measurement inspection	Package	Confirm according to calculation, etc.	To be 23.2×10^3 kg or less.	
4. Surface containation measurement inspection	Package	Measure surface radiation level of package with smear method.	To be ; α : 0.4 Bq/cm^2 or less β, γ : 4 Bq/cm^2 or less	
5. Radiation dose rate measurement inspection	Package	Measure γ ray dose equivalent ratio and neutron dose equivalent ratio on condition that the fuel element is loaded.	To be 2 mSv/hr or less on surface and 100 μSv/hr or less at a point 1 m away from surface.	
6. Sub-criticality inspection	Basket	Inspect visually outside appearance of basket.	To have no crack, abnormal flaw, deformation, or any defects.	

(III)-Table A.1 Prior to shipping inspection points (No.2)

Inspection item		Inspection method	Successful standard	Remarks
7. Contents inspection	Contents	1) Inspect visually loaded conditions. 2) Confirm records relating to radioactive level, burning degree, calorific value, number of days of cooling, etc.	1) To be no existence of anything unusual on outside appearance. 2) To satisfy values described in SAR for vehicle transportation confirmation.	
8. Surface temperature measurement inspection	Package	Measure temperature of surface of package before transport, after the fuel element is loaded.	To be 85°C or less.	
9. Leakage inspection	Lid, vent valve and drain valve	Carry out pressurize test with compressed N_2 gas at above 4.2 MPaG, and inspect quantity of pressure drop.	Quantity of pressure drop shall be 0.00608 MPa or less per hour.	Refer to paragraph (II)-C.6
10. Package internal pressure measurement inspection	Vent valve and drain valve	Confirm to be opened in the air.	To be opened in the air.	

A.3 Unloading method

The unloading method of fuel elements and the typical action necessary for safety, etc., are summarized as follows;

1. The crane and handling instruments which are used for movement of the package, and the crane and fuel handling instruments which are used for unloading the fuel element, etc., shall be checked before handle and confirm their soundness.
2. When the package is received, perform necessary inspection such as visual inspection, etc.
3. Before unloading the fuel element, [redacted]
4. [redacted]
5. The fuel element shall be [redacted]

A.4 Preparation of empty packaging

Perform the following inspections for the packaging before use, and confirm safety of the operation and integrity of the packaging;

- Visual Inspection
- Surface Contamination Level Measurement
- Radiation Dose Equivalent Ratio Measurement
- Internal Air Radioactivity Density Measurement
- Lifting Inspection of the Packaging Body and Lid
- Visual Inspection of Packaging Inside and Basket
- Visual Inspection of Packaging Body, Lid, Contact Surface and O-ring

B Maintenance conditions

In order to guarantee the specification of packaging over a long period of time, perform the periodical voluntary inspection shown in (III)-Table B.1, confirm integrity of this packaging, and also maintain its record for the necessary period of time. The inspection frequency shall be 1 time per year, but it shall be 1 time or more per every 10 times of use for the packaging which number of use per year exceeds 10 times.

B.1 Visual inspections

Visual inspection is to visually examine the appearance of the packaging in order to confirm that no crack, abnormal flaw, deformation, or any defects exists.

B.2 Internal pressure inspections

Internal pressure inspection is to apply the water pressure at above 0.98 MPaG over a period of 30 min. to the inside of packaging, and to confirm no generation of leakage and permanent deformation, etc., especially on the packaging body, lid, contact portion, and penetration portions (valve).

B.3 Leakage inspection

This inspection shall be carried out for every transport. Pressurize the inside of packaging at above 0.42 MPaG, and perform leaktight inspection by measurement of pressure drop.

If the amount of pressure drop is 0.00608 MPa or less, it be successful, and in case of failure adequate remedy such as exchange of O-ring, etc., shall be done, and then inspect again.

(Refer to (II)-C.6 for detailed information.)

B.4 Shielding inspection

Visual inspection should be performed to examine the appearance of the important portions for shielding performance to confirm that no crack, abnormal flaw, deformation, or any defects exists.

In addition, visual inspection should be performed on the fuel baskets installed in the package in every transport to confirm that no crack, abnormal flaw, deformation, or any defects exists.

B.5 Subcriticality inspection

Visual inspection should be performed on the fuel baskets important for subcriticality performance to confirm that no crack, abnormal flaw, deformation, or any defects exists.

B.6 Thermal inspection

Visual inspection should be performed on the fins for heat dissipation and shock absorption that are important for heat dissipation performance to confirm that no crack, abnormal flaw, deformation, or any defects exists.

B.7 Lifting inspection

Visual inspection should be performed by way of outside appearance, etc., on condition that the empty packaging is lifted up, and confirm to have nounusualness on lifting lug, etc.

B.8 Operational inspection

This inspection is not applicable because the packaging has no special parts, such as valve etc.

B.9 Maintenance of auxiliary system

This packaging is not applicable to the subject due to the reason as follows ;

For this packaging are not used the cooling system attached, neutron shield tank, and the other auxiliary systems.

B.10 Maintenance of valve and gasket, etc., of containment vessel

During every periodic inspection, visual inspection should be performed on O-rings and O-ring grooves to confirm that no crack, harmful flaw, or any defects, which would affect sealing performance, or no abnormal shape exists. Note that the O-rings shall be replaced for every transport.

B.11 Stoarge of transport packaging

Tranport package should be stored indoors.

B.12 Storage of records

Fabriction records and periodical inspection records should be stored for in-service transport packaging.

B.13 Others

None

(III)-Table B.1 Periodical voluntary inspection points

Inspection Item	Scope of Inspection	Inspection method	Successful standard	Remarks
1. Visual inspection	Container body, lid, basket for box type, vent valve and drain valve	Inspect visually outside appearance of packaging.	To have no such unusualness as harmful flaw, crack, and shape, etc.	
2. Leakage inspection	Lid, vent valve and drain valve	Carry out pressurize test with compressed N_2 gas at above 0.42 MPaG, and inspect quantity of pressure drop.	Quantity of pressure drop shall be 0.00608 MPa or less per hour.	Refer to paragraph (II)-C.6
3. Shielding inspection	Container bodyand lid	Inspect visually outside appearance of shield portion of packaging.	To have no unusualness such as harmful flaw, crack, and shape, etc.	
4. Sub-criticality inspection	Basket for box type	To be according to visual inspection of basket.	To have no unusualness on outside appearance such as deformation, damage, etc.	
5. Thermal inspection	Fin Spacer	Fins for heat release and buffer and spacers used as heat transfer components are to be visually inspected.	To have no unusualness such as harmful deformation, and damage, etc.	
6. Lifting inspection	Lifting fittings of container body	Inspect by way of outside appearance, etc., on condition that the empty packaging is lifted up	To have nounusualness on lifting lug, etc.	

Chapter IV -I : Fabrication of packaging

This chapter shows the procedure when the packaging is newly produced as follows. (It is hereafter indicated as "fabrication").

A. Fabrication procedure of packaging

A.1 General description

This packaging is fabricated in accordance with the following procedure. The general processes concerned with the fabrication, or the material procurement, forming, cutting, welding, heat-treatment, repair, inspection and test are executed in accordance with JIS or ASME Code Section-III, Subsection NE.

The overall fabrication process in the fabrication of the packaging, and the flow chart are shown in (IV)-I-Fig.A.1 and (IV)-I-Fig.A.2, respectively.

The following describes the fabrication procedure and process of main components.

The flow charts of the fabrication process of the body and the lid are shown in (IV)-I-Fig.A.3 and (IV)-I-Fig.A.4.

The heavy wall part making up the body and the lid are made by forging, and welded with the fin, lifting lug, etc. after machining.

The flow charts of the fabrication process of the baskets are shown in (IV)-I-Fig.A.5 and (IV)-I-Fig.A.6.

The basket for box type fuel is made by retaining the circumference of the lattice structure made up of partition plate and compartment plate, by the frame of forged stainless steel. The basket for MNU fuel is fixed by the support plate and guide plate after integrating 160 square shape pipes by welding.

A.2 Description of materials

The materials are subjected to fabrication, marking, inspection and test in accordance with JIS or ASME Code Section-III, Subsection NE, Article 2000 and the applicable specification given in Section-II.

[redacted]

(IV)-I-Fig.A.1　Manufacturing process of packaging

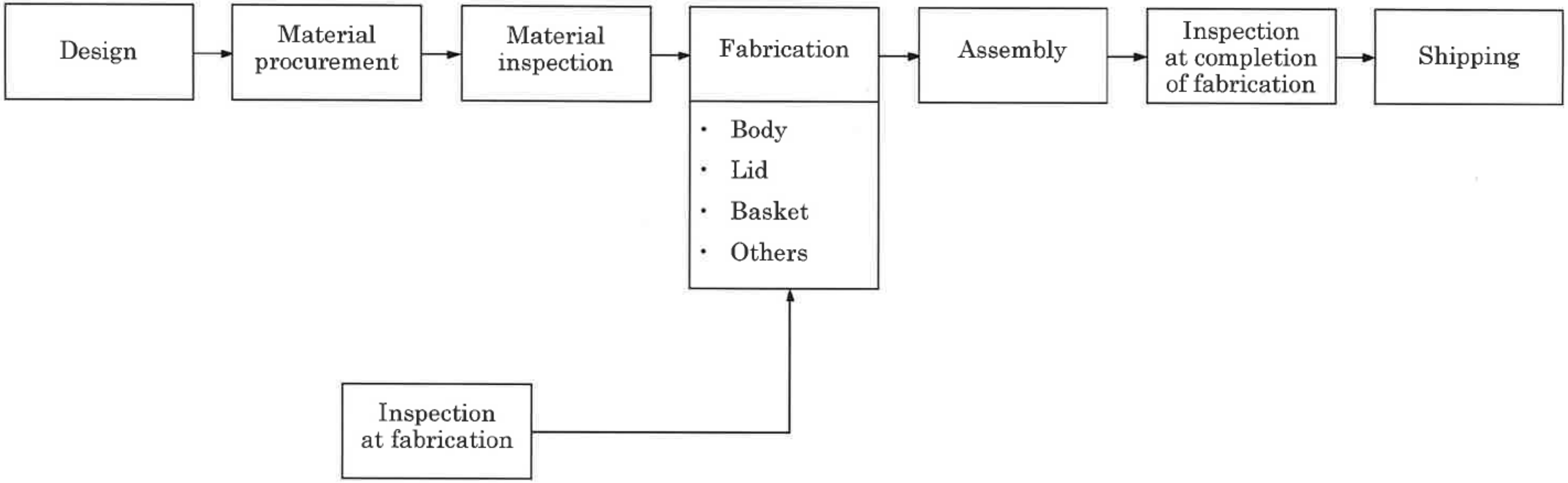

(IV)-I-Fig.A.2　Flow chart of the fabrication process of the packaging

Body

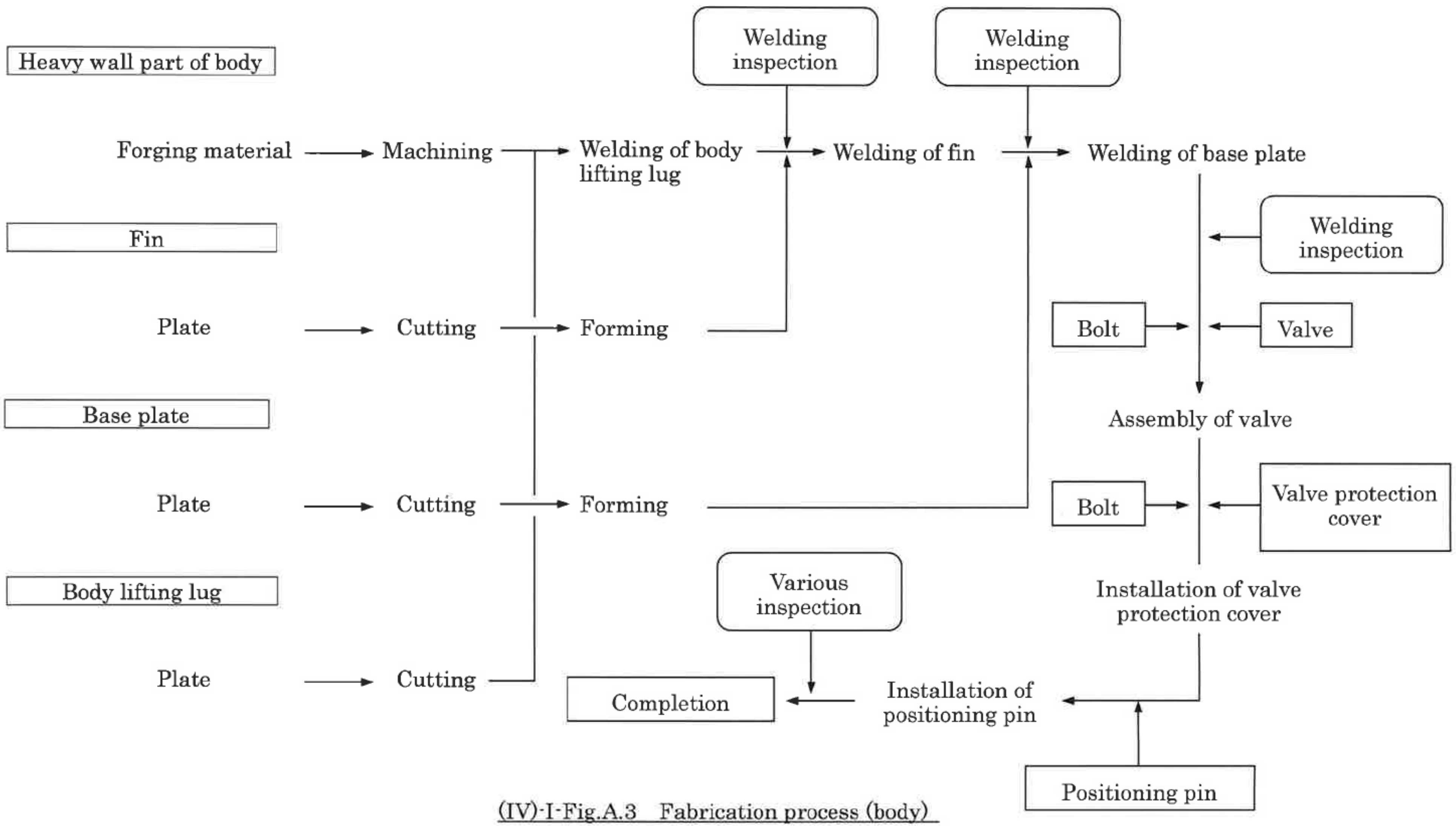

(IV)-I-Fig.A.3 Fabrication process (body)

Lid

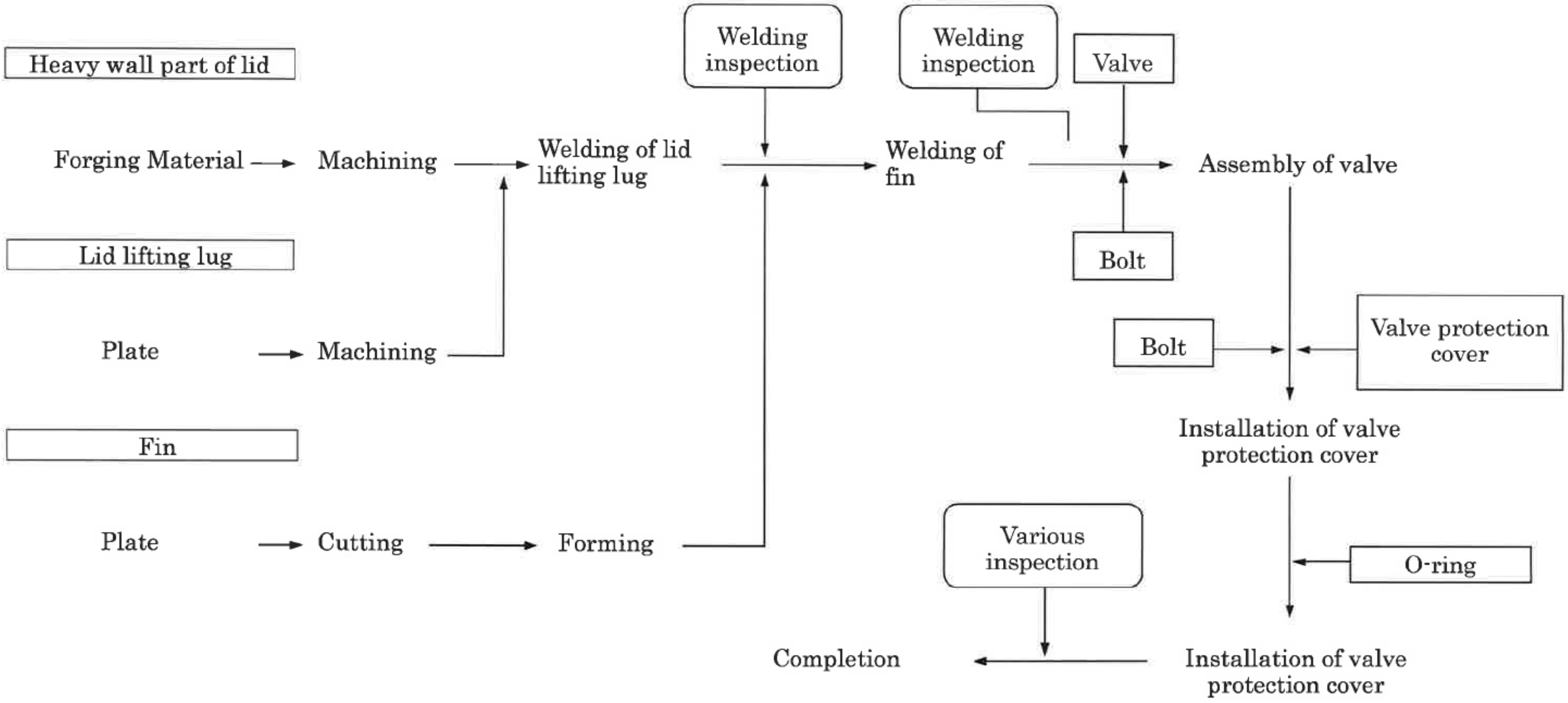

(IV)-I-Fig.A.4　Fabrication process (lid)

Basket for box type fuel

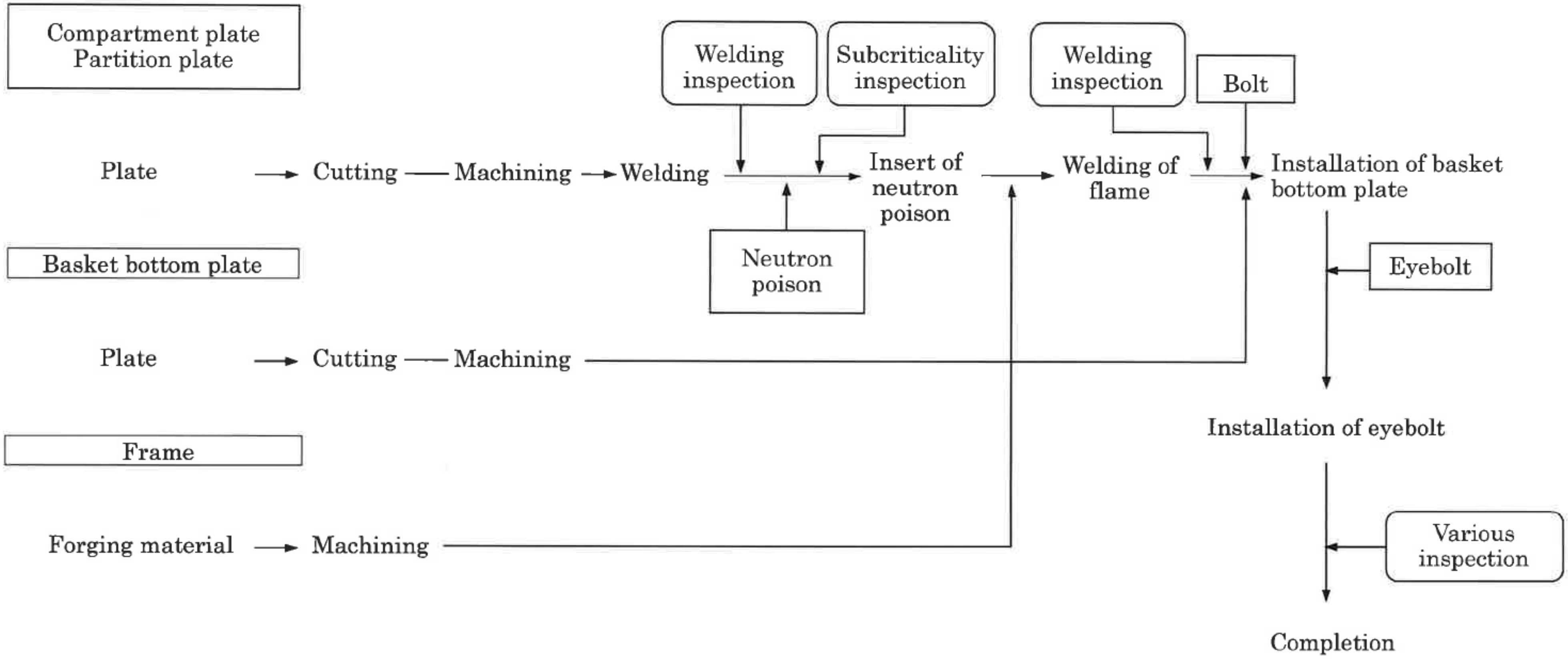

(IV)-I-Fig.A.5 Fabrication process (Basket for box type fuel)

Basket for MNU type fuel

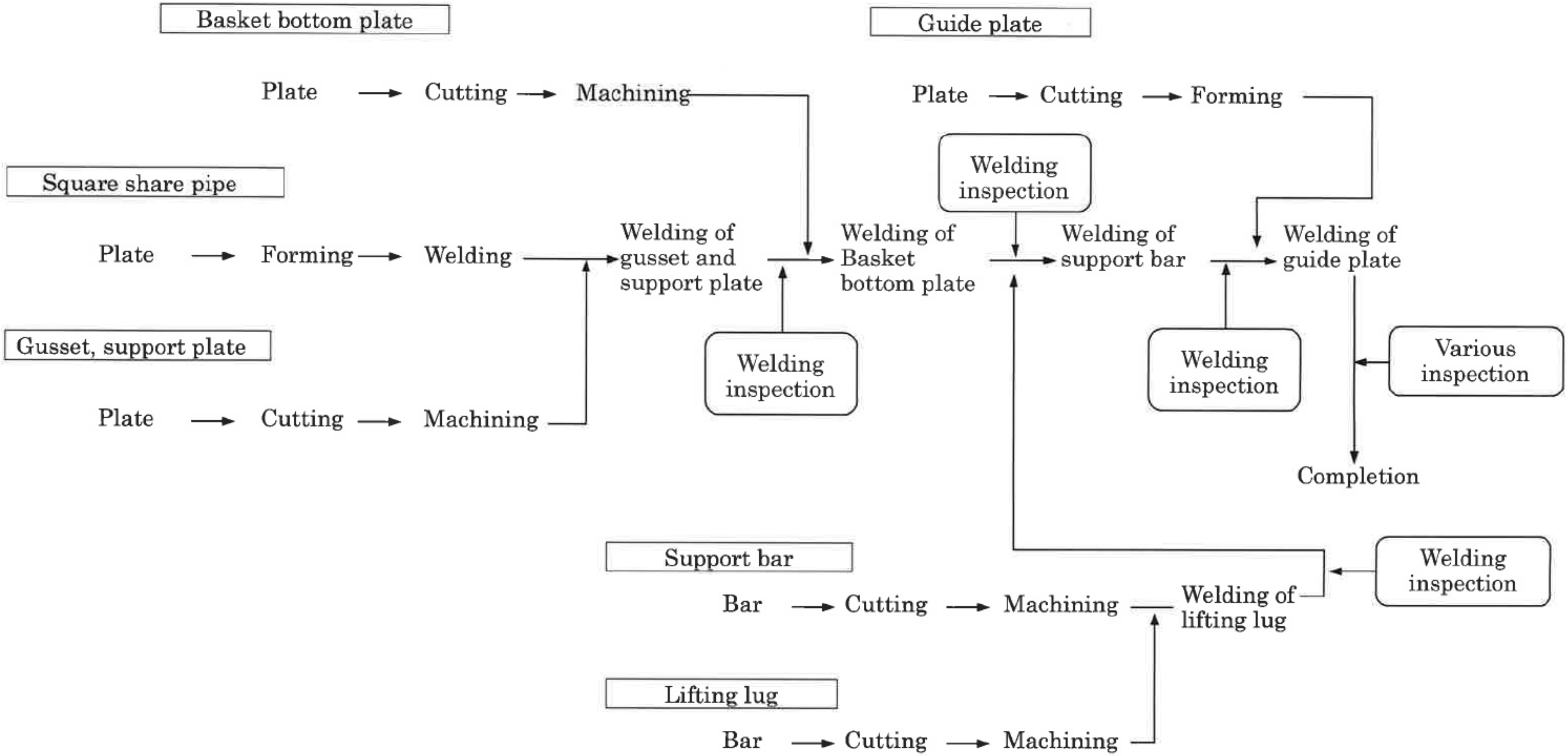

(IV)-I-Fig.A.6 Fabrication process (Basket for MNU type fuel)

A.2.1 Plate material

All materials used for fabrication of this packaging and lifting instrument are the stainless steel, and conform to ASME SA-240 [redacted] (equivalent to [redacted]. These stainless steel plate materials are applied with solution heat treatment to improve corrosion-proof performance.

Since these materials are provided with sufficient strength and excellent corrosion-proof performance, they can be subjected to machining without losing characteristics under any fabrication conditions.

A.2.2 Pipe materials

All pipe materials used for the fabrication of this packaging are stainless steel, and conform to the Grade TP304 specified in ASME SA-312 [redacted]

The stainless steel materials are applied with solution heat treatment to increase the corrosion-proof performance.

A.2.3 Forged parts, bolts, nuts

The forged parts and steel rod used for fabrication of this packaging are all made of stainless steel and conform to the Grade F304 specified in ASME SA-182 ([redacted]

The forged stainless steel parts are applied with solution heat treatment to increase the corrosion-proof performance.

All bolts, plugs, etc. used for fabrication of this packaging are made of stainless steel and conform to the Type-630 *) specified in ASME SA-564 ([redacted].

Since these materials are provided with sufficient strength and excellent corrosion-proof performance, they can be subjected to machining without losing characteristics under any fabrication conditions.

---

*) [redacted] stainless steel of which final heat-treatment temperature [redacted]

A.2.4 Electrodes, rods, wires for welding

The following codes are applied to the rod and wire used at the weld of this packaging.

- Shielded metal arc welding

  AWS (American welding Association) A5.4 E308-16 (equivalent to JIS Z3221 D308-16)

- TIG welding

  AWS A5.9 ER308 (equivalent to JIS Z3321 Y308)

- Welding electrode

  The welding electrode used for fabrication is made of tungsten, etc. and will not be consumed. AWS A5.1 E7016 (equivalent to JIS Z3211 D4316) is applied to the rods and wires to be used at the weld of the tie down device.

  The strength, corrosion-proof performance and weldability required for the material are as shown below to describe that the materials can satisfy the use conditions fully.

1. AWS A5.4 E308-16 (equivalent to JIS Z3221 D308-16) and AWS A5.9 ER308 (equivalent to JIS Z3321 Y308)

- Strength

  - Yield strength : Min. 206 MPa (Min. 21 kgf/mm^2)
  - Tensile strength : Min. 519 MPa (Min. 53 kgf/mm^2)

- Corrosion-proof performance

  The welded joint of stainless steel welded by the use of welding rod, wire having corrosion-proof performance equivalent to that of base metal can provide the corrosion-proof performance equivalent to that of base metal.

- Weldability

  Since the welding rod, wire used provide almost the same component as that of base metal, the excellent weldability is assured with the base metal.

2. AWS A5.1 E7016 (equivalent to JIS Z3211 D4316)

- Strength
  - Yield strength : Min. 206 MPa (Min. 21 kgf/mm^2)
  - Tensile strength : Min. 402 MPa (Min. 41 kgf/mm^2)
- Corrosion-proof performance

  The welded joint of mild steel arc-welded by the use of welding rod having the corrosion-proof performance equivalent to that of base metal provides the corrosion-proof performance equivalent to that of base metal.
- Weldability

  Since the welding rod used provides almost the same component as that of base metal, excellent weldability can be assured with the base metal.

A.2.5 Special materials

The special material used for this packaging will include the neutron poison for critical control and [redacted] used for sealing of containment boundary.

1. Neutron poison
   - Applicable code

     Aluminum alloy : Equivalent to [redacted]

     [redacted] : ASTM [redacted]
   - Strength

     Yield strength : Min. [redacted] MPa (Min. [redacted]gf/mm^2)
2. [redacted]
   - Standard : JIS [redacted]
   - Standard working temperature range (normal) : –[redacted]C – +[redacted]°C

A.2.6 Mill sheet

The main steel materials used for this packaging are attached with the mill sheet which will contain the chemical component, mechanical property and other physical property values required by the applicable specification, code or standard (JIS, ASME, etc.).

A.2.7 Repair of material defect

The defect of forged material and plate material is repaired basically in accordance with requirements specified in JIS or ASME Code, Section-III, Subsection NE, Article 2500.

A.2.8 Cutting of material

The plasma arc cutting method *1) or the other proper method is employed to cut the stainless steel material used for heat dissipating and shock absorbing fin, lifting lug, compartment plate, partition plate, etc.

The plasma cutting method is also used to cut the raw materials of plug, bolt, etc. which are made by machining the rod shape metal.

The details of material cutting are subject to the requirement as stipulated in JIS or the Article NE 4000 of ASME Code.

A.2.9 Forming of material

The body, the lid and the frame of basket are subjected to machining by using a grinder, lathe, etc. after forming to the desired shape by forging the stainless steel ingot.

A.3 Welding

A.3.1 Welding procedure and material

The welding materials of the packaging are stainless steel, of which welding procedure and the welding material are as described below.

1) Stainless steel - stainless steel

1).1 Welding location (main welding procedure)

a) Body, lid

- Shielded metal arc welding *2)

  Fin - body, fin - lid, bottom fin-base plate, lifting lug - lid,
  lifting lug - body

---

*1) Plasma arc cutting method
Method to generate high-density heat by using arc having plasma column converged mechanically and electrically.

*2) Shielded metal arc welding
Welding procedure to execute welding by using arc heat generated between welding rod covered with covering material, and base metal.

b) Basket

- Shielded metal arc welding

  Frame - frame

- TIG welding *1)

  Compartment plate – partition plate, support plate – guide plate, square shape pipe – square shape pipe

- Electric beam welding *2)

  Square shape pipe – square shape pipe

c) Others

1).2 Welding materials

Welding materials used for shield metal arc welding and TIG welding are chosen so as to have the mechanical properties and the corrosion – proof performance equivalent to that of base materials.

A.3.2 Control of welding machine and qualification of welder

1) Control of welding machine

Welding machines are periodically checked and maintained by fabricators of the packaging according to the maintenance plan. The check is to be confirmed that the desired electric current, voltage, welding rod and delivery speed of welding wire are secured while operating the machine.

2) Qualification of welders

Welders of the packaging fabrication are qualified to have the welding ability specified in ASME Code Section IX and pass the qualified welding performance test based upon JIS Z 3801.

---

*1) TIG (Tungsten Inert Gas) welding

Non-consumable inert gas arc welding employing a welding wire as electrode

*2) Electric beam welding

Welding procedure to execute by applying electric beams of high speed generated in vacuum, and using the impact heat.

Welding materials are unnecessary.

A.3.3 Description concerned with main items of welding

1) Maximum allowable temperature

The stainless steel needs not be pre-heated due to properties of crystalline particles as stipulated in ASME Code Section-III, NE4000 (or JIS Z3600).

Accordingly, no pre-heating is executed when the packaging is welded.

The maximum allowable temperature during welding is controlled to less than 200°C.

2) Main dimension/shape of groove face, etc.

The groove face dimension and shape at the main welds of the packaging are as shown in (IV)-I-Fig. A.7 through (IV)-I-Fig. A.10.

3) Cleaning of weld surface

To prevent the lack of fusion and crack at the weld after welding, the foreign matters such as oxides, oil, etc. are removed from the surface of each weld prior to welding. Such cleaning is available in mechanical method or chemical method, each of which is used selectively, depending upon the condition.

4) Finishing of weld

The weld reinforcement and welding condition at each weld are within the allowable range specified in the JIS or ASME Code.

The excess reinforcement, finishing, etc. at each weld are finished smoothly by using a grinder, etc.

A.3.4 Repair of weld defect

The weld defect rejected in the welding inspection described later in paragraph (IV)-I-B.3 is repaired by either one of the following methods.

(1) to re-make the part completely after removing welded joint

(2) to partially re-make the part after removing the defect by using a grinder, etc.

The repaired weld is subjected to the inspection equivalent to that for practical welding.

[redacted]

(IV)-I-Fig.A.7　Example of groove face dimension/shape at weld of fin - packaging body

[redacted]

(IV)-I-Fig.A.8　Groove face dimension/shape at weld of lid lifting lug – lid

[redacted]

(IV)-I-Fig.A.9 Groove face dimension/shape at weld of body lifting lug - body lifting lug

[redacted]

(IV)-I-Fig.A.10 Groove face dimension/shape at weld of basket frame - frame

A.3.5 Heat-treatment after welding

The heat treatment is not applied to the stainless steel after welding, as it will not require heat-treatment after welding.

A.3.6 Special welding

No special welding is executed in the fabrication of this packaging.

A.3.7 Quality assurance program, etc. for welding

The quality assurance for welding work, inspection, etc. is performed in accordance with JIS or ASME Code Section-III.

The general detailed application of the quality assurance program is described later in paragraph (IV)-I-D.2. This section describes the items to be assured for quality in the welding of this packaging.

1) Pre-welding precautions
   a) Check that the welding materials are examined, stored and handled properly.
   b) Check that the main dimensions, shape (paragraph (IV)-I-A.3.3.2)) of groove face, etc. are correct.
   c) Check that the weld surface is cleaned properly (paragraph (IV)-I-A.3.3.3)).
2) Check that the welding machine control and welder qualification are proper. (paragraph (IV)-I-A.3.2)
3) Welding/finishing
   a) Check that the weld is finished properly (paragraph (IV)-I-A.3.3.4)).
4) Welding inspection

   Check that the welding inspection performed properly
   (paragraph (IV)-I-B.3).
5) Repair of weld defect

   Check that the weld defect is repaired correctly (paragraph (IV)-I-A.3.4).

A.4 Fabrication procedure of shielding

The shielding of this packaging is mainly composed of a stainless steel lid, body and basket frame.

This paragraph will not be applied, as the packaging does not use any special shielding such as lead, etc.

A.4.1 Casting of lead shielding material

Not applicable

A.4.2 Fabrication procedure of uranium shielding material

Not applicable

A.4.3 Fabrication procedure of other shielding materials

Not applicable

A.5 Fabrication procedure of accessories such as valve, etc.

a) Vent valve, drain valve

The bellows, stem, bolt, etc. used for the valve are all made of stainless steel. They are fabricated by cutting the plate and steel rod to the desired dimension for forming, welding and machining. The O-ring and gasket are all made of [redacted] and are incorporated moulding articles.

b) Plug (for leaktightness inspection)

The stainless steel rod is cut to the desired size for machining.

c) Positioning pin for lid installation

The stainless steel rod is cut to the desired size for machining.

d) Bolts

The stainless steel rod is cut to the desired size for machining.

A.6 Fabrication procedure such as assembling, etc.

The body, lid and basket are subjected to visual inspection after fabrication, and corrected with a grinder, etc. in such case when there are some harmful irregularities, burrs at the cutting part due to machining, which may fear to allow the water to deposit, or the other defect on appearance.

The assembling sequence and procedure for each part are as shown in (IV)-I-Fig. A.1 through (IV)-I-Fig.A.6.

B. Test, inspection procedure, etc.

This paragraph describes the test/inspection procedure, period and judgement criteria by each test/inspection item.

B.1 Materials inspection

The essential materials are checked for conformity to those specified, referring to the marking and mill sheet attached to the material concerned, or further checked as required by confirmation test (mechanical test, chemical analysis, etc.).

B.2 Dimensional inspection

This dimensional inspection is performed at the time of intermediate inspection during fabrication, and at the time of final inspection after completion of fabrication respectively.

The measurement instruments such as slide calipers, etc. are used for the measurement of dimension. The main dimensions and judgement criteria are within the tolerance shown in (IV)-I-Fig.B.1 through (IV)-I-Fig.B.3. The simulative fuel element for dimensional inspection or dimension checking jig, etc. is used for the dimensional inspection of fuel insertion hole of basket.

B.3 Welding inspection

The body and lid are incorporated body of forging. Accordingly, there is no weld at the containment boundary, etc. which is essential from the viewpoints of safety analysis.

This inspection is performed to check the heat dissipating and shock absorbing fin, lifting lug and basket for bevelling dimension at the weld point. After the welding, the visual inspection, liquid penetrant test, etc. are performed to check for absence of harmful defect at the weld.

B.4 Visual inspection

The body, inner/outer surfaces of lid, basket, packing surface, etc. are checked visually for absence of harmful defects such as crack, etc., and for finish condition to make ascertain that the requirements shown in this application are satisfied.

[redacted]

(IV)-I-Fig.B.1　Main Dimension Tolerance of Packaging

[redacted]

(IV)-I-Fig.B.2 Main Dimension Tolerances of Basket for Box type fuel

[redacted]

(IV)-I-Fig.B.3 Basket for MNU type fuel

B.5 Pressurized inspection

The pressurized inspection is performed on the fabricated packaging (excluding basket) after the completion of fabrication.

The inspection is performed to visually check for absence of failures such as leakage from containment boundary (through part such as connection between the body and lid, valve, etc.), for shape, etc. after leaving for more than 30 minutes with the hydrostatic pressure of 0.98 MPaG and over applied.

B.6 Leaktightness inspection

The packaging is subjected to the leaktightness inspection after completion of fabrication. In this case, the nitrogen gas is used to pressurize the [redacted] (connection between body and lid, vent valve and drain valve) at 0.42 MPaG and over, and measure the amount of pressure dropped at the [redacted]. The amount of pressure dropped up to 0.00608 MPa and less per hour is acceptable.

B.7 Shielding performance inspection

Gamma ray source such as ^{60}Co, etc. is inserted in the packaging, and the equivalent does ratio is measured to check that there is not any defective part in the shielding material, and further to check that the shielding performance specified in this application is satisfied.

B.8 Shielding dimensional inspection

The similar inspection to the dimensional inspection shown in the paragraph B.2 is executed for the shield material (body and lid) to check that the dimensions are within the tolerances.

B.9 Thermal inspection

The thermal inspection is performed to confirm the heat transfer performance of the packaging. In other words, the confirmation is made on the heat radiation performance defined in the thermal analysis against the temperature evaluation (paragraph (II)-B.4) in the absence of insolation.

1) Inspection instrument

The inspection is performed by heating the electric heater set in the fuel lodgement within the packaging.

The amount of heat is simulated to more than 2.25 kW described in chapter (II)-B "Thermal analysis".

The temperature is measured by using a thermocouple, thermister thermometer, etc. set at the fuel basket, inner wall surface of packaging, end of fin, outer surface of shell and in the air around the circumference respectively, to gain the maximum temperature at each part of the packaging and temperatures at major parts.

2) Inspection procedure

The heat input and temperature are recorded continuously until they almost reach the balanced point.

3) Criteria

The inspection result is compensated to the value at the ambient temperature of 38°C, and compared with the thermal analysis result.

Checking is made to see that the maximum temperature on the surface of packaging will not exceed 85°C.

B.10 Lifting load inspection

The following lifting lugs are checked.

- Body lifting lug
- Lid lifting lug

Each lifting lug is checked by applying the force of two times static load during normal operation. The welds of each lifting lug are subjected to the liquid penetrant test, etc. after the lifting load test.

The product is accepted if it is free from any harmful defect, deformation, etc.

B.11 Weight inspection

The weight inspection is performed after completion of fabrication. The total weight is determined either by measuring the weight of each unit to find the total weight, or by measuring the total assembly weight.

The product is accepted if the total weight is less than 22.8×10^3 kg.

B.12 Subcritical inspection

The basket, etc. are checked for appearance and dimension. ^{10}B concentration, content ratio, etc. of neutron poison are checked, referring to the mill sheet. The rejected basket is repaired and then rechecked or disposed.

B.13 Operation inspection

The product is accepted if the valve opens/closes smoothly and is free from any functional problem as a valve.

B.14 Handling inspection

This packaging is accepted if it has no problem in handling when tested for the following items after completion of fabrication.

1. Check that the baskets (2 types) are properly assembled to the packaging.
2. Insert the dummy fuel (simulated in its outside dimension) into the fuel lodgement of the basket to check that the fuel element can be loaded/unloaded readily, and further that the fuel element is stored properly.
3. Check that the O-ring is assembled properly in the O-ring groove.
4. Check that the lid is mounted/demounted readily to/from the packaging and is properly assembled.
5. Check that the packaging can be mounted/demounted readily to/from the lifting instrument and the tie down device readily, and further that these units are assembled properly.
6. Check that the valve body is mounted/demounted readily to the valve storage part, and further that it can be operated properly.

7. Check that the plug and protective cover are mounted/demounted readily, and that they are assembled properly.
8. Check that the lid bolts and valve mounting bolts are tightened properly, and that they can be removed readily.
9. Check that the plug operation tool can operate properly.

C. Packaging fabrication schedule

The fabrication process of packaging is disassembled to each process, depending upon the contents of fabrication such as member material, etc. and then each process is plotted in accordance with the axis of time, of which typical example is shown in (IV)-I-Fig.C.1.

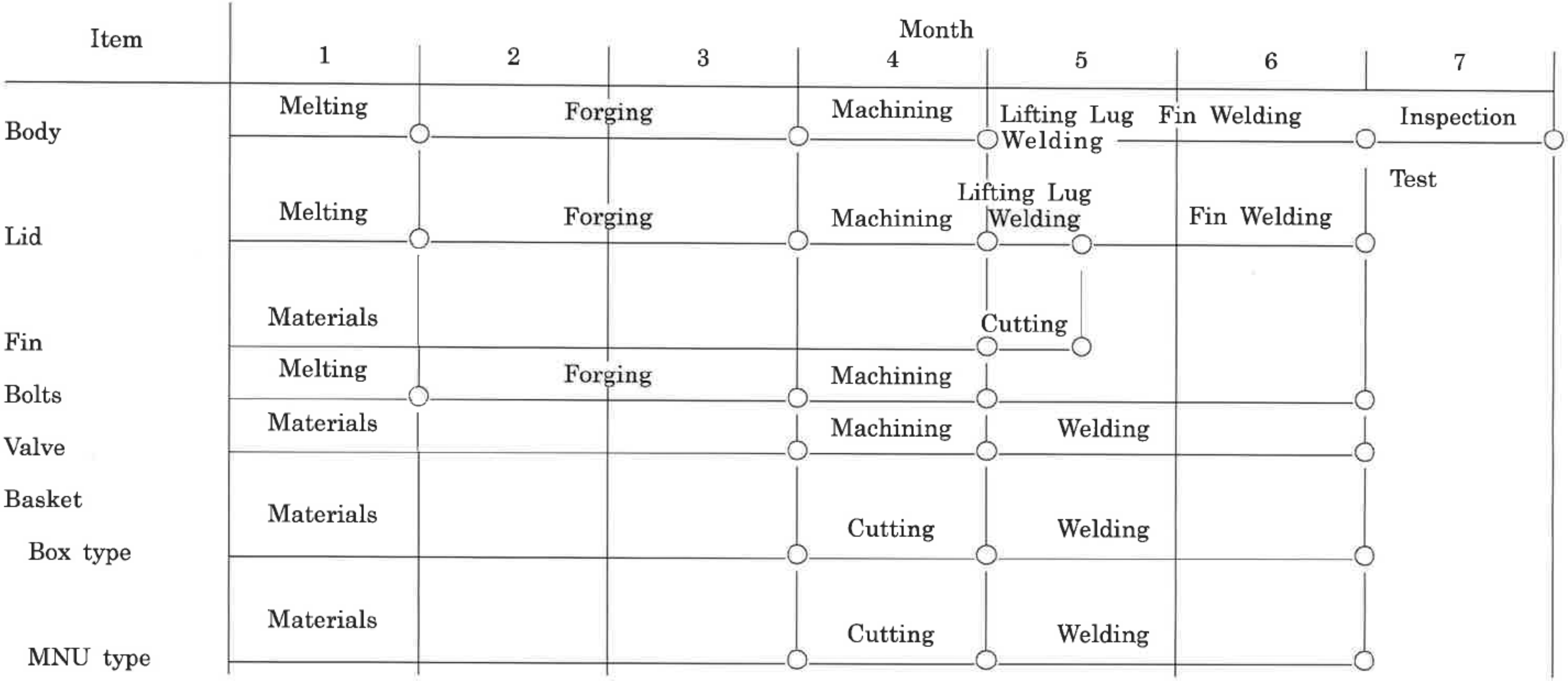

(IV)-I-Fig.C.1 Packaging fabrication schedule

D. Quality control

D.1 System

The quality control for this packaging is executed by the system shown in (IV)-I-Fig. D.1.

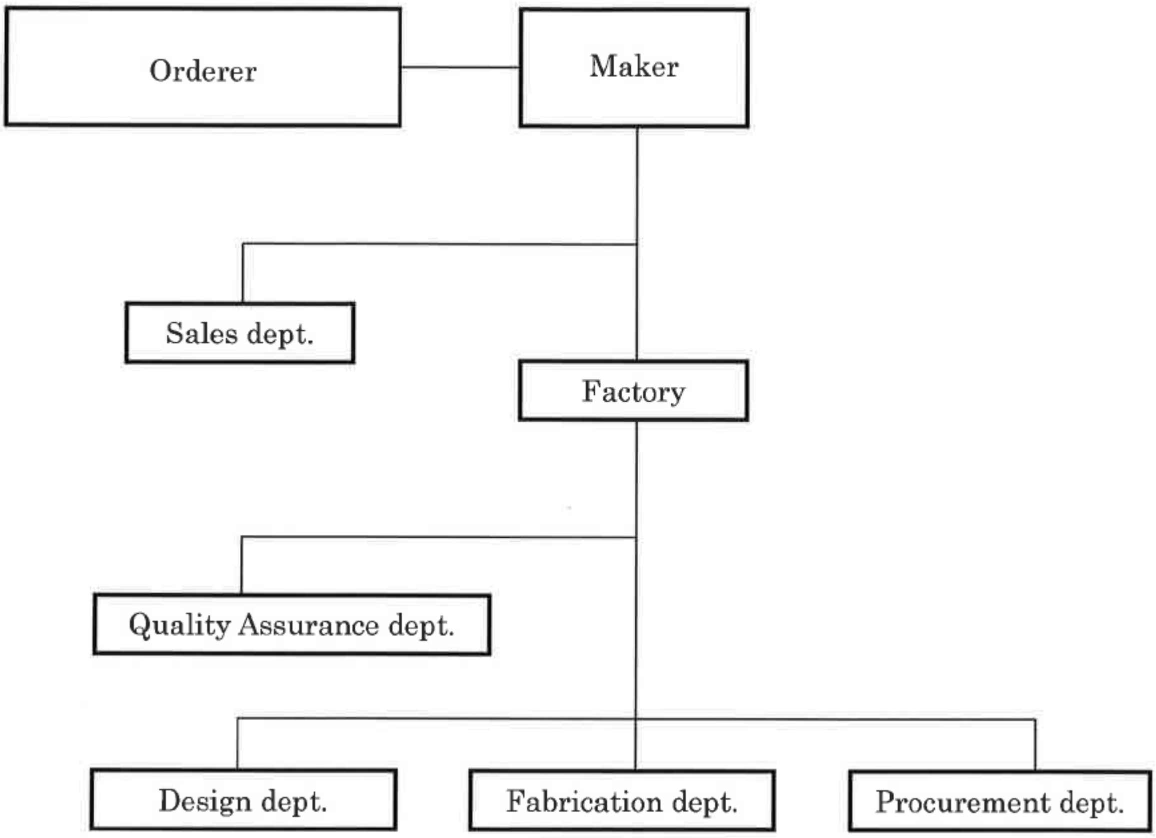

(IV)-I-Fig.D.1 Quality Control System

D.2 Quality assurance program

The following shows the implementation procedure for quality assurance program.

1) Functional failure or trouble of equipment

The most important units in this packaging from the viewpoint of its function will include the [redacted] at the containment boundary.

[redacted] to be protected against the external factor by using the protective cover, therefore, there is no problem in the functional failure or trouble.

2) Relationship between design and fabrication

All items required in design are described in the documents such as drawing, specification, manual, etc. and the fabrication is all executed on the basis of instructions given in these documents.

Since various inspections are performed during the fabrication process to check that all the items required for design are satisfied, the consistency can be secured between the design and fabrication.

3) Management and supervision of process and equipment

The main items to be managed and supervised during the fabrication process include the handling, fabrication and test of materials. In handling the materials, the proper measures are taken such as to prevent the misuse of material, corrosion, damage, etc. including the maintenance, storage and marking of material, etc.

The packaging is fabricated in accordance with the fabrication procedure set up with the mechanical/chemical properties taken into consideration to suit the construction, dimension and accuracy by using the processing unit corresponding to each fabrication procedure under the strict management and supervision.

The test and inspection are performed in the manner with the main points, contents and criteria of the work taken into consideration.

4) Functional adaptability verified by inspection/test

The procedures of test/inspection carried out during the fabrication of this packaging are those that are widely approved as industrial inspection/test procedures, and it is possible to confirm the function of the packaging required by using these inspection/test.

When the packaging is accepted by these inspection and test, it is verified to provide the functions described in chapter (II) "Safety design of package" and chapter (III) "Handling of package".

5) Degree of standard, quality history and standardization

The ASME Code is partially introduced to practice the desired quality assurance/quality control program in the fabrication of packaging, so the packaging can be fabricated in accordance with standardized procedure.

6) Other items required for quality assurance

Nothing in particular

D.3 Design control

The quality control section checks that the items concerning the quality specified in the safety analysis sheet are described correctly in the fabrication specification, drawing, etc. to gain consent from the orderer.

D.4 Instruction and its procedure

All works (purchase of materials, fabrication, test, inspection, etc.) which may affect the quality in the fabrication, use and maintenance are stipulated to be practiced in accordance with the relevant documents (drawing, manual, instruction sheet), etc.

The main items to be strictly observed in accordance with the regulation are shown below ;

Fabrication : All fabrication behaviors are instructed by the manual and instruction sheet which are prepared by the design dept. The confirmation test is performed prior to the execution in the special processes such as welding, etc. and the manual is prepared by the design dept. in accordance with the approved procedure, in the basis of which the instruction are given.

Maintenance inspection： All parts are handled in accordance with the manual prepared by the design dept. to avoid the quality deterioration of parts during the period after receipt till shipment.

D.5 Document control

The documents such as instruction, manual, drawing, etc. concerned with the quality are controlled in accordance with the following procedure.

The documents such as purchase specification, drawing, test/inspection reports, etc. which can affect the quality of packaging are controlled in accordance with the quality control system of the maker. These documents are submitted from the maker to the orderer for approval at the time of completion, and kept by the maker at the same time.

D.6 Procurement of materials, equipment and services

The materials and equipment used for the packaging are purchased in accordance with the purchase specification that defines the specifications such as type, function of material, etc. Such materials and equipment are checked for conformity to those shown in the purchase specification by the receiving inspection when they are supplied.

The receiving inspection record is controlled as quality record.

D.7 Control concerning confirmation of materials, parts and equipment

The main materials, parts and constituent equipment are checked, referring to the mill sheet and equipment inspection certificate, and controlled with markings by using stamping, paint etc.

D.8 Control of special process

The special process such as welding, non-destructive examination, etc. are controlled so that such works can be performed by the qualified personnel described in (IV)-I-described in paragraph (IV)-I A.3.2 or the inspector described in paragraph (IV)-I-D.9 in accordance with the manual prepared on the basis of proper standard.

D.9 Inspection control

The following shows the data sheet, inspection method, etc. concerned with quality.

(1) Data sheet

The data sheet is controlled by the quality control dept. in accordance with the maker's quality record storage regulation.

(2) Inspection procedure

The inspection is performed in accordance with the manual which defines the purpose of inspection, inspection procedure, instruments to use, material designation, criteria and recording method.

(3) Qualification of inspector

The inspector of fabrication maker belongs to the quality assurance dept. which is independent of fabrication dept. The non-destructive examination is performed by the inspector in accordance with the standard conforming to ASNT # SNT-TC-1A. The dimension, weight, etc. are inspected by the fully experienced inspector by using the calibrated instrument, etc. in accordance with the weights and measures law.

(4) Calibration of instrument

The measuring instrument, testing unit, etc. are calibrated by the quality control dept. periodically or as required in accordance with the weights and measures law and other relevant regulations to make sure that such instruments are assured of required accuracy.

(5) Inspection manual

The inspection manual is prepared by the design dept, which defines the inspection procedure, sequence, etc. concerned with the inspection of the packaging.

(6) Repair, improvement and replacement

When any non-conformities such as failure, etc, are found in the inspection, such defective unit is repaired with a new one before it is subjected to another inspection.

D.10 Control of measuring instrument, testing instrument

The measuring instrument, testing instrument, etc. used for fabrication and test are registered in the control ledger card by the quality control dept. and controlled by defining the handling/storage method.

D.11 Handling, storage

The equipment, member materials used, etc. of this packaging are controlled totally and properly to avoid any non-conformity due to handling and storage.

D.12 Control of inspection/fabrication progresses

The inspection/fabrication progresses of the packaging are controlled in accordance with the fabrication plan sheet and schedule list prepared on the basis of plan sheet. The progress of each work in each process is controlled in such a manner as to be checked any time, and further as not to occur any error in the process.

D.13 Correction control

When there occurs any non-conformity in the inspection and fabrication, which may affect the quality, the non-conformity report (indicating non-conforming items, contents and corrective measures) immediately for the approval by the orderer.

D.14 Quality assurance records

The quality control records such as specifications, manual, mill sheet, inspection record, etc. concerning the fabrication are controlled by the quality control dept. in accordance with the maker's quality control system. These records are submitted to the orderer for approval, and kept by the maker at the same time.

D.15 Quality assurance audit

The quality assurance audit is executed to check that the quality assurance is practised correctly. Such audit is executed as required in accordance with the check sheet based on the maker's quality assurance system. These check sheets are submitted to the orderer for approval, and kept by the maker at the same time.

Chapter IV -II : Modification of packaging

This chapter shows the procedure when the packaging is modified and/or only the part is newly produced by design change of the packaging. (It is hereafter indicated as "modification")

A. Modification procedure of packaging

A.1 General description

This packaging is modified in accordance with the following procedure. The general processes concerned with the modification, or the material procurement, forming, cutting, welding, heat-treatment, repair, inspection and test are executed in accordance with JIS or ASME Code Section-III, Subsection NE.

The flow chart and the overall process in the modification of the packaging are shown in (IV)-II-Fig.A.1 and (IV)-II-Fig.A.2, respectively.

The following describes the modification procedure and process of lid and adapters.

On the circumferences of the lid, the supplementary fins newly produced by machining are welded to the edge of top fins. The top edges of type A fins and type B fins are chamfered off. (The configuration of top fins is shown in (I)-Fig.C.15.) The lid lifting lugs and the bottom corner of the lid inner surface are also chamfered off, and the two short fins (location 0° and 180°) are cut off by machining. Furthermore, the difference of 5 mm of the flange surface is removed and flattened by machining. That includes removeing the O-ring grooves, clad welding and reworking the O-ring grooves.

Adapters, box tubular shape and made of aluminum alloy, are newly produced by extrusion.

Those components are assembled into the packaging body that is not modified.

A.2 Description of materials

The materials are subjected to fabrication, marking, inspection and test in accordance with JIS or ASME Code Section-III, Subsection NE, Article 2000 and the applicable specification given in Section-II.

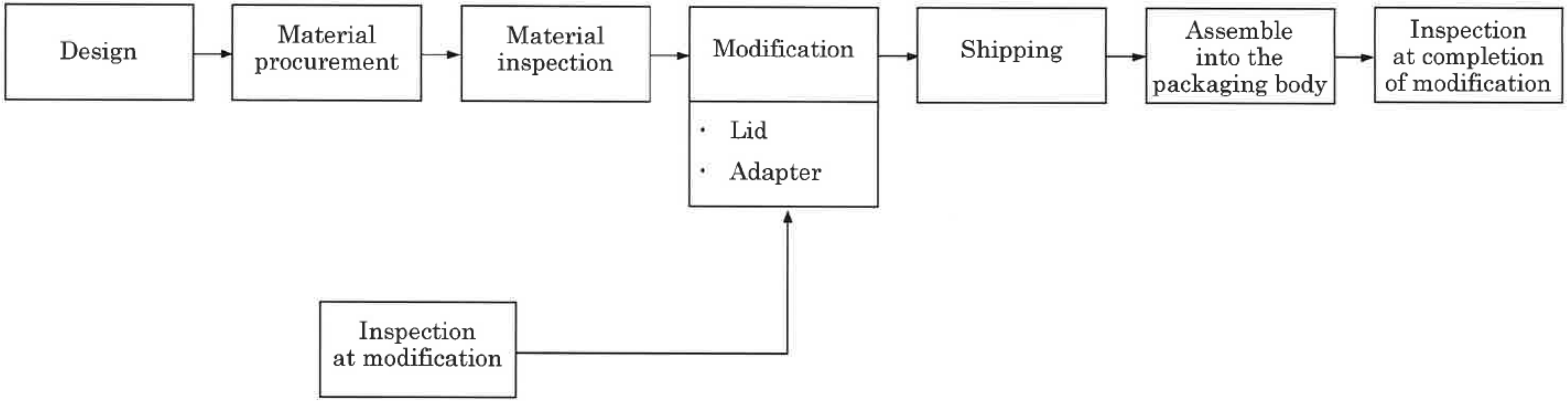

(IV)-II-Fig.A.1　Flow chart of the modification of the packaging

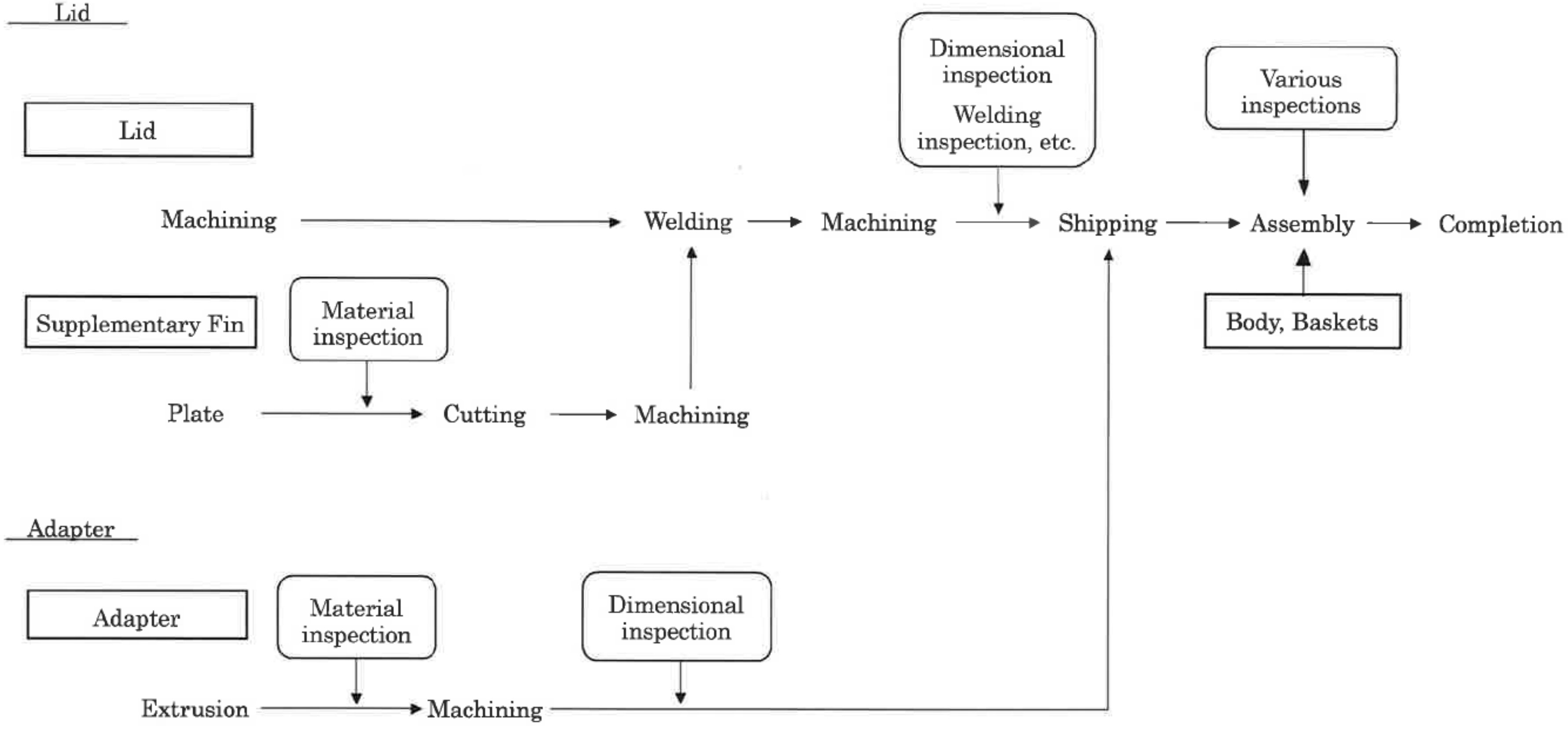

(IV)-II-Fig.A.2 Modification process

A.2.1 Plate material

The material used for supplementary fins is the stainless steel, and conform to ASME SA-240 [redacted] which is applied with solution heat treatment to improve corrosion-proof performance.

Since this material is provided with sufficient strength and excellent corrosion-proof performance, it can be subjected to machining without losing characteristics under any fabrication conditions.

A.2.2 Pipe materials

The pipe material used for adapters is aluminum alloy specified in JIS[redacted]

A.2.3 Forged parts, bolts, nuts

There are neither forged materials nor bolts nuts used for modification.

A.2.4 Electrodes, rods, wires for welding

The following codes and equivalents are applied to the rod and wire used at the weld of this modification.

- Shielded metal arc welding

  AWS (American welding Association) A5.4 E308-16 (equivalent to JIS Z3221 D308-16)

- TIG welding

  AWS A5.9 ER308 (equivalent to JIS Z3321 Y308)

- Flaxcored ark welding

  AWS A5.22 ER308T-1 (equivalent to JIS Z3323 Y308)

- Welding electrode

  The welding electrode used for TIG welding is made of tungsten, etc. and will not be consumed.

Since the welding rod, wire used provide almost the same component as that of base metal, the excellent weldability is assured with the base metal. The welded joint of those materials can provide the corrosion-proof performance and the strength equivalent to those of base metal.

A.2.5 Special materials

There are no special materials used for modification.

A.2.6 Mill sheet

The materials used for this modification are attached with the mill sheet which will contain the chemical component, mechanical property and other physical property values required by the applicable specification, code or standard (JIS, ASME, etc.).

A.2.7 Repair of material defect

The defect of plate material is repaired basically in accordance with requirements specified in JIS or ASME Code, Section-III, Subsection NE, Article 2500.

A.2.8 Cutting of material

The plasma arc cutting method or the other proper method is employed to cut the stainless steel plates.

A.2.9 Forming of material

No forming of material is executed in the modification.

A.3 Welding

A.3.1 Welding procedure and material

The welding materials of the modification are stainless steel, of which welding procedure is qualified in accordance with ASME Code Section-IX or equivalent standard.

The welding is performed by either of shielded metal arc welding, TIG welding or fluxcored ark welding or the combination.

The welding procedure and the welding material are as described below.

1) Welding procedure

- Shielded metal arc welding

  Manual welding uses welding rod as electrode. Welding procedure to execute welding by using arc heat generated between welding rod covered with covering material, and base metal.

- TIG welding

  Non-consumable electrode inert gas arc welding employing tungsten or tungsten alloy as electrode and using Ar gas as shielding gas.

- Flaxcored arc welding

  Automatic arc welding with the electrode of welding wire in the form of a pipe, in which flux is filled, by using shielding gas such as carbonic acid gas.

2) Welding materials

Welding materials used for shield metal arc welding, TIG welding and flaxcored arc welding are chosen so as to have the mechanical properties and the corrosion – proof performance equivalent to that of base materials.

A.3.2 Control of welding machine and qualification of welder

1) Control of welding machine

Welding machines are periodically checked and maintained by fabricators of the packaging according to the maintenance plan. The check is to be confirmed that the desired electric current, voltage, welding rod and delivery speed of welding wire are secured while operating the machine.

2) Qualification of welders

Welders of the packaging fabrication are qualified to have the welding ability specified in ASME Code Section IX and pass the qualified welding performance test based upon JIS Z 3801.

A.3.3 Description concerned with main items of welding

1) Maximum allowable temperature

The stainless steel needs not be pre-heated due to properties of crystalline particles as stipulated in ASME Code Section-III, NE4000 (or JIS Z3600).

Accordingly, no pre-heating is executed when the packaging is welded.

The maximum allowable temperature during welding is controlled to less than 200°C.

2) Main dimension/shape of groove face, etc.

The groove face dimension and shape at the welds of the modifications are as shown in (IV)-II-Fig. A.3 and (IV)-II-Fig. A.4.

3) Cleaning of weld surface

To prevent the lack of fusion and crack at the weld after welding, the foreign matters such as oxides, oil, etc. are removed from the surface of each weld prior to welding. Such cleaning is available in mechanical method or chemical method, each of which is used selectively, depending upon the condition.

4) Finishing of weld

The excess reinforcement, finishing, etc. at each weld are finished smoothly by using a grinder, etc.

A.3.4 Repair of weld defect

The weld defect rejected in the welding inspection described later in paragraph (IV)-II-B.3 is repaired in accordance with ASME Code Section-III Subsection NE Article 4000 after removing the defect by using a grinder, etc.

The repaired weld is subjected to the inspection equivalent to that for practical welding.

A.3.5 Heat-treatment after welding

The heat treatment is not applied to the stainless steel after welding, as it will not require heat-treatment after welding.

[redacted]

(IV)-II-Fig.A.3 Example of groove face dimension/shape at weld of supplementary fin

[redacted]

(IV)-II-Fig.A.4 Groove face dimension/shape at weld of O-ring grooves of the lid

A.3.6 Special welding

No special welding is executed in the modification.

A.3.7 Quality assurance program, etc. for welding

The quality assurance for welding work, inspection, etc. is performed in accordance with JIS or ASME Code Section-III.

The general detailed application of the quality assurance program is described later in paragraph (IV)-II-D.2. This section describes the items to be assured for quality in the welding of this packaging.

1) Pre-welding precautions
   a) Check that the welding materials are examined, stored and handled properly.
   b) Check that the main dimensions, shape (paragraph (IV)-II-A.3.3.2)) of groove face, etc. are correct.
   c) Check that the weld surface is cleaned properly (paragraph (IV)-II-A.3.3.3)).
2) Check that the welding machine control and welder qualification are proper. (paragraph (IV)-II-A.3.2)
3) Welding/finishing
   a) Check that the weld is finished properly (paragraph (IV)-II-A.3.3.4)).
4) Welding inspection

Check that the welding inspection performed properly (paragraph (IV)-II-B.3).

5) Repair of weld defect

Check that the weld defect is repaired correctly (paragraph (IV)-II-A.3.4).

A.4 Fabrication procedure of shielding

Not applicable

A.4.1 Casting of lead shielding material

Not applicable

A.4.2 Fabrication procedure of uranium shielding material

Not applicable

A.4.3 Fabrication procedure of other shielding materials

Not applicable

A.5 Fabrication procedure of accessories such as valve, etc.

Not applicable

A.6 Modification procedure such as assembling, etc.

The cutting off of two (short) top fins and the chamferings of the top edges of (long) top fins, the lid lifting lugs and the bottom corner of the lid inner surface are executed by machining.

The lids and adapters are subjected to visual inspection after modification, and corrected with a grinder, etc. in such case when there are some harmful irregularities, burrs at the cutting part due to machining, which may fear to allow the water to deposit, or the other defect on appearance.

The assembling sequence and procedure for each part are as shown in (IV)-II-Fig. A.1 and (IV)-II-Fig.A.2.

B. Test, inspection procedure, etc.

This paragraph describes the test/inspection procedure, period and judgement criteria by each test/inspection item.

B.1 Materials inspection

The essential materials are checked for conformity to those specified, referring to the marking and mill sheet attached to the material concerned. The material inspection for the materials of supplementary fin and adapter is performed before it begins to modify, and the other materials are checked by confirming the record when producing the packaging.

B.2 Dimensional inspection

The measurement instruments such as slide calipers, etc. are used for the measurement of dimension. The main dimensions and judgement criteria are within the tolerance shown in (IV)-II-Fig.B.1 and (IV)-II-Fig.B.2. The dimensional inspection on the modified part of the lid and adapter is performed after completion of the modification, and the dimentions of other parts are checked by confirming the record when producing the packaging.

B.3 Welding inspection

This inspection is performed to check the supplementary fin and the O-ring grooves for bevelling dimension and shapes at the weld point. After the welding, the visual inspection and the liquid penetrant test are performed to check for absence of harmful defect at the weld. The ASME Code Section-III Subsection NE Article 2500 is applied to the judgement criteria of the liquid penetrant test. The other weld parts of the packaging are checked by confirming the record when producing it.

B.4 Visual inspection

The modified part includes adapter and the outer surface of the body are checked visually for absence of harmful defects such as crack, etc., and for finish condition to make ascertain that the requirements shown in this application are satisfied.

[redacted]

*1: Dimension is confirmed by the record of the packaging producing.

*2: Dimension is measured when the modification was completed.

(IV)-II-Fig.B.1　Main Dimension Tolerance of Packaging

[redacted]

(IV)-II-Fig.B.2　Main Dimension Tolerance of Adapter

Other compornrnts of the packaging such as the inner surface of the body, the baskets, etc. are checkd by confirming the record when producing the packaging.

B.5 Pressurized inspection

The pressurized inspection is performed on the modified packaging (excluding basket) after completion of the modification. The inspection is performed to visually check for absence of failures such as leakage from containment boundary, for shape, etc. after leaving for more than 30 minutes with the hydrostatic pressure of 0.98 MPaG and over applied.

B.6 Leaktightness inspection

The packaging is subjected to the leaktightness inspection after completion of the modification. In this case, the nitrogen gas is used to pressurize the [redacted] (connection between body and lid, vent valve and drain valve) at 0.42 MPaG and over, and measure the amount of pressure dropped at the [redacted] The amount of pressure dropped up to 0.00608 MPa and less per hour is acceptable.

B.7 Shielding performance inspection

Gamma ray source such as ^{60}Co, etc. is inserted in the packaging, and the equivalent does ratio is measured to check that there is not any defective part in the shielding material, and further to check that the shielding performance specified in this application is satisfied. The shielding performance is checked by confirming the record when producing the packaging.

B.8 Shielding dimensional inspection

The similar inspection to the dimensional inspection shown in the paragraph B.2 is performed for the shield material (body and lid) to check that the dimensions are within the tolerances. This inspection is performed on the modified part of the lid after completion of the modification, and the shielding dimensions for other parts is checked by confirming the record when producing the packaging.

B.9 Thermal inspection

The thermal inspection is performed to confirm the heat transfer performance of the packaging. In other words, the confirmation is made on the heat radiation performance defined in the thermal analysis against the temperature evaluation (paragraph (II)-B.4) in the absence of insolation. This thermal inspection is performed by confirming the record when producing the packaging.

1) Inspection instrument

The inspection is performed by heating the electric heater set in the fuel lodgement within the packaging.

The amount of heat is simulated to more than 2.25 kW described in chapter (II)-B "Thermal analysis".

The temperature is measured by using a thermocouple, thermister thermometer, etc. set at the fuel basket, inner wall surface of packaging, end of fin, outer surface of shell and in the air around the circumference respectively, to gain the maximum temperature at each part of the packaging and temperatures at major parts.

2) Inspection procedure

The heat input and temperature are recorded continuously until they almost reach the balanced point.

3) Criteria

The inspection result is compensated to the value at the ambient temperature of 38°C, and compared with the thermal analysis result.

Checking is made to see that the maximum temperature on the surface of packaging will not exceed 85°C.

B.10 Lifting load inspection

The following lifting lugs are checked after completion of the modification.

- Body lifting lug
- Lid lifting lug

Each lifting lug is checked by applying the force of two times static load during normal operation.

The welds of each lifting lug are subjected to the liquid penetrant test, etc.

after the lifting load test. The product is accepted if it is free from any harmful defect, deformation, etc. The body lifting lug is checked by confirming the record when producing the packaging.

B.11 Weight inspection

The weight of lids and adapters are measured after completion of the modification. The weights of other compornrnts of the packaging such as the body, the baskets, etc. are checkd by confirming the record when producing the packaging. The total weight is determined either by measuring the weight of each unit to find the total weight, or by measuring the total assembly weight.

It is accepted if the total weight is less than 22.8×10^3 kg.

B.12 Subcritical inspection

The basket, etc. are checked for appearance and dimension. ^{10}B concentration, content ratio, etc. of neutron poison are checked, referring to the mill sheet. This subcritical inspection is performed by confirming the record when producing the packaging.

B.13 Operation inspection

The product is accepted if the valve opens/closes smoothly and is free from any functional problem as a valve. This operastional inspection is performed by confirming the record when producing the packaging.

B.14 Handling inspection

This packaging is accepted if it has no problem in handling when tested for the following items after completion of the modification.

1. Check that the O-ring is assembled properly in the O-ring groove.
2. Check that the lid is mounted/demounted readily to/from the packaging, and is properly assembled.
3. Insert the adapter into the basket for box type fuel and take off.
4. Check that the follower type fuel element can be loaded/unloaded readily into/from the basket for box type fuel (with adapter). A dummy fuel

(simulated in its outside dimension) is used for this checking.

Following items are checked by confirming the record when producing the packaging.

5. Check that the baskets are properly assembled to the packaging.
6. Insert the dummy fuels (simulated in their outside dimensions except the follower type fuel element) into the fuel lodgement of the basket to check that the fuel element can be loaded/unloaded readily.
7. Check that the packaging can be mounted/demounted readily to/from the lifting instrument and the tie down device readily, and further that these units are assembled properly.
8. Check that the valve body is mounted/demounted readily to the valve storage part, and further that it can be operated properly.
9. Check that the lid bolts and valve mounting bolts are tightened properly, and that they can be removed readily.
10. Check that the plug and protective cover are mounted/demounted readily, and that they are assembled properly.
11. Check that the plug operation tool can operate properly.

C. Modification schedule

The modificaion process is disassembled to each process, depending upon the contents of fabrication such as member material, etc. and then each process is plotted in accordance with the axis of time, of which typical example is shown in (IV)-II-Fig.C.1.

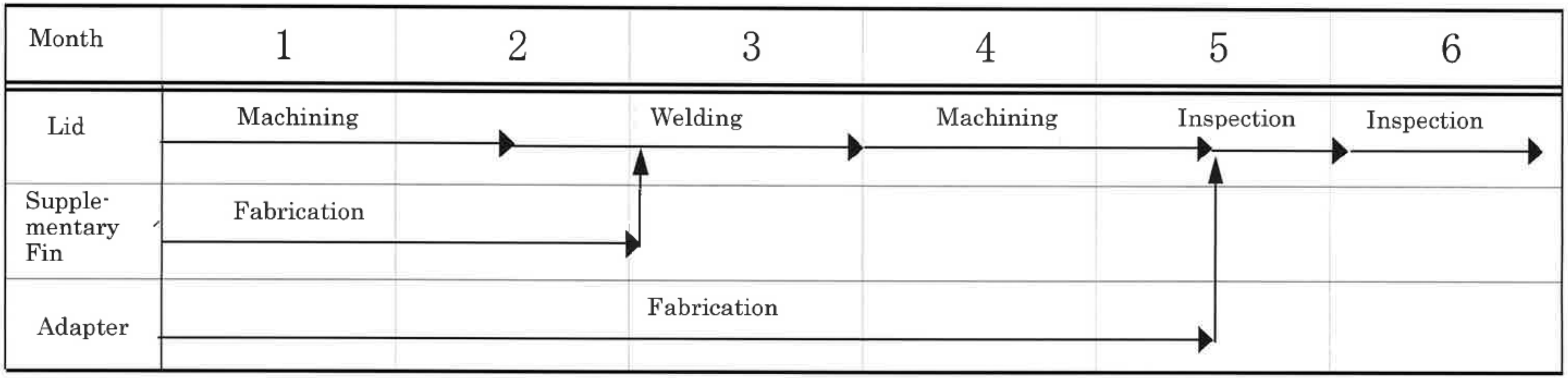

(IV)-II-Fig.C.1 Packaging modification schedule

D. Quality control

D.1 System

The quality control for this packaging is executed by the system shown in (IV)-II-Fig. D.1.

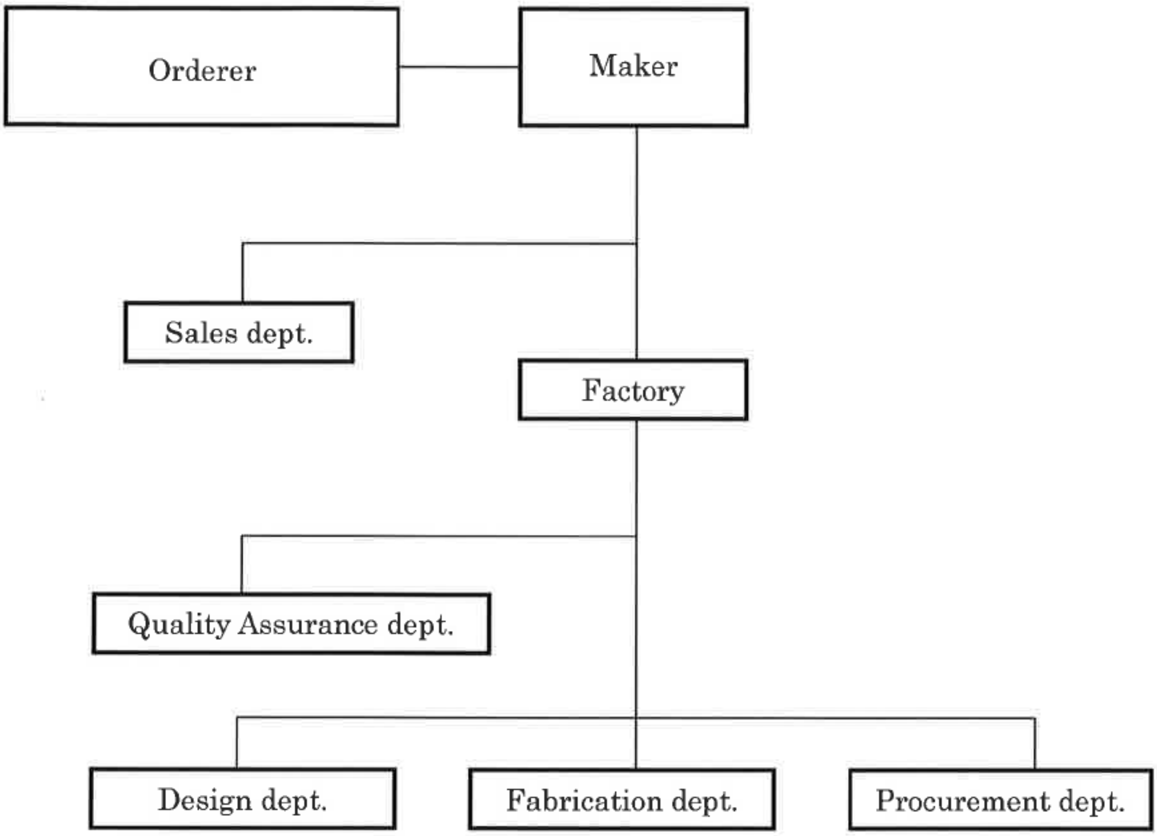

(IV)-II-Fig.D.1 Quality Control System

D.2 Quality assurance program

The following shows the implementation procedure for quality assurance program.

1) Functional failure or trouble of equipment

The most important units in this packaging from the viewpoint of its function will include [redacted] in which the modification is not excuted. [redacted] [redacted] to be protected against the external factor by using the protective cover, therefore, there is no problem in the functional failure or trouble.

2) Relationship between design and fabrication

All items required in design are described in the documents such as drawing, specification, manual, etc. and the modification is all executed on the basis of instructions given in these documents. Since various inspections are performed during the modification process to check that all the items required for design are satisfied, the consistency can be secured between the design and fabrication.

3) Management and supervision of process and equipment

The main items to be managed and supervised during the modification process include the handling, modification and test of materials. In handling the materials, the proper measures are taken such as to prevent the misuse of material, corrosion, damage, etc. including the maintenance, storage and marking of material, etc.

The lid is modified and the adapter is produced in accordance with the modification procedure set up with the mechanical/chemical properties taken into consideration to suit the construction, dimension and accuracy by using the processing unit corresponding to each fabrication procedure under the strict management and supervision.

The test and inspection are performed in the manner with the main points, contents and criteria of the work taken into consideration.

4) Functional adaptability verified by inspection/test

The procedures of test/inspection carried out during the modification of this packaging are those that are widely approved as industrial inspection/test procedures, and it is possible to confirm the function of the packaging required by using these inspection/test.

When the packaging is accepted by these inspection and test, it is verified to provide the functions described in chapter (II) "Safety design of package" and chapter (III) "Handling of package".

5) Degree of standard, quality history and standardization

The ISO Standard 9001 (2000) is introduced to practice the desired quality assurance/quality control program in the modification of packaging, so the packaging can be modified in accordance with standardized procedure.

6) Other items required for quality assurance

Nothing in particular

D.3 Design control

The quality control section checks that the items concerning the quality specified in the safety analysis sheet are described correctly in the modification specification, drawing, etc. to gain consent from the orderer.

D.4 Instruction and its procedure

All works (purchase of materials, modification, test, inspection, etc.) which may affect the quality in the modification, use and maintenance are stipulated to be practiced in accordance with the relevant documents (drawing, manual, instruction sheet), etc.

The main items to be strictly observed in accordance with the regulation are shown below ;

Modification : All modification behaviors are instructed by the manual and instruction sheet which are prepared by the design dept. The confirmation test is performed prior to the execution in the special processes such as welding, etc. and the manual is prepared by the design dept. in accordance with the approved procedure, in the basis of which the instruction are given.

Maintenance inspection： All parts are handled in accordance with the manual prepared by the design dept. to avoid the quality deterioration of parts during the period after receipt till shipment.

D.5 Document control

The documents such as instruction, manual, drawing, etc. concerned with the quality are controlled in accordance with the following procedure.

The documents such as purchase specification, drawing, test/inspection reports, etc. which can affect the quality of packaging are controlled in accordance with the quality control system of the maker. These documents are submitted from the maker to the orderer for approval at the time of completion, and kept by the maker at the same time.

D.6 Procurement of materials, equipment and services

The materials and equipment used for the packaging are purchased in accordance with the purchase specification that defines the specifications such as type, function of material, etc. Such materials and equipment are checked for conformity to those shown in the purchase specification by the receiving inspection when they are supplied.

The receiving inspection record is controlled as quality record.

D.7 Control concerning confirmation of materials, parts and equipment

The main materials, parts and constituent equipment are checked, referring to the mill sheet and equipment inspection certificate, and controlled with markings by using stamping, paint etc.

D.8 Control of special process

The special process such as welding, non-destructive examination, etc. are controlled so that such works can be performed by the qualified personnel described in (IV)-II-described in paragraph (IV)-II A.3.2 or the inspector described in paragraph (IV)-II-D.9 in accordance with the manual prepared on the basis of proper standard.

D.9 Inspection control

The following shows the data sheet, inspection method, etc. concerned with quality.

(1) Data sheet

The data sheet is controlled by the quality control dept. in accordance with the maker's quality record storage regulation.

(2) Inspection procedure

The inspection is performed in accordance with the manual which defines the purpose of inspection, inspection procedure, instruments to use, material designation, criteria and recording method.

(3) Qualification of inspector

The inspector of fabrication maker belongs to the quality assurance dept. which is independent of fabrication dept. The non-destructive examination is performed by the inspector in accordance with the standard conforming to ASNT # SNT-TC-1A. The dimension, weight, etc. are inspected by the fully experienced inspector by using the calibrated instrument, etc. in accordance with the weights and measures law.

(4) Calibration of instrument

The measuring instrument, testing unit, etc. are calibrated by the quality control dept. periodically or as required in accordance with the weights and measures law and other relevant regulations to make sure that such instruments are assured of required accuracy.

(5) Inspection manual

The inspection manual is prepared by the design dept, which defines the inspection procedure, sequence, etc. concerned with the inspection of the packaging.

(6) Repair, improvement and replacement

When any non-conformities such as failure, etc, are found in the inspection, such defective unit is repaired with a new one before it is subjected to another inspection.

D.10 Control of measuring instrument, testing instrument

The measuring instrument, testing instrument, etc. used for modification and test are registered in the control ledger card by the quality control dept. and controlled by defining the handling/storage method.

D.11 Handling, storage

The equipment, member materials used, etc. of this packaging are controlled totally and properly to avoid any non-conformity due to handling and storage.

D.12 Control of inspection/fabrication progresses

The inspection/modification progresses of the packaging are controlled in accordance with the fabrication plan sheet and schedule list prepared on the basis of plan sheet. The progress of each work in each process is controlled in such a manner as to be checked any time, and further as not to occur any error in the process.

D.13 Correction control

When there occurs any non-conformity in the inspection and modification, which may affect the quality, the non-conformity report (indicating non-conforming items, contents and corrective measures) immediately for the approval by the orderer.

D.14 Quality assurance records

The quality control records such as specifications, manual, mill sheet, inspection record, etc. concerning the modification are controlled by the quality control dept. in accordance with the maker's quality control system. These records are submitted to the orderer for approval, and kept by the maker at the same time.

D.15 Quality assurance audit

The quality assurance audit and survey is executed according to the ISO

Standard 9001 (2000) to check that the quality assurance is practised correctly.

APPENDIX-2

Type JRC-80Y-20T nuclear fuel Transport Package Basic policy for the quality management

Basic policy for quality management

This quality management system stipulates the requirements for quality assurance activities by reference to the "Rules of Quality Assurance for Safety of Nuclear Power Plants (JEAC4111-2009)."

A. Quality management system

A.1 General requirements

(1) An organization shall establish, document, implement, and maintain a quality management system for transportation, etc. An organization shall also continue to improve the effectiveness of this quality management system.

(2) An organization shall implement the following matters:

- (a) Clarifying processes required for a quality management system and their application to an organization.
- (b) Clarifying the order and correlation of the processes.
- (c) Defining required judgment criteria and methods to ensure that both operation and management of the processes are effective.
- (d) Ensuring that the resources and information required to operate and monitor the processes are available.
- (e) Monitoring, measuring, and analyzing the processes. However, the measurement can be skipped when it is difficult to measure.
- (f) For the processes, taking measures required to obtain results as planned and continue to improve them.
- (g) Matching the processes and the organization with a quality management system.
- (h) Promoting work based on the knowledge of social science and behavioral science.

A.2 Requirements for documentation

A.2.1 General

The quality management system documents shall be each item of the following:

(1) Quality policy and quality objective

(2) Primary document (quality assurance program)

(3) Secondary document (documents required by primary documents and documents such as rules determined necessary by an organization)

(4) Tertiary documents (documents such as procedures and guides determined necessary by an

organization other than primary documents and secondary documents)

(5) Records required by documents of (1) to (4)

A.2.2 Quality assurance plan

The Director General shall develop, review as necessary, and maintain a quality assurance plan that includes the followings:

(1) Matters related to planning, implementation, evaluation, and improvement of the quality management system

(2) Scope of application of the quality management system

(3) Established "documented procedures" for the quality management system or information that makes it possible to refer to them

(4) A description of the interrelationships among the processes of the quality management system.

A.2.3 Document management

A director general and a manager (research reactor accelerator administration manager. The same shall apply hereinafter) shall define procedures for the document and record management to certainly implement the following matters:

(1) Managing documents required by a quality management system. However, although records are a kind of documents, they are managed in accordance with the requirements specified in A.3 Record management.

(2) Specifying the management required for the following activities:

  (a) Approving documents prior to the issuance from the viewpoint of whether they are appropriate.

  (b) Reviewing, renewing as necessary, and reapproving documents.

  (c) Clarifying the identification of document changes and the identification state of the currently effective version, by a management ledger, etc.

  (d) Ensuring that the appropriate version of the corresponding document is available when and where it is required, by a management ledger, etc.

  (e) Ensuring that documents can be easily read and easily distinguishable.

  (f) Clarifying external documents determined to be required for the quality management system planning and operation and ensuring that their distribution is managed by a management ledger, etc.

(g) Preventing an abolished document from being used by mistake. Also, identifying it appropriately when it is retained for a certain purpose.

A.3 Quality record management

A director general and a manager shall define procedures for the document and record management to certainly implement the following matters:

(1)Clarifying the target for creating records and maintaining them to provide evidence of conforming to requirements and effectively operating a quality management system.

(2)Making records easy to read, easily distinguishable, and retrievable.

(3)Specifying the management required for identification, storage, protection, retrieval, storage time, and disposal of records.

B. An applicant's responsibilities

B.1 Commitment

A director general shall conduct the following matters as the top's commitment to construct and implement a quality management system and continue to improve its effectiveness:

(1) Making it public in an organization to observe laws and ordinances and regulatory requirements.

(2) Setting up a quality policy.

(3) Promoting activities for fostering nuclear safety.

(4) Ensuring that quality objectives are set up.

(5) Conducting a management review.

(6) Ensuring that resources are available.

B.2 Emphasis on nuclear safety

A director general shall give top priority to nuclear safety, determine requirements for work, and ensure that they are met.

B.3 Quality policy and quality objective

B.3.1 Quality record

A director general shall certainly conduct the following matters concerning the quality policy related to transportation, etc.:

(1) Being appropriate in regard to Article 4 of the Act on the Japan Atomic Energy Agency,

Independent Administrative Agency (Purpose of the agency.)

(2) Being appropriate in regard to the quality policy concerning nuclear safety specified by the chief director.

(3) Incorporating the commitment to conform to requirements and continue to improve the effectiveness of a quality management system.

(4) Giving the framework for set-up and review of quality objectives.

(5) Making them transmitted to and understood by the whole organization.

(6) Reviewing to maintain their adequacy.

B.3.2 Quality objective

The Director General should establish manuals for the management of quality objectives to ensure that the followings are implemented.

(1) The Director General shall have the Director set quality objectives. Such quality objectives shall include those necessary to meet the requirements for the work, if any.

(2) The quality objectives shall be consistent with the quality policy and the degree of the achievement of those objectives shall be judgeable.

B.4 Responsibility and authority

B.4.1 Structure

The quality assurance organization for work concerning transportation containers, etc. is shown in (c)-Fig. B.2.

B.4.2 Responsibility and authority

The following persons have responsibility and authority in the matters described for each:

(1) Director general

A director general integrates and promotes quality assurance activities for transportation, etc. carried out at the research institute.

(2) Person in charge of quality assurance control

A person in charge of quality assurance control has the following responsibility and authority:

(a) To ensure that a process required for a quality management system is established, implemented, and maintained.

(b) To report to a director general on the quality management system's implementation status and whether improvements need to be made.

(c) To ensure that the consciousness of compliance with applicable laws and ordinances and nuclear safety is enhanced across the organization.

(3) Manager

A manager integrates and promotes quality assurance activities for transportation, etc. in a department under his/her jurisdiction.

(4) Section chief

A section chief conducts quality assurance activities for transportation, etc. in a department under his/her jurisdiction.

(5) Quality assurance promotion committee

The quality assurance promotion committee reviews important matters for promoting quality assurance activities and for quality assurance activities in the research institute and matters inquired by a director general.

(6) Safety review committee for nuclear facilities and safety review committee for facilities used

The safety review committee for nuclear facilities and the safety review committee for facilities used review important matters for promoting operational safety activities and for operational safety activities in the research institute and matters inquired by a director general.

B.4.3 Internal communication

An organization shall use meetings, business communication memorandums, etc. to ensure information exchange to allow better internal communication. It shall also ensure that the information about the effectiveness of a quality management system is exchanged.

B.5 Management review

A director general shall define procedures for the management review to certainly implement the following matters:

B.5.1 General

(1) For the work concerning transportation, etc., a director general shall conduct a management review at least once a year to confirm that a quality management system continues to function appropriately, validly, and effectively.

(2) In this review, the evaluation of opportunities for improving a quality management system and the evaluation of the necessity for changes of a quality management system including a quality policy shall be conducted.

(3) Records of the result of a management review shall be maintained.

B.5.2 Input to a management review

A person in charge of quality assurance control shall incorporate the following matters in the input to a management review:

(a) Audit results
(b) How outsiders view the achievement of nuclear safety
(c) Implementation status of a process (including the achievement status of quality objectives) and inspection and test results
(d) Implementation status of activities for fostering the nuclear safety culture
(e) Status of compliance with applicable laws and ordinances
(f) Status of preventative measures and corrective actions
(g) Follow-up to results of previous management reviews
(h) Changes which may affect a quality management system
(i) Proposals for improvement

B.5.3 Output from a management review

A director general shall incorporate the decisions and measures on the following matters in the output from a management review:

(a) Improvement of the effectiveness of a quality management system and its processes
(b) Improvements required for work planning and implementation
(c) Necessity for resources

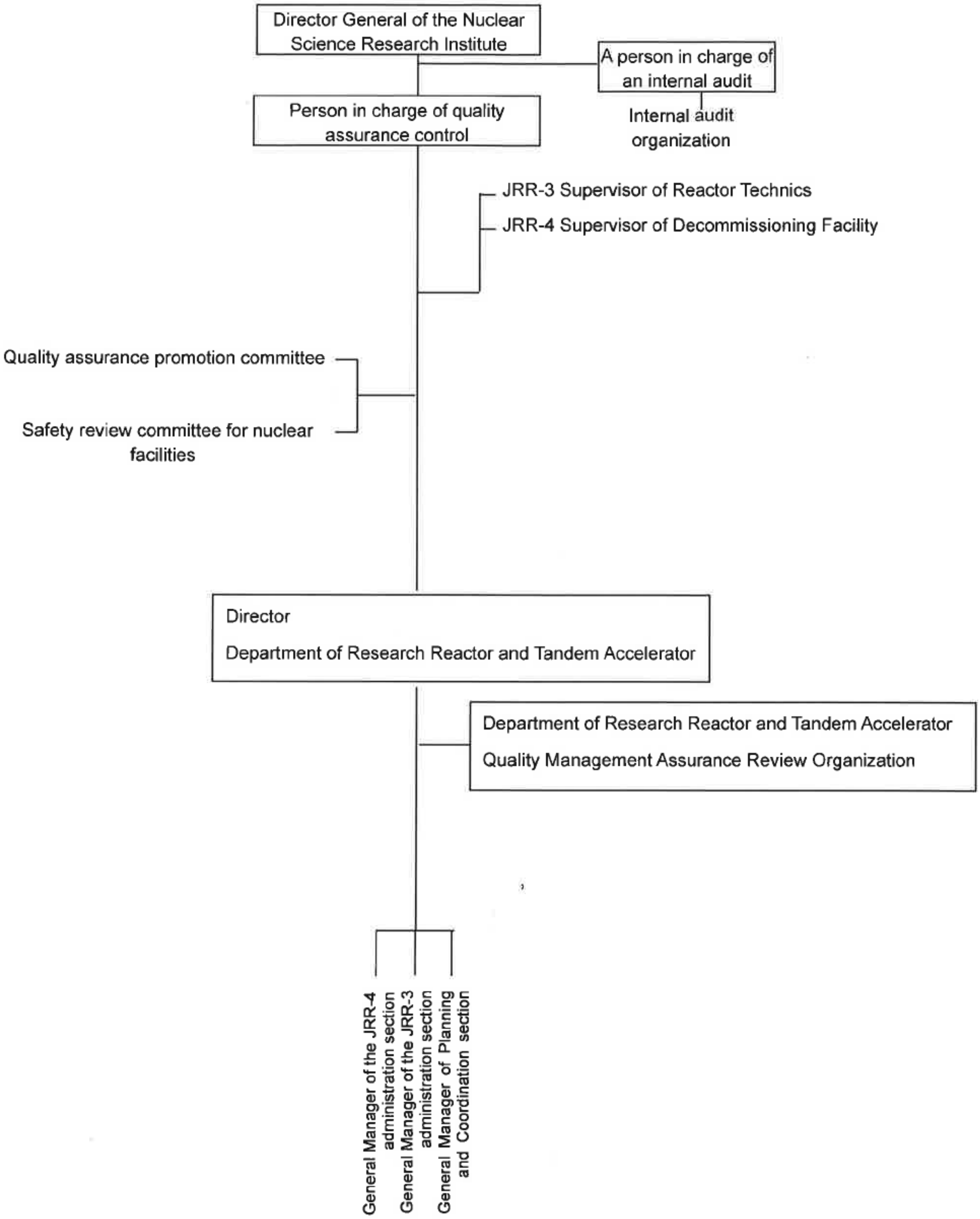

(C)-Fig. B.2 Quality assurance organization concerning design, etc. of nuclear fuel package

C. Education and training

A manager shall define procedures for the education and training management to certainly implement the following matters:

(1) To clarify the competence required for the personnel engaged in the work.

(2) To assign a person capable of carrying out the work, using the required education, training, skills, and experience as the basis of judgment.

(3) To carry out education and training or OJT, etc. so that personnel can have the required competence.

(4) To evaluate the effectiveness of conducted education and training, etc.

(5) To make personnel recognize the meaning and importance of their activities and how they can contribute to achieving quality objectives.

(6) To maintain records concerning education and training track records, skills, and experience.

D. Design management

D.1 Design and development program

(1) A manager shall define procedures for design and development management to clarify processes required for designing and developing a transportation container (including a prototype container).

(2) A section chief shall formulate and manage a design and development program in accordance with the procedures for design and development management.

(3) A section chief shall clarify the following matters in the design and development program:

- (a) Stage of design and development
- (b) Review, verification, and validation suitable for each stage of design and development
- (c) Responsibility and authority for design and development

(4) The design and development program shall incorporate the following matters and clearly indicate them to those who carry out design and development (employees, etc. and contractors):

- (a) To clarify design/development requirements, such as applicable laws and ordinances, standards, and design/development conditions, persons in charge of the review, approval, etc., and required design analysis, design verification, etc., as design documents.
- (b) To define procedures for selecting the components important for transportation containers' functions and the construction method applied to them and evaluating the validity, etc., and

evaluate them.

- (c) To define procedures for selecting, documenting, and approving an appropriate disposition method when a change (including a deviation) from design and development requirements arises.
- (d) To assign those who have appropriate experience and knowledge to the design and development work and make the required information and means available.
- (e) To allow the persons other than an original designer to evaluate design and development documents.

(5) A section chief shall clarify the following matters and operate and manage the interface between the organizations involved in design and development to ensure effective communication and clear assignment of responsibility. It shall incorporate the design interface with a section in charge of manufacturing transportation containers and a section in charge of maintaining transportation containers. The interface shall also be provided with contractors as necessary.

- (a) Interface between organizations or between contractors
- (i) Clarifying the responsibility for the interface of design and development
- (ii) Clarifying methods for creating, reviewing, approving, issuing, distributing, and revising design documents on the interface of design and development and responsible organizations
- (b) Communication between organizations or between contractors
- (i) Clarifying methods to position, examine, and approve the information about design and development information communication
- (ii) Clarifying the interface between the organization carrying out design and development and the one related to each stage of procurement, manufacturing, and maintenance (or the external organization)

(6) A section chief shall renew the program formulated in accordance with the progress of design and development as appropriate.

D.2 Input to design and development

(1) A section chief shall clarify the requirement-related input, reflect it in design and development, and keep and manage the records. The following matters shall be incorporated in the input:

- (a) Requirements for the function and performance of a transportation container (including a prototype container)
- (b) Requirements, such as applicable laws and ordinances

- (c) Requirements for a quality assurance program
- (d) Information obtained from a previous similar design when applicable
- (e) Other requirements essential for design and development

(2) A section chief shall clarify in writing and implement the method for review and approval to prevent inappropriate data use in clarifying design and development requirements.

(3) A section chief shall review the input's adequacy. It shall be noted that there is no omission, no ambiguity, and no incompatibility in requirements.

D.3 Output from design and development

(1) A section chief shall present the output from design and development in the form of a drawing, a specification, a report, a check sheet, etc. to allow the verification comparing it with the input to design and development. In that case, it shall be ensured that the output from design and development is in the following states:

- (a) The requirements given in the input to design and development are satisfied.
- (b) The information suitable for performing procurement and work is provided.
- (c) The characteristics of a transportation container essential for safe use and proper use are clarified.
- (d) When a demonstration test and manufacturing of prototype containers are outsourced for the validation of design and development, the judgment of acceptance of the related inspection and test is incorporated, or it is referenced.

(2) A section chief shall approve the output from design and development before proceeding to the next stage.

D.4 Review of design and development

(1) A section chief shall perform a systematic review as planned, aiming at the following matters at an appropriate design and development stage. In this review, those who have screening skills, such as experts in other departments, shall be included, as necessary.

- (a) To evaluate whether design and development results can satisfy the requirements.
- (b) To clarify problems and propose necessary measures.

(2) A section chief shall keep and manage review result records and disposition records if any disposition is required.

D.5 Design and development verification

(1) A section chief shall perform a verification as planned to ensure that the output from design and development satisfies the requirements given in the input to design and development at an appropriate design and development stage, considering the following matters:

(a) Method of design and development verification

(i) The verification for one or more designs and developments, such as a review of design and development, alternative calculation, a demonstration test, and the comparison with previous similar designs, are performed as appropriate.

(ii) Design and development are verified by the persons other than an original designer.

(b) Alternative calculation

The design and development requirements, the adequacy of a calculation code, etc. are confirmed as well as an original design.

(c) Demonstration test

Tests, such as a verification test and a performance test, are carried out considering the structural material and the structural system of a transportation container, environmental conditions, etc.

(d) Comparison with previous similar designs and development

The comparison with design and development requirements, a structural system, a calculation code, etc. for a comparison target is performed to confirm the validity of design and development.

(2) A section chief shall keep verification result records and disposition records if any disposition is required.

D.6 Validation of design and development

(1) A section chief shall perform a validation as planned at an appropriate stage of design and development to ensure that the design documents as a result of design and development (including safety analysis reports) satisfy the requirements according to the designated use or the intended use. Whenever feasible, a validation shall be completed prior to delivering or providing design documents (including safety analysis reports).

(2) A section chief shall keep validation result records and disposition records if any disposition is required.

D.7 Change management of design and development

(1) When changing design and development, an organization shall clarify the reasons for change, sections changed, changed contents, the existence of the influence due to the change, circumstances of the change, etc. before changing them, appropriately perform a review, verification, and validation, and approve the change before implementation in accordance with the procedure for design and development management.

(a) Changing design and development

(i) Design and development are changed by the same management method of design and development as the one applied to the original design.

(ii) The influence of the change in design and development on the safety of a transportation container (including components, etc.) and design documents (including safety analysis reports) and the validity are evaluated.

(b) Transmitting changes of design and development

The information concerning design change is transmitted to related organizations in writing as specified by a design and development program.

(2) An organization shall keep change review result records and disposition records if any disposition is required.

E. Manufacturing order of a transportation container

E.1 Procurement management

A director general shall define procedures for the procurement management to ensure the following matters:

E.1.1 Procurement process

(1) An organization shall ensure that procured products, etc. comply with specified procurement requirements.

(2) The method and degree of management for suppliers, procured products, etc. shall be defined depending on the influence of procured products, etc. on nuclear safety.

(3) An organization shall evaluate and select a supplier, using the supplier's capability of supplying procured products, etc. in accordance with the organization's requirements as the basis of judgment, based on the criteria of selection, evaluation, and reevaluation defined in the procedure for

procurement management.

(4) An organization shall keep evaluation result records and disposition records if any disposition is required by the evaluation.

(5) An organization shall define the method for obtaining the technical information concerning nuclear safety required for maintenance or operation after the procurement of procured products, etc. and the method for the necessary disposition when sharing them with other departments.

E.1.2 Procurement requirements

(1) A section chief shall clarify the requirements for procured products, etc. and include the relevant items among the following when necessary:

- (a) Requirements for the approval of a product, a procedure, a process, and equipment
- (b) Requirements for qualification confirmation of personnel
- (c) Requirements for a quality management system
- (d) Requirements for a nonconformity report and nonconformity disposition
- (e) Matters necessary for activities to foster a nuclear safety culture
- (f) Matters for information management
- (g) Other matters necessary for procured products, etc.

(2) An organization shall ensure that specified procurement requirements are valid before transmitting them to a supplier.

E.1.3 Verification of procured products

(1) A section chief shall define and perform required inspections or other activities to ensure that procured products satisfy specified procurement requirements.

(2) When a verification is performed at a supplier's facility, a section chief shall clarify the verification procedure and procured products' release method (permission for shipment) in procurement requirements.

(3) When receiving procured products, an organization shall make a procured products supplier submit a document recording the conformity status to procurement requirements.

F. Handling and maintenance

An organization shall plan and conduct the handling and maintenance management of a transportation container in accordance with the following:

(1) Considering the following matters, a manager shall define a procedure for handling transportation containers to prevent erroneous operation of and damage on a transportation container while handling a transportation container under his/her jurisdiction.

(a) Inspection of handling equipment and preventive measures against erroneous operation of and damage on a transportation container during handling

(b) Handling conditions of a transportation container

(c) The shipping in/out conditions and method of a transportation container from a storage facility

(d) Person responsible for handling

(2) A section chief shall clearly indicate requirements while handling a transportation container and reflect them in preventing erroneous operation of and damage on a transportation container in accordance with a procedure for handling transportation containers.

(3) Considering the following matters, a manager shall define a procedure for maintenance management of a transportation container to maintain the design performance of a transportation container under his/her jurisdiction.

(a) Requirements of laws and ordinances, design documents, authorized or licensed matters, etc.

(b) Inspection method and procedure for a transportation container

(c) Damage prevention measures in storage

(d) Setting up storage method and storage areas considering environmental conditions, etc.

(e) Person responsible for maintenance and storage

(4) A section chief shall clarify requirements of applicable laws and ordinances/regulations, design documents, authorized or licensed matters, etc. and reflect them in maintenance management of transportation containers in accordance with a procedure for maintenance management of transportation containers.

(5) A section chief shall clarify and manage persons responsible for work to those who perform maintenance or storage (employees, etc. and contractors).

(6) When maintenance work of transportation containers is outsourced, a section chief shall make a contractor submit management manuals clarifying the following matters and manage them after obtaining the manager's approval, as necessary.

(a) Requirements of laws and ordinances/regulations, etc.

(b) Persons responsible for approval, review, work instructions, etc. of rules, manuals, instructions, etc. required for management

(7) Considering safety importance, etc., a section chief shall conduct witness confirmation and record confirmation in the maintenance inspection of transportation containers (including components).

G. Measurement, analysis and improvement

G.1 General

(1) Organization shall plan and implement the process for monitoring, measurement and improvement required for the following matters:

a) Verify conformity of requirements for the duties.

b) Ensure conformity of the quality management system.

c) Continuously improve effectiveness of the quality management system.

(2) This shall include statistical methods, applicable methods, and determination on the extent to which they are used.

G.2 Internal audit

The Director General shall establish manuals for internal audits to ensure the following.

(1) The Director General shall conduct an internal audit at least once a year on transportation and other activities during the relevant fiscal year to verify whether the following items of the quality management system are fulfilled:

a) Whether the quality management system conforms to the plan of operations, the requirements of the quality assurance plan, and the quality management system requirements determined by the organization.

b) Whether the quality management plan has been effectively operated and maintained.

(2) The Director General should implement the internal program which specifies the following matters by taking into account the process to be the audited, its importance, the past audit results etc.

a) Criteria, scope and methods of audit

b) Objectivity and fairness shall be ensured in selecting the auditor and implementing the audit. Further, the auditor shall not audit his or her own duty.

(3) The manual for internal audits shall specify responsibilities and authorities (authority to order

special internal audits) and requirements for planning and conducting audits, reporting results, and management of records.

(4) Records of audits and the results of them shall be retained.

(5) The person responsible for the audited area shall ensure that the necessary corrective and preventive actions are taken without delay to eliminate the nonconformity found and its cause. The follow-up shall include the verification of the actions taken and the report of the verification result.

G.3 Nonconformity control

The Director General shall establish manuals for nonconformity management and corrective and preventive actions to ensure the followings:

(1) The organization shall ensure that nonconformities are identified and controlled to prevent them from being left unresolved. The manuals for nonconformity and corrective and preventive actions shall specify the controls over the handling of nonconformities and the responsibilities and authorities related thereto. The manual for internal audits shall specify the controls over, and the responsibility and authority for, the handling of nonconformities in quality assurance activities identified during internal audits.

(2) The organization shall take actions for nonconformity in either of the following ways:

a) Take action to remove detected nonconformity.

b) An authorized person may determine its use, release, or acceptance by special employment.

c) Take action to prevent its original intended use or application

d) If a nonconformity is detected after delivery, the organization should take an appropriate action for the effects or possible effects of the nonconformity.

(3) The organization should maintain records of the nature of the nonconformity.

(4) When nonconformities are corrected, the organization shall reverify them to demonstrate conformance to the requirements.

(5) If a nonconformity is detected after delivery, the organization shall take appropriate action to address the effects or potential effects of the nonconformity.

G.4 Corrective actions

The Director General shall establish manuals for nonconformity management and corrective and preventive actions, and for internal audits to ensure the followings.

(1) The organization shall take action to eliminate the causes of nonconformities to prevent

recurrence.

(2) Corrective actions shall be commensurate with the impact of the nonconformity that has been found.

(3) The following requirements shall be specified in the manuals for nonconformity management and corrective and preventive actions:

a) Confirmation of the nonconformity details

b) Identification of the cause of nonconformity

c) Evaluation of the necessity of the actions to certainly prevent nonconformity from occurring again

d) Decision and performance of necessary actions

e) Record of the results of the investigation and the corrective actions taken based on those results, when an investigation is conducted into corrective actions.

f) Review of activities performed in corrective actions

(4) The following requirements shall be specified in the manual for internal audits:

a) Confirmation of the nonconformity details

b) Identification of the cause of nonconformity

c) Decision and performance of necessary actions

d) Record of the results of actions that have been taken

G.5 Preventative actions

The Director General should establish manuals for nonconformity management and corrective and preventive actions, as well as manuals for horizontal deployment, to ensure the following.

(1) The organization should determine actions to eliminate the causes of possible nonconformities, including the acquisition and utilization of knowledge obtained through the implementation of safety activities and technical information obtained from inside and outside the institute, in order to prevent the occurrence of possible nonconformity. This utilization includes sharing the knowledge obtained through the implementation of nuclear safety and security-related activities with other organizations.

(2) Preventive actions shall be commensurate with the impact of possible problems.

(3) The organization shall specify requirements for the followings.

a) Identification of possible nonconformity and its cause

b) Assessment of necessity of actions to ensure the prevention of non-conformity

c) Determination and performance of necessary actions

d) Record of the results of the investigation and the preventive actions taken based on those results, when an investigation is conducted into preventive actions.

e) Review of activities performed in preventive actions